TRW REPORT NO. 33631-6006-RU-00
November 14, 1978

FINAL REPORT

EFFECTS OF ARCING DUE TO SPACECRAFT CHARGING ON SPACECRAFT SURVIVAL

A. Rosen
N. L. Sanders
J. M. Sellen, Jr.
G. T. Inouye

Prepared for

NASA/LEWIS RESEARCH CENTER
Cleveland, Ohio 44135

Under Contract No. NAS3-21363

TRW
DEFENSE AND SPACE SYSTEMS GROUP
SYSTEMS ENGINEERING
ONE SPACE PARK REDONDO BEACH CALIFORNIA 90278

GLOSSARY

DCNM	DC NOISE MARGIN
DSCS	DEFENSE SATELLITE COMMUNICATION SYSTEM
D_T	PULSE DURATION
EMC	ELECTROMAGNETIC COMPATIBILITY
EMCD	ELECTROMAGNETIC CONTROL DEPARTMENT
EMI	ELECTROMAGNETIC INTERFERENCE
ESD	ELECTROSTATIC DISCHARGE
EST	ELECTRON SWARM TUNNEL
F_C	CUT OFF FREQUENCY
FLTSATCOM	FLEET SATELLITE COMMUNICATIONS SYSTEM
FSS	FREQUENCY SELECTIVE SUBSYSTEM
IST	INTEGRATED SYSTEM TEST
LECP	LOW ENERGY CHARGED PARTICLES
LI	LOW IMPEDANCE
MIRIS	MULTIPLE INFRARED INTERFERENCE SPECTROMETER
NASCAP	NASA CHARGING ANALYZER PROGRAM
OSR	OPTICAL SOLAR REFLECTORS
PTM	PROOF TEST MODEL
RF	RADIO FREQUENCY
RFI	RADIO FREQUENCY INTERFERENCE
RTG	RADIOISOTOPE THERMAL GENERATOR
SCATHA	SPACECRAFT CHARGING AT HIGH ALTITUDES
SEMCAP	SPECIFICATION & ELECTROMAGNETIC COMPATIBILITY ANALYSIS PROGRAM
SLOPE	FREQUENCY RESPONSE ROLL-OFF RATE
SSM	SECOND SURFACE MIRRORS
VDA	VACUUM DEPOSITED ALUMINUM

REFERENCES APPEAR IMMEDIATELY AFTER THE APPROPRIATE SECTION.

1. Report No.	2. Government Accession No.	3. Recipient's Catalog No.
CR 159593		

4. Title and Subtitle	5. Report Date
FINAL REPORT - EFFECTS OF ARCING DUE TO SPACECRAFT CHARGING ON SPACECRAFT SURVIVAL	NOV. 14, 1978
	6. Performing Organization Code
7. Author(s)	8. Performing Organization Report No.
A. ROSEN, N. L. SANDERS, J. M. SELLEN, JR., & G.T. INOUYE	TRW 33631-6006-RU-00
	10. Work Unit No
	YOS 8352
9. Performing Organization Name and Address	11. Contract or Grant No.
TRW DEFENSE AND SPACE SYSTEMS GROUP ONE SPACE PARK REDONDO BEACH, CA 90278	NAS3-21363
	13. Type of Report and Period Covered
12. Sponsoring Agency Name and Address	FINAL MAY 1978-NOV 1978
NATIONAL AERONAUTICS AND SPACE ADMINISTRATION LEWIS RESEARCH CENTER 21000 BROOKPARK ROAD, CLEVELAND, OH 44135	14. Sponsoring Agency Code
	6124

15. Supplementary Notes

16. Abstract

THIS REPORT PRESENTS A QUANTITATIVE ASSESSMENT OF THE HAZARD ASSOCIATED WITH SPACECRAFT CHARGING AND ARCING ON SPACECRAFT SYSTEMS. IT IS MADE UP OF A COMPILATION OF DATA GATHERED AS A RESULT OF FOUR STUDY TASKS. TASK 1, ARC DISCHARGE CHARACTERIZATION INCLUDES A LITERATURE SURVEY THAT TABULATES AND DISCUSSES THE AVAILABLE DATA ON ARC DISCHARGE THRESHOLDS AND CHARACTERISTICS, AND ALSO IDENTIFIED GAPS IN THE DATA AND REQUIREMENTS FOR ADDITIONAL EXPERIMENTS. TASK 2, COUPLING DETERMINATIONS PRESENTS CALCULATIONS OF COUPLING OF ARC DISCHARGES INTO TYPICAL SPACECRAFT SYSTEMS. TASK 3, THREAT DETERMINATION, PRESENTS A QUANTITATIVE ANALYSIS OF THE SUSCEPTIBILITY OF TYPICAL SPACECRAFT TO DISRUPTION BY ARC DISCHARGES. TASK 4, SPACECRAFT DESIGN PRACTICE REVIEW PRESENTS A SUMMARY OF DESIGN GUIDELINES AND RECOMMENDED PRACTICES TO REDUCE OR ELIMINATE THE THREAT OF MALFUNCTION AND FAILURES DUE TO SPACECRAFT CHARGING/ARCING.

17. Key Words (Suggested by Author(s))	18. Distribution Statement
SPACECRAFT CHARGING DISCHARGE ELECTROSTATIC DISCHARGE (ESD) ARC DISCHARGES	PUBLICLY AVAILABLE

19. Security Classif. (of this report)	20. Security Classif. (of this page)	21. No. of Pages	22 Price*
UNCLASSIFIED	UNCLASSIFIED	152	

* For sale by the National Technical Information Service, Springfield, Virginia 22161

TRW REPORT NO. 33631-6006-RU-00
November 14, 1978

FINAL REPORT

EFFECTS OF ARCING DUE TO SPACECRAFT CHARGING ON SPACECRAFT SURVIVAL

A. Rosen
N. L. Sanders
J. M. Sellen, Jr.
G. T. Inouye

Prepared for

NASA/LEWIS RESEARCH CENTER
Cleveland, Ohio 44135

Under Contract No. NAS3-21363

TRW
DEFENSE AND SPACE SYSTEMS GROUP
SYSTEMS ENGINEERING
ONE SPACE PARK REDONDO BEACH CALIFORNIA 90278

TABLE OF CONTENTS

INTRODUCTION

The study of the "Effects of Arcing Due to Spacecraft Charging on Spacecraft Survival" was initiated on May 17, 1978. A description of the four tasks encompassed by the study is presented in Table I; with the associated schedule given in Figure I. This document, the final report for the study, presents a detailed description of the data generated for Tasks 1 through 4, and summarizes the major conclusions reached as a result of the generated data.

The study of the "Effects of Arcing Due to Spacecraft Charging on Spacecraft Survival" was motivated by the following rationale and assumptions:

1. At this time a quantitative assessment has not been made of the hazard associated with spacecraft charging and arcing.

2. The quantitative evidence gathered to date proves that environmental charging and arcing occur at synchronous altitudes, however the degree to which this charging and arcing affect typical space systems has not been quantitatively determined.

3. The purpose of this study was to determine from the literature the best known arc characterization data, couple these arcs with typical space systems and quantitatively determine the magnitude of the hazard.

4. A successful quantitative determination of the magnitude of the hazard to real space systems would represent a strong motivational factor for system designers to undertake the necessary countermeasures to assure the integrity and reliability of space systems.

CONCLUSIONS

The major conclusions reached in this study, after performing the four technical tasks outlined in Table I, are

- The magnitude of the hazard of spacecraft charging to typical space systems is determined by (a) the arc discharge characteristics, (b) the coupling of the discharge with typical spacecraft subsystems, and (c) the vulnerability of the subsystem to the coupled, environmentally induced arc. Although a large body of charging/discharging experimental and analytic data has been obtained, additional data is required to make a quantitative determination of the hazardous effects of spacecraft charging on typical space systems.

TABLE I

WORK PLAN - EFFECTS OF ARCING DUE TO SPACECRAFT CHARGING ON SPACECRAFT SURVIVAL

TASK 1 - ARC DISCHARGE CHARACTERIZATION

TRW SHALL DETERMINE THE THRESHOLDS FOR AND CURRENT-VOLTAGE CHARACTERISTICS OF ARC DISCHARGES ON THERMAL BLANKETS MADE OF FEB TEFLON, KAPTON AND MYLAR, ON SOLAR ARRAYS AND ON OPTICAL SOLAR REFLECTORS (OSR'S) OR SECOND SURFACE MIRRORS.

1.1 TRW SHALL REVIEW EXISTING DATA ON ARC DISCHARGING OF THE ABOVE NAMED SPACECRAFT INSULATORS, AND DETERMINE FROM THIS DATA THE EXPECTED DISCHARGE THRESHOLDS AND CHARACTERISTICS. BEST ESTIMATES AND WORST CASE ESTIMATES SHALL BE DETERMINED.

1.2 TRW SHALL IDENTIFY REQUIREMENTS FOR ADDITIONAL EXPERIMENTS, AND SHALL RECOMMEND EXPERIMENTS NEEDED. THE RECOMMENDATIONS SHALL INCLUDE ADDITIONAL DATA TYPES, ADDITIONAL MATERIALS, IMPROVED MEASUREMENT TECHNIQUES, AND IDENTIFICATION OF SPECIFIC MEASUREMENTS REQUIRED TO DETERMINE THE THRESHOLDS FOR AND CHARACTERISTICS OF ARC DISCHARGES ON SPACECRAFT INSULATORS.

TASK 2 - COUPLING DETERMINATION

TRW SHALL DETERMINE THE COUPLING OF ARC DISCHARGES AND TYPICAL SPACECRAFT SUBSYSTEMS UTILIZING THE COMPUTER PROGRAM SPECIFICATION AND ELECTROMAGNETIC COMPATIBILITY ANALYSIS PROGRAM (SEMCAP), FOR CONFIGURATIONS TYPICAL OF THERMAL BLANKETS SOLAR ARRAY PANELS (3-AXIS STABILIZED CONFIGURATION) AND OPTICAL SOLAR REFLECTORS.

2.1 TRW SHALL MODEL THE ARC DISCHARGE CHARACTERISTICS DETERMINED IN TASK 1 AS VOLTAGE AND CURRENT SOURCES FOR SEMCAP ON THE CONFIGURATIONS IDENTIFIED BELOW. BOTH BEST ESTIMATES AND WORST CASE ESTIMATES OF DISCHARGE CHARACTERISTICS SHALL BE SO MODELED.

2.2 TRW SHALL DETERMINE THE COUPLING BETWEEN ARC DISCHARGES AND SPACECRAFT ELECTRONICS COMPONENTS FOR THE THREE CONFIGURATIONS LISTED BELOW. IN EACH CASE, THE SIZE AND SOLAR ASPECT OF THE CONFIGURATION SHALL BE MODELED APPROPRIATELY TO AN ON ORBIT SPACECRAFT CONFIGURATION.

2.2.1 TRW SHALL DETERMINE THE COUPLING BETWEEN SPACECRAFT ELECTRONICS AND ARC DISCHARGES ON THERMAL BLANKETS MOUNTED ON THE EXTERIOR SURFACE OF THE BODY OF A SPACECRAFT, UTILIZING THE DISCHARGE CURRENT AND VOLTAGE CHARACTERISTICS MODELED IN 1.1 FOR THERMAL BLANKET MATERIALS.

2.2.2 TRW SHALL DETERMINE THE COUPLING BETWEEN SPACECRAFT ELECTRONICS AND ARC DISCHARGES ON OPTICAL SOLAR REFLECTORS MOUNTED ON THE EXTERIOR SURFACE OF THE BODY OF A SPACECRAFT, UTILIZING THE DISCHARGE CURRENT AND VOLTAGE CHARACTERISTICS MODELED IN 1.1 FOR OPTICAL SOLAR REFLECTORS.

2.2.3 TRW SHALL DETERMINE THE COUPLING BETWEEN SPACECRAFT ELECTRONICS AND ARC DISCHARGES ON BOOM-MOUNTED SOLAR ARRAYS ON A THREE-AXIS STABILIZED SPACECRAFT, UTILIZING THE DISCHARGE CURRENT AND VOLTAGE CHARACTERISTICS MODELED IN 1.1 FOR SOLAR ARRAYS.

TASK 3 - THREAT DETERMINATION

TRW SHALL DETERMINE THE SUSCEPTIBILITY OF TYPICAL SPACECRAFT COMPONENTS TO DISRUPTION BY ARC DISCHARGES AND SHALL IDENTIFY POSSIBLE MODES OF ANOMALOUS BEHAVIOR OF OR DAMAGE TO SUCH COMPONENTS. SPACECRAFT COMPONENTS TO BE EVALUATED SHALL INCLUDE, BUT NEED NOT NECESSARILY BE LIMITED TO, COMMAND DECODERS, POWER CONTROL AND DISTRIBUTION UNITS, RECEIVERS AND TRANSMITTERS OF STANDARD DESIGN FOR SPACE APPLICATIONS.

TASK 4 - SPACECRAFT DESIGN PRACTICES REVIEW

TRW SHALL REVIEW SPACECRAFT DESIGN GUIDELINES AND RECOMMENDED PRACTICES DATA AVAILABLE AT TRW'S FACILITY. TRW SHALL SUMMARIZE THIS INFORMATION AND RECOMMEND CHANGES IN DESIGN GUIDELINES AND RECOMMENDED PRACTICES WHICH ARE INDICATED BY THE RESULTS OF TASKS 1 THROUGH 3 ABOVE.

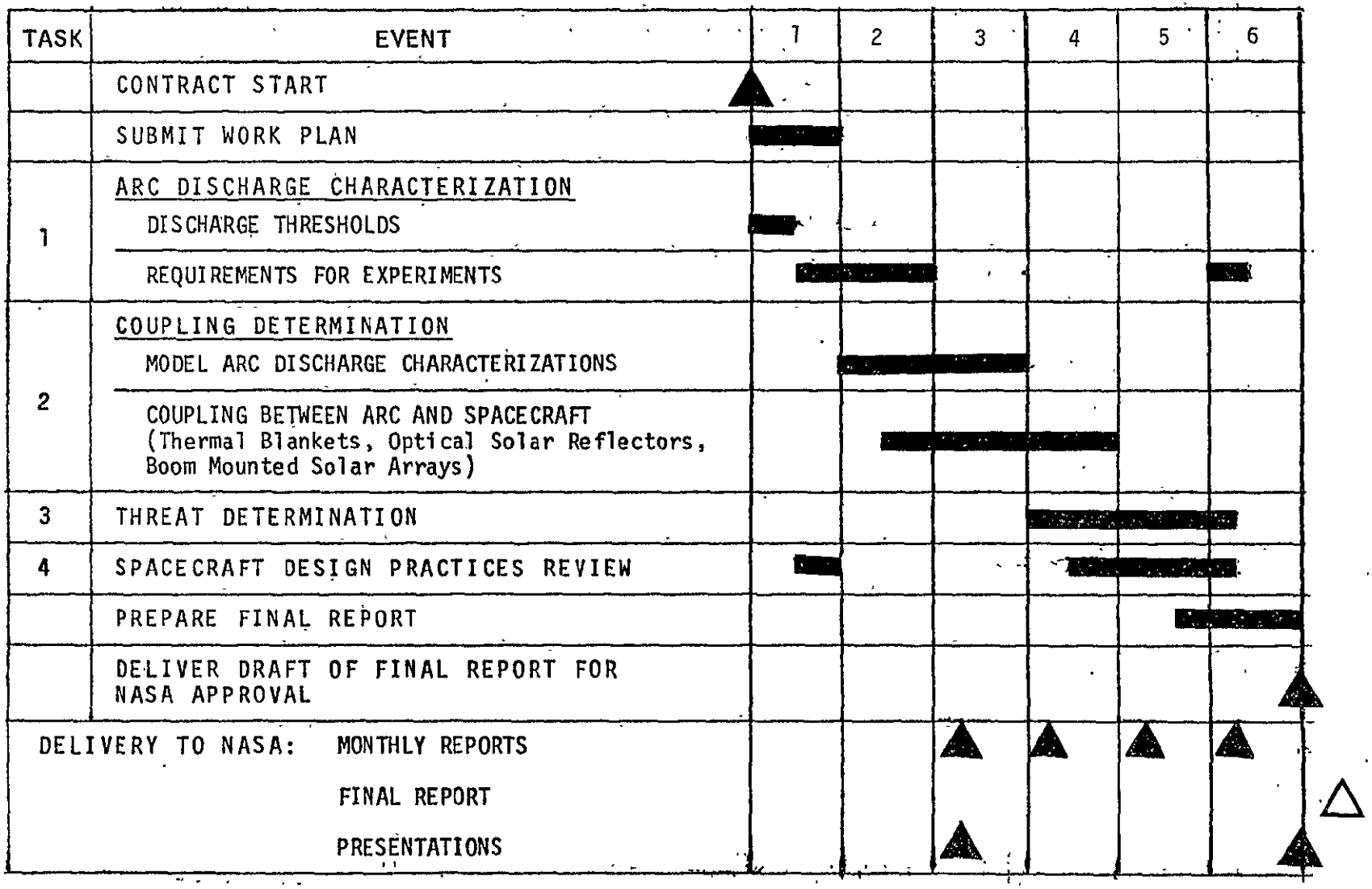

Figure I. Effects of Arcing Study Project Schedule

- If the arc characteristics are well known, then a simple coupling model such as SEMCAP can be used to determine the effects of the arcs on spacecraft subsystems (however spacecraft susceptibility depends strongly on the arc characterization).

- The major problem in determining arc characteristics experimentally is in establishing the fraction of arc current (G´) that goes to space. Where G´ is high, SEMCAP indicates high upset levels. Where G´ is low, SEMCAP indicates a more benign level.

- Design guidelines and recommended practices are developed from studies of charging and discharge models. Most of the general design guides and recommended practices have already been developed. It is important that detailed configuration-specific guidelines be developed for grounding, solar panel design, filtering, shielding, and verification testing.

A brief summary of the results obtained for each of the tasks undertaken in the study is presented in the following sections.

SUMMARY

Task 1.1 - Review of Literature and Characterization of Arcs

A literature review for dielectric arc characterization data for spacecraft material was undertaken (teflon, kapton, mylar, solar array, OSR), and is presented in more detail in Section 1.1 page 8 of this report. Approximately fifty papers were examined including TRW internal documentation. A "first cut" determination of expected discharge thresholds and characteristics was made from these data. In studies of experimental results nominal and worst case results were estimated, results of "similar" experiments were averaged (material, configuration, loading), area effects for discharge pulse peak current were estimated, area effects for discharge pulse width were estimated, effects of stress polarity on solar cell coverglasses were included, and effects of diagnostic loading on discharge pulse peak current and pulse width were examined.

It was concluded that the available arc characterization data cast doubt on the validity of combining results because a) a discharge is a stochastic process, b) very few experiments set out to characterize arcs systematically, c) each experiment usually examines a limited number of parameters, d) experiments were performed on a variety of sample configurations using different techniques and different chargeup conditions, e) descriptions on which results

depend are often incomplete (sample, facility, diagnostic, technique, beam voltage, current, etc.), and f) most area effect data were taken with small samples (electron microscope).

Improvements in experimental techniques and recommendations for more standardized experimental procedures were discussed in order to assure that the results of each experiment can be compared to and correlated with others performed in this field.

Task 1.2 - Identification of Requirements for Additional Experiments

The more detailed identification of requirements for additional experiments are presented in Section 1.2 page 33 of this report.

Key questions to be posed in identifying requirements for additional experiments to characterize arc discharges on spacecraft were: a) Were the test sample configurations representative of those applicable to the real spacecraft? b) What fraction of the arc current went to space? c) Was the environment adequately simulated? d) Were the test diagnostics appropriate to the phenomena involved and did they affect the test results? e) Are the test results valid and useful for spacecraft design and immunity verification procedures?

A phenomenological assessment and evaluation of the experimental data guides in the selection of future experiments and also gives rise to many problem areas: a) Although propagation is an essential element of all models, wave propagation speeds have not been measured directly, but have been inferred from sample size and discharge duration. b) The very high current ($\sim$ 500 A) discharges in the electron swarm tunnel have not yet been demonstrated to be discharges which could occur on spacecraft. c) Transport of electrons in a plasma film has been postulated but has not been experimentally verified. d) The significance of the light emission patterns during surface discharge clean off has not been determined. e) The possible role of surface contaminant gas layers has not been evaluated as a source of the conducting plasma film in the surface plasma conduction model. f) Transient bulk conduction has been postulated but has no direct experimental evidence to support the model. g) Q and I limitations and dependence on area, chargeup voltage, and incident J_E have not yet been rigorously determined.

Task 2.0 - Coupling Determination

The coupling of the arc discharges characterized in Task 1 has been determined utilizing the computer program SEMCAP. A detailed discussion of coupling is presented in Section 2.0 page 53 of this report. The specific spacecraft system considered was the Voyager. The SEMCAP program was used as an analytic tool during I.S.T. of the Voyager spacecraft, and experimental validation of the coupling has been performed.

For the Voyager spacecraft a) 12 arc generators and 77 receptor circuits were identified for SEMCAP, b) arc generators included teflon, kapton, mylar, solar cells, OSR's, and thermal blankets, c) each arc generator was characterized by as many as 12 parameters, and d) the voltages coupled into each of the receptor circuits, for various arc generators with various generator characteristics, were obtained from SEMCAP computer runs.

Task 3.0 - Threat Determination

The threat of circuit upset was assessed by studying circuit sensitivities for receptor circuits and the voltages coupled into the receptor via SEMCAP. A detailed discussion of the threat determination is presented in Section 3.0 page 92 of this report. The negative margins of immunity in each of the Voyager receptors, obtained in Task 2, do not yield a sufficient condition to predict a circuit malfunction. Individual, detailed circuit analysis is required to quantitatively determine circuit susceptibility. In each case, it was clear that an arc to space was more likely to cause circuit malfunctions than flashover or punch-through arcs.

Task 4.0 - Spacecraft Design Practices Review

Design guidelines and recommended practices were reviewed and additional guidelines have been generated as a result of the study. Spacecraft charging countermeasures were reviewed and analyzed. Figure II is a summary of the various countermeasure parameters discussed in this report. A more detailed discussion of design practices and spacecraft charging/arcing countermeasures is presented in Section 4.0 page 103 of this report.

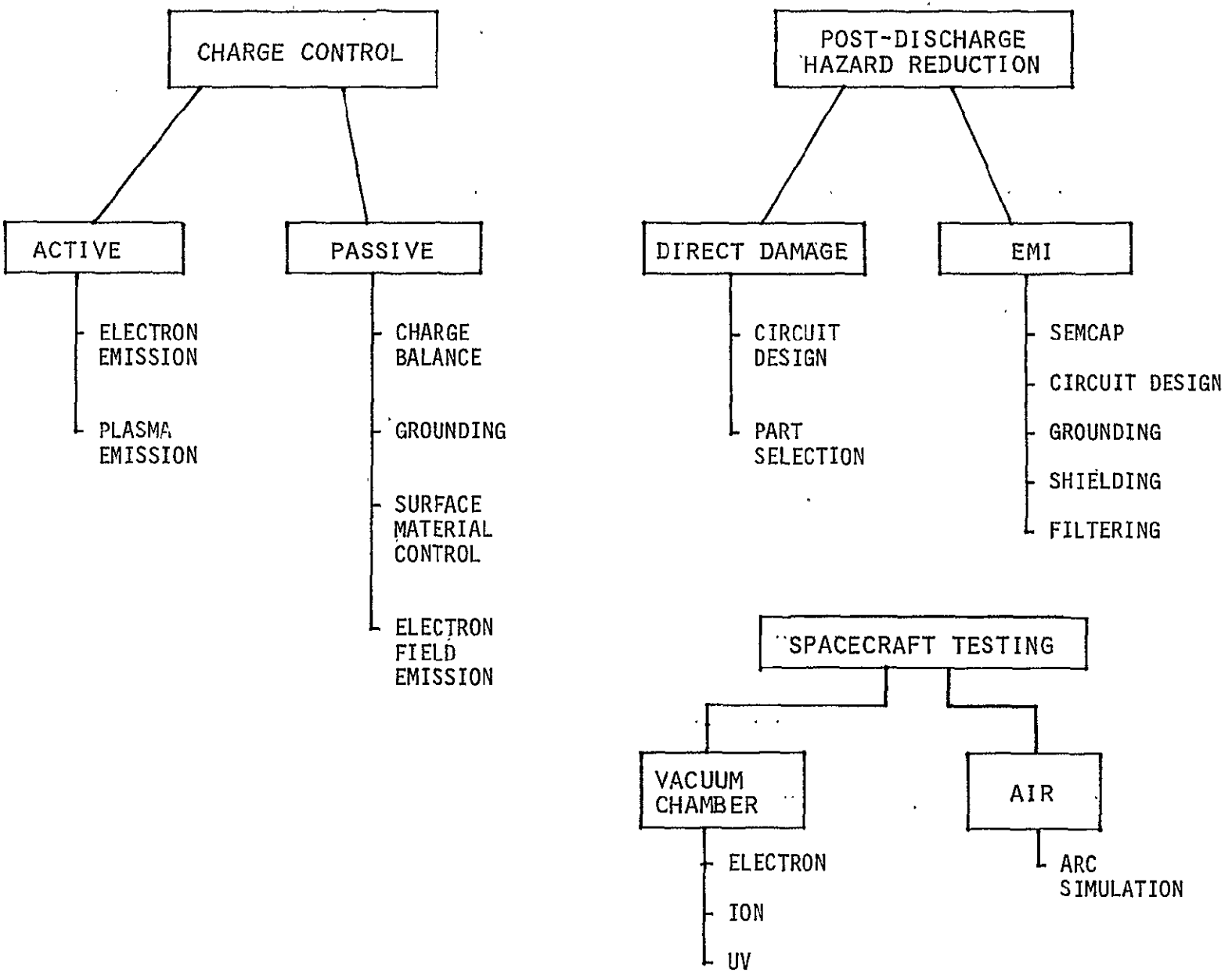
CHARGE CONTROL
ACTIVE
PASSIVE
ELECTRON EMISSION
PLASMA EMISSION
CHARGE BALANCE
GROUNDING
SURFACE MATERIAL CONTROL
ELECTRON FIELD EMISSION
POST-DISCHARGE HAZARD REDUCTION
DIRECT DAMAGE
EMI
CIRCUIT DESIGN
PART SELECTION
SEMCAP
CIRCUIT DESIGN
GROUNDING
SHIELDING
FILTERING
SPACECRAFT TESTING
VACUUM CHAMBER
AIR
ELECTRON
ION
UV
ARC SIMULATION

Figure II.

1. TASK 1 - ARC DISCHARGE CHARACTERIZATION

1.1 TASK 1.1 - ARC CHARACTERIZATION FROM A LITERATURE SURVEY—REVIEW OF EXISTING DATA ON ARC DISCHARGING

1.1.1 Introduction

The characterization of arc discharges resulting from environmental plasma charging is essential for the determining of the possible effects of charging on spacecraft survival.

In the past eight years many laboratory tests have been performed at TRW and other institutions on dielectrics such as FEP Teflon, kapton, and mylar, as well as on solar arrays and second surface mirrors. In Task 1.1 we have reviewed this data in an attempt to define the best- and worst-case estimates of expected discharge characteristics. We have also examined the effect of dielectric "wipe off" (the area effect) on the discharge parameters.

The grounding of isolated metallic spacecraft configurations exposed to the plasma environment is presently being implemented by many spacecraft contractors as a design guideline for the prevention of arcing on synchronous orbit spacecraft. The threat caused by arc discharges from dielectrics exposed to the geosynchronous orbit environment, however, is still not clearly defined. Tests at TRW and other laboratories have shown that a "wipe off", cleaning off of areas as large as 3600 cm^2, could occur in a single dielectric discharge. Complete characterization of discharges from a dielectric must include an examination of the impact of this area effect on the discharge parameters so that one can scale up the parameters obtained on laboratory samples to the actual areas used on spacecraft.

1.1.2 Spacecraft Dielectric Materials

A literature survey was performed with the specific purpose of identifying and describing the discharges that take place in geosynchronous orbit for the following spacecraft materials:

- Teflon
- Kapton
- Mylar
- Solar arrays (substrate and coverslide)
- Second surface mirrors
- Thermal blankets.

These materials were chosen since they are the most commonly used dielectrics on the external surface of a spacecraft and also since a significant amount of laboratory effort has been expended on examining discharges on these materials. All the teflon, kapton and mylar samples discussed in this report had either a thin VDA or a silvered substrate. Two different thermal blanket types were included, mylar and teflon. Furthermore in the review of the arcing of solar arrays, we included arrays using both fused silica and ceria glass coverslides. Arc characterization for two kinds of solar array experiments were considered, e.g., those were the coverslide was irradiated with electrons and those where electrons were deposited on the substrate while the coverslide was exposed to ultraviolet radiation.

1.1.3 Papers Reviewed

Approximately 50 papers were examined including TRW internal documentation for the arc discharge characterization study. Most of these papers did not specifically characterize the discharge which could occur on spacecraft dielectric materials and therefore could not be used in this study. All the contributions to the study came from fourteen different papers, unpublished reports and interoffice correspondence. A list of the references actually used is given in Table 1-1.

Table 1-1. References Used in Report

IN SPACECRAFT CHARGING IN MAGNETOSPHERIC PLASMAS, A. ROSEN, EDITOR, THE MIT PRESS, CAMBRIDGE, MASS

1. ADAMS, R. C. AND NANEVIEZ, J. E. (1975), SPACECRAFT CHARGING STUDIES OF VOLTAGE BREAKDOWN PROCESSES IN SPACECRAFT THERMAL CONTROL MIRRORS.
2. BALMAIN, K.G., ET AL. (1975), SURFACE DISCHARGES IN SPACECRAFT DIELECTRICS IN A SCANNING ELECTRON MICROSCOPE.
3. STEVENS, N. J., ET AL. (1975), SPACECRAFT CHARGING INVESTIGATION FOR THE CTS PROJECT.

IN PROCEEDINGS OF THE SPACECRAFT CHARGING TECHNOLOGY CONFERENCE, C. P. PIKE AND R. R. LOVELL, EDITORS

1. BALMAIN, K. G., (1977), SURFACE MICRODISCHARGES ON SPACECRAFT DIELECTRICS.
2. BOGUS, K. P. (1977), INVESTIGATION OF A CTS SOLAR CELL TEST PATCH UNDER SIMULATED GEOMAGNETIC SUBSTORM CHARGING CONDITIONS.
3. STEVENS, N. J. ET AL. (1977), TESTING OF TYPICAL SPACECRAFT MATERIALS IN A SUBSTORM ENVIRONMENT.

IN PROCEEDINGS OF 1978 SYMPOSIUM ON THE EFFECT OF THE IONSOPHERE ON SPACE AND TERRESTRIAL SYSTEMS

1. BALMAIN, K.G., (1978), CHARGED AREA EFFECTS ON SPACECRAFT DIELECTRIC ARC DISCHARGES.

REPORTS, IOC's, AND UNPUBLISHED PAPERS

BOEING (1977), ELECTROSTATIC CHARGING AND DISCHARGING OF MJS SPACECRAFT PARTS, APRIL 1977.

BALMAIN (1977), CHARGE/DISCHARGE AND ELECTROMAGNETIC RADIATION STUDIES ON SPACECRAFT MATERIALS AND STRUCTURES, APRIL 1977.

BOGUS, K. P. (1978), PRIVATE COMMUNICATION. TO BE PUBLISHED IN PROCEEDINGS OF THE SPACECRAFT MATERIAL CONFERENCE AT TOULOUSE.

TRW (1972), ROSEN, A., FREDRICKS, R., INOUYE, G., SANDERS, N., REPORT ON RGA ANALYSIS: FINDINGS REGARDING CORRELATION OF SATELLITE ANOMALIES WITH MAGNETOSPHERIC SUBSTORMS AND LABORATORY TEST RESULTS, AUGUST 1972.

TRW (1978a), INOUYE, G., AND SELLEN, M., REPORT ON TDRSS SOLAR ARRAY DESIGN GUIDELINES FOR IMMUNITY TO GEOMAGNETIC STORMS.

TRW (1978b), INOUYE, G., ET AL., REPORT ON THERMAL BLANKET ARC DISCHARGES AND METALLIC FILM GROUNDSTRAP DURABILITY

TRW (1978c), SANDERS, N. L., AND INOUYE, G. T., REPORT ON SSM CHARGING TESTS, MAY 1978.

1.1.4 Arc Characterization Parameters

A large number of parameters is required to describe the discharge occurring on spacecraft dielectrics. These can be limited to a relatively few parameters that are applicable to the problem of determining the spacecraft threat resulting from environmental plasma charging. For example, the spectrum of the light emitted during the discharge is required for a complete description of the discharge but can usually be disregarded when evaluating the spacecraft threat. However, the parameters required to describe the arc discharge are not only dependent on the material in which the discharge occurs, but also on the size and configuration of the material and that of neighboring

materials. Furthermore, when these parameters are determined by test, the results obtained are seriously affected not only by the sample configuration but also by the facility used and the test configuration. For example, the voltage at which a sample will breakdown will depend not only on the sample material, size and configuration, but also on test conditions such as the beam voltage, the proximity of the chamber walls, the kinds of diagnostics used and whether the facility was a swarm tunnel or an electron microscope.

The value of the impedance from the sample to ground is also known to affect the experimental determination of arc discharge parameters. Tests performed at TRW (TRW '72a and '78b, Table 1-1) have shown that the peak current obtained in a dielectric discharge pulse from solar cells and teflon samples depends strongly on the load resistor from the sample substrate to ground which serves as a load for the current measurements. These tests were performed in the TRW 2' x 4' vacuum tank using the configuration shown in Figure 1-1. In these tests electrons from a 20 kilovolt electron gun were used to charge up the substrate of a solar array sample. A removable Faraday cup was used to determine the beam current, and removable electrostatic probes, the surface potential. Charging was performed with and without ultraviolet radiation on the coverslides of the solar cells, as shown in the figure. The peak current in the discharge was measured in the following alternative ways:

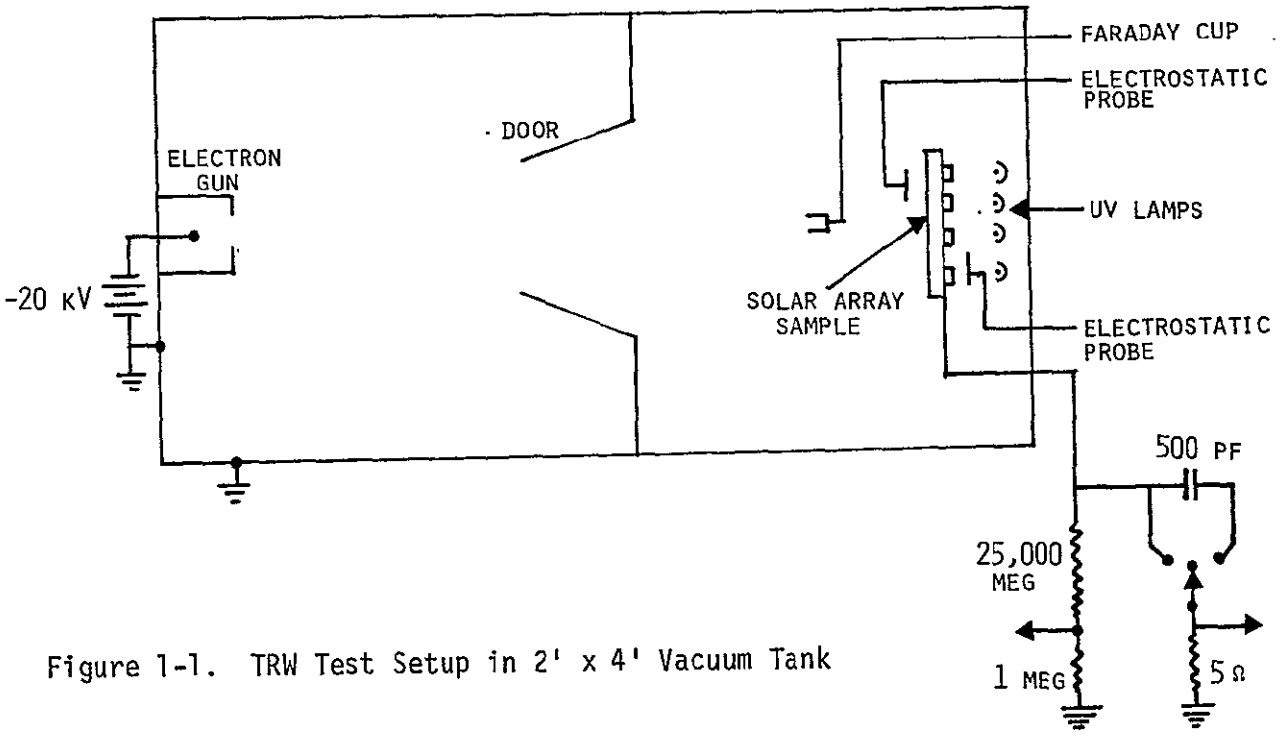

Figure 1-1. TRW Test Setup in 2' x 4' Vacuum Tank

a. Measuring the drop across a one megohm resistor to tank wall ground which was in series with a 25,000 megohm resistor from the sample substrate.

b. Measuring the drop across a 5 ohm resistor from the sample substrate to ground.

c. Measuring the drop across the grounded 5 ohm resistor capacitively coupled to the sample substrates.

The peak discharge currents changed. Similar tests were performed with electrons on the coverglass with substrate loaded to ground and also on a kapton sample with the vacuum deposited aluminum loaded to ground. The results of these tests showing the peak current in the discharge as a function of the load are shown in Figure 1-2. Also shown in the figure is the discharge pulse duration as a function of load resistor. In this case the dependence is not as significant as in the case of the peak current.

A variety of sample load impedances has been used in the arc parameter determination experiments performed to date. Usually the impedance utilized is small (50 Ω or less) and frequently the sample load is not given in the experiment report. Furthermore, little, if any, effort has been expended to determine which load best simulates the space flight condition.

1.1.5 Information Tabulated to Characterize the Arc

In view of the earlier discussion we decided that 16 items of information would be required to characterize the arc for each different dielectric material considered. These are

- Sample Characteristics
  - Material
  - Size
  - Thickness
  - Configuration
  - Load to ground
- Experimental Approach
  - Technique utilized
- Electrical Characteristics
  - Breakdown voltage
  - Beam voltage
  - Beam current
  - Total charge lost
  - Energy in discharge
  - Pulse duration
  - Peak pulse current
  - Charge in pulse
  - Area effect
  - Pulse (EMI) characteristics

Very few of the experiments reported in the literature set out to characterize arcs systematically, but rather each experiment usually examines a limited number of parameters on one or two samples. In reviewing

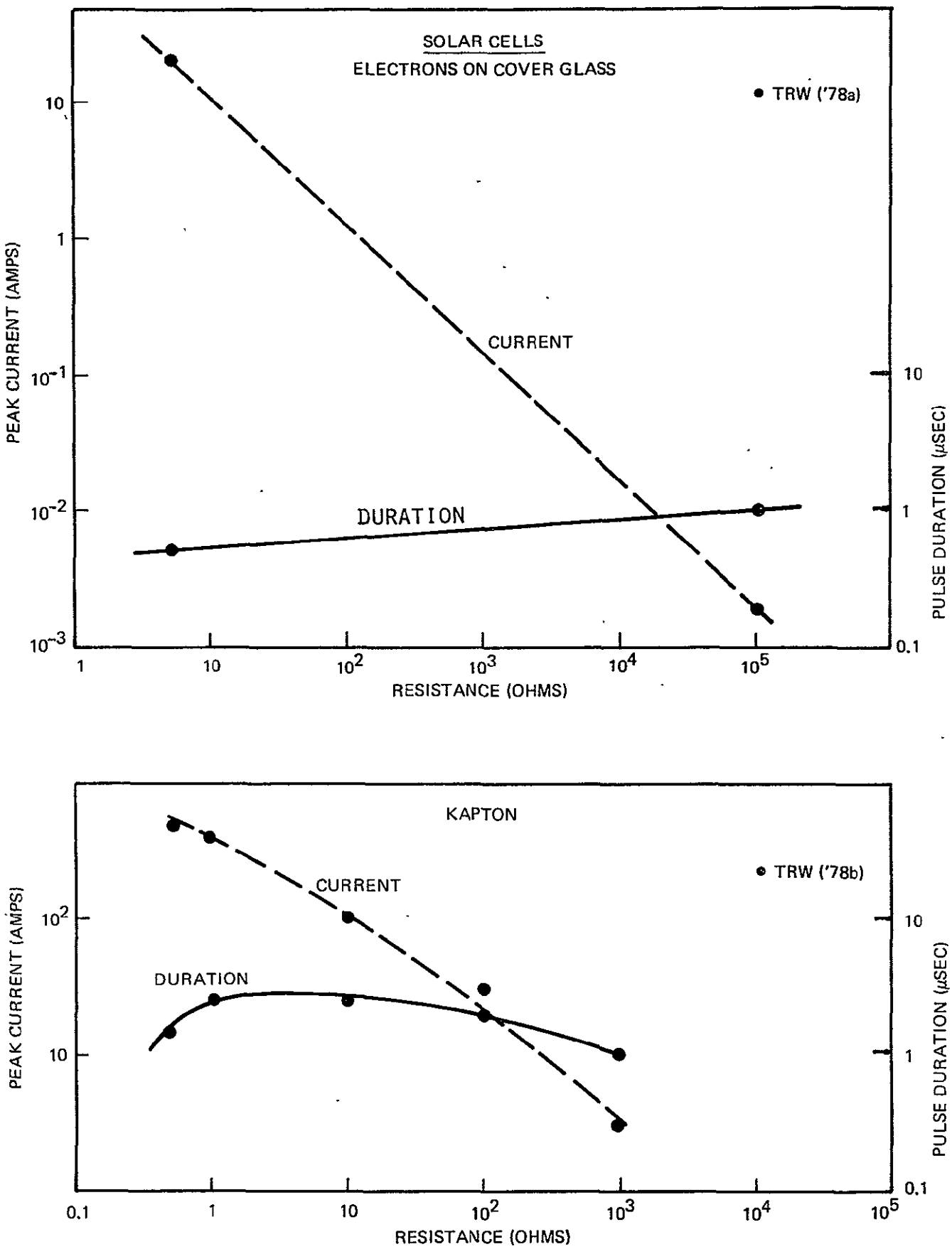

Figure 1-2. Effect of Diagnostic Load Resistor on Arc Pulse Characteristics

the literature one notices that the experiments performed to date are not readily compared or summarized since they have been performed on a variety of sample configurations, using different techniques and different chargeup conditions. In many cases the descriptions of the sample, diagnostic and test configuration, upon which the results depend critically are incomplete.

1.1.6 Information Tabulation

The information obtained in the literature survey is tabulated in Tables 1-2 through 1-9. Each table summarizes the results of experiments performed on each of the spacecraft surface materials listed in Section 1.1.2. Each column in the table corresponds to an individual experiment identified in the column heading by the investigators' name and year of publication for correlation with the references given in Table 1-1. Each row in the table is one of the items of information or arc parameters discussed in Section 1.1.5. Where information is omitted, it was not available or could not be deduced from the published report.

1.1.7 Discussion of Tables

1.1.7.1 Solar Cell Segments. Tables 1-2, -3 and -4 describe a set of experiments performed on solar array segments. Several different types of experiments are included. In the first set of experiments the solar cell coverslide is exposed to electrons in an electron swarm tunnel and the resulting discharge characteristics are observed. In the TRW experiment in this category, the experiment is repeated using different load resistors. In a second set of experiments, electrons were incident on the substrate and ultraviolet radiation on the coverslides. In these experiments none of the arc characteristics except the breakdown voltage was reported. Furthermore, the diagnostics were capacitance coupled to the substrate. In a third set of experiments, the substrate was biased in the vacuum system by a power supply and the coverglass irradiated with ultraviolet radiation. Breakdown occurred at voltages as low as 1 kilovolt but the discharge pulse had a relatively small peak current, i.e., < 0.6 A, demonstrating the "zenering" effect of the cells when exposed to ultraviolet light. In this case, too, the diagnostics were capacitively loaded. Another experiment included was an old experiment performed at TRW to determine a solar array segment breakdown voltage in air. Aluminum plates were placed across the array and the power supply voltage raised until breakdown occurred.

Table 1-2. Solar Cells

	STEVENS ('77)	TRW ('78a)	TRW ('78a)	TRW ('78a)	TRW ('78a)	TRW ('78a)
1. SUBSTRATE	KAPTON ON FIBERGLASS ON METAL GROUND PLATE	LIGHTWEIGHT INSULATOR	LIGHTWEIGHT INSULATOR	METALLIC	PERFORATED KAPTON	CONDUCTIVE COATED PERFORATED KAPTON
2. COVERGLASS MATERIAL	FUSED SILICA	CERIA GLASS	CERIA GLASS	FUSED SILICA	CERIA GLASS	CERIA GLASS
3. COVERGLASS THICKNESS	12 mils			12 mils	12 mils	12 mils
4. CELL THICKNESS	10 mils			10 mils	10 mils	10 mils
5. SAMPLE SIZE	96 cm^2	18.5 x 23 cm	18.5 x 23 cm	28.6 x 35.6 cm	18.5 x 23 cm	18.5 x 23 cm
6. CONFIGURATION	24, 2 x 2 cm CELLS	12, 2 x 4 cm CELLS	12, 2 x 4 cm CELLS	48, 2 x 4 cm CELLS	20 CELLS	20 CELLS
7. TECHNIQUE	e^- ON COVERGLASS	e^- ON COVER-GLASS	e^- ON COVER GLASS	UV ON COVERGLASS e^- ON SUBSTRATE	UV ON COVERGLASS e^- ON SUBSTRATE	UV ON COVERGLASS e^- ON SUBSTRATE
8. BEAM VOLTAGE AT BREAKDOWN	14 kV	20 kV*	20 kV*	16 kV. ONLY WITH UV OFF	15 kV. UV ON AND OFF	15 kV. UV OFF
9. BEAM CURRENT DENSITY	10 na/cm^2	10 na/cm^2	10 na/cm^2	10 na/cm^2	10 na/cm^2	
10. LOAD TO GROUND FROM METALLIC PORTION OF CELLS	FEW OHMS	R = 5 Ω	R = 100 kΩ	R = 2.5 x 10^{10} Ω. C COUPLED TO DIAGNOSTICS.	R = 2.5 x 10^{10} Ω. C COUPLED TO DIAGNOSTICS.	R = 2.5 x 10^{10} Ω. C COUPLED TO DIAGNOSTICS.
11. BREAKDOWN VOLTAGE	8.1 to 9.4 kV					
12. PEAK PULSE CURRENT		20 A	20 mA			
13. PULSE EMI CHARACTERISTICS						
14. PULSE DURATION		0.5 μS	1 μS			
15. ENERGY IN DISCHARGE	25 to 62 mJ					
16. TOTAL CHARGE LOST	4 - 12 μC					
17. CHARGE IN PULSE						

*NO BREAKDOWN AT 10 kV.

Table 1-3. Solar Cells

	TRW ('78a)	TRW ('78a)	TRW ('78a)	TRW ('78a)	TRW ('78a)	TRW ('78a)	TRW ('72)
1. SUBSTRATE	← CONDUCTIVE COATED PERFORATED KAPTON →						
2. COVERGLASS MATERIAL	← CERIA GLASS →						
3. COVERGLASS THICKNESS	← 12 mils →						
4. CELL THICKNESS	← 10 mils →						
5. SAMPLE SIZE	← 18.5 x 23 cm →						
6. CONFIGURATION	← 20 CELLS (2 cm x 4 cm) →						
7. TECHNIQUE	← UV ON COVERGLASS. POWER SUPPLY BIASED SUBSTRATE →						POWER SUPPLY AND TERMINALS IN AIR
8 BEAM VOLTAGE AT BREAKDOWN							
9. BEAM CURRENT							
10. LOAD TO GROUND FROM METALLIC PORTION OF CELLS	← 2.5×10^{10} Ω, CAPACITANCE COUPLED TO DIAGNOSTICS →						
11. BREAKDOWN VOLTAGE	1.75 kV	2.0 kV	2.5 kV	5.0 kV	10.0 kV	15 kV	7 kV
	← BREAKDOWN OCCURS FOR V ≥ 1 KILOVOLT →						
12. PEAK PULSE CURRENT	0 6 A	0.8 A	0.9 A	1.6 A	2.8 A	3.6 A	
13. PULSE EMI CHARACTERISTICS							
14. PULSE DURATION	2 μS	2 μS	2 μS	2 μS	2 μS	2 μS	
15. ENERGY IN DISCHARGE							
16 TOTAL CHARGE LOST							
17 CHARGE IN PULSE							

Table 1-4. Kapton Solar Cell Substrate

	STEVENS('77)	BOGUS('77)	BOGUS('78)	BOGUS('78)
1. SAMPLE SIZE	180 cm^2		180 cm^2	3600 cm^2
2. COVERGLASS MATERIAL	CERIA GLASS	CERIA GLASS	CERIA GLASS	CERIA GLASS
3. COVERGLASS THICKNESS	4 mils	4 mils	4 mils	4 mils
4. CELL THICKNESS	8 mils	8 mils	8 mils	8 mils
5. SUBSTRATE THICKNESS	← 25 μ KAPTON ON 35 μ GLASS FIBER →			
6. CONFIGURATION	27, 2 cm x 2 cm CELLS	3 CELLS x 9 CELLS	3 CELLS x 9 CELLS	
7. TECHNIQUE	THERMAL LAMP ON CELLS. e^- ON SUBSTRATE	UV ON CELLS. e^- ON SUBSTRATE	UV ON CELLS. e^- ON SUBSTRATE	UV ON CELLS. e^- ON SUBSTRATE
8. LOAD TO GROUND		2 KΩ		
9. BEAM VOLTAGE AT BREAKDOWN	∿ 10 kV	>15 kV	> 15 kV	> 15 kV
10. BEAM CURRENT	10 na/cm^2	60 na/cm^2		
11. BREAKDOWN VOLTAGE	8-9 kV WITH LAMPS OFF	∿ 15 kV		
12. PEAK PULSE CURRENT			30 - 40 A	200 to 300 A
13. PULSE (EMI) CHARACTERISTICS				
14. PULSE DURATION		3 - 5 μS	0.5 TO 0.75 μS	1.5 TO 1.75 μS
15. ENERGY IN DISCHARGE		100 mJ	0.25 J	5 J
16. TOTAL CHARGE LOST		60 μC		
17. CHARGE IN PULSE		13 μC	20 - 30 μC	400 to 600 μC
18. AREA EFFECT			$I = 1.2\ A^{.65}$	$I = 1.2\ A^{.65}$

A different kind of solar cell test is summarized in Table 1-4. In these experiments the substrate was irradiated with electrons and the coverslides were irradiated with ultraviolet, but in contrast to the UV experiment discussed in the last paragraph, the ultraviolet lamps served primarily as a thermal source so that thermal effects rather than photoemission effects were studied. This test was primarily a test of the arc discharge on the kapton substrate.

No experimenter studied the effect of increasing the area of the solar cell coverglass on the pulse characteristics. The effect of increasing the area was studied by Bogus ('78) as shown in Table 1-4, but as we discussed in the previous paragraph this test demonstrated the area effect for a kapton substrate and not the solar cell coverglass. We have generated the expression for the current in the case of the kapton substrate by using the data from Bogus ('78). The resulting expression is listed in Table 1-4 under Bogus ('78). In this expression I is in amperes and A in cm^2.

Furthermore, no measurements were made in any of the solar cell experiments of the radiated electromagnetic energy emitted during the discharge, i.e., the pulse EMI characteristics, and thus these entries are left blank.

1.1.7.2 Thermal Blankets. The experiments on thermal blankets consist of electron-gun irradiations of thermal blankets with both sewn and open edges as well as an experiment using a high voltage power supply with aluminum plates across a mylar thermal blanket sample. The available results and information are shown in Table 1-5. In the case of this TRW ('72) experiment performed in a bell jar, both $\dot{E}$ and $\dot{B}$ were measured during the discharge at distance of 50 and 100 cm from the discharge. In none of the experiments on thermal blankets was the effect of varying the blanket areas examined.

1.1.7.3 Teflon, Kapton and Mylar with VDA or Silvered Backing. Numerous experiments have been performed on thin layers of dielectric (teflon, kapton or mylar) with one side covered with VDA or silvered. The parameters and information obtained from these experiments are tabulated in Tables 1-6, -7 and -8.

Three types of facilities have been used for these experiments, electron swarm tunnels (electron guns), scanning electron microscopes and

Table 1-5. Thermal Blankets

	STEVENS ('77)	STEVENS('77)	TRW ('72)
1. SAMPLE SIZE			20 cm x 20 cm
2. SAMPLE MATERIAL	Kapton	Kapton	Mylar
3. THICKNESS	5 mil	5 mil	10 Layers
4. CONFIGURATION	Sewn Edge	Open Edge	Open Edge
5. TECHNIQUE	Electron Swarm Tunnel (EST)	EST	Power supply - Terminals
6. BEAM VOLTAGE AT BREAKDOWN	∿ 10 kV		
7. BEAM CURRENT	1 na/cm^2	1 na/cm^2	
8. LOAD TO GROUND	Few ohms	Few ohms	
9. BREAKDOWN VOLTAGE	10.4 kV	16.5 kV	5 kV
10. PEAK PULSE CURRENT			
11. PULSE (EMI) CHARACTERISTICS			Measure E and B. Rise time 15 ns each. E = 700 V/m at 50 cm, 250 V/m at 100 cm. B = < .02 γ for distances greater than 50 cm.
12. PULSE DURATION			
13. ENERGY IN DISCHARGE	0.3 to 0.7 J	2J	
14. TOTAL CHARGE LOST	50-90 μC	200 μC	
15. CHARGE IN PULSE			
16. AREA EFFECT			

Table 1-6. Teflon (VDA or Silvered)

	TRW('72)	STEVENS('75)	BALMAIN('77)	STEVENS('77)	BOEING('77)	BALMAIN('78)	BALMAIN('78)
1. SAMPLE SIZE	20 cm x 20 cm	15 x 20 cm	1 x 1 cm*	15 x 20 cm	3.8 cm dia.	10 cm^2	4.5×10^{-4} cm^2**
2. THICKNESS	5 mils	5 mils	20 mils	5 mils	5 mils	4 mils	4 - 32 mils
3. CONFIGURATION							
4. TECHNIQUE	POWER SUPPLY AND TERMINALS	ELECTRON SWARM TUNNEL (EST)	SCANNING ELECTRON MICROSCOPE (SEM)	EST	EST	EST	SEM
5. BEAM VOLTAGE AT BREAKDOWN		> 10 kV	18 kV	> 12 kV		20 kV	15 - 30 kV
6. BEAM CURRENT		1 and 10 na/cm^2		1 na/cm^2		1-2 $\mu A/cm^2$	
7. LOAD TO GROUND FROM METALLIC BACK		FEW OHMS	12.5 Ω	FEW OHMS	FEW OHMS	12.5 Ω	12.5 Ω
8. BREAKDOWN VOLTAGE	4 kV			12 kV ± 1.5 kV			
9. PEAK PULSE CURRENT			100 mA	20 - 100 A	10 - 250 A	20 A	25 - 150 ma
10. PULSE (EMI) CHARACTERISTICS			SPECTRUM † FLAT TO 100 MHz 40 db/ DECADE DROPOFF		NEAR FIELD ANTENNA - 0.5 to 3 V		
11. PULSE DURATION		200-300 nsec	2 - 3 nsec	500 nsec	20-300 nsec	125 nsec	1.2 - 22 nsec
12. ENERGY IN DISCHARGE				150 to 400 mJ			
13. TOTAL CHARGE LOST				20 - 60 μC			
14. CHARGE IN PULSE				15 μC			
15. AREA EFFECT							$I=7A^{0.575}$ Amps †† (A in cm^2)

*EFFECTIVE AREA 10^{-5} cm^2
**EFFECTIVE AREA
†BALMAIN ('75)
††EFFECTIVE AREAS FROM 10^{-5} TO 20 cm^2

Table 1-7. Kapton (Silvered or VDA)

	BALMIAN ('75 & '77)	BALMAIN ('78)	TRW('78b)	TRW('78b)	TRW('78b)	TRW('78b)	TRW('78b)	TRW('78b)	TRW('78b)
1. SAMPLE SIZE	10^{-5} * cm^2	5 x 5 cm	14x28 cm	12x12 cm	8 x 8 cm	14x28 cm	14x28 cm	14x28 cm	14x28 cm
2. THICKNESS	4 - 20 mils		2 mils	2 mils	2 mils	2 mils	2 mils	2 mils	2 mils
3. CONFIGURATION			EDGE FOLDED OVER METAL PLATE	EDGE FOLDED OVER METAL PLATE	EDGE FOLDED OVER METAL PLATE (GUARD RING)	EDGE FOLDED OVER METAL PLATE	EDGE FOLDED OVER METAL PLATE	EDGE FOLDED OVER METAL PLATE	EDGE FOLDED OVER METAL PLATE
4. TECHNIQUE	SCANNING ELECTRON MICROSCOPE (SEM)MICRO-DISCHARGE	SEM MACRO-DISCHARGE	ELECTRON SWARM TUNNEL (EST)	EST	EST	EST	EST	EST	EST
5. BEAM VOLTAGE AT BREAKDOWN	16 - 18 kV	20 kV	20 KV	20 kV	20 kV	20 kV	20 kV	20 kV	20 kV
6. BEAM CURRENT	10 na/cm^2	1-2 $\mu A/cm^2$	10 na/cm^2	10 na/cm^2	10 na/cm^2	10 na/cm^2	10 na/cm^2	10 na/cm^2	10 na/cm^2
7. LOAD TO GROUND FROM METALLIC BACK	FEW OHMS	FEW OHMS	0.5 OHMS	0.5 OHMS	0.5 OHMS	1 OHM	10 OHMS	100 OHMS	1000 OHMS
8. BREAKDOWN VOLTAGE									
9. PEAK PULSE CURRENT	100 mA**	9 A	500 A 720 A***	100 A	12 A	400 A	100 A	30 A	3 A
10. PULSE (EMI) CHARACTER-ISTICS	FLAT TO 100 MHz 40 db/DECADE DROPOFF								
11. PULSE DURATION	5 - 10 ns**	200 ns	1.5 μs 0.75 μs***	1 μs	0.5 μs	2.5 μs	2.5 μs	2 μs	1 μs
12. ENERGY IN DISCHARGE									
13. TOTAL CHARGE LOST									
14. CHARGE IN PULSE									
15. AREA EFFECT									

*EFFECTIVE AREA

**BALMAIN '77

***CURRENT AND DURATION CHANGED WHEN CONNECTIONS BROUGHT OUT WITH COPPER BARS $\sim$ 1/2" DIAMETER

Table 1-8. Mylar (VDA)

	BALMAIN('77)	BALMAIN ('78)	BALMAIN ('78)
1. SAMPLE SIZE	2.6 x 4.8 cm	10 cm^2	4.5×10^{-4} cm^2*
2. THICKNESS	5 mils	4 mils	4 mils
3. CONFIGURATION			
4. TECHNIQUE	SCANNING ELECTRON MICROSCOPE (SEM)	SEM	SEM
5. BEAM VOLTAGE AT BREAKDOWN	20 kV	20 kV	20, 25, 30 kV
6. BEAM CURRENT	50 na/cm^2	1-2 $\mu A/cm^2$	1-2 $\mu A/cm^2$
7. LOAD TO GROUND	12.5 Ω	12.5 Ω	12.5 Ω
8. BREAKDOWN VOLTAGE			
9. PEAK PULSE CURRENT	40 A	100 A	0.22 - .35 A
10. PULSE EMI CHARACTERISTICS			
11. PULSE DURATION	80 - 150 ns	20 - 50 ns	1.2 - 1.3 ns
12. ENERGY IN DISCHARGE	2 mJ		
13. TOTAL CHARGE LOST			
14. CHARGE IN PULSE			
15. AREA EFFECT		$I = 17.2\ A^{.764}$ amps** (A in cm^2)	

* EFFECTIVE IRRADIATED AREA

** EFFECTIVE AREAS FROM 5×10^{-5} cm^2 TO 20 cm^2

power supply applied voltages. Almost all of the parameters required have been examined by at least one investigator, but because of the different facilities, test configuration and sample configurations used, the validity of combining the results of the different experiments is questionable. In many of the experiments the sample configuration is not even specified.

Balmain ('78) has performed detailed area effect studies on these materials using an electron microscope as an electron source. This approach, however, limits the areas covered by electrons to values from about 10^{-5} cm^2 to 20 cm^2. The relationships between current and area resulting from these efforts are given in the tables.

Furthermore, TRW ('78b) has examined the effect of varying diagnostic load resistances on the peak discharge pulse current and pulse duration for a thin kapton sample. The information and data resulting from this experiment are also included in Table 1-7.

1.1.7.4 Second Surface Mirrors (SSM)

Two different experiments on the arc discharging of quartz window second surface mirrors are summarized in Table 1-9. In the first experiment (Adamo '75), the sample is irradiated with an electron gun in a bell jar and the arc effluents measured. In this experiment the electric field of the discharge pulse is recorded by a dipole placed three inches from the sample.

In the second experiment the mirror is irradiated by an electron gun in a 2' x 4' vacuum chamber and the current resulting from the discharge is recorded by means of a 1Ω load resistor from an aluminum substrate to ground.

Neither experiment yields sufficient information to examine any area effect that would permit scaling of the experiment results to spacecraft SSM array dimensions.

Table 1-9. Second Surface Mirrors

	ADAMO ('75)	TRW ('78c)
1. SAMPLE SIZE	1 in^2 MIRRORS	15 cm x 2.5 cm
2. THICKNESS		8 mil SSM'S
3. CONFIGURATION	SSM'S ON METAL SUBSTRATE	QUARTZ SSM'S ON ALUMINUM PLATE
4. TECHNIQUE	ELECTRON GUN. MEASURED ARC EFFLUENTS	EST
5. BEAM VOLTAGE AT BREAKDOWN	10 kV	20 kV
6. BEAM CURRENT	1 na/cm^2	10 na/cm^2
7. LOAD TO GROUND	FEW OHMS	R = 1 Ω
8. BREAKDOWN VOLTAGE	2 - 3 kV	11 kV
9. PEAK PULSE CURRENT		40 A
10. PULSE EMI CHARACTERISTICS	MEASURED E AT 3" (DIPOLE) RISETIME - 5 μS DURATION - 3 μS 60 mA PEAK	
11. PULSE DURATION		300 nsec
12. ENERGY IN DISCHARGE		
13. TOTAL CHARGE LOST		
14. CHARGE IN PULSE		
15. AREA EFFECT		

1.1.8 Experiment Result Analysis

In this section we attempt to meet the objective of the task, i.e., to obtain best-and worst-case estimates from the data obtained in the literature survey.

As discussed in Section 1.1.5, the non-uniformity in facilities, test configurations, techniques, sample sizes and configurations, sample history and parameters measured in each experiment results in a large number of independent measurements of discharge parameters in dielectrics which cannot be readily combined.

In order to obtain results as required by this task, we have taken liberties to combine and average the results of experiments that were similar in a gross sense even though we were aware of some differences. We combined the results of experiments that used similar materials even though the material thickness varied from experiment to experiment. For example, kapton sample thickness varied from 4 to 32 mils. Actually, in many cases, thicknesses were not even given. Experiment results were put together in spite of the difference in facilities used. We did, however, separate experiments that used obviously different test and sample configurations such as edges turned under a metal plate (see Section 1.1.8.1.1) rather than open edges or experiments that used large substrate to ground load resistances for diagnostics rather than the more commonly used low resistance (see Section 1.1.4). In this regard we have examined the effect of the load resistance on both the peak discharge pulse current and the discharge pulse width (see Fig. 1-2) for both kapton and solar arrays. Furthermore, we separated parameter results for each material by sample area and, where the data was available, determined an area effect for both the peak discharge current and the discharge pulse width.

1.1.8.1 Area Effect

Balmain (Balmain '78) has shown that peak discharge current of spacecraft dielectric materials apparently increases with sample area and the increase over the range of sample areas that he investigated fit reasonably well to a power law. In order to permit scaling up of the data given in the tables to spacecraft areas, we have fit the peak discharge peak current vs area, and discharge pulse width vs area data, with power law curves.

Sufficient data for this effort were available only in the cases of kapton, mylar and teflon samples, i.e., Tables 1-6, -7 and -8.

1.1.8.1.1 The Effect of Area on Peak Discharge Current for Teflon

The peak discharge current from the experiment results summarized in Table 1-7 is plotted versus the area of the sample and shown in Fig. 1-3. The best-fit power law to all the data is given by $I = 9.9A^{0.43}$ amps where A is in cm^2. The scatter in the data points in Fig. 1-3 is significantly reduced if one ignores a set of data points taken on a special configuration sample at TRW. In this sample, the kapton is wrapped around a plastic frame, so that no edges are exposed. A second small piece of kapton with exposed edges is mounted nearby to act as a trigger for the discharge. The configuration is shown in Fig. 1-4. Experiments with this kind of sample configuration have produced peak discharge currents of over 700 amperes for areas of approximately 400 cm^2. We have therefore used as a worst case fit to the data for large areas the power law fit to the folded-over sample configuration data. In this case, $I = 0.002\ A^{2.1}$ amps. This is a good example of the effect of sample configuration on the arc discharge parameters.

Notice that in the curves of Fig. 1-3, the current in both the best-fit and worst-case-fit increases with area with no apparent limit. This is typical for all the materials examined as will be seen later in this section. If limitations do exist to the area that contributes to the current in a dielectric "wipe off", results of tests on samples of sufficient area to demonstrate those limits have yet to be reported.

1.1.8.1.2 Teflon and Mylar Peak Discharge Current

The relationships between the sample area and the discharge pulse peak current for teflon and mylar were derived directly from the work of Balmain ('78) and are shown in Fig. 1-5. The solid data points are the actual data points taken by Balmain, who also derived the best fit value of the slopes. We have derived the power law expressions that fit those curves using the Balmain slopes and also made an estimate of the worst case fit to the data. We have also shown on the curves the data points for other "similar" experiments from Tables 1-6 and 1-8.

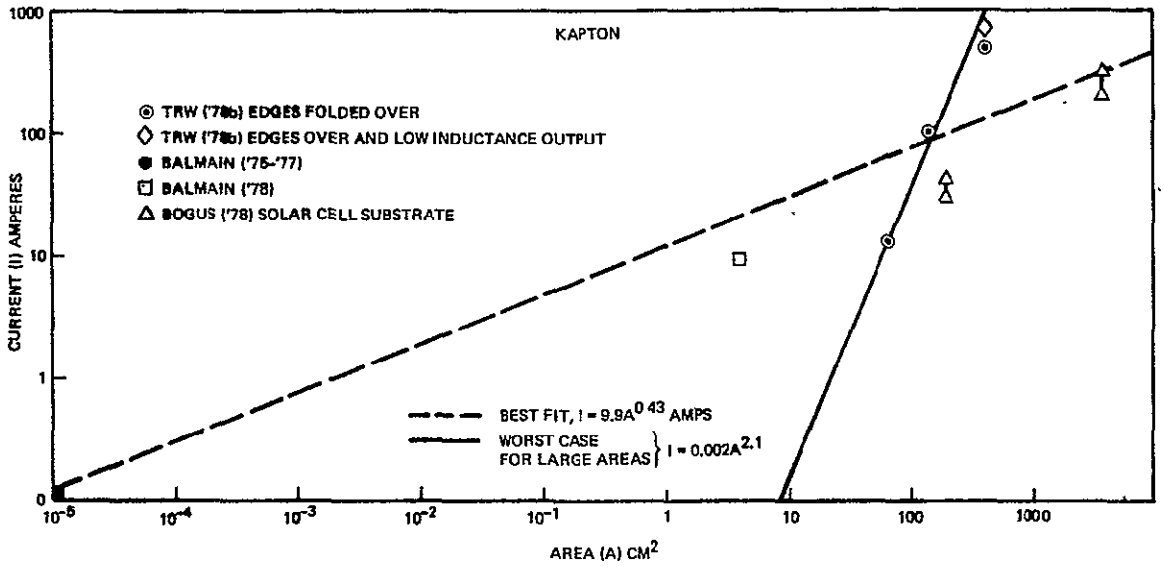

Figure 1-3. Discharge Peak Current-Area Effect

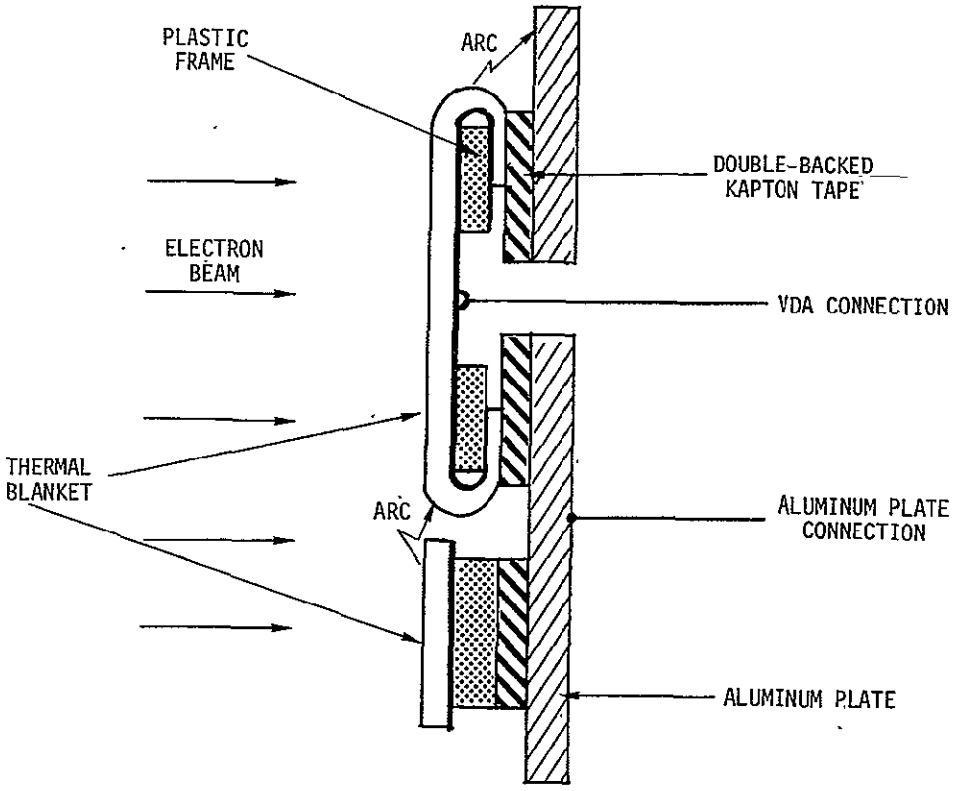

Figure 1-4. Test Sample Configuration

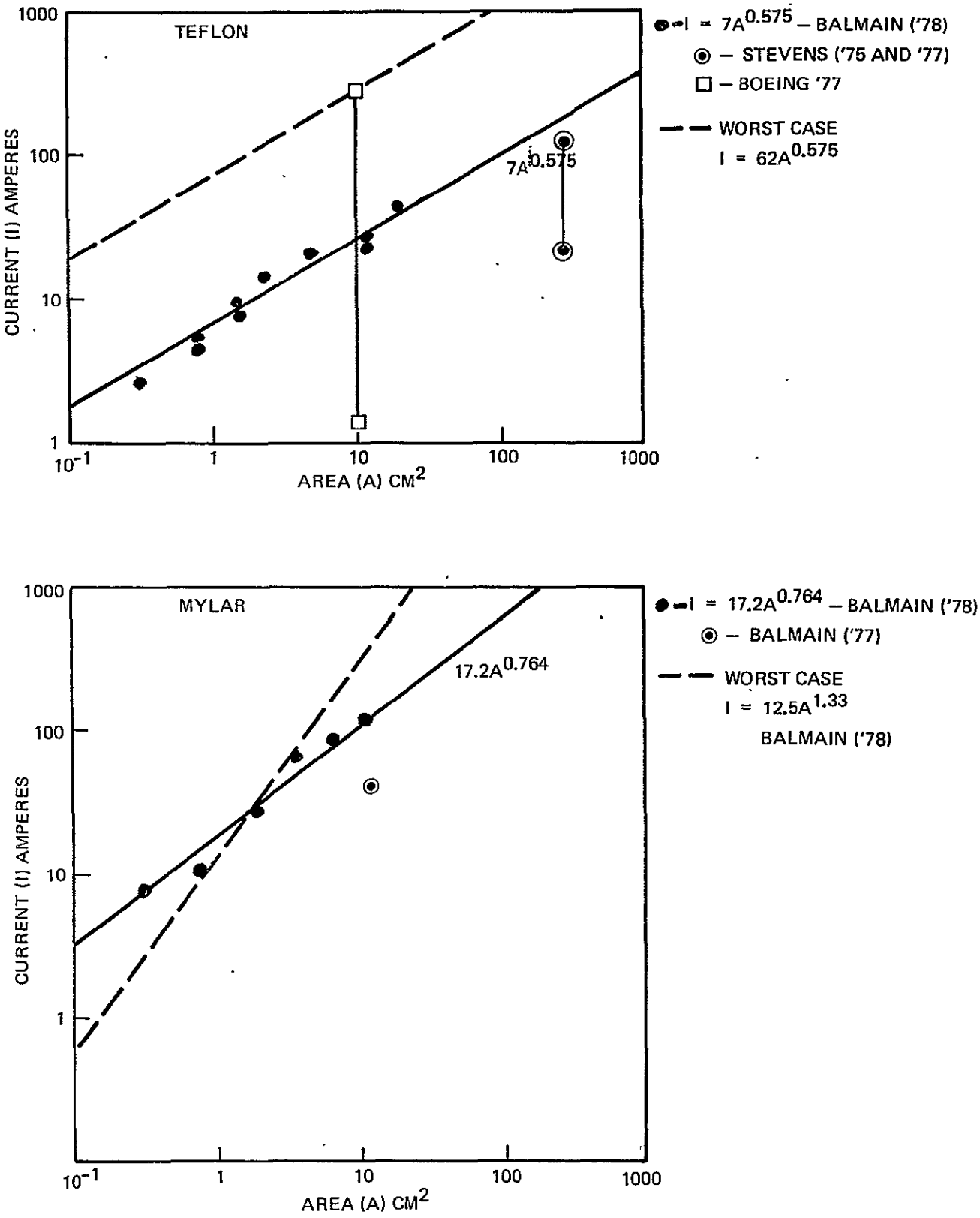

Figure 1-5. Discharge Peak Current-Area Effect

1.1.8.1.3 Area Dependence of Discharge Pulse-Width

As part of Task 1.1, we have made an estimate of the best fit and worst case fit to the area dependence of the discharge pulse width. As in the case of the current-area effect, we have assumed that the data can be fit by a power law curve, and once again only sufficient data were available for teflon, kapton and mylar samples. The results are shown in Figures 1-6, -7 and -8.

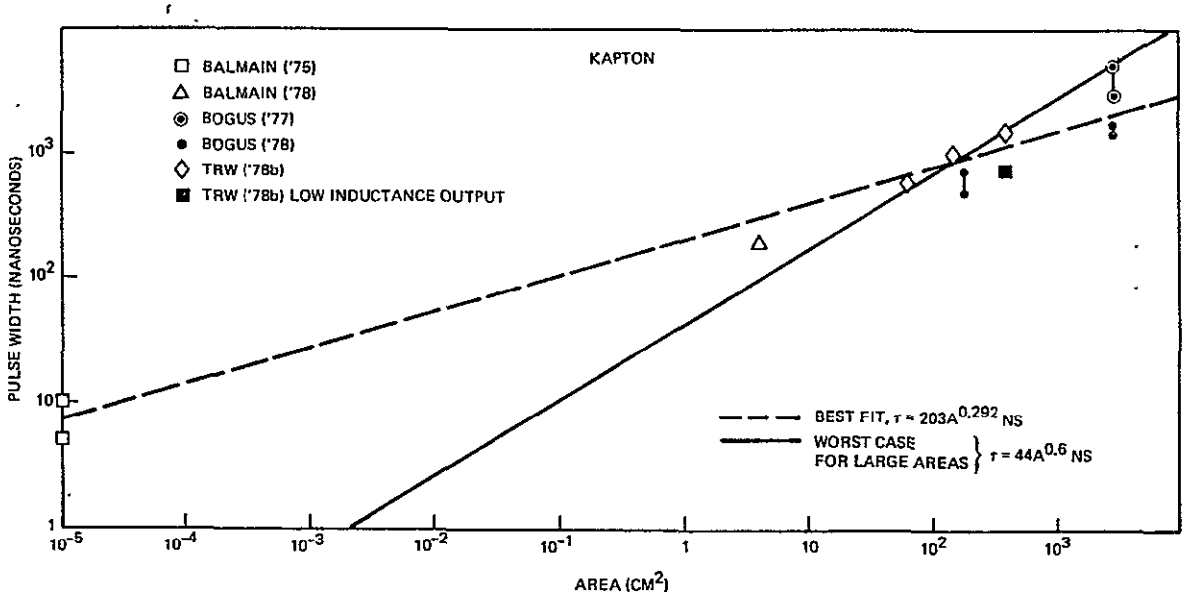

Figure 1-6. Area Dependence of Discharge Pulse-Width

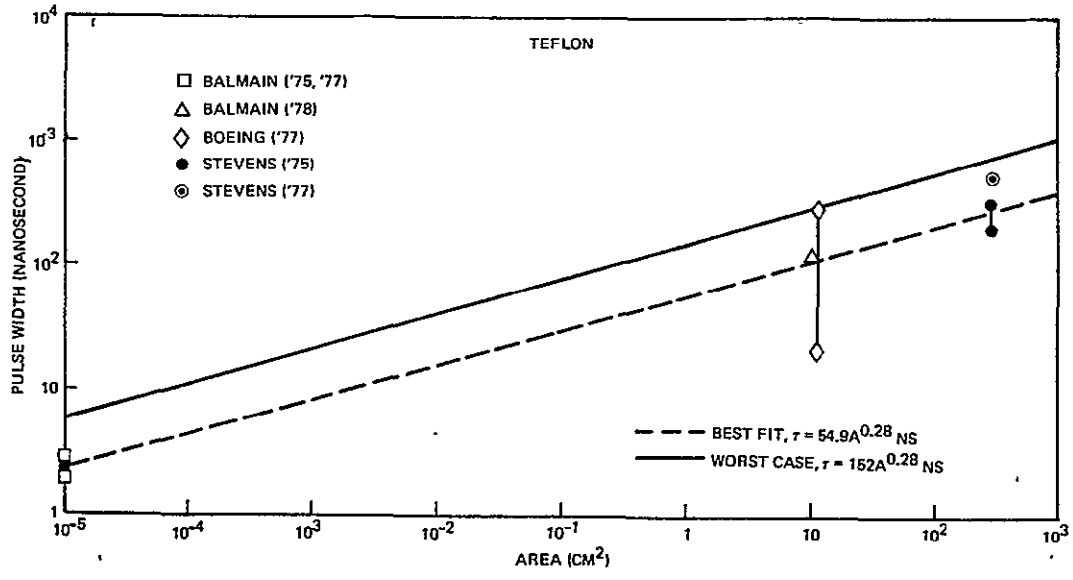

Figure 1-7. Area Dependence of Discharge Pulse-Width

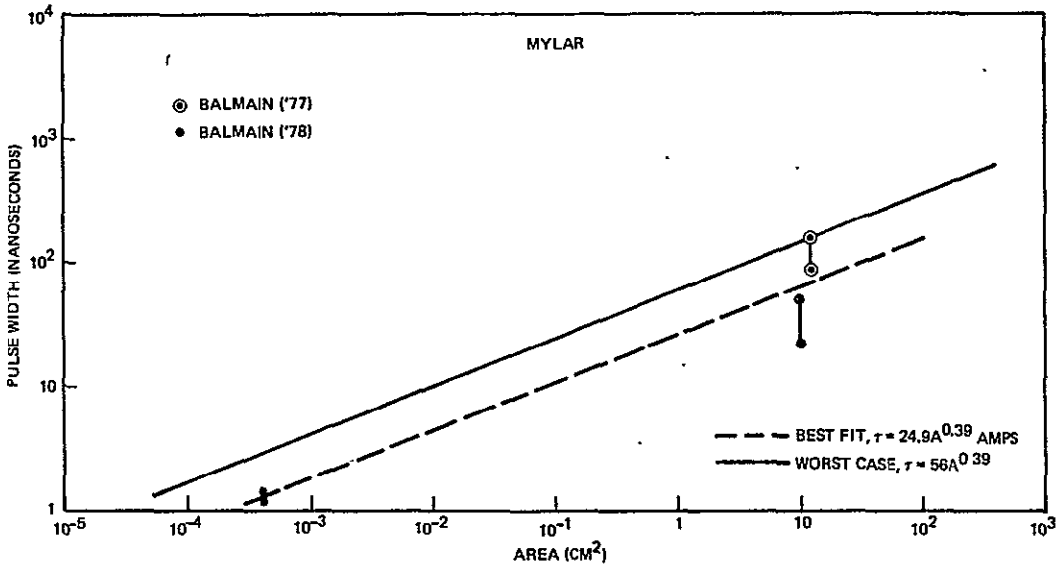

Figure 1-8. Area Dependence of Discharge Pulse-Width

1.1.8.1.4 Estimated Charge-Area Effect

The charge measured during the discharge is given by

$$Q = \int I \, dt, \text{ where}$$

I is the discharge current and the integral is over the duration of the discharge pulse. The charge is, therefore, roughly given by the product of the peak discharge current and the pulse width. Therefore,

$$Q \propto A^{n_s} A^{n_\tau} = A^{n_i + n_\tau}, \text{ where}$$

A is the area of the sample

n_i is the area exponent for the peak current

n_τ is the area exponent for the pulse width.

Averaging the values of n_i over all the materials for which a power fit curve was made we find that $n_i = 0.59$. Similarly we find that $n_\tau = 0.32$. Therefore $Q \propto A^{0.91}$ which indicates that the charge is roughly proportional to the area of the sample.

1.1.9 Summary of Arc Discharge Characterization

A summary of the best and worst case estimates of the breakdown voltage, peak pulse current and the pulse width for all the materials considered is given in Table 1-10. Also shown are notes explaining the basis for each of the entries in the matrix. These notes are identified in the matrix by numbers.

Table 1-10. Summary of Arc Discharge Characterization*

MATERIAL		BREAKDOWN VOLTAGE		PEAK PULSE CURRENT (AMPS)		PULSE WIDTH (ns)	
		ESTIMATE	WORST CASE	ESTIMATE	WORST CASE(1)	ESTIMATE	WORST CASE (1)
TEFLON		12 kV (2)	4 kV (3)	$I=7A^{.575}$ (A in cm^2) (4)	$I=62A^{.575}$ (5)	$\tau=54.9A^{.28}$ (4)	$\tau=152A^{.28}$
KAPTON		12 kV (6)	8 kV (6)	$I=9.9A^{.43}$ (7)	$I=.002A^{2.1}$ (8)	$\tau=203A^{.292}$ (7)	$\tau=44A^{.6}$ (8)
MYLAR		<20 kV (9)	<20 kV (9)	$I=17.2A^{.764}$ (4)	$I=12.5A^{1.33}$ (10)	$\tau=24.9A^{.39}$ (4)	$\tau=56A^{.39}$ (5)
SOLAR CELLS COVERGLASS NEGATIVE		9 kV (11)	9.4 kV (11)	20 (12)	20 (12)	500 (12)	500 (12)
SOLAR CELLS COVERGLASS POSITIVE		1 kV (13)	1 kV (13)	0.5 (13)	0.6 (13)	2000 (13)	2000 (13)
SECOND SURFACE MIRRORS (QUARTZ WINDOW)		7 kV	2 kV	40 (14)	40 (14)	300 (14)	300 (14)
THERMAL BLANKETS	SEWN EDGE	10.4 kV (15)	10.4 kV (15)	(17)	(17)	(17)	(17)
	OPEN EDGE	16.5 kV (15)	5 kV (16)	(17)	(17)	(17)	(17)

* LOAD FOR DIAGNOSTICS FOR ALL EXPERIMENTS USED IN SUMMARY IS R < 2000 Ω. INSUFFICIENT DATA TO DETERMINE THICKNESS DEPENDENCE.

NOTES
(1) WORST CASE DEFINED AS LARGEST PEAK PULSE CURRENT AND PULSE WIDTH AND LOWEST VOLTAGE AT WHICH BREAKDOWN OCCURS.
(2) BASED ON ONE EXPERIMENT ONLY. SAMPLE 5 MILS THICK.
(3) BASED ON EXPERIMENT PERFORMED IN AIR.
(4) BASED PREDOMINANTLY ON MEASUREMENTS MADE WITH ELECTRON MICROSCOPE ON SMALL SIZE SAMPLES.
(5) ASSUME AREA DEPENDENCE UNCHANGED FOR WORST CASE MEASUREMENT.
(6) SAMPLE THICKNESS 1-2 MILS. BEAM VOLTAGES, 10 kV AND >15 kV.
(7) BASED ON SEVERAL EXPERIMENTS USING DIFFERENT TECHNIQUES AND CONFIGURATIONS.
(8) BASED ON TRW EXPERIMENT IN SWARM TUNNEL. SAMPLE EDGES FOLDED OVER METAL PLATE. WORST CASE FOR LARGE AREAS.
(9) NO BREAKDOWN VOLTAGES REPORTED. BASED ON BEAM VOLTAGE AT BREAKDOWN. SAMPLE THICKNESS 4-5 MILS.
(10) BASED ON MEASUREMENTS MADE WITH ELECTRON MICROSCOPE ON SMALL SIZE SAMPLES. WORST CASE FOR LARGE AREAS.
(11) BASED ON ONE EXPERIMENT ONLY. FUSED SILICA COVERGLASS - 12 MILS THICK - 14 kV BEAM VOLTAGE.
(12) BASED ON ONE EXPERIMENT ONLY. CERIA COVERGLASS - 12 MILS THICK - 20 kV BEAM VOLTAGE 18.5 X 23 CM SAMPLE.
(13) BASED ON ONE EXPERIMENT ONLY. HIGHER BREAKDOWN VOLTAGE IS ASSUMED TO BE WORST CASE.
(14) BASED ON ONE EXPERIMENT. 15 X 2.5 CM SAMPLE. SIX QUARTZ SSM'S - 8 MIL THICK - BEAM VOLTAGE 20 kV.
(15) BASED ON ONE EXPERIMENT. 5 MIL KAPTON BLANKETS.
(16) BASED ON ONE EXPERIMENT IN AIR. 5 MIL MYLAR BLANKET.
(17) NO DATA REPORTED.

1.1.10 Assessment and Conclusions

The validity of the arc characterization performed in Task 1.1 is questionable. A discharge is a stochastic process and the results of experiments defining many of the parameters required for the characterization are not repeatable. The results often depend on the condition of the sample surface, as well as the history of exposure to the electron beam. Furthermore, the results depend on a large number of factors (such as sample configuration, test technique, etc.) which are clearly different from experiment-to-experiment. Furthermore, very few of the experiments that have been reported in the literature and used in this study have set out to characterize the arcs systematically. Most of the experiments were examining a specific aspect of the discharge and in the process measured a limited number of the parameters of interest. For this reason, descriptions and information required to fully utilize the data were not given. For example, descriptions of the samples, facility, diagnostics and even the techniques used were frequently not given or incomplete. Often the beam voltage and current used in a swarm tunnel test are not included.

In spite of this, a rough cut of the parameters which characterize the arc discharges occurring in an environmentally induced chargeup has been made for several spacecraft materials. The area effect for both the peak discharge current and the pulse width has been estimated. There is some problem in using this data for an estimate of the current and pulse width that would result from spacecraft size samples since the area effects derived to date have apparently no current limit. Both experimental work on large samples and analytical work to develop a good physical understanding of the discharge process on spacecraft dielectrics are required to determine any limit to the current that might exist.

Recent experiments performed at NASA LeRC have added a large amount of data on the area effect of teflon (P. R. Aron and J. V. Staskus, "Area Scaling Investigations of Charging Phenomena"). We have obtained a preliminary report of this data which was obtained after Task 1.1 had been completed and we, therefore, have modified the results of Task 1.1 accordingly and made this the subject of Appendix A to this report.

1.2 TASK 1.2 - IDENTIFICATION OF REQUIREMENTS FOR ADDITIONAL EXPERIMENTS

In identifying the requirements for additional experiments that should be performed in the laboratory to characterize arc discharges, it is important to consider how the results of these tests will be used in the design and test of spacecraft.

In this section, 1.2, the following elements will be considered:

- Spacecraft design and test requirements
  - Impact on arc characterization
- Requirements for additional experiments
  - Measurement techniques improvements
  - Arc breakdown thresholds
  - Arc characterization
- Recommended key experiments

Table 1-11 lists specific data requirements, and the corresponding applications of that data in spacecraft design and test procedures. With regard to the kind of data required, it is clear from Task 1.1 that a systematic approach to obtaining useful data has not been undertaken. The experiments to be recommended in this task have been broken down into three subtasks, Tasks 1.2.1, 1.2.2 and 1.2.3 as shown in Table 1-12. Task 1.2.1 considers those experiments which will develop improved measurement techniques. Task 1.2.2 considers those experiments which will characterize arc breakdown thresholds, and Task 1.2.3 those which characterize the arc discharges per se. Note that a distinction is made between arc breakdown thresholds and the arc discharge itself. As may be seen in Table 1-12, each subtask has an associated set of recommended key experiments that should be performed.

Under Task 1.2.1, experiments to develop improved measurement techniques, a further subdivision into three areas is indicated in Table 1-12. These are

- Sample Configuration Experiments (Table 1-13)
- Environment Simulation Experiments (Table 1-14)
- Diagnostic Development Experiments (Table 1-15).

These three areas are defined with objectives and rationales in the corresponding tables as indicated. In Table 1-13, the lack of a consistent or comparable test sample configuration in prior experiments is discussed. As indicated, a basic understanding of what the important features of the test samples are is not well understood at the present time. In Table 1-14, experiments to define the adequacy or inadequacy of the environment simulation in ground based vacuum system tests are discussed. Table 1-15 addresses the experiments required to develop improved diagnostics. As our understanding of the arc discharge phenomenon is improved, the quality of the diagnostics must be "bootstrapped" to provide better information which is more useful and appropriate in spacecraft design and test procedures. Figure 1-9 shows some of the elements of an improved experimental setup. The test sample is a minisatellite in that it is electrically isolated from the test chamber. The onboard diagnostics have their data transmitted to external recording equipment via a wideband telemetry system. UV lamps for photoemission are included as well as a source of high energy electrons. The output of Task 1.2.1, the key recommended experiments to develop improved measurement techniques, is shown in Table 1-16. Experiments to characterize arc breakdown thresholds are discussed in Table 1-17 with objectives and rationales. Key recommended experiments are summarized in Table 1.-18. The phenomena and spacecraft configuration parameters associated with arc breakdown are distinct from the arc discharge itself. For example, edge conditions are the most important factor in defining the breakdown threshold, but the characteristics of the remainder of the discharge may depend on many other factors which should be investigated separately.

Experiments to characterize arc discharges are discussed in Table 1-19 with objectives and rationales. Key recommended experiments in this area are summarized in Table 1-20. Since arc breakdown thresholds are to be studied separately, a very useful and time-saving tool for this series of experiments would be a "sure-fire" trigger which initiates a discharge independent of a real-life trigger. Possible approaches are a spark coil or a laser-type trigger.

Table 1.-11. Specific Arc Data Requirements and their Applicability to Spacecraft Design and Test

SPECIFIC DATA REQUIREMENTS	DATA APPLICATIONS
• LOCATION OF ARC AND ITS SPATIAL EXTENT	AFFECTS EMI COUPLING INTO SPECIFIC SUBSYSTEMS OR CABLING OR IN DEPOSITION OF CONTAMINANTS
• CURRENT WAVEFORM, $I(t)$	
- PEAK CURRENT, I	COUPLES DIRECTLY INTO CABLES, ETC; ALSO COUPLES AS REPLACEMENT CURRENTS ON BOOMS, ANTENNAS, ETC.
- PULSE WIDTH, w	AFFECTS COUPLING AND HAZARD (VIA FREQUENCY SPECTRUM)
- PEAK $\frac{dI}{dt}$	DIRECTLY RELATED TO INDUCED VOLTAGE
• VOLTAGE WAVEFORMS $V(t)$	
- BREAKDOWN VOLTAGE, V_b	AFFECTS MATERIAL SELECTION AND CONFIGURATION DESIGN
- CHANGE IN VOLTAGE ($=V_b$?)	COUPLES DIRECTLY AS A CAPACITANCE VOLTAGE DIVIDER
- PEAK dV/dt	COUPLES CAPACITIVELY AS $C\cdot(dV/dt)$
• OTHER DATA	
- STORED CHARGE	AFFECTS SELECTION OF MATERIALS AND CONFIGURATION DESIGN. AREA INVOLVED DEFINES AVAILABLE CHARGE AND ENERGY AND ACTUAL CHARGE AND ENERGY DISSIPATED IN THE DISCHARGE. PULSE ENERGY AND PEAK POWER DEFINES DAMAGE OR DETERIORATION OF ARCING MATERIAL AND THE POSSIBLE REDISTRIBUTION OF CONTAMINANTS.
- CHARGE IN PULSE	
- STORED ENERGY	
- ENERGY IN PULSE	
- PEAK POWER	

Table 1-12. Types of Recommended Experiments

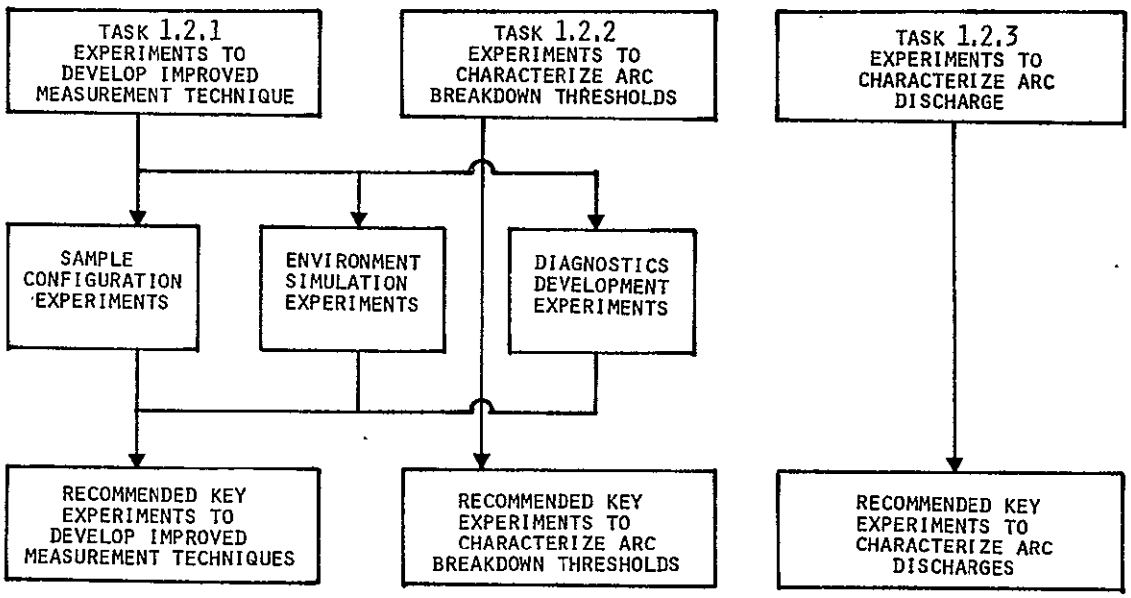

Table 1-13. Sample Configuration Improvement Experiments

EXPERIMENT	OBJECTIVE	RATIONALE
DETERMINE EFFECTS OF TEST SAMPLE MOUNTING TECHNIQUES, SAMPLE LOADING RESISTANCES AND LOCATION OF DIAGNOSTICS	DEFINE A STANDARD TEST SAMPLE MOUNTING CONFIGURATION	• ARC DISCHARGE CHARACTERISTICS HAVE BEEN SHOWN TO BE AFFECTED BY SAMPLE MOUNTING TECHNIQUES AND LOAD RESISTANCES • THE ACHIEVABILITY OF POSITIVE DIELECTRIC STRESSES HAS BEEN SHOWN TO BE LIMITED BY THE LOAD RESISTANCE
DETERMINE EFFECTS OF SAMPLE CONFIGURATION - CLEANLINESS, OUTGASSING, PRIOR EXPOSURE, PRIOR ARCING - EDGES, CORNERS, THICKNESS - LOCATION OF ADJACENT METALS AND UNCHARGED DIELECTRICS	DEFINE WHAT SAMPLE CONFIGURATION PARAMETERS ARE IMPORTANT IN ARC BREAKDOWN AND IN THE RESULTING CHARACTERISTICS	• SAMPLE CLEANLINESS/CONTAMINATION REQUIREMENTS FOR OBTAINING VALID TEST DATA HAVE NOT BEEN DETERMINED • EFFECTS OF PRIOR EXPOSURE AND ARCING ON PROGRESSIVE CHANGES HAS NOT BEEN DETERMINED • EDGES AND CORNER CONFIGURATIONS AND THE LOCATION OF ADJACENT MATERIALS HAVE BEEN SHOWN TO AFFECT ARC BREAKDOWN CHARACTERISTICS

Table 1-14. Environment Simulation Improvement Experiments

EXPERIMENT	OBJECTIVE	RATIONALE
INVESTIGATE EFFECTS OF STRESS POLARITY	VERIFY THAT POSITIVE DIELECTRICS HAVE DIFFERENT ARC DISCHARGE CHARACTERISTICS FROM NEGATIVE DIELECTRICS	THE INITIAL EXPERIMENTS ON THE TDRSS SOLAR ARRAY SAMPLE INDICATE THAT POSITIVE DIELECTRICS BEHAVE DIFFERENTLY FROM THE NEGATIVE DIELECTRIC STRESS CONFIGURATION
INVESTIGATE EFFICACY OF UV SIMULATION - COMPARED TO ONE-SUN - THERMAL AS WELL AS PHOTOEMISSION AND PHOTOCONDUCTION EFFECTS	DEFINE METHODS OF SIMULATING PHOTOEMISSION AND THEIR LIMITATIONS	UV SIMULATION AT THE ONE-SUN LEVEL IS DIFFICULT TO ACHIEVE, PARTICULARLY OVER LARGE AREAS. THE USE OF ION SOURCES TO GENERATE POSITIVE STRESSES HAS BEEN SUGGESTED.
INVESTIGATE EFFECTS OF LACK OF ELECTRON OMNIDIRECTIONALITY AND SPREAD ENERGY SPECTRUM. ABSENCE OF IONS.	VERIFY THAT THE USE OF MONOENERGETIC ELECTRON BEAMS IS A VALID SIMULATION	THE LACK OF ELECTRON OMNIDIRECTIONALITY AND SPREAD ENERGY SPECTRUM HAS BEEN CRITICIZED AS AN INCOMPLETE SIMULATION. ANY EXPERIMENTAL VERIFICATION THAT THESE SHORTCOMINGS ARE NOT CRUCIAL WILL HELP.
INVESTIGATE ROLE OF ELECTRON PENETRATION IN ARC DISCHARGES	DETERMINE UNDER WHAT CONDITIONS THE PENETRATION OF ELECTRONS MUST BE CONSIDERED	HIGHER ENERGY ELECTRONS PENETRATE INTO THE SURFACE OF DIELECTRICS AND MAY CAUSE A DIFFERENT ARCING MODE
INVESTIGATE CHAMBER EFFECTS - VACUUM LEVEL (10^{-5}-10^{-8} torr) - ION GAUGES, FARADAY CUPS - ELECTRON GUN EMISSION OF IONS AND IR/UV - NON-UNIFORMITY OF IRRADIATION - VACUUM CHAMBER RESONANCES	DETERMINE EFFECTS OF VACUUM CHAMBER EFFECTS ON ARC DISCHARGE CHARACTERISTICS	VACUUM CHAMBER EFFECTS ON THE ARC DISCHARGE TEST RESULTS HAVE BEEN OBSERVED AND OTHERS HAVE BEEN POSTULATED. THE CONDITIONS UNDER WHICH VALID TEST RESULTS ARE OBTAINABLE MUST BE DETERMINED.

Table 1-15. Improved Diagnostics Development Experiments

EXPERIMENT	OBJECTIVE	RATIONALE
DEVELOP STATIC AND DYANMIC E-FIELD AND $\dot{B}$-FIELD PROBES. ALSO, DATA TELEMETERING METHODS.	DEVELOP DIAGNOSTICS COMPATIBLE WITH AN ISOLATED TEST SAMPLE	DIAGNOSTIC GROUNDING TO THE TANK WALL HAS BEEN USED EXTENSIVELY IN THE PAST. SAMPLE ISOLATION IS MORE REALISTIC BUT REQUIRES IMPROVED DIAGNOSTIC TECHNIQUES.
DEVELOP DETECTION TECHNIQUES FOR IONS AND NEUTRALS	DETECT FLOWS OF PARTICLES OTHER THAN ELECTRONS IN AN ARC DISCHARGE	ARC DISCHARGES INVOLVE IONS AND NEUTRALS AS WELL AS ELECTRONS. WHERE THESE PARTICLES GO IS AN IMPORTANT ASPECT OF CHARACTERIZING ARC DISCHARGES.
DEVELOP TECHNIQUES TO DETERMINE TEMPORAL AND SPATIAL HISTORY OF ARC DISCHARGES	DEVELOP TECHNIQUES TO STUDY MULTIPLE OR PROPAGATING DISCHARGE WAVEFRONTS	MULTIPLE OR PROPAGATING ARC DISCHARGES HAVE BEEN OBSERVED WHICH MAY BE RELATED TO THE AREA EFFECT. IN ADDITION TO THE AREA EFFECT FURTHER ENHANCEMENT OF ARC CURRENTS IS POSSIBLE WITH THESE EFFECTS.
DEVELOP A SURE-FIRE TRIGGER TO INITIATE ARC DISCHARGES	DEVELOP A TOOL FOR STUDYING ARC DISCHARGES APART FROM THE ARC BREAKDOWN PROCESS	THE STUDY OF ARC DISCHARGE CHARACTERISTICS AS DISTINGUISHED FROM ARC BREAKDOWN IS TIME CONSUMING IF ARCS DO NOT OCCUR. A SURE-FIRE TRIGGER WOULD PERMIT A MORE COST EFFECTIVE USE OF EFFORT IN CHARACTERIZING ARC DISCHARGES.

Table 1-16. Output of Task 1.2.1: Recommended Key Experiments to Develop Improved Measurement Techniques

- SAMPLE CONFIGURATION
  - — SELECT ONE TYPICAL THERMAL BLANKET CONFIGURATION, VIZ, FSC OR DSCS II OR A TDRSS SOLAR ARRAY SAMPLE
  - — ISOLATE SAMPLE FROM TANK WALLS
  - — DETERMINE EFFECTS OF SAMPLE GROUNDING, EDGE TREATMENT, ADJACENT GROUNDED METALS AND UNCHARGED DIELECTRICS, PRIOR EXPOSURE, ETC.
- ENVIRONMENT SIMULATION
  - — VERIFY DIFFERENCE OF TEST RESULTS DEPENDING ON STRESS POLARITY
  - — IDENTIFY VACUUM CHAMBER EFFECTS: VACUUM LEVEL, ELECTRON GUN, UNIFORMITY OF IRRADIATION
- DIAGNOSTICS
  - — DEVELOP E AND $\dot{B}$ SENSORS
  - — DEVELOP TECHNIQUES TO IDENTIFY DISCHARGE PARTICLE SPECIES AND WHERE THEY GO
  - — DEVELOP A SURE-FIRE TRIGGER

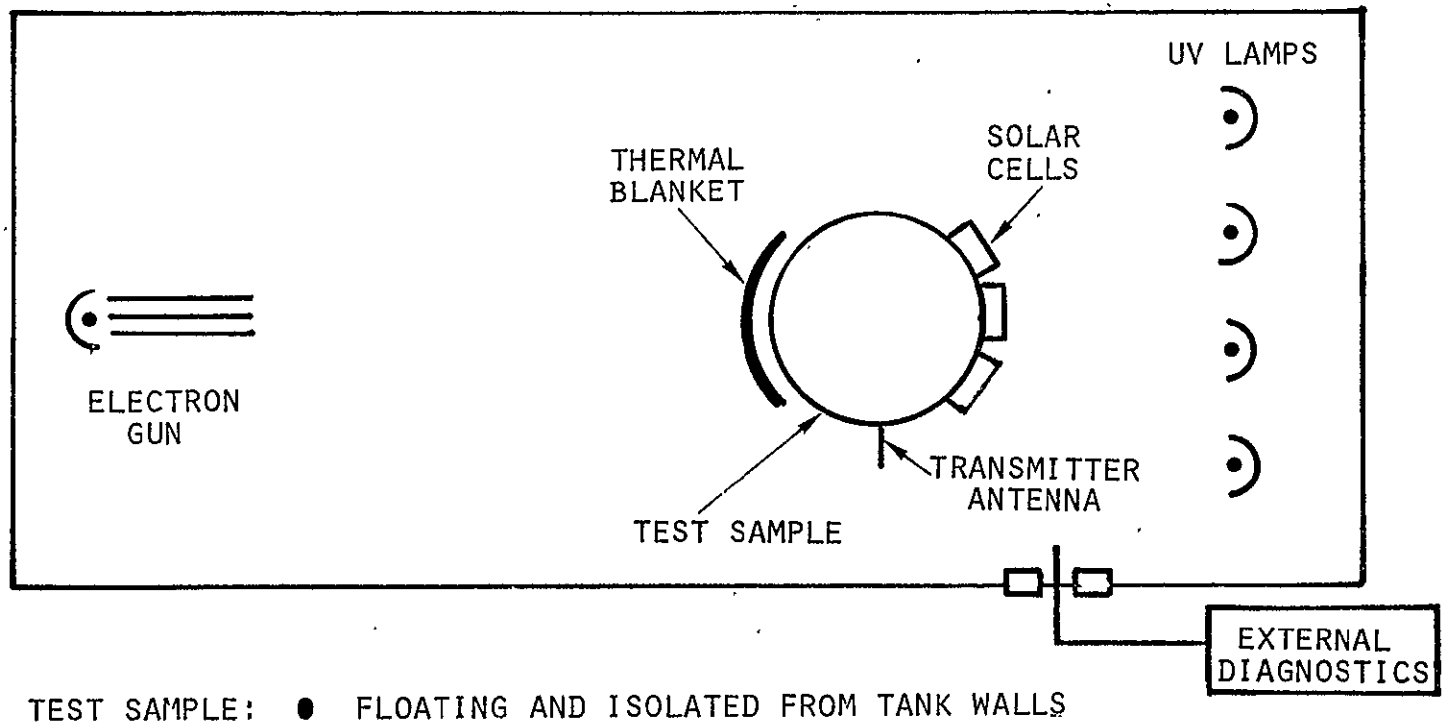

TEST SAMPLE:
- FLOATING AND ISOLATED FROM TANK WALLS
- ON-BOARD DIAGNOSTICS
- ON-BOARD POWER (BATTERIES)
- WIDEBAND TELEMETRY SYSTEM

Figure 1-9. Laboratory Test Verification Study of the Validity of Swarm Tunnel Tests

Table 1-17. Experiments to Characterize Arc Breakdown Thresholds

EXPERIMENT	OBJECTIVE	RATIONALE
DETERMINE EFFECTS ON ARC BREAKDOWN OF • EDGES AND CORNERS • LOCATION AND CONFIGURATION OF ADJACENT METALS AND UNCHARGED DIELECTRICS • SAMPLE THICKNESS, CLEANLINESS, SMOOTHNESS • DIFFERENT MATERIALS • DEGRADATION FROM PRIOR EXPOSURE AND PRIOR ARCING	DETERMINE WHAT PARAMETERS ARE IMPORTANT IN ARC BREAKDOWN. DEFINE A PRIORITY OF FACTORS.	A SYSTEMATIC APPROACH TO DEFINING ARC BREAKDOWN THRESHOLDS, APART FROM THE ARC DISCHARGE ITSELF, IS NEEDED. THIS DISTINCTION HAS NOT BEEN EMPHASIZED IN PRIOR TESTS. WE HAVE FOUND THAT ALL OF THE FACTORS LISTED DO AFFECT THE VOLTAGE AT WHICH BREAKDOWN OCCURS.
DETERMINE EFFECTS ON ARC BREAKDOWN OF STRESS POLARITY	VERIFY THAT STRESS POLARITY AFFECTS ARC BREAKDOWN THRESHOLDS	WE HAVE OBTAINED INITIAL INDICATIONS THAT STRESS POLARITY DOES AFFECT ARC BREAKDOWN THRESHOLDS. IT IS IMPORTANT TO PURSUE THIS EFFECT FURTHER.
DETERMINE EFFECTS OF NEARBY ARCS IN TRIGGERING OTHER ARC DISCHARGES	DETERMINE THE MAXIMUM DISTANCE THAT AN ARC CAN BE TRIGGERED FROM ANOTHER ARC	WE HAVE OBSERVED ARCS WHICH CAN "JUMP" ~1 cm. WHAT IS THE LIMIT AND UNDER WHAT CONDITIONS?
DETERMINE EFFECTS ON ARC BREAKDOWN OF - TEMPERATURE, OUTGASSING - CHARGING RATE - BEAM VOLTAGE	DEFINE OTHER FACTORS WHICH MAY AFFECT BREAKDOWN THRESHOLDS	OTHER ENVIRONMENTAL PARAMETERS HAVE BEEN POSTULATED AS HAVING EFFECTS IN ARC BREAKDOWN—THESE SHOULD BE INVESTIGATED TO ASSURE THE VALIDITY OF THE ENVIRONMENTAL SIMULATION
INVESTIGATE THE ROLE OF PENETRATING ELECTRONS ON ARC DISCHARGE THRESHOLDS	DETERMINE UNDER WHAT CONDITIONS THE PENETRATION OF ELECTRONS MUST BE CONSIDERED	PENETRATING ELECTRONS COULD AFFECT ARC DISCHARGE BREAKDOWN THRESHOLDS. (MALTER EFFECT AND MEULENBERG EFFECT)
DETERMINE RELATIVE TIMING OF ARCS AT DIFFERENT LOCATIONS ON THE TEST SAMPLE	DETERMINE WHETHER AND HOW "LARGE ARCS" ARE CAUSED BY "SMALL ARCS"	"LARGE ARCS" MAY BE HAZARDOUS AND THE STUDY OF HOW THEY ARISE IS IMPORTANT
DETERMINE WHETHER OTHER SOURCES CAN CAUSE TRIGGERING - MECHANICAL ACOUSTIC, UV FLASH, ETC.	DEFINE OTHER SOURCES OF ARC DISCHARGE TRIGGERING	OTHER TRIGGERING SOURCES HAVE BEEN POSTULATED. THESE SHOULD BE INVESTIGATED TO SEE WHETHER THEY APPLY TO SPACECRAFT IN ORBIT

Table 1-18. Output of Task 1.2.2: Recommended Key Experiments to Characterize Arc Breakdown Thresholds

- SAMPLE CONFIGURATION
  - — USE THE TYPICAL SAMPLE CONFIGURATION SELECTED IN TASK 1.2.1
  - — INVESTIGATE EFFECTS OF SAMPLE EDGE TREATMENT, ADJACENT GROUNDED METALS OR UNCHARGED DIELECTRICS, PRIOR ARCING, ETC.
- ENVIRONMENT SIMULATION
  - — DETERMINE EFFECT ON BREAKDOWN THRESHOLD OF STRESS POLARITY
  - — DETERMINE EFFICACY OF TRIGGERING FROM NEARBY SPARKS
  - — DETERMINE EFFECTS OF TEMPERATURE, OUTGASSING, CONTAMINATION, ETC.
- DIAGNOSTICS
  - — USE DIAGNOSTICS DEVELOPED IN TASK 1.2.1

Table 1-19. Experiments to Characterize Arc Discharges

EXPERIMENT	OBJECTIVE	RATIONALE
DETERMINE SAMPLE AREA EFFECT VS - SAMPLE MATERIAL - THICKNESS, EDGES AND CORNERS - SAMPLE UNIFORMITY, CLEANLINESS, OUTGASSING, PRIOR EXPOSURE, PRIOR ARCING - ADJACENT METALS AND UNCHARGED DIELECTRICS	CHARACTERIZE ARC DISCHARGE PARAMETERS IN A SYSTEMATIC WAY. DEFINE PRIORITY OF PARAMETERS WHICH DETERMINE ARC DISCHARGE CHARACTERISTICS.	A SYSTEMATIC APPROACH USING STANDARDIZED TECHNIQUES IS NEEDED WHICH WILL PROVIDE VALID AND USEFUL DATA (>10 cm). A SURE-FIRE TRIGGER WILL BE EXTREMELY USEFUL IN THIS STUDY WHICH IS DISTINCT FROM THAT OF THE ARC BREAKDOWN PROCESS. E AND B PROBES AND/OR TELEMETERING OF DATA MAY BE REQUIRED.
DETERMINE EFFECTS OF STRESS POLARITY ON ARC CHARACTERISTICS	VERIFY THAT STRESS POLARITY MUST BE TAKEN INTO ACCOUNT	WE HAVE OBTAINED INITIAL INDICATION THAT STRESS POLARITY STRONGLY AFFECTS THE CHARACTER OF ARCING. THE EMI IMPLICATIONS OF POSITIVE AND NEGATIVE ARC DISCHARGE PULSES ARE DIFFERENT
DETERMINE EFFECTS OF THE TEST ENVIRONMENT - SAMPLE POTENTIAL - BEAM CURRENT AND VOLTAGE - TEMPERATURE, MAGNETIC FIELDS, VACUUM LEVEL	DEFINE ACCEPTABLE TEST CHAMBER CONDITIONS FOR CHARACTERIZING ARC DISCHARGES	THESE ENVIRONMENTAL SIMULATION FACTORS MUST BE SHOWN TO NOT INVALIDATE THE TEST RESULTS. SAMPLE ISOLATION MAY REQUIRE PROVISION FOR SUPPLYING REPLACEMENT CHARGE OR CURRENT (VIA CAPACITANCE TO WALL) TO SIMULATE PROPER SAMPLE POTENTIAL DURING THE ARC.
INVESTIGATE EFFECTS OF PENETRATING ELECTRONS ON ARC CHARACTERISTICS	DETERMINE UNDER WHAT CONDITIONS THE PENETRATION OF ELECTRONS MUST BE CONSIDERED	PENETRATING ELECTRONS MAY AFFECT THE CHARACTER OF ARC DISCHARGES (MALTER EFFECT AND MEULENBERG EFFECTS)
IDENTIFY DISCHARGE PARTICLE SPECIES AND WHERE THEY GO	DETERMINE ALL VOLTAGES AND CURRENT FLOWS IN THE DISCHARGE	IONS AND NEUTRALS PARTICIPATE IN ARC DISCHARGES. WHERE THEY COME FROM AND WHERE THEY GO AFFECT THE CHARACTERISTICS OF THE ARC DISCHARGE

Table 1-20. Output of Task 1.2.3: Recommended Key Experiments to Characterize Arc Discharges

- SAMPLE CONFIGURATION
  - — USE THE TYPICAL SAMPLE CONFGIGURATION SELECTED IN TASK 1.2.1
  - — INVESTIGATE EFFECTS OF SAMPLE SIZE (AREA EFFECT)
  - — INVESTIGATE EFFECTS OF DIFFERENT SAMPLE MATERIALS
- ENVIRONMENT SIMULATION
  - — DETERMINE EFFECT ON ARC CHARACTERISTICS OF STRESS POLARITY
  - — DETERMINE EFFECT ON ARC CHARACTERISTICS OF CHARGING RATE, TEMPERATURE, MAGNETIC FIELDS, ETC.
- DIAGNOSTICS
  - — USE SURE-FIRE TRIGGER AND OTHER DIAGNOSTICS DEVELOPED IN TASK 1.2.1

1.3 THE PHYSICS OF DIELECTRIC (CATHODE)-TO-METAL ARC DISCHARGES

An understanding of the physical phenomena involved in arc discharges is a crucial element in performing experiments to define the characteristics of arc discharges. The type of diagnostic measurements taken, the configuration of the test sample and the adequacy of environment simulation are all influenced by the physical model of the arc discharge which is in the mind of the experimenter performing the experiments. Furthermore, a synergistic development of experiment and analytical modeling as with one cross-coupling to the other is essential if a characterization of arcs which truly reflects the in-flight situations is to be obtained in the shortest possible time.

This section will examine electron transport from the forward (exposed) face of a dielectric film to a rear face metallized layer. The electron transport to be examined specifically excludes "punch-through" in which the charge moves from the front surface to the rear surface via a (bulk) breakdown channel. It should be noted, however, that a bulk breakdown process may be invoked as the triggering mechanism for the dielectric surface charge clean off.

A discharge model has been advanced to describe the clean off of surface charge on the dielectric surface. This discharge model has the following tenets:

1. An initial breakdown point (either in the bulk or on the surface) creates a region of very high potential gradient on the dielectric surface.

2. Electron extraction from the uppermost monolayers of the dielectric occurs at the region of high negative potential and high surface gradient.

3. Electrons extracted from the dielectric move along the surface and re-intercept the surface with sufficient energy to emit secondary electrons at greater than unity gain.

4. The secondary electron cloud released from and generated by the surface is transported to regions of more positive potential via one or another of several possible transport modes.

5. Steepening of the potential gradients on the dielectric surface by secondary electron multiplication causes the discharge wave to propagate and thus causes a clean off of surface charge over large areas of the dielectric. In summary to the above, the surface discharge wave requires a triggering mechanism, a discharge wave propagating mechanism, and an electron transport process.

The discussion will now examine the electron transport processes.

1.3.1 Electron Transport Modes

1.3.1.1 Electron Transport in Vacuum

The subject of electron transport in vacuum has been examined at very great lengths in the development of vacuum tubes. The principal feature of this previous (and extensive) work as it affects dielectric-to-metal arcs is the recognition that space charge forces in the electron flow will limit the total current which may be transported across an intervening space. The term usually involved in such charge transport treatments is that of "perveance" ($I/V^{3/2}$, where I is the electron current transported by the potential difference V). If the electrons must be transported over large distances, say meters, the perveance is comparatively low (of the order of 10^{-6} ampere/volt$^{3/2}$) and, even for potential differences of the order of 10^4 volts, electron currents are limited to the order of a few amperes. It is for this current limitation reason that "blow off" (electron transport to space from a spacecraft surface) is probably not a significant threat to spacecraft systems. Figure 1-10 (top) illustrates the transport mode over large distances from the discharge wave.

As the electron transport distance is reduced, the perveance of the flow increases and larger electron currents can be transported for a given potential difference, V. Reducing the distance to tens of centimeters can increase allowable electron transport to tens of amperes (for the example of $V \sim 10^4$ volts) and reduction of the transport distance to a few centimeters can cause the allowable electron transport to rise to levels of the order of 100 A. Such discharge paths could take place, for example, in a discharge between a spacecraft dielectric surface and a nearby metal portion of the spacecraft. Figure 1-10 (bottom) illustrates such a transport process. It should be noted, however, that the total area of a spacecraft dielectric

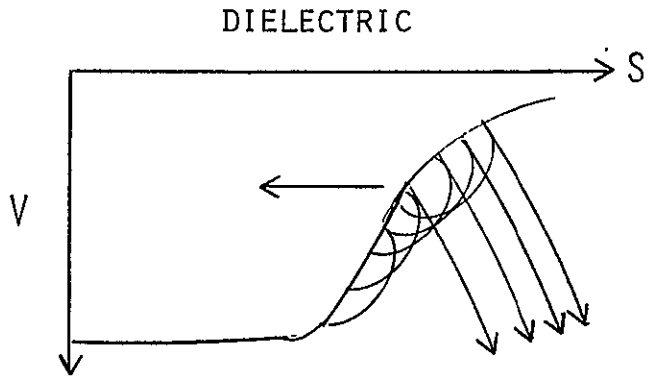

PROPAGATING WAVE AND TRANSPORT
(OVER LARGE DISTANCES) IN VACUUM

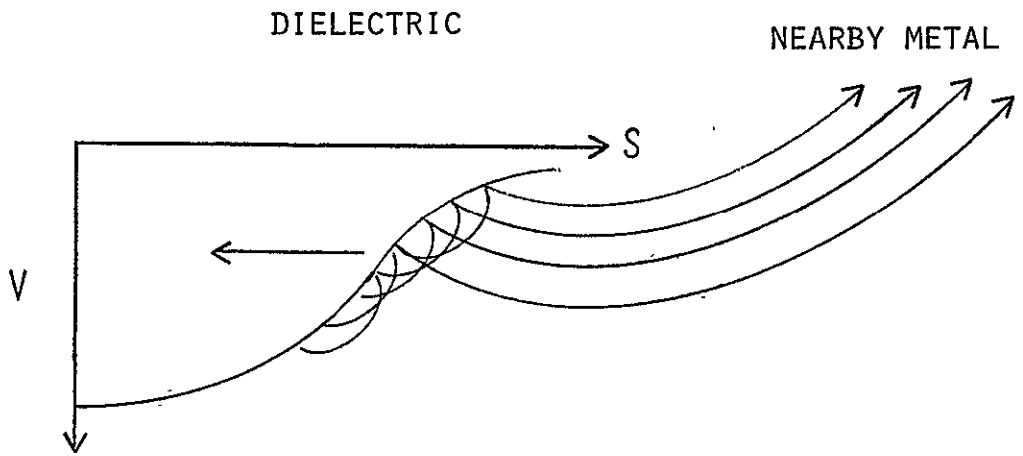

PROPAGATING WAVE AND TRANSPORT
(OVER MID-RANGE, OR SMALL) DISTANCES
IN VACUUM.

Figure 1-10. Surface Discharge and Transport Model I

within a few centimeters of a given spacecraft metal surface is limited and that the high current portion of the discharge would be limited to the clean off of these "nearby" areas. In this transport-in-vacuum case the electrons moving from more distant regions of the dielectric surface to the metal would become progressively fewer as the discharge wave propagated away from the nearby metal. The experimental results, however, indicate that comparatively large areas of dielectric can clean off at very high current levels during the majority of the clean off. This observed behavior clearly violates the perveance limitations of the electron transport-in-vacuum model and causes the model to consider other (and lower impedance) transport modes. Specifically, the discharge model is driven toward plasma processes in order to have high current electron flow over increasing distances and for (presumably) small transport potentials.

1.3.1.2 Electron Transport-in-Plasma

If the electrons from the discharge wave to the nearby metal can cause the formation of a surface plasma, then large currents of electrons can be transported over the required distance from the discharge wave to the metal with only small required potential gradients. Figure 1-11 (top) illustrates such a surface plasma film.

The model for the surface plasma conduction has the following postulated processes:

1. Impacting electrons cause desorption of adsorbed surface atoms.
2. Impacting electrons also cause depolymerization of dielectric molecules.
3. Ionization of the released atoms causes the release of still further electrons and the formation of a charge neutralizing layer of positive ions.
4. The diminution of electron transport resistance causes still further growths in the transported electron current.
5. Because of the low resistance transport, large surface areas of the dielectric may clean off to nearby metals at high current levels.
6. Plasma constriction (pinch effects) may occur.
7. Plasma film blow off may occur at higher currents (from $\vec{J} \times \vec{B}$ effects).

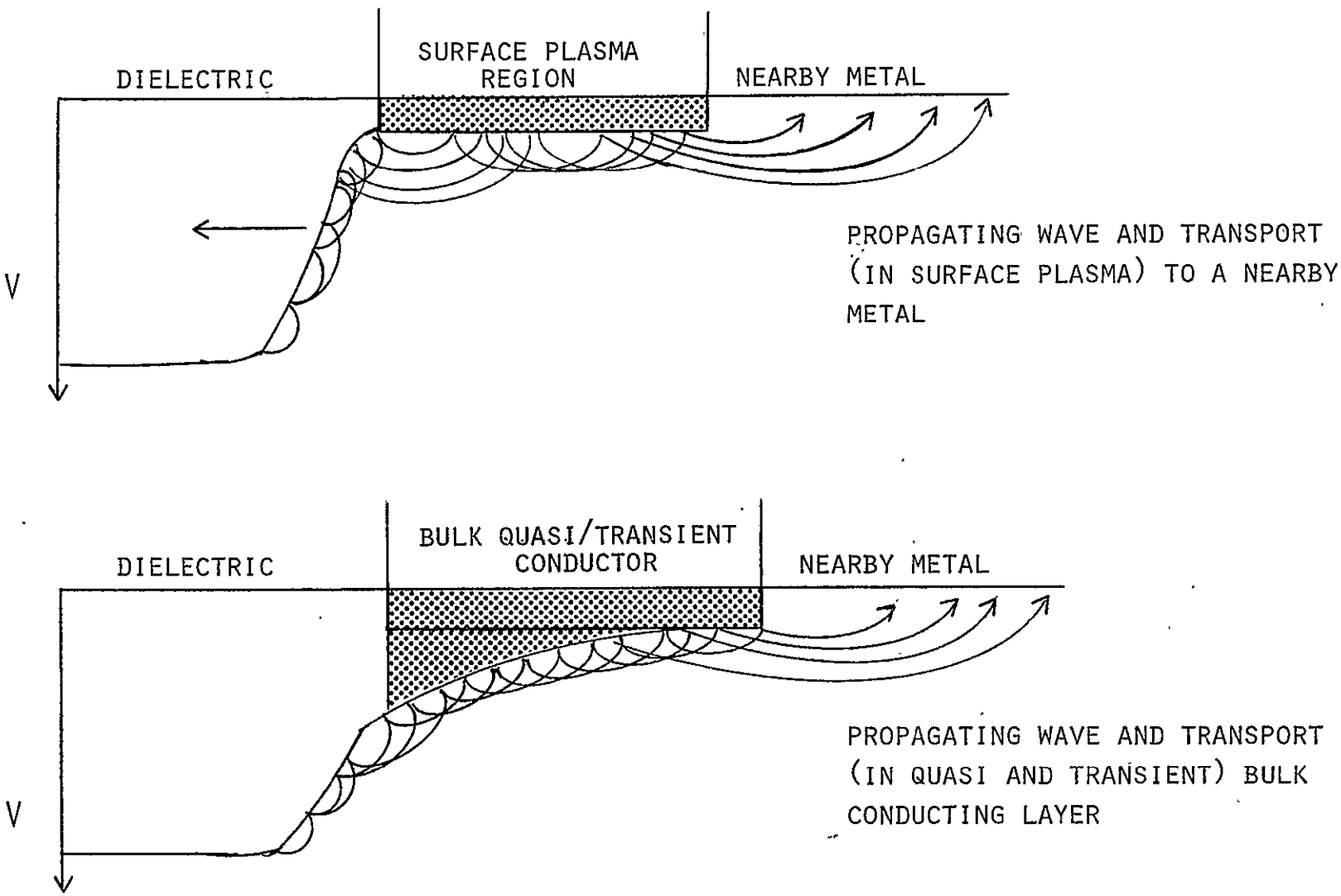

Figure 1-11. Surface Discharge and Transport Model II

The plasma film model described above is somewhat conjectural in nature. The model is, however, supported by the observed high discharge currents ($\sim$ 500 amperes) for dielectric-to-metal arcs in electron swarm tunnels, and from the previous work in "sliding spark" discharges and those pulsed plasma thrusters which use surface discharges of solid dielectric materials to create the plasma thrust plume.

1.3.1.3 Electron Transport in (Quasi/Transient) Bulk Conductor

Figure 1-11 (bottom) has illustrated an electron transport model in which the bulk of the dielectric becomes a quasi-conductor on a transient basis and under the action of the discharge wave currents. Figure 1-12 provides an additional illustration of this model.

It should be emphasized that the quasi/transient bulk conduction model is highly conjectural and is advanced largely in the interests of examining all possible modes of electron transport and in the hope that discussion of the various transport processes may lead to additional insights into these (rather complex) processes.

The bulk (transient/quasi) conduction model has the following (postulated) processes:

1. Secondary electron impact in the (multiplied) flow causes a transient "conduction band" group of electrons in the dielectric material.

2. The depth of the transiently conducting dielectric material is small (of the order of 10 Å to 50 Å) but the electron conduction density is high (of the order of a metal).

3. Continued secondary electron impact over the period of the discharge ($\sim$ 1 μsec) keeps the quasi-conduction band populated.

The model described above does appear to require higher potential gradients in the electron transport direction than the surface plasma conduction model. Some estimates of required properties to create the transiently conducting zone are that for a region 1mm in width and 100 Å in depth, and a conduction band density of 10^{22} electrons/cm^3, a current of $\sim$ 1000 amperes would be conducted, provided that the average velocity of the (electron) charge carriers remains at $\sim 10^7$ cm/sec. For electrons to retain these flow velocities in

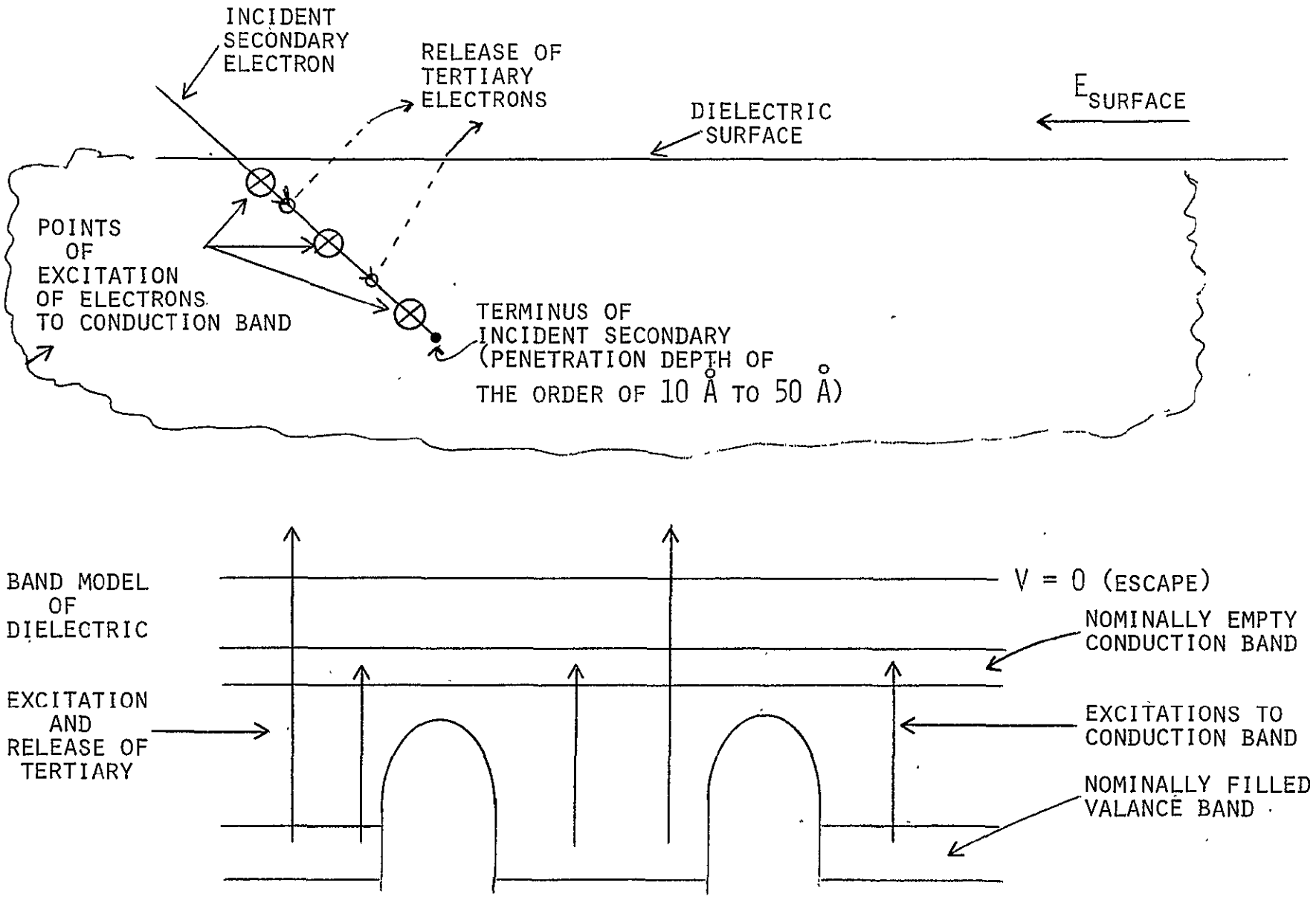

Figure 1-12. Bulk (Transient/Quasi) Conduction Model II

the bulk of the material may require larger potential gradients than can, in the ultimate reality, be sustained over any appreciable distance. In principle the energy storage in the dielectric film is sufficient to create a very high density of "conduction band" electrons in the material. For a kapton film, for example, at 20 kilovolts chargeup potential and at 3×10^{-3} inch thickness, the energy density is $\sim 5 \times 10^{17}$ eV/cm^2. If this stored energy were to be converted to conduction band electrons at a cost of 10 eV per electron, the conduction band electrons would have a surface (area) density of 5×10^{16} electrons/cm^2. If the conduction layer were 100 Å in thickness, the conduction band density would be 5×10^{22} electrons/cm^3. As noted above, the model does have problems in maintaining the electron in the conduction band for sufficient times ($\sim$ 1 μsec) before its return to a valence band state. The model also has problems in terms of the comparatively high energy expenditure for the conduction band alone (considering that other elements of the total discharge process are also energy absorbing and that the overall driver for the discharge is the stored electrical energy in the polymer film). The model is, nevertheless, of some interest and should be examined further, possibly in terms of the presence of this process in the dielectric material during the (more limited) period of the passage of the discharge wave (steeply varying potential portion) over a surface element.

1.3.2 Potential Watersheds and the Depth of Deposited Charge

The surface discharge model discussed in Sections 1.3 and 1.3.1 has treated all charge on the dielectric as though it was deposited in the very uppermost monolayers of the dielectric and, thus, would be easily accessible to the secondary electron multiplication method of clean off proposed in the discharge model. In practice the charge in the dielectric is at somewhat greater depths. An estimate of the mean depth of charge deposition can be gained from the known chargeup potential on the surface and the subsequent range of electrons entering the dielectric with an energy given by their "initial" energy (at infinity) minus the potential of the surface.

For an incident flow of electrons at a single acceleration energy in an electron swarm tunnel (and for sufficient deposition rates to reach the "saturation" potential), the surface ultimately moves to $\sim$2 kilovolts from the apparent source potential of the electrons. For 20 keV electrons, for

example, the surface will charge to ∿ -18 kilovolts and electrons will impact on the surface at 2 keV of energy which is approximately at the second crossover for secondary electron emission (i.e., one secondary electron released for each incident electron). The primary electrons encountering the dielectric will possess ∿ 2 keV and will have ranges in the dielectric material of ∿ 1000 Å. The presence of charge within the dielectric also sets up a retarding electric field for the penetrating primary electrons, but the potential increment of this in-bulk electric field is probably only of the order of 10 to 100 volts between the surface and the potential watershed (most negative potential in the dielectric) and, thus will not materially reduce the range of the primaries.

From their principal deposition point at ∿1000 Å beneath the dielectric surface, the electrons then move in two, opposite, directions. A portion of the flow (which deposits beyond the watershed) moves to the rear face metal film of the dielectric, and the electrons which deposit in the region between the watershed and the front surface move back to the front surface to replace the electrons released by secondary emission.

The average depth of the deposited negative charge in the dielectric is determined by integrating the depth of penetration for incident electrons from the time that the surface is at 0 volts to its final value. In the example considered above, the integration would proceed from the time that the surface is at 0 volts to the time that it reaches -18 kV or when the beam in turned off. For 20 kev electrons the depth of the deposited negative charge will range from 1000 Å to a few microns. When the surface discharge wave propagates across the surface, these "buried" charges make their way to the surface and participate in the surface discharge. It is not particularly difficult to move the electrons back to the surface in view of the relative small required voltage (∿1000 volts) over this very small distance (10^{-4} centimeters) in order to attain breakdown field levels (∿10^{7} volts/cm) in the dielectric. The surface discharge wave process does, thus, also create a certain amount of bulk breakdown in the dielectric in the region from 0 to ∿1000 Å below the surface.

1.3.3 Discharge Wave Propagation Problem Areas

The discharge waves discussed in the preceeding sections are presently advanced as a simple, two dimensional clean off of the surface with a single broad wavefront propagating over the surface in a single direction of motion.

In practice, it is known, that the discharges of these surfaces exhibit filamentary structures in the emitted light. This "pinching" of the light emission patterns was particularly true for the ORCON-10 samples in the TRW Electron Swarm Tunnel measurements. Thus, while the discharge wave model may be of some use in understanding dielectric clean off behavior, there are many problem areas in the total discharge modeling. A list of problem areas includes the following:

1. Although propagation is an essential element of all models, wave propagation speeds have not been measured directly, but have been inferred from sample size and discharge duration.

2. The very high current ($\sim$500 A) discharges observed in the electron swarm tunnel have not yet been demonstrated to be discharges which could occur on spacecraft and in space.

3. Transport of electrons in a plasma film has been postulated but has not been experimentally verified.

4. The significance of the light emission patterns observed during surface discharge clean off has not yet been determined relative to the total surface discharge.

5. The possible role of surface contaminant gas layers has not been evaluated in terms of their possible contributions to a conducting plasma film in the surface plasma conduction model.

6. Transient bulk conduction has been postulated but there is no direct experimental evidence to support this aspect of the discharge model.

7. Q and I limitations and dependence on area, chargeup voltage, and incident J_E have not yet been rigorously determined.

The observed behavior relative to Item 7 in the list above is that the majority of dielectric-to-metal arcs have increasing peak discharge current with increasing surface area. By altering the dielectric/metal configuration, however, the discharge current-area relationship can be dramatically altered so that even small dielectric samples can produce large peak discharge currents. It is probable that only Q ($=\int I dt$) is area-dependent in the strict sense and that I_{max} and $\dot{I}_{max}$ are more strongly dependent on dielectric/metal configuration than on dielectric surface area. For the (somewhat analogous) cases of metal-to-metal arcs, the R-C limited transmission of energy into the arc and the blow offs of arc current (from $\vec{J} \times \vec{B}$ forces) tend to limit the role of dielectric surface area in both I_{max} and $\dot{I}_{max}$. Arc currents may also be limited by inductive effects ($L\dot{I}$) for rapidly rising arc currents (for example, $\dot{I} > 10^{10}$ amperes/second).

A final area to note here in the discussion of problems is that of sample alteration. For electric stress levels above 10^6 V/cm, bulk conductivity in dielectrics undergoes a comparatively rapid growth as a function of continued exposure. For further increases in potentials and electric stress, surface discharges do occur and do cause alteration of both bulk and surface properties in the dielectric. For these reasons, arc discharge behavior cannot be expected to result in repetitive I_{max}, $\dot{I}_{max}$, and Q. For the (somewhat analogous) case of metal-to-metal arcs, material blow offs affect not only the metals but also the intervening dielectric surfaces.

1.3.4 Metal(Cathode)-to-Dielectric Arcs

The discussion in Sections 1.3 through 1.3.3 has been concerned with negative dielectrics discharging to positive metals. The situation of "reversed polarity" (negative metals and positive dielectrics) can occur, however, for certain 3-axis stabilized spacecraft (those having large areas of dark metals and equally large areas of sununlit dielectrics). For the metal cathode discharges, electron release (for electrons stored over a broad area of the metal) does not require a propagating wave but can use a single electron emissive point and the natural conductivity of the metal. The high release of electrons at the single emissive point has been observed to cause vaporization of the metal for both metal-to-metal arcs and metal-to-dielectric arcs. There are questions over the discharge of large areas of dielectric by a metal cathode in a metal-to-dielectric arc and whether the dielectric portion of this total discharge process may or may not require a propagating wave. Conclusions regarding the behavior of both metals and dielectrics in those arcs must be limited because of the limited number of experiments and because of the limited diagnostics in these experiments. There is some evidence to suggest that the discharge process in these metal-to-dielectric areas may be strongly dependent (in the initial phases of the discharge) on the details of the dielectric-to-metal interface.

2. TASK 2 - COUPLING DETERMINATION

The coupling of arc discharges to typical spacecraft systems has been determined utilizing the computer program SEMCAP. The specific spacecraft system considered was the Voyager, for which a SEMCAP analysis was implemented on two prior instances. The first instance was for the EMC purpose in which only the usual interactions of spacecraft electrical subsystems are considered. The second application[1] of SEMCAP to Voyager was implemented to verify its immunity to arc discharges in the Jovian magnetosphere. The techniques used were very similar to those for the present work. The major difference is in the characterization of the arc discharges. In the earlier effort, the arcs were characterized by special vacuum chamber tests performed at Boeing[2] under contract from JPL. In the present work, the arc characteristics derived from a survey of existing literature, in Task 1, have been utilized. The Boeing work was included in the survey.

2.1 TASK 2.1 - MODELING OF SOURCES FOR SEMCAP

Arc discharges of dielectric or insulated conductor surfaces create remote structural replacement currents as well as producing local capacitively and inductively coupled currents. Two surface discharge source models were required to simulate these effects. The structure replacement current effect is shown in Figure 2-1 for a surface discharge on a box situated on one of the payload booms. The replacement current restores potential equilibrium in the structure as the surface is discharged. The boom current will be a small fraction of the arc current and can be modeled by a filter which has a current transfer ratio equal to the ratio of impedances of the two paths shown in Figure 2-1. These impedances were approximated by a simplified electrically equivalent model of the structure. The necessary equations are also shown in Figure 2-1. The induced voltage on the boom was modeled by a second filter function multiplied by the boom current. This filter is characterized by a "gain", G'', equal to the impedance of the boom groundstrap at 10^9 Hz. The localized capacitive and inductive coupling effects of the surface discharge are most easily modeled by translating the surface into an approximately equivalent fat wire as shown in Figure 2-2. This equivalent wire capacitive coupling is driven directly by the step voltage change, V, of the discharged surface, and the arc current, I_{arc}, drives the inductive coupling.

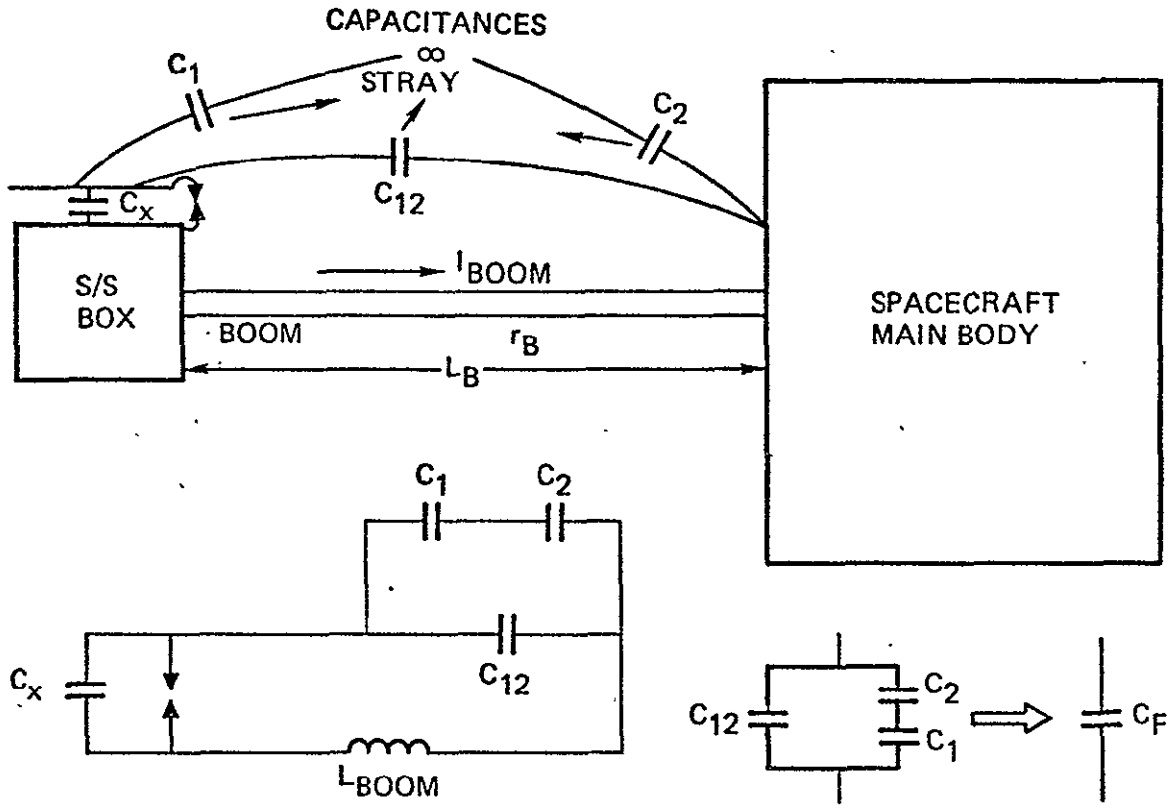

$$I_{BOOM} = I_{ARC}\left(\frac{X_{CX}}{X_{LB} + X_F + X_{CX}}\right)$$

$$= I_{ARC}\left(\frac{1/2\pi fC_X}{2\pi fL_B + 1/2\pi fC_F + 1/2\pi fC_X}\right)$$

$$= I_{ARC}\,[C_F/(C_F + C_X)]\,(4\pi^2 f^2 C_{eq} L_B + 1)^{-1}$$

$$= I_{ARC} \cdot P_1(f)$$

P(f) = LOW PASS (TYPE = 1)

G′ = INBAND GAIN = $C_F/(C_F + C_X)$

$f_c = (2\pi\sqrt{L_B C_{eq}})^{-1}$

ORDER = 2

$C_{eq} = C_F C_X/(C_F + C_X)$

$V_{BOOM} = I_{BOOM} \cdot X_{LB}$

$V_B = I_{ARC} \cdot P_1(f) \cdot P_2(f)$

$P_2(f)$ = HIGH PASS (TYPE = 2)

G_I'' = INBAND GAIN = $2\pi L_B f_c$

$f_c = 10^9$ (ARBITRARILY HIGH)

ORDER = 1

L_B = INDUCTANCE OF BOOM GROUND STRAP

Figure 2-1. Model for Boom Replacement Current

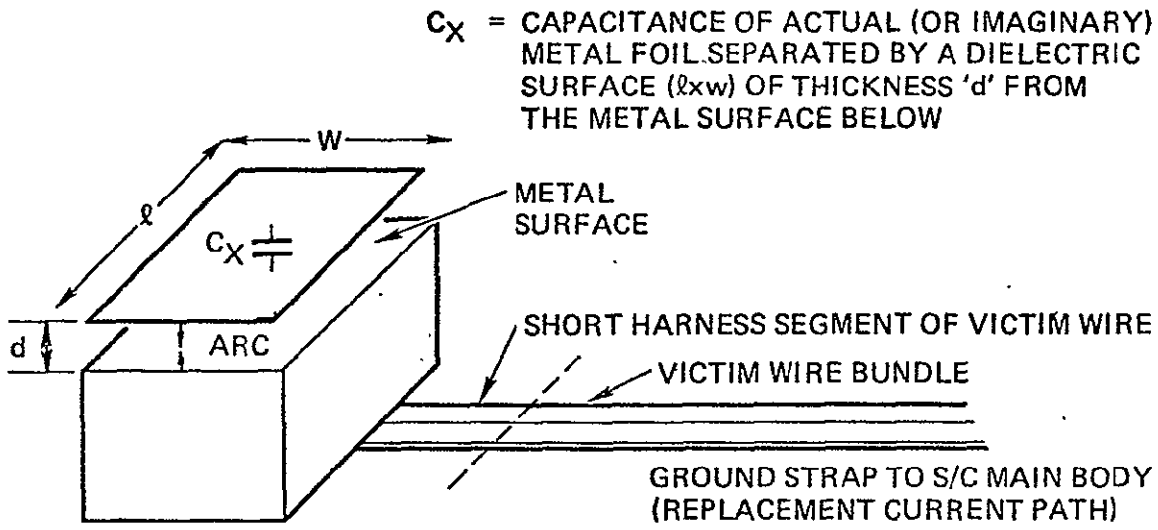

(a) REPLACEMENT CURRENT MODEL

THE METAL FOIL (ℓxw) IS MODELED AS A WIRE OF RADIUS w/2 AND LENGTH ℓ, AT HEIGHT h (= w) ABOVE GROUND PLANE; THUS, FORMING A (RECTANGULAR) LOOP WITH ITS IMAGE IN GROUND PLANE

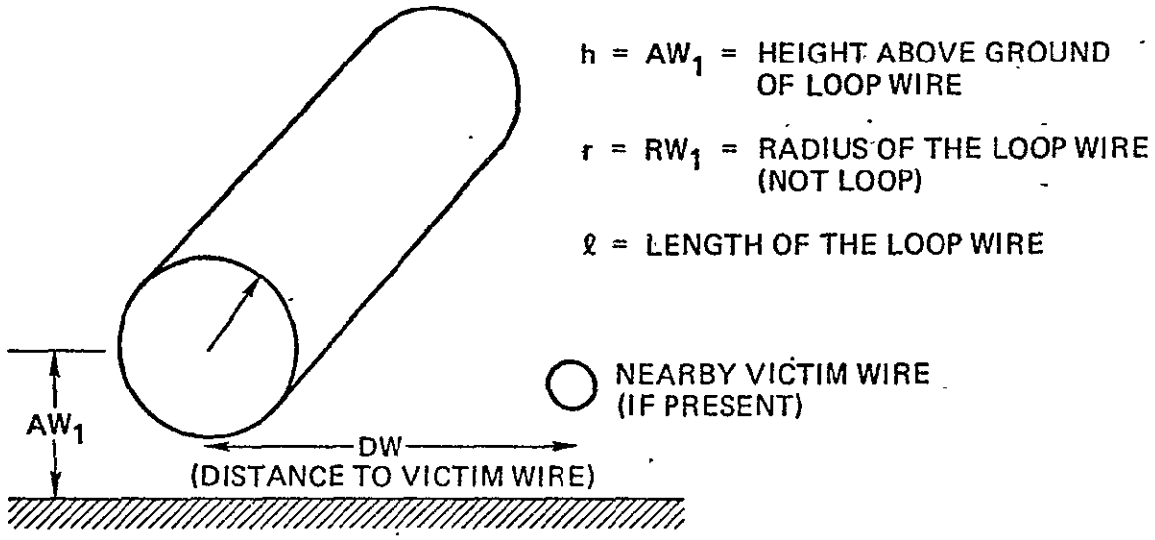

(b) LOCALIZED DISCHARGE LOOP

Figure 2-2. Surface Discharge Model for Local Replacement Current Coupling

For the Voyager spacecraft, twelve exposed dielectric surfaces were identified as potentially hazardous arc discharge sources. These are shown across the top of Table 2-1 which lists the parameters of these generators for Run 8. Run 8 corresponds to the case which was analyzed using the arc parameters derived from the Boeing tests, and constitutes the baseline case. These parameters are not the direct test results, but rather, represent the best estimates of parameters as expected to be appropriate to inflight conditions as derived from the Boeing test data.

As per the requirements for this task, three of the sources were modeled to represent thermal blankets, optical solar reflectors and boom-mounted solar arrays. The items on Voyager selected were, respectively, the high gain antenna outboard paint (HGA OB Paint), the Brewster Plate and the radioisotope thermal generator oxide layer (RTG Oxide). The physical geometry, size and location of these three sources were retained unchanged. Thus the coupling from these sources to the 77 receptors aboard the spacecraft are unchanged from Run 8. Runs 11 and 12 are the worst-case and best-estimate values of the three sources obtained from the literature survey of Task 1.1. The summary chart of Task 1.1 is reproduced as Table 2-2.

For an arcing source of known capacitance, the peak arc current, I_{arc}, is not independently specifiable if the breakdown voltage, $V_{Breakdown}$, and the pulse waveform are characterized. Assuming that the waveform is describable as the sum of two exponentials of the form

$$I_{arc}(t) = I_o(e^{-\alpha t} - e^{-\beta t}) \text{ where } \beta = 10\alpha,$$

it may be shown that the pulsewidth, t_p, risetime, t_r, charge, Q, and peak current, I_{max}, are given by

$$t_p = 1/\alpha, \quad t_r = 1/\beta, \quad I_{max} = .697\ I_o$$

$$Q = C_x \cdot V_{Breakdown} = \int_0^\infty Idt = .9\ I_o\ t_p = 1.291\ I_{max}\ t_p$$

$$I_{max} = .774\ Q/t_p = .774\ C_x\ V_{Breakdown}/t_p.$$

Table 2-1. Generator Parameters for Voyager SEMCAP Run 8

	1	2	3	4	5	6	7	8	9	10	11	12
	BREWSTER PLATE	MAG CABLE	SEP CONN	MAG TEFLON	HGA OB PAINT	PLUME SH SEP CONN	LECP TEFLON	FSS	HGA 1B PAINT	PLUME SH RTG	RTG OXIDE	MIRIS KAPTON
BREAKDOWN VOLTAGE, V(kV)	1	5	5	1	1	1	1	7	1	1	3.5	1
ARC CURRENT, I_A (AMPS)	2	20	36	3	150	16	.26	80	150	16	925	160
RISETIME, t_r (ns)	3	10	10	5	5	20	3	8	5	20	20	5
PULSE WIDTH, t_p (ns)	10	1700	15	13	3000	285	8	80	2400	330	3700	26
REPLACEMENT CURRENT PATH INDUCTANCE, L_B(μh)	0.25	2.3	1.5	7.7	0.4	1.5	1.8	1.9	0.4	0.8	2.8	4
DISCHARGE CAPACITANCE, C_x (pf)	2E4	5E4	150	38	4E5	4500	12	14	3E5	5200	3.4E5	40
STRAY CAPACITANCE, C_f(pf)	12	30	1.0	1.5	500	.2	4	53	70	2.5	90	.032
$V_{repl.}/I_{arc}$ (ohms)	1.25E3	82E3	9.5E3	3.8E4	1.25E3	9.4E3	1.6E4	12E3	1.25E3	9.5E3	1.1E4	2.5E4
CORNER FREQUENCY, f_c(MHz)	102	8	159	81	15.9	290	49	34	42	83	12	12
LOOP LENGTH, ℓ (m)	.2	.6	.025	.025	1.8	.2	.1	.35	1.0	.17	.85	.24
LOOP HEIGHT, h (m)	.006	6E-5	.025	1.6E-3	2E-4	5E-5	3E-3	.025	2E-4	5E-5	7.6E-5	5E-5
WIRE RADIUS, r (m)	5E-5	2.5E-4	4E-4	2E-4	5E-5	2.5E-5	1.6E-3	5E-5	5E-5	2.5E-5	3.8E-5	2.5E-5

Table 2-2. Arc Discharge Characterization Summary*
(From Task 1.1)

MATERIAL		BREAKDOWN VOLTAGE		PEAK PULSE CURRENT (AMPS)		PULSE WIDTH (ns)	
		ESTIMATE	WORST CASE	ESTIMATE	WORST CASE(1)	ESTIMATE	WORST CASE (1)
TEFLON		12 kV (2)	4 kV (3)	$I=7A^{.575}$ (A in cm^2) (4)	$I=52A^{.575}$ (5)	$\tau=54.9A^{.28}$ (4)	$\tau=152A^{.28}$
KAPTON		12 kV (6)	8 kV (6)	$I=9.9A^{.43}$ (7)	$I=.002A^{2.1}$ (8)	$\tau=203A^{.292}$ (7)	$\tau=44A^{.6}$ (8)
MYLAR		<20 kV (9)	<20 kV (9)	$I=17.2A^{.764}$ (4)	$I=12.5A^{1.33}$ (10)	$\tau=24.9A^{.39}$ (4)	$\tau=56A^{.39}$ (5)
SOLAR CELLS COVERGLASS NEGATIVE		9 kV (11)	9.4 kV (11)	20 (12)	20 (12)	500 (12)	500 (12)
SOLAR CELLS COVERGLASS POSITIVE		1 kV (13)	1 kV (13)	0.5 (13)	0.6 (13)	2000 (13)	2000 (13)
SECOND SURFACE MIRRORS(QUARTZ WINDOW)		7 kV	2 kV	40 (14)	40 (14)	300 (14)	300 (14)
THERMAL BLANKETS	SEWN EDGE	10.4 kV (15)	10.4 kV (15)	(17)	(17)	(17)	(17)
	OPEN EDGE	16.5 kV (15)	5 kV (16)	(17)	(17)	(17)	(17)

* LOAD FOR DIAGNOSTICS FOR ALL EXPERIMENTS USED IN SUMMARY IS R < 2000 Ω. INSUFFICIENT DATA TO DETERMINE THICKNESS DEPENDENCE.

NOTES

(1) WORST CASE DEFINED AS LARGEST PEAK PULSE CURRENT AND PULSE WIDTH AND LOWEST VOLTAGE AT WHICH BREAKDOWN OCCURS.

(2) BASED ON ONE EXPERIMENT ONLY. SAMPLE 5 MILS THICK.

(3) BASED ON EXPERIMENT PERFORMED IN AIR.

(4) BASED PREDOMINANTLY ON MEASUREMENTS MADE WITH ELECTRON MICROSCOPE ON SMALL SIZE SAMPLES.

(5) ASSUME AREA DEPENDENCE UNCHANGED FOR WORST CASE MEASUREMENT.

(6) SAMPLE THICKNESS 1-2 MILS. BEAM VOLTAGES, 10 kV AND >15 kV.

(7) BASED ON SEVERAL EXPERIMENTS USING DIFFERENT TECHNIQUES AND CONFIGURATIONS.

(8) BASED ON TRW EXPERIMENT IN SWARM TUNNEL. SAMPLE EDGES FOLDED OVER METAL PLATE. WORST CASE FOR LARGE AREAS.

(9) NO BREAKDOWN VOLTAGES REPORTED. BASED ON BEAM VOLTAGE AT BREAKDOWN. SAMPLE THICKNESS 4-5 MILS.

(10) BASED ON MEASUREMENTS MADE WITH ELECTRON MICROSCOPE ON SMALL SIZE SAMPLES. WORST CASE FOR LARGE AREAS.

(11) BASED ON ONE EXPERIMENT ONLY. FUSED SILICA COVERGLASS - 12 MILS THICK - 14 kV BEAM VOLTAGE.

(12) BASED ON ONE EXPERIMENT ONLY. CERIA COVERGLASS - 12 MILS THICK - 20 kV BEAM VOLTAGE 18.5 X 25 CM SAMPLE.

(13) BASED ON ONE EXPERIMENT ONLY. HIGHER BREAKDOWN VOLTAGE IS ASSUMED TO BE WORST CASE.

(14) BASED ON ONE EXPERIMENT. 15 X 2.5 CM SAMPLE. SIX QUARTZ SSM'S - 8 MIL THICK - BEAM VOLTAGE 20 kV.

(15) BASED ON ONE EXPERIMENT. 5 MIL KAPTON BLANKETS.

(16) BASED ON ONE EXPERIMENT IN AIR. 5 MIL MYLAR BLANKET.

(17) NO DATA REPORTED.

The equation for I_{max}, or I_{arc}, gives the largest value for smallest t_p. Thus, the expression for area dependent t_p which gave the smaller t_p was used for the kapton thermal blanket:

$$t_p = 203\ A^{.292} = 3805 \text{ nanoseconds.}$$

The area of the thermal blanket (HGA OB Paint) was 22,857 cm^2 or 2.3 m^2. Using the above value for I_{max}, and the largest breakdown voltage, 12 kV, the peak arc current was obtained as

$$I_{arc} = \frac{.774\ CV}{t_p} = \frac{.774 \cdot 4 \cdot 10^{-7} \cdot 12 \cdot 10^{3}}{3805 \cdot 10^{-9}} = 977 \text{ amperes.}$$

For the best estimate case, the peak current was obtained from

$$I_{arc} = 9.9\ A^{.43} = 741 \text{ amperes,}$$

and the pulse width, t_p, was calculated using the 8 kV breakdown voltage as:

$$t_p = \frac{.774\ CV}{I_{arc}} = 3.3 \text{ microseconds.}$$

Using the Task 1.1 expression giving the largest t_p gives:

$$t_p = 44\ A^{.16} = 18.15 \text{ microseconds.}$$

This value of t_p was considered to be too large, and therefore the 6.9 microseconds value was used for the best estimate case, Run 12. Similarly, using the worst case expression for the peak current:

$$I_{arc} = .002\ A^{2.1} = 2.85 \cdot 10^{6} \text{ amperes}$$

gave a result which seemed to be much too large and therefore the 977 ampere current was used for the worst case, Run 11.

For the optical solar reflector (Brewster Plate), the capacitance and area, 20,000 pf and 571 cm^2 were retained unchanged. The pulse width, 300 nanoseconds, as obtained from the literature survey, as well as the worst and best estimate breakdown voltages, 7 kV and 2 kV, were used. The peak arc currents were computed as

$$I_{arc} = \frac{.774\ CV}{t_p} = 121 \text{ amperes and } 34.4 \text{ amperes.}$$

For the solar array (RTG Oxide), the area of 9714 cm^2 was retained, but the capacitance was reduced by a factor of 3 to .113 microfarads because solar cell coverglasses are typically 6 mils thickness rather than the 2 mils of the RTG oxide layer. As with the optical solar reflector, the literature survey value for t_p of 500 nanoseconds was used, and the peak arc current values calculated from the 9 kV and 1 kV breakdown voltages

$$I_{arc} = \frac{.774\ CV}{t_p} = 1575 \text{ amperes and } 43.8 \text{ amperes.}$$

Table 2-3 lists the generator parameters for the kapton thermal blanket, optical solar reflector and solar array as they were simulated for running on the Voyager SEMCAP model.*

Although only kapton thermal blankets were considered, the results for mylar and teflon could have been considered also. The worst case parameters are compared below as derived from the literature survey

	Kapton	Mylar	Teflon
Voltage (kilovolts)	12	9.4	12
I_{max} (amperes)	977	2232	4074
t_p (microseconds)	3.81	1.25	0.91

*A factor of 2 or 6 dB was inadvertently included in the magnitude of the arc current. The induced voltages shown in Tables 2-7, -8, -11, -12 and -14 through -18 are therefore high by a factor of two. To obtain the correct values, the induced voltages or currents should be decreased by a factor of 2 and the negative margins of immunity should be decreased by 6 dB as noted in the appropriate tables. These numerical corrections do not affect any of the conclusions resulting from the analysis.

Table 2-3. SEMCAP Generator Parameters for Runs 11 and 12

	Kapton Thermal Blanket	Optical Solar Reflector	Solar Array
RUN 11 (WORST CASE)			
$V_{Breakdown}$ (kilovolts)	12	7	9
Peak Current I_{arc} (amperes)	977	121	1575
Risetime t_r (nanoseconds)	380.5	30	50
Pulse Width t_p (nanoseconds)	3805	300	500
RUN 12 (BEST-ESTIMATE CASE)			
$V_{Breakdown}$ (kilovolts)	8	2	1
Peak Current I_{arc} (amperes)	741	34.4	43.8
Risetime t_r (nanoseconds)	330	30	200
Pulse Width t_p (nanoseconds)	3300	300	2000
PARAMETERS COMMON TO RUNS 11 AND 12			
Dielectric Thickness (mils)	2	6	6
Area (cm^2)	22,857	571	9,714
Capacitance C_x (μf)	0.4	0.02	0.113
Stray Capacitance C_f (pf)	500	12	90
G' (I_{repl}/I_{arc}) (ratio)	1.25E-3	1.8E-3	7.5E-4
L_{Boom} (μh)	0.4	0.25	2.8
G'' (V_{repl}/I_{arc}) (ohms)	1,250	1,250	11,000
f_c (mhz)	15.9	104	12
Loop Length (meters)	1.8	0.2	0.85
Loop Height (meters)	2E-4	.006	7.6E-5
Wire Radius (meters)	5E-5	5E-5	3.8E-5

For voltage related effects the induced voltages would not be materially affected. However, for current related coupling, the induced voltages on mylar would be roughly twice that for kapton, and four times larger for teflon.

2.2 TASK 2.2 - COUPLED VOLTAGES

The voltages coupled into the various receptor circuits are printed in the computer output of each SEMCAP run. For the Voyager spacecraft, 77 receptor circuits were modeled and these are shown in Table 2-4. As a part of the receptor characterization, the anomalous operation voltage threshold is listed for each receptor in Table 2-4. SEMCAP, as a part of its printout, lists db's of margin of the induced voltages for each threshold. Other parts of the printout summarize, in quickly recognizable form, those receptors for which margins are negative or near zero. It should be re-emphasized at this point that the three arcing sources modeled do not exist on Voyager. The Voyager SEMCAP model was used because it was available and had been used before for analysis of effects of arc discharges. Thus, the voltages coupled into the various receptors do not represent in any manner the actual voltages to be expected on Voyager in its encounter with the Jovian magnetosphere.

What these results do represent are examples of the induced voltages that would be expected for a spacecraft which is similar to Voyager if it had kapton thermal blankets, second surface mirrors and solar arrays with the characteristics assumed for this analysis. The coupling between the twelve generators and 77 receptors is defined by four different matrices involving all generators and receptors:

1. Close Coupling (DW) (Two 13 x 13 matrices)
2. Field Coupling (DF) (27 x 27 matrix)
3. Bulkhead Attenuation (FT) (27 x 27 matrix)
4. Common Resistance (RC) (Two 24 x 24 matrices)

These matrices have been retained unchanged for all of the cases considered. The actual numerical values for these matrices are available as a part of the computer printout for each SEMCAP run. Details of inputting the data for the coupling matrices and for reading the printouts are given in "SEMCAP Engineering Handbook Electromagnetic Compatibility Analysis Program, Version 7.3,

TABLE 2-4. VOYAGER PARAMETERS AND SUSCEPTIBILITY THRESHOLDS

RECEPTORS NO.	RECEPTORS NAME	WIRE TYPE	VOLTAGE THRESHOLD (VOLTS)	CUTOFF FREQUENCY (HZ)	SOURCE RESISTANCE (OHMS)	LOAD RESISTANCE (OHMS)	WIRE LENGTH (CM)	WIRE HEIGHT ABOVE GROUND (CM)	SOURCE CAPACITANCE (PF)	LOAD CAPACITANCE (PF)
1	TLM BAY 6 TEMP	24 TP	0.01	1.00 E8	5.00 E2	1.00 E6	380	1.00	5	1
2	S-TWTA HI/LO STAT	24 TP	2.00	1.00 E8	1.00 E7	3.90 E4	108	1.00	5	20
3	S-TWTAI ON STAT<	24 TP	10.00	1.00 E8	7.20 E4	4.50 E6	108	1.00	5	5
4	50.4 KHz % 02-06	24 SH	2.00	1.00 E8	7.50 E2	1.00 E4	210	1.00	20	5
5	TLM S-BAND TWT REG V	24 TP	0.01	1.00 E8	3.16 E3	1.00 E6	142	1.00	5	100,000
6	S-TWTA RF DR MONITOR	24 SH	0.01	1.00 E8	9.00 E3	6.00 E6	108	1.00	5	10,000
7	CMPST CMD, RCVR 1 TO CDU-A	24 TPS	0.01	1.00 E8	4.00 E3	1.00 E5	74	1.00	1	1
8	TLM S-BAND EX CURR	24 SC	0.01	1.00 E8	1.10 E3	2.20 E7	210	1.00	5	1,000,000
9	TLM RCVR VCO TEMP	24 TP	0.01	1.00 E8	7.00 E2	1.00 E6	210	1.00	5	1,200
10	TLM RCVR LO DR	24 TP	0.01	1.00 E8	4.50 E3	1.00 E6	210	1.00	5	10
11	TLM S-BAND TWT DR	24 TP	0.01	1.00 E8	3.90 E3	1.00 E6	210	1.00	5	5
12	CDU-A COMMAND DATA, XR	24 SC	2.0	1.00 E8	1.00 E6	1.00 E6	142	1.00	100	1
13	TMU A SYMBOL SYNC	24 SH	2.0	1.00 E8	5.00 E2	2.00 E3	176	1.00	5	5
14	HGH RATE CHAN DATA TMU-A	24 TP	1.5	1.00 E8	1.00 E2	2.00 E3	176	1.00	1	1
15	CC STROBE XR	24 SC	4.5	1.00 E8	1.00 E6	5.00 E3	74	1.00	10	1
16	CCS BIT SYNC 1	24 SC	4.5	1.00 E8	1.00 E6	1.00 E6	74	1.00	100	1
17	CCS DATA TO AACS XR	24 SC	4.0	1.00 E8	1.00 E6	3.60 E4	108	1.00	1	1
18	POWER CODE B XR	24 SC	1.2	1.00 E8	2.00 E2	1.00 E2	108	1.00	100	1
19	BOT/EOT XR	24 SC	1.2	1.00 E8	1.00 E6	1.00 E6	74	1.00	100	1
20	POWER CODE	24 SC	1.0	1.00 E8	1.00 E6	2.50 E5	108	1.00	300	300
21	POWER CODE	24 SC	1.0	1.00 E8	2.00 E1	1.00 E4	108	1.00	300	100
22	TLM SUN SENSOR TEMP	24 TP	0.01	1.00 E8	5.00 E2	1.00 E6	238	1.00	10	5
23	AACS DATA	24 SC	4.0	7.40 E4	1.00 E6	5.00 E3	74	1.00	10	5
24	AACS ADDRESS DATA	24 SC	2.0	1.00 E8	5.00 E2	2.00 E4	74	1.00	10	10
25	TLM PYRO AMP IND A	24 SC	4.0	7.40 E4	1.00 E6	5.00 E3	176	1.00	10	10
26	TLM TCAPU TANK TEMP 1	24 SH	0.01	1.00 E8	5.00 E2	1.00 E7	182	1.00	5	10
27	CC DATA 2	24 SH	4.0	1.00 E8	4.00 E2	7.50 E3	108	1.00	1	1
28	PLAYBACK DATA	24 SH	4.0	7.40 E4	1.00 E6	5.60 E4	108	1.00	1	1
29	TLM DSS MOTOR V	24 SC	0.01	1.00 E8	1.00 E2	1.00 E5	108	1.00	1	1
30	CRS CMD WORD	24 SC	4.0	8.20 E4	5.00 E2	5.60 E4	177	1.00	10	1
31	CRS TELESCOPE TEMP	24 TP	0.01	1.00 E8	5.00 E2	1.00 E6	177	1.00	5	1
32	PWS ADC BIT SYNC	24 TP	2.0	7.20 E5	5.00 E2	1.00 E4	180	1.00	47	10
33	PRA ANALOG MUX DATA	24 TP	0.01	1.00 E8	1.00 E3	1.00 E6	180	1.00	5	68
34	PRA ELECTRONICS TEMP	24 TP	0.01	1.00 E8	5.00 E2	1.00 E6	180	1.00	5	5
35	PRA CMD WORD	24 TP	2.0	1.00 E6	5.00 E2	1.00 E4	180	1.00	10	10
36	LECP CMD WORD A	24 SC	4.0	7.40 E4	5.00 E2	5.60 E4	177	1.00	10	5
37	LECP ANALOG DATA	24 SC	0.01	1.00 E8	4.00 E3	1.00 E6	177	1.00	5	1
38	PPS COMMAND WORD	24 SC	4.0	7.40 E4	5.00 E2	5.60 E4	373	1.00	10	5
39	PPS SOLAR SENSOR	24 SC	0.01	1.00 E8	5.00 E3	1.00 E6	373	1.00	5	1
40	UVS MODE CONTROL	24 SC	4.0	7.40 E4	5.00 E2	5.60 E4	393	1.00	10	5
41	UVS HV MONITOR	24 SC	0.01	1.00 E8	1.00 E4	1.00 E7	393	1.00	5	10
42	UVS SCIENCE DATA I	24 SC	2.0	7.40 E4	5.00 E2	5.60 E4	393	1.00	10	1
43	MAG SAMPLE B	24 SC	4.0	8.20 E4	5.00 E2	5.60 E4	176	1.00	10	1
44	MAG IBHFM CLOCK 50.4 KHz	24 SH	4.0	5.80 E5	5.00 E2	5.60 E4	176	1.00	5	1
45	MAG OBLFM SENSOR TEMP	24 TPS	0.01	6.00 E5	5.00 E2	1.00 E7	166.6	1.00	5	1
46	ISS-WA ADC START	24 TP	2.0	9.60 E5	5.00 E2	5.60 E4	368	1.00	10	1
47	ISS-WA ADC VIDEO DATA	24 TP	4.0	4.80 E5	5.00 E2	5.60 E4	368	1.00	10	1
48	ISS-NA ANALOG ENGR TLM	24 TP	0.01	1.00 E8	2.00 E3	1.00 E6	368	1.00	10	10
49	MAG OBLFM SENSOR TEMP	24 TPS	0.01	6.00 E5	5.00 E2	1.00 E7	386	1.00	5	1
50	IRIS FRAME START	24 SC	4.0	8.15 E4	5.00 E2	5.00 E3	388	1.00	5	5
51	IRIS RAD-MTR H-G ANALOG	24 SH	0.01	1.00 E8	8.00 E3	1.00 E7	368	1.00	5	5
52	IRIS PLL CARRIER	24 SH	0.2	1.00 E8	5.00 E2	5.00 E1	368	1.00	5	5
53	PITCH CRUISE SS/1 POSN	24 SH	0.01	4.50 E2	2.00 E2	1.00 E5	238	1.00	100,000	5
54	CSTI CONE ANGLE CMD A	24 SC	3.5	3.00 E2	6.80 E3	5.61 E4	215	1.00	1	1
55	CSTI STAR INTENSITY	24 SH	0.01	3.00 E2	1.00 E3	1.00 E5	215	1.00	1	1
56	CSTI CONE ANGLE POSITION	24 SC	0.8	3.00 E2	1.00 E4	1.00 E5	215	1.00	1	1
57	OBLFM X OUT % COAX <	SOLID	1.0 E7	1.00 E8	1.00 E1	1.60 E4	1490	1.00	5	100
58	IBHFM X OUT % COAX <	SOLID	9.99999 E7	1.00 E8	1.00 E1	1.60 E4	180	1.00	5	100
59	CRS ANALOG DATA	24 SC	0.01	1.00 E8	5.00 E2	1.00 E6	177	1.00	1	1
60	HGA S-BAND FEED TEMP	ALSTP	1.0	8.00 E4	5.00 E2	2.20 E7	402	1.00	6000	5
61	X-BAND FEED TEMP	ALSTP	1.0	8.00 E4	5.00 E2	2.20 E7	342	1.00	5000	5
62	IRIS SEC MIRROR TEMP	24 TP	1.0	1.00 E8	5.00 E2	2.20 E7	388	1.00	1000	10
63	IRIS SEC MIRROR HTR ANLG	24 SC	1.0	1.00 E8	1.00 E4	2.20 E7	388	1.00	1000	820
64	SS 1 SYNC	24 SH	1.0	1.60 E5	6.80 E3	2.00 E4	238	1.00	100	5
65	PITCH SS BIAS	24 SH	1.0	1.00 E1	1.00 E3	8.00 E4	238	1.00	5,000,000	5
66	RTG CASE TEMP	ALSTP	1.0	6.00 E5	5.00 E2	2.20 E7	280	1.00	5000	5
67	RTG POWER	ALFTP	1.0	1.00 E8	6.00 E0	1.00 E0	280	1.00	500,000,000	200
68	X-BAND FEED TEMP	ALSTP	1.0	8.00 E4	5.00 E2	2.20 E7	342	1.00	5	5
69	X-BAND FEED TEMP	ALSTP	1.0	8.00 E4	5.00 E2	2.20 E7	342	1.00	5	5
70	X-BAND FEED TEMP	ALSTP	1.0	8.00 E4	5.00 E2	2.20 E7	342	1.00	5	5
71	X-BAND FEED TEMP	ALSTP	1.0	8.00 E4	5.00 E2	2.20 E7	342	1.00	5,600	5
72	X-BAND FEED TEMP	ALSTP	1.0	8.00 E4	5.00 E2	3.00 E2	342	1.00	5	5
73	HGA DISH TEMP	ALSTP	1.0	8.00 E4	5.00 E2	2.20 E7	302	1.00	5	5
74	HGA DISH TEMP	ALSTP	1.0	8.00 E4	5.00 E2	2.20 E7	302	1.00	5	5
75	HGA DISH TEMP	ALSTP	1.0	8.00 E4	5.00 E2	2.20 E7	302	1.00	5	5
76	HGA DISH TEMP	ALSTP	1.0	8.00 E4	5.00 E2	2.20 E7	302	1.00	5,600	5
77	HGA DISH TEMP	ALSTP	1.0	8.00 E4	5.00 E2	3.00 E2	302	1.00	5	5

April 1973" by the TRW Electromagnetic Compatibility Department. These matrices are not all of the maximum size, 77 x 77, because many of the wires run in harnesses with common routing, and therefore the input information required is not as great as 77^2 or 5929 per matrix. Table 2-5 shows the common run separation matrix which has 13 x 13 elements. It may be noted, first of all, that a_{ij} and a_{ji} elements are equal. Furthermore, many other elements are identical in a systematic way. Table 2-6 shows all of the necessary array elements as they are put into the SEMCAP program.

Tables 2-7 and 2-8 are the voltages coupled into the 77 receptors by each of the three sources. There are six generators listed because each source was modeled as a replacement current generator and a close coupling "loop" generator. Table 2-7 (Run 11) is for the worst-case generator parameters, and Table 2-8 (Run 12) is for the best-estimate generator parameters. Also shown in Tables 2-7 and 2-8 are the threshold voltages for each receptor and the db margin of immunity if the margin is negative, i.e., the induced voltage is greater than the threshold.

The induced voltages for Run 8, the run with the arc parameters derived from the Boeing tests are shown in Table 2-9. 24 generators, for 12 sources, are included. In Table 2-10, the threshold voltage and the negative db margins for Run 8 are shown. Leaving out the positive margins permits easy visual identification of possibly hazardous induced voltage levels. The fact that negative db margins are shown in the tables is not necessarily an indication that a real hazard exists. In the first place, it must be recognized that the threshold voltage listed for each receptor is that level which gives an erroneous reading. In the temperature reading of Receptor No. 1 (TLM Bay 6 Temp), for example, the threshold of .01 volt probably represents one quantization increment of the telemetry system. It does not represent any damage threshold. Furthermore, in the case of temperature readings, for example, the probability that a perturbation occurs during readout is remote, and even more, successive readouts will indicate whether any particular readout was anomalous or not.

Another example in which negative margins should be viewed with similar caution are Receptors 57 and 58 (OBLFM X out coax and IBHFM X out coax), the coaxial signal cables from the outboard low-field and inboard

Table 2-5. One of the Two Close Coupling Parameter Matrices (DW)

(Common Run Separation Distance in Meters)

RECEPTORS ↓	GENERATORS → 1	2	3	4	5	6	7	8	9	10	11	12	13
1	.005	.049	.036	.2	.005	.008	.02	.15	.02	.01	.005	.004	.004
2	.049	.005	.023	.005	.005	.008	.02	.15	.02	.01	.005	.004	.004
3	.036	.023	.005	.005	.005	.008	.02	.15	.02	.01	.005	.004	.004
4	.2	.005	.005	.005	.02	.008	.02	.15	.02	.01	.2	.004	.004
5	.005	.005	.005	.02	.005	.008	.02	.15	.02	.01	.005	.004	.004
6	.008	.008	.008	.008	.008	.005	.02	.15	.02	.01	.005	.004	.004
7	.02	.02	.02	.02	.02	.02	.005	.15	.02	.01	.005	.004	.004
8	.15	.15	.15	.15	.15	.15	.15	.15	.02	.01	.005	.004	.004
9	.02	.02	.02	.02	.02	.02	.02	.02	.02	.01	.005	.004	.004
10	.01	.01	.01	.01	.01	.01	.01	.01	.01	.01	.005	.004	.004
11	.005	.005	.005	.005	.005	.005	.005	.005	.005	.005	.005	.004	.004
12	.004	.004	.004	.004	.004	.004	.004	.004	.004	.004	.004	.004	.004
13	.004	.004	.004	.004	.004	.004	.004	.004	.004	.004	.004	.004	.004

Table 2-6. DW Matrix Input Data for SEMCAP

DW ARRAY INPUT CARDS

	GEN CLASS		REC CLASS						
DW	1	13	1	13	4.00000E-03	1.00000E 00	0.0	0.0	
DW	12	12	2	2	4.00000E-03	1.00000E 00	0.0	0.0	
DW	2	2	12	12	4.00000E-03	1.00000E 00	0.0	0.0	
DW	1	11	1	11	5.00000E-03	1.00000E-01	0.0	0.0	
DW	1	10	1	10	1.00000E-02	1.00000E 00	0.0	0.0	
DW	1	9	1	9	2.00000E-02	1.00000E 00	0.0	0.0	
DW	1	8	1	8	1.50000E-01	1.00000E 00	0.0	0.0	A 1
DW	1	7	1	7	5.00000E-03	1.00000E 00	0.0	0.0	A 1
DW	2	2	1	1	4.90000E-02	3.16000E-01	0.0	0.0	B 2
DW	1	1	2	2	4.90000E-02	3.16000E-01	0.0	0.0	B 3
DW	3	3	1	1	3.60000E-02	1.00000E 00	0.0	0.0	C 4
DW	1	1	3	3	3.60000E-02	1.00000E 00	0.0	0.0	C 5
DW	2	2	3	3	2.30000E-02	3.16000E-01	0.0	0.0	D 6
DW	3	3	2	2	2.30000E-02	3.16000E-01	0.0	0.0	D 7
DW	6	6	1	5	8.00000E-03	1.00000E 00	0.0	0.0	E 8
DW	1	5	6	6	8.00000E-03	1.00000E 00	0.0	0.0	E 9
DW	7	7	1	6	2.00000E-02	1.00000E-02	0.0	0.0	F 10
DW	1	6	7	7	2.00000E-02	1.00000E-02	0.0	0.0	F 11
DW	5	5	4	4	2.00000E-01	3.16000E-01	0.0	0.0	G 12
DW	4	4	5	5	2.00000E-01	3.16000E-01	0.0	0.0	G 13
DW	1	1	4	4	2.00000E-01	1.00000E-01	0.0	0.0	
DW	4	4	1	1	2.00000E-01	1.00000E-01	0.0	0.0	
DW	1	1	5	5	5.00000E-03	1.00000E-01	0.0	0.0	
DW	5	5	1	1	5.00000E-03	1.00000E-01	0.0	0.0	
DW	4	4	11	11	2.00000E-01	1.00000E-01	0.0	0.0	
DW	11	11	4	4	2.00000E-01	1.00000E-01	0.0	0.0	
/	0	0	0	0	0.0	0.0	0.0	0.0	

FOLDOUT FRAME

FOLDOUT FRAME

Table 2-7. Voltage Thresholds, Induced Voltages, and Negative dB Margins of Immunity

Run 11 10/19/78

RECEPTORS			GENERATOR PARAMETERS											
			SECOND SURFACE MIRROR *				KAPTON THERMAL BLANKET				SOLAR ARRAY *			
			RECPL		LOOP		RECPL		LOOP		RECPL		LOOP	
NO.	NAME	VOLTAGE THRESHOLD												
1	TLM BAY 6 TEMP	0.01	1.52E-3		1.59E-1	-24	1.99E-2		1.84E-2	-5	1.57E-2	-4	6.17E-4	
2	S-TWTA HI/LO STAT	2.00	2.75E-6		4.42E-2		5.58E-3		5.67E-3		5.43E-3		8.06E-5	
3	S-TWTAI ON STAT<	10.00	8.24E-4		1.25E-1		8.76E-3		1.84E-2		5.75E-3		4.27E-4	
4	50.4 KHz % 02-06	2.00	8.10E-3		6.76E-1		3.36E-2		1.03E-1		4.28E-3		3.09E-3	
5	TLM S-BAND TWT REG V	0.01	1.69E-6		1.67E-2	-4	6.21E-3		3.83E-4	-16	6.54E-3		1.74E-5	
6	S-TWTA RF DR MONITOR	0.01	5.28E-3		4.31E-1	-33	2.00E-2		6.38E-2		2.28E-3		2.03E-3	
7	CMPST CMD, RCVR 1 TO CDU-A	0.01	7.43E-5		2.88E-2	-9	2.54E-3		3.12E-3	-21	2.04E-3		6.98E-5	
8	TLM S-BAND EX CURR	0.01	8.87E-3		7.16E-1	-37	4.23E-2		1.12E-1		1.09E-2	-1	3.38E-3	
9	TLM RCVR VCO TEMP	0.01	1.35E-4		3.34E-2	-11	9.42E-3		2.36E-3	-4	9.45E-3		7.75E-5	
10	TLM RCVR LO DR	0.01	1.14E-3		1.33E-1	-22	1.38E-2		1.65E-2	-4	1.01E-2		4.96E-4	
11	TLM S-BAND TWT DR	0.01	1.18E-3		1.35E-1	-23	1.39E-2		1.66E-2		1.01E-2		5.07E-4	
12	CDU-A COMMAND DATA, XR	2.00	3.29E-3		3.10E-1		1.85E-2		4.94E-2		7.31E-3		1.34E-3	
13	TMU A SYMBOL SYNC	2.00	1.68E-3		1.43E-1		9.54E-3		2.31E-2		3.08E-3		6.55E-4	
14	HGH RATE CHAN DATA TMU-A	1.50	4.50E-4		5.76E-2		9.04E-3		4.46E-3		8.36E-3		1.89E-4	
15	CC STROBE XR	4.50	1.92E-5		2.29E-2		4.02E-3		1.57E-3		3.80E-3		3.92E-5	
16	CCS BIT SYNC 1	4.50	1.93E-3		1.87E-1		9.99E-3		2.81E-2		3.66E-3		7.98E-4	
17	CCS DATA TO AACS XR	4.00	1.79E-4		6.60E-2		6.72E-3		8.13E-3		5.78E-3		1.62E-4	
18	POWER CODE B XR	1.20	1.26E-3		1.09E-1		9.92E-3		1.72E-2		5.20E-3		4.91E-4	
19	BOT/EOT XR	1.20	1.93E-3		1.87E-1		9.99E-3		2.81E-2		3.66E-3		7.98E-4	
20	POWER CODE	1.00	1.06E-3		1.07E-1		8.54E-3		1.53E-2		5.15E-3		4.37E-4	
21	POWER CODE	1.00	5.20E-3		4.32E-1		2.33E-2		6.31E-2		5.83E-3		2.00E-3	
22	TLM SUN SENSOR TEMP	0.01	6.65E-4		1.68E-2	5	2.79E-3		2.84E-3		6.39E-3		3.06E-4	
23	AACS DATA	4.00	1.79E-7		2.08E-3		1.94E-5		4.53E-4		6.10E-6		4.79E-6	
24	AACS ADDRESS DATA	2.00	3.74E-3		3.20E-1		1.64E-2		4.47E-2		4.17E-3		1.46E-3	
25	TLM PYRO AMP IND A	4.00	4.05E-7		4.30E-3		3.62E-5		9.92E-4		1.21E-5		1.00E-5	
26	TLM TCAPU TANK TEMP 1	0.01	7.97E-3		6.37E-1	-36	3.16E-2		9.95E-2	-20	3.46E-3		3.04E-3	
27	CC DATA 2	4.00	1.17E-3		1.01E-1		6.06E-3		1.53E-2		1.79E-3		4.58E-4	
28	PLAYBACK DATA	4.00	2.73E-6		1.50E-2		7.09E-5		4.84E-3		5.12E-6		3.77E-5	
29	TLM DSS MOTOR V	0.01	5.28E-3		4.40E-1	-33	2.37E-2		6.38E-2	-16	6.11E-3		2.04E-3	
30	CRS CMD WORD	4.00	6.61E-6		3.66E-4		2.39E-5		7.78E-5		2.47E-6		3.37E-6	
31	CRS TELESCOPE TEMP	0.01	4.97E-5		5.31E-3		1.72E-4		1.59E-4		6.87E-4		3.00E-5	
32	PWS ADC BIT SYNC	2.00	1.39E-4		1.26E-2		1.05E-3		3.26E-3		1.22E-4		6.22E-5	
33	PRA ANALOG MUX DATA	0.01	6.97E-4		8.14E-2	-18	1.04E-2		8.61E-3		8.57E-3		2.94E-4	
34	PRA ELECTRONICS TEMP	0.01	9.28E-4		9.96E-2	-20	1.10E-2		1.01E-2		8.76E-3		3.76E-4	
35	PRA CMD WORD	2.00	8.95E-5		9.82E-3		7.39E-4		2.11E-3		1.58E-4		4.27E-5	
36	LECP CMD WORD A	4.00	4.27E-6		3.40E-4		2.25E-5		7.33E-5		2.28E-6		3.13E-6	
37	LECP ANALOG DATA	0.01	4.10E-4		3.43E-2	-11	5.83E-4		1.54E-3		7.90E-4		2.37E-4	
38	PPS COMMAND WORD	4.00	8.37E-6		6.65E-4		4.66E-5		1.52E-4		4.45E-6		6.22E-6	
39	PPS SOLAR SENSOR	0.01	6.96E-4		5.66E-2	-15	1.07E-3		2.82E-3		1.39E-3		4.00E-4	

*VOLTAGES SHOULD BE DIVIDED BY 2 AND NEGATIVE MARGINS BY 6 dB.

Table 2-7. Voltage Thresholds, Induced Voltages, and Negative dB Margins of Immunity (Cont)

Run 11 10/19/78

RECEPTORS			GENERATOR PARAMETERS											
			SECOND SURFACE MIRROR *				KAPTON THERMAL BLANKET				SOLAR ARRAY *			
			RECPL		LOOP		RECPL		LOOP		RECPL		LOOP	
NO.	NAME	VOLTAGE THRESHOLD												
40	UVS MODE CONTROL	4.00	8.77E-6		6.96E-4		4.90E-5		1.60E-4		4.66E-6		6.52E-6	
41	UVS HV MONITOR	0.01	7.24E-4		5.91E-2	-15	1.12E-3		2.98E-3		1.44E-3		4.18E-4	
42	UVS SCIENCE DATA I	2.00	8.77E-6		6.96E-4		4.90E-5		1.60E-4		4.66E-6		6.53E-6	
43	MAG SAMPLE B	4.00	8.69E-5		6.90E-3		1.52E-3		4.95E-3		3.11E-5		4.25E-5	
44	MAG IBHFM CLOCK 50.4 KHz	4.00	5.52E-4		4.18E-2		6.46E-3		2.09E-2		1.45E-4		2.53E-4	
45	MAG OBLFM SENSOR TEMP	0.01	1.93E-8		3.53E-6		2.04E-6		5.35E-6		3.08E-3		3.62E-4	
46	ISS-WA ADC START	2.00	9.02E-6		9.54E-4		2.46E-5		7.28E-5		2.23E-5		6.55E-6	
47	ISS-WA ADC VIDEO DATA	4.00	4.79E-6		5.71E-4		1.43E-5		4.60E-5		1.14E-5		3.75E-6	
48	ISS-NA ANALOG ENGR TLM	0.01	9.38E-5		9.88E-3		3.32E-4		3.84E-4		1.21E-3		5.82E-5	
49	MAG OBLFM SENSOR TEMP	0.01	1.68E-6		3.32E-4		2.71E-6		1.10E-5		1.17E-3		3.80E-4	
50	IRIS FRAME START	4.00	8.05E-6		6.39E-4		4.45E-5		1.45E-4		4.44E-6		5.99E-6	
51	IRIS RAD-MTR H-G ANALOG	0.01	6.93E-4		5.39E-2	-15	8.71E-4		2.76E-3		3.97E-4		3.93E-4	
52	IRIS PLL CARRIER	0.20	9.40E-6		1.14E-3		7.59E-5		5.08E-5		3.29E-4		6.25E-6	
53	PITCH CRUISE SS/1 POSN	0.01	8.74E-8		6.88E-6		2.88E-6		9.43E-6		1.30E-7		2.02E-7	
54	CSTI CONE ANGLE CMD A	3.50	3.78E-7		1.24E-4		8.16E-6		6.02E-5		3.89E-7		4.15E-7	
55	CSTI STAR INTENSITY	0.01	4.19E-7		5.05E-5		8.69E-6		3.48E-5		1.61E-7		2.50E-7	
56	CSTI CONE ANGLE POSITION	0.60	3.85E-7		1.66E-4		8.33E-6		7.73E-5		3.92E-7		5.21E-7	
57	OBLFM X OUT % COAX <	1.00E-7	7.74E-8		2.10E-5	-46	3.34E-5	-50	6.58E-6	-36	1.62E-1	-124	1.30E-3	-82
58	IBHFM X OUT % COAX <	9.99E-7	4.93E-6	-14	7.11E-4	-57	1.78E-5	-25	7.14E-6	-17	3.78E-2	- 92	7.27E-4	-57
59	CRS ANALOG DATA	0.01	4.11E-4		3.37E-2	-11	5.80E-4		1.52E-3		7.80E-4		2.35E-4	
60	HGA S-BAND FEED TEMP	1.00	6.79E-6		5.16E-4		5.92E-4		1.91E-3		2.78E-8		4.09E-8	
61	X-BAND FEED TEMP	1.00	5.74E-6		4.41E-4		1.54E-4		5.00E-4		2.05E-6		3.00E-6	
62	IRIS SEC MIRROR TEMP	1.00	5.62E-4		4.50E-2		8.50E-4		2.08E-3		1.36E-3		3.18E-4	
63	IRIS SEC MIRROR HTR ANLG	1.00	7.18E-4		5.70E-2		1.09E-3		2.88E-3		1.40E-3		4.09E-4	
64	SS 1 SYNC	1.00	2.06E-5		1.91E-3		5.09E-4		1.79E-3		2.57E-5		4.96E-5	
65	PITCH SS BIAS	1.00	2.37E-9		2.12E-7		6.25E-8		2.08E-7		5.50E-9		5.39E-9	
66	RTG CASE TEMP	1.00	4.09E-5		3.01E-3		4.77E-4		1.53E-3		3.03E-1		2.99E-1	
67	RTG POWER	1.00	6.55E-6		8.89E-4		4.67E-4		2.37E-4		3.22E-1		7.80E-2	
68	X-BAND FEED TEMP	1.00	7.59E-8		8.88E-5		2.26E-6		1.92E-5		8.11E-7		2.23E-7	
69	X-BAND FEED TEMP	1.00	7.59E-8		8.88E-5		2.26E-6		1.92E-5		8.11E-7		2.23E-7	
70	X-BAND FEED TEMP	1.00	7.59E-8		8.88E-5		2.26E-6		1.92E-5		8.11E-7		2.23E-7	
71	X-BAND FEED TEMP	1.00	5.82E-6		4.45E-4		1.59E-4		5.15E-4		2.07E-6		3.04E-6	
72	X-BAND FEED TEMP	1.00	1.71E-8		3.58E-5		1.15E-6		6.91E-6		7.27E-7		8.42E-8	
73	HGA DISH TEMP	1.00	2.73E-7		3.00E-4		2.82E-7		2.41E-6		2.96E-7		8.68E-8	
74	HGA DISH TEMP	1.00	2.73E-7		3.00E-4		2.82E-7		2.41-6		2.96E-7		8.68E-8	
75	HGA DISH TEMP	1.00	2.73E-7		3.00E-4		2.81E-7		2.41E-6		2.96E-7		8.68E-8	
76	HGA DISH TEMP	1.00	1.91E-5		1.46E-3		1.86E-5		6.04E-5		7.47E-7		1.11E-6	
77	HGA DISH TEMP	1.00	6.16E-8		1.20E-4		1.41E-7		8.63E-7		2.61E-7		3.26E-8	

*VOLTAGES SHOULD BE DIVIDED BY 2 AND NEGATIVE MARGINS BY 6 dB.

Table 2-8. Voltage Thresholds, Induced Voltages, and Negative dB Margins of Immunity

Run 12 10/20/78

RECEPTORS			GENERATOR PARAMETERS											
			SECOND SURFACE MIRROR *				KAPTON THERMAL BLANKET				SOLAR ARRAY *			
		VOLTAGE	RECPL		LOOP		RECPL		LOOP		RECPL		LOOP	
NO.	NAME	THRESHOLD												
1	TLM BAY 6 TEMP	0.01	2.66E-3		4.55E-2	-13	4.15E-3		6.37E-1	-36	1.16E-4		1.77E-3	
2	S-TWTA HI/LO STAT	2.00	8.09E-4		1.26E-2		1.15E-3		2.71E-0	-3	4.04E-5		4.64E-3	
3	S-TWTA ON STAT<	10.00	1.07E-3		3.57E-2		1.89E-3		4.25E-0		4.38E-5		6.94E-3	
4	50.4 KHz % 02-06	2.00	2.73E-3		1.84E-1		7.80E-3		4.23E-1		3.76E-5		9.16E-4	
5	TLM S-BAND TWT REG V	0.01	9.64E-4		4.70E-3		1.26E-3		1.38E-1	-23	4.71E-5		4.77E-4	
6	S-TWTA RF DR MONITOR	0.01	1.72E-3		1.23E-1	-22	4.61E-3		1.64E-1	-24	1.99E-5		2.72E-4	
7	CMPST CMD, RCVR 1 TO CDU-A	0.01	3.25E-4		8.23E-3		5.36E-4		1.05E-0	-40	1.61E-5		2.09E-3	
8	TLM S-BAND EX CURR	0.01	3.90E-3		2.05E-1	-26	9.63E-3		1.98E-1	-26	8.56E-5		6.61E-4	
9	TLM RCVR VCO TEMP	0.01	1.41E-3		9.89E-3		1.93E-3		3.04E-1	-30	6.86E-5		8.61E-4	
10	TLM RCVR LO DR	0.01	1.77E-3		3.79E-2	-12	2.91E-3		1.35E-0	-43	7.52E-5		2.91E-3	
11	TLM S-BAND TWT DR	0.01	1.78E-3		3.84E-2	-12	2.94E-3		1.26E-0	-42	7.55E-5		2.77E-3	
12	CDU-A COMMAND DATA, XR	2.00	1.93E-3		8.84E-2		4.13E-3		5.15E-0	-8	5.56E-5		6.55E-3	
13	TMU A SYMBOL SYNC	2.00	8.87E-4		4.08E-2		2.20E-3		3.11E-1		2.42E-5		7.30E-4	
14	HGH RATE CHAN DATA TMU-A	1.50	1.34E-3		1.64E-2		1.85E-3		1.95E-1		6.08E-5		6.54E-4	
15	CC STROBE XR	4.50	5.81E-4		6.54E-3		8.30E-4		5.70E-1		2.84E-5		1.32E-3	
16	CCS BIT SYNC 1	4.50	1.06E-3		5.34E-2		2.22E-3		2.95E-0		2.78E-5		3.80E-3	
17	CCS DATA TO AACS XR	4.00	9.06E-4		1.89E-2		1.41E-3		2.78E-0		4.39E-5		5.12E-3	
18	POWER CODE B XR	1.20	1.10E-3		3.10E-2		2.19E-3		1.07E-1		3.85E-5		3.64E-4	
19	BOT/EOT XR	1.20	1.06E-3		5.34E-2		2.22E-3		2.95E-0	-8	2.78E-5		3.80E-3	
20	POWER CODE	1.00	1.06E-3		3.04E-2		1.85E-3		1.41E-0	-3	3.79E-5		1.94E-3	
21	POWER CODE	1.00	2.23E-3		1.23E-1		5.27E-3		1.20E-1		4.54E-5		4.08E-4	
22	TLM SUN SENSOR TEMP	0.01	2.44E-4		4.81E-3		5.81E-4		8.44E-2	-19	4.72E-5		7.18E-4	
23	AACS DATA	4.00	9.27E-7		5.84E-4		5.26E-6		2.20E-1		7.81E-8		3.41E-4	
24	AACS ADDRESS DATA	2.00	1.61E-3		9.18E-2		3.71E-3		1.60E-1		3.27E-5		4.72E-4	
25	TLM PYRO AMP IND A	4.00	1.82E-6		1.23E-3		9.98E-6		4.87E-1		1.43E-7		7.36E-4	
26	TLM TCAPU TANK TEMP 1	0.01	2.58E-3		1.82E-1	-25	7.34E-3		2.29E-1	-27	3.10E-5		5.18E-4	
27	CC DATA 2	4.00	5.72E-4		2.89E-2		1.40E-3		1.78E-1		1.42E-5		4.36E-4	
28	PLAYBACK DATA	4.00	1.39E-6		4.28E-3		2.31E-5		2.59E-0		1.03E-7		3.23E-3	
29	TLM DSS MOTOR V	0.01	2.28E-3		1.26E-1	-22	5.36E-3		1.44E-1	-23	4.76E-5		4.68E-4	
30	CRS CMD WORD	4.00	1.40E-6		1.04E-4		7.88E-6		9.40E-4		5.05E-8		7.64E-6	
31	CRS TELESCOPE TEMP	0.01	7.98E-5		1.52E-3		3.55E-5		5.46E-3		5.07E-6		7.91E-5	
32	PWS ADC BIT SYNC	2.00	5.33E-5		3.58E-3		2.56E-4		1.28E-1		1.25E-6		2.57E-4	
33	PRA ANALOG MUX DATA	0.01	1.43E-3		2.33E-3	-7	2.16E-3		4.50E-1	-33	6.29E-5		1.18E-3	
34	PRA ELECTRONICS TEMP	0.01	1.52E-3		2.84E-2	-9	2.29E-3		3.52E-1	-31	6.46E-5		1.10E-3	
35	PRA CMD WORD	2.00	4.59E-5		2.81E-3		1.75E-4		1.46E-1		1.48E-6		3.07E-4	
36	LECP CMD WORD A	4.00	1.29E-6		9.70E-5		7.47E-6		9.26E-4		4.71E-8		7.43E-6	
37	LECP ANALOG DATA	0.01	1.84E-4		9.79E-3		1.33E-4		1.62E-2	-4	8.28E-6		1.85E-4	
38	PPS COMMAND WORD	4.00	2.53E-6		1.90E-4		1.55E-5		1.91E-3		9.53E-8		1.52E-5	
39	PPS SOLAR SENSOR	0.01	3.15E-4		1.62E-2	-4	2.46E-4		3.18E-2	-10	1.11E-5		3.35E-4	

*VOLTAGES SHOULD BE DIVIDED BY 2 AND NEGATIVE MARGINS BY 6 dB.

Table 2-8. Voltage Thresholds, Induced Voltages, and Negative dB Margins of Immunity (Cont)

Run 12 10/20/78

RECEPTORS			GENERATOR PARAMETERS											
			SECOND SURFACE MIRROR *				KAPTON THERMAL BLANKET				SOLAR ARRAY *			
			RECPL		LOOP		RECPL		LOOP		RECPL		LOOP	
NO.	NAME	VOLTAGE THRESHOLD												
40	UVS MODE CONTROL	4.00	2.65E-6		1.99E-4		1.63E-5		2.01E-3		1.00E-7		1.59E-5	
41	UVS HV MONITOR	0.01	3.27E-4		1.69E-2	-5	2.57E-4		7.74E-2	-14	1.15E-5		4.54E-4	
42	UVS SCIENCE DATA 1	2.00	2.65E-6		1.99E-4		1.63E-5		2.01E-3		1.00E-7		1.60E-5	
43	MAG SAMPLE B	4.00	2.64E-5		1.97E-3		5.01E-4		5.99E-2		6.36E-7		9.67E-5	
44	MAG IBHFM CLOCK 50.4 KHz	4.00	1.61E-4		1.19E-2		1.87E-3		1.39E-1		2.87E-6		2.60E-4	
45	MAG OBLFM SENSOR TEMP	0.01	2.18E-8		1.01E-6		5.07E-7		7.26E-4		2.98E-5		6.56E-3	
46	ISS-WA ADC START	2.00	4.44E-6		2.73E-4		5.99E-6		4.48E-3		2.15E-7		4.61E-5	
47	ISS-WA ADC VIDEO DATA	4.00	2.31E-6		1.63E-4		3.60E-6		3.93E-3		1.14E-7		3.84E-5	
48	ISS-NA ANALOG ENGR TLM	0.01	1.42E-4		2.82E-3		7.03E-5		1.97E-2	-6	9.06E-6		2.30E-4	
49	MAG OBLFM SENSOR TEMP	0.01	9.37E-7		9.48E-5		6.23E-7		2.19E-3		1.19E-5		8.77E-3	
50	IRIS FRAME START	4.00	2.45E-6		1.83E-4		1.47E-5		1.76E-3		9.27E-8		1.42E-5	
51	IRIS RAD-MTR H-G ANALOG	0.01	2.19E-4		1.54E-2	-4	2.05E-4		1.41E-2	-3	3.77E-6		1.17E-4	
52	IRIS PLL CARRIER	0.20	3.39E-5		3.26E-4		1.62E-5		1.86E-3		2.43E-6		2.71E-5	
53	PITCH CRUISE SS/1 POSN	0.01	2.62E-8		1.96E-6		1.06E-6		1.55E-4		3.06E-9		4.46E-7	
54	CSTI CONE ANGLE CMD A	3.50	1.57E-7		3.55E-5		2.96E-6		2.16E-2		5.01E-9		2.25E-5	
55	CSTI STAR INTENSITY	0.01	1.30E-7		1.44E-5		3.20E-6		4.22E-3		3.55E-9		4.40E-6	
56	CSTI CONE ANGLE POSITION	0.60	1.59E-7		4.74E-5		3.02E-6		3.19E-2		5.12E-9		3.29E-5	
57	OBLFM X OUT % COAX <	1.00E-7	8.78E-7	-19	6.00E-6	-36	6.85E-6	-37	8.98E-4	-79	1.24E-3	-82	1.51E-2	-104
58	IBHFM X OUT % COAX <	9.99E-7	1.80E-5	-25	2.03E-4	-46	3.62E-6	-11	3.24E-4	-50	2.74E-4	-49	2.54E-3	-68
59	CRS ANALOG DATA	0.01	1.83E-4		9.64E-3		1.32E-4		5.39E-3		6.14E-6		7.73E-5	
60	HGA S-BAND FEED TEMP	1.00	2.05E-6		1.47E-4		2.19E-4		1.41E-2		7.55E-10		1.54E-7	
61	X-BAND FEED TEMP	1.00	1.72E-6		1.26E-4		5.61E-5		4.46E-3		5.36E-8		6.02E-6	
62	IRIS SEC MIRROR TEMP	1.00	2.78E-4		1.29E-2		1.89E-4		7.97E-3		1.05E-5		1.11E-4	
63	IRIS SEC MIRROR HTR ANLG	1.00	3.22E-4		1.63E-2		2.52E-4		1.50E-2		1.11E-5		1.49E-4	
64	SS 1 SYNC	1.00	6.00E-6		5.47E-4		1.81E-4		8.64E-2		6.06E-7		3.74E-4	
65	PITCH SS BIAS	1.00	7.87E-10		6.05E-8		2.27E-8		5.81E-6		8.40E-11		1.63E-8	
66	RTG CASE TEMP	1.00	1.24E-5		8.59E-4		1.38E-4		7.01E-3		6.68E-3		2.97E-2	
67	RTG POWER	1.00	6.47E-5		2.54E-4		1.02E-4		4.35E-3		2.98E-3		1.54E-2	
68	X-BAND FEED TEMP	1.00	1.33E-7		2.54E-5		5.95E-7		7.93E-3		8.06E-9		1.30E-5	
69	X-BAND FEED TEMP	1.00	1.33E-7		2.54E-5		5.75E-7		7.43E-3		8.06E-9		1.30E-5	
70	X-BAND FEED TEMP	1.00	1.33E-7		2.54E-5		5.95E-7		7.93E-3		8.06E-9		1.30E-5	
71	X-BAND FEED TEMP	1.00	1.75E-6		1.27E-4		5.82E-5		4.30E-3		5.49E-8		5.76E-6	
72	X-BAND FEED TEMP	1.00	1.07E-7		1.02E-5		2.70E-7		3.08E-3		6.37E-9		5.12E-6	
73	HGA DISH TEMP	1.00	4.40E-7		8.57E-5		7.39E-8		9.93E-4		2.98E-9		5.01E-6	
74	HGA DISH TEMP	1.00	4.40E-7		8.57E-5		7.39E-8		9.93E-4		2.98E-9		5.10E-6	
75	HGA DISH TEMP	1.00	4.40E-7		8.57E-5		7.39E-8		9.93E-4		2.98E-9		5.10E-6	
76	HGA DISH TEMP	1.00	5.71E-6		4.16E-4		6.76E-6		5.35E-4		1.95E-8		2.20E-6	
77	HGA DISH TEMP	1.00	3.43E-7		3.43E-5		3.30E-8		3.84E-4		2.31E-9		1.97E-6	

*VOLTAGES SHOULD BE DIVIDED BY 2 AND NEGATIVE MARGINS BY 6 dB.

FOLDOUT FRAME 1

FOLDOUT FRAME 2

TABLE 2-9. TABLE OF INDUCED VOLTAGES. RUN 8, 6-17-78

RECEPTORS		GENERATOR PARAMETERS																					
		BREWSTER PLATE		MAG CABLE		SEP CONN		MAG TEFLON		HGA OB PAINT		PLUME SH SEP CONN		LECP TEFLON		FSS		HGA IB PAINT		PLUME SH RTG		RTG OXIDE		MIRIS KAPTON	
NO.	NAME	RECPL	LOOP	RECPL	LOOP	RECPL	LOOP	RECPL	LOOP	RECPL	LOOP	RECPL	LOOP	RECPL	LOOP	RECPL	LOOP	RECPL	LOOP	RECPL	LOOP	RECPL	LOOP	RECPL	LOOP
1	TLM BAY 6 TEMP	1.21E-4	1.02E-1	8.17E-5	3.27E-5	2.46E-2	8.27E-2	2.33E-2	6.18E-4	5.03E-3	1.99E-2	7.87E-5	2.67E-5	2.82E-4	6.43E-4	4.68E-2	2.51E-3	3.42E-3	1.99E-2	1.16E-4	2.78E-5	1.56E-4	3.04E-4	1.98E-2	4.25E-6
2	S-TWTA HI/LO STAT	4.54E-5	5.01E-2	2.67E-5	4.34E-5	9.62E-3	5.15E-2	8.48E-3	3.71E-4	9.84E-4	6.21E-4	3.23E-5	2.22E-5	1.00E-4	3.64E-4	1.46E-2	1.05E-3	0 9.09E-4	6.88E-4	3.96E-5	2.34E-5	-5.49E-5	1.36E-5	6.58E-3	1.28E-6
3	S-TWTAI ON STAT<	4.92E-5	5.48E-2	3.34E-5	7.27E-5	9.77E-3	7.03E-2	8.64E-3	4.50E-4	2.30E-3	1.29E-2	3.28E-5	3.59E-5	1.03E-4	4.30E-4	1.63E-2	1.81E-3	1.35E-3	1.30E-2	4.22E-5	3.87E-5	7.74E-5	1.92E-4	7.40E-3	2.68E-6
4	50.4 KHz % 02-06	5.16E-5	2.97E-2	2.31E-5	8.73E-5	5.20E-3	6.80E-2	4.55E-3	2.08E-4	1.31E-2	1.08E-1	1.89E-5	5.67E-5	8.08E-5	1.54E-4	1.51E-2	5.32E-3	4.84E-3	1.09E-1	3.73E-5	6.39E-5	1.50E-4	1.64E-3	5.97E-3	1.25E-6
5	TLM S-BAND TWT REG V	5.60E-5	5.01E-2	1.48E-5	5.07E-6	1.19E-2	2.70E-2	1.06E-2	2.60E-4	8.62E-4	6.88E-5	3.94E-5	5.69E-6	1.24E-4	2.64E-4	1.68E-2	7.09E-4	1.05E-3	7.73E-5	4.80E-5	5.48E-6	3.32E-5	1.43E-6	6.74E-3	9.05E-7
6	S-TWTA RF DR MONITOR	3.44E-5	1.90E-2	8.20E-6	5.69E-5	3.09E-3	4.34E-2	2.44E-3	1.06E-4	7.84E-3	7.70E-2	1.04E-5	3.62E-5	3.29E-5	6.63E-5	7.69E-3	3.72E-3	2.79E-3	7.88E-2	1.83E-5	4.09E-5	7.74E-5	1.11E-3	2.81E-3	9.20E-6
7	CMPST CMD, RCVR 1 TO CDU-A	1.54E-5	2.08E-2	2.02E-5	2.09E-5	3.18E-3	2.98E-2	2.88E-3	1.96E-4	6.77E-4	1.42E-3	1.03E-5	1.26E-5	3.60E-5	1.89E-4	6.401E-3	5.67E-4	4.12E-4	1.45E-3	1.48E-5	1.33E-5	4.11E-5	2.14E-5	3.30E-3	7.85E-7
8	TLM S-BAND EX CURR	1.09E-4	7.51E-2	3.33E-6	9.32E-5	1.58E-2	9.19E-2	1.51E-2	4.03E-4	1.50E-2	1.19E-1	5.48E-6	6.31E-5	1.86E-4	3.63E-4	3.28E-2	8.38E-3	5.90E-3	1.19E-1	8.30E-3	7.05E-5	1.84E-4	1.80E-3	1.28E-2	1.45E-5
9	TLM RCVR VCO TEMP	7.65E-5	6.60E-2	2.51E-5	1.02E-5	1.62E-2	3.99E-2	1.49E-2	3.49E-4	1.54E-3	1.92E-2	5.26E-6	9.54E-6	1.76E-4	3.89E-4	2.57E-2	1.05E-3	1.62E-3	1.93E-3	6.97E-5	9.46E-6	5.88E-5	2.94E-5	1.04E-2	1.44E-6
10	TLM RCVR LO DR	8.11E-5	7.42E-2	4.43E-5	3.99E-5	1.64E-2	7.01E-2	1.51E-2	4.93E-4	3.45E-3	1.58E-2	5.33E-5	2.72E-5	1.82E-4	4.95E-4	2.88E-2	2.03E-3	2.23E-3	1.59E-3	7.43E-5	2.87E-5	1.00E-4	2.39E-4	1.24E-4	3.39E-6
11	TLM S-BAND TWT DR	8.13E-5	7.43E-2	4.52E-5	3.90E-5	1.64E-2	7.03E-2	1.52E-2	4.94E-4	3.52E-3	1.63E-2	5.33E-5	2.71E-5	1.82E-4	4.96E-4	2.90E-2	2.04E-3	2.26E-3	1.63E-2	7.46E-5	2.86E-5	1.10E-4	2.45E-4	1.25E-2	3.45E-6
12	CDU-A COMMAND DATA, XR	6.95E-5	6.06E-2	2.57E-5	8.03E-5	1.22E-2	7.27E-2	1.08E-2	4.07E-4	5.91E-3	4.73E-2	4.05E-5	4.44E-5	1.30E-4	3.80E-4	2.05E-2	3.24E-3	2.71E-3	4.72E-2	5.45E-5	4.88E-5	9.33E-5	7.00E-4	8.36E-3	6.36E-6
13	TMU A SYMBOL SYNC	2.79E-5	2.29E-2	1.65E-5	2.35E-5	4.75E-3	2.91E-2	4.28E-3	1.56E-4	3.18E-3	2.23E-2	1.55E-5	1.61E-5	5.21E-5	1.48E-4	9.20E-3	1.39E-3	1.30E-3	2.22E-2	2.30E-5	1.76E-5	5.57E-5	3.42E-4	4.01E-3	2.94E-6
14	HGH RATE CHAN DATA TMU-A	8.94E-5	5.93E-2	2.49E-5	1.19E-5	1.43E-2	3.92E-2	1.30E-2	3.17E-4	1.77E-3	7.29E-3	4.67E-5	1.08E-5	1.65E-4	3.32E-4	2.30E-2	1.21E-3	1.59E-3	7.38E-3	6.17E-5	1.08E-5	5.98E-5	9.87E-5	9.46E-3	2.01E-6
15	CC STROBE XR	3.26E-5	3.58E-2	2.19E-5	1.35E-5	6.83E-3	3.21E-2	5.92E-3	2.47E-4	7.92E-4	4.45E-4	2.36E-5	1.01E-5	7.05E-5	2.47E-4	1.05E-2	6.96E-4	6.62E-4	4.69E-4	2.77E-5	1.04E-5	4.52E-5	7.41E-5	4.97E-3	8.67E-7
16	CCS BIT SYNC 1	3.95E-5	3.83E-2	1.28E-5	5.41E-5	6.71E-3	4.43E-2	5.56E-3	2.48E-4	3.22E-3	2.99E-2	2.34E-5	2.66E-5	6.71E-5	2.27E-4	9.87E-3	2.03E-3	1.47E-3	2.98E-2	2.73E-5	2.93E-5	4.78E-5	4.23E-4	4.09E-3	4.30E-6
17	CCS DATA TO AACS XR	4.69E-5	5.38E-2	3.68E-5	6.06E-5	9.79E-3	6.39E-2	8.73E-3	4.37E-4	1.46E-3	3.24E-3	3.28E-5	2.78E-5	1.04E-4	4.25E-4	1.64E-2	1.32E-3	1.08E-3	3 31E-3	4.22E-5	2.95E-5	7.68E-5	5.14E-5	7.69E-3	1.75E-6
18	POWER CODE B XR	4.80E-5	3.84E-2	1.37E-5	1.56E-5	9.40E-3	2.68E-2	8.15E-3	1.76E-4	2.76E-3	1.58E-2	3.16E-5	1.18E-5	9.65E-5	1.86E-4	1.36E-2	1.24E-3	1.42E-3	1.58E-3	3.84E-5	1.27E-5	4.73E-5	2.52E-4	-5.55E-3	2.31E-6
19	BOT/EOT XR	3.95E-5	3.83E-2	1.28E-5	5.41E-5	6.71E-3	4.43E-2	5.56E-3	2.48E-4	3.22E-3	2.99E-2	2.34E-5	2.66E-5	6.71E-5	2.27E-4	9.87E-3	2.03E-3	1.47E-3	2.98E-3	2.73E-5	2.93E-5	4.78E-5	4.23E-4	4.09E-3	4.30E-6
20	POWER CODE	4.87E-5	4.45E-2	1.34E-5	2.83E-5	9.49E-3	3.50E-2	8.10E-3	2.45E-4	2.20E-3	1.57E-2	3.20E-5	1.60E-5	9.69E-5	2.42E-4	1.33E-2	1.39E-3	1.31E-3	1.56E-2	3.80E-5	1.72E-5	4.09E-5	2.27E-4	5.39E-3	2.64E-6
21	POWER CODE	6.56E-5	4.82E-2	1.62E-5	5.76E-5	9.80E-3	5.77E-2	8.28E-3	2.48E-4	8.24E-3	7.55E-2	3.30E-5	3.85E-5	1.01E-4	2.17E-4	1.66E-2	4.04E-3	3.32E-3	7.50E-2	4.43E-5	4.30E-5	9.47E-5	1.09E-3	6.43E-3	9.47E-6
22	TLM SUN SENSOR TEMP	1.12E-5	9.52E-3	2.62E-5	1.65E-5	2.52E-3	3.59E-3	1.05E-2	2.83E-4	7.12E-4	3.58E-3	8.15E-8	2.92E-6	2.00E-4	4.60E-4	1.07E-1	4.81E-3	3.10E-4	2.32E-3	2.42E-5	6.46E-6	6.10E-5	1.56E-4	1.99E-2	5.43E-6
23	AACS DATA	2.81E-8	4.20E-4	2.34E-7	3.11E-6	5.69E-6	1.53E-3	5.05E-6	8.25E-6	4.41E-6	4.62E-5	2.09E-8	1.17E-6	6.83E-8	7.16E-6	1.88E-5	2.72E-5	1.34E-6	5.02E-5	3.97E-8	1.29E-6	4.23E-7	1.04E-6	1.31E-5	2.68E-8
24	AACS ADDRESS DATA	4.80E-5	3.83E-2	1.65E-5	4.46E-5	7.02E-3	4.83E-2	5.85E-3	2.18E-4	5.87E-3	5.68E-2	2.42E-5	2.99E-5	7.23E-5	1.91E-4	1.24E-2	3.11E-3	2.40E-3	5.67E-2	3.17E-5	3.32E-5	7.64E-5	7.98E-4	- 5.71E-3	7.39E-6
25	TLM PYRO AMP IND A	6.01E-8	8.25E-4	3.56E-7	6.57E-6	1.27E-5	3.04E-3	1.26E-5	1.63E-5	7.38E-6	1.00E-4	4.18E-8	2.42E-6	1.55E-7	1.41E-5	3.69E-5	5.46E-5	2.60E-6	1.09E-4	8.17E-8	2.66E-6	6.55E-7	2.27E-5	2.20E-5	5.31E-8
26	TLM TCAPU TANK TEMP 1	4.62E-6	2.41E-2	1.83E-5	8.36E-5	3.94E-3	6.36E-2	3.35E-3	1.62E-4	1.25E-2	1.09E-1	1.28E-5	5.42E-5	4.65E-5	1.08E-4	1.26E-2	5.26E-3	4.27E-3	1.09E-1	2.76E-5	6.11E-5	1.36E-4	1.63E-3	4.87E-3	1.26E-5
27	CC DATA 2	1.77E-5	1.54E-2	1.11E-5	1.63E-5	2.85E-3	2.04E-2	2.45E-3	1.05E-4	2.07E-3	1.68E-2	9.63E-6	1.11E-5	3.02E-5	9.76E-5	5.50E-3	1.01E-3	8.47E-4	1.67E-2	1.34E-5	1.22E-5	3.68E-5	2.45E-4	2.49E-3	2.25E-6
28	PLAYBACK DATA	1.57E-8	2.34E-3	2.72E-7	2.72E-5	2.77E-6	9.19E-3	2.75E-6	4.84E-5	1.17E-5	4.64E-4	1.05E-8	8.33E-6	3.56E-8	4.13E-5	1.42E-5	1.71E-4	2.51E-6	4.86E-4	3.05E-8	9.28E-6	5.88E-7	1.09E-5	9.95E-6	1.67E-7
29	TLM DSS MOTOR V	6.70E-5	4.95E-2	1.96E-5	5.82E-5	1.00E-2	6.09E-2	8.57E-3	2.56E-4	8.41E-3	7.68E-2	3.35E-5	3.97E-5	1.05E-4	2.33E-4	1.79E-2	4.16E-3	3.42E-3	7.67E-2	4.64E-5	4,43E-5	1.03E-4	1.10E-3	7.10E-3	9.74E-6
30	CRS CMD WORD	8.12E-9	1.13E-5	5.15E-8	2.00E-7	6.72E-6	3.09E-4	1.70E-6	3.94E-7	3.89E-6	1.45E-5	2.59E-8	3.39E-7	5.91E-5	6.51E-4	1.08E-5	5.09E-6	6.25E-6	4.73E-10	4.73E-10	2.14E-8	2.91E-7	1.80E-6	4.43E-2	2.98E-6
31	CRS TELESCOPE TEMP	3.79E-6	3.32E-3	2.97E-6	2.42E-6	6.11E-3	2.09E-2	1.56E-3	4.34E-5	4.22E-5	2.17E-4	1.99E-5	6.89E-6	4.01E-2	8.60E-2	3 08E-3	2.45E-4	2.36E-4	1.74E-3	1.49E-7	3.99E-8	6.66E-6	1.54E-5	4.88E 0	1.73E-4
32	PWS ADC BIT SYNC	8.01E-7	1.17E-3	1.62E-6	3.58E-6	1.29E-4	3.08E-3	1.24E-4	1.62E-5	3.30E4	1.34E-3	4.24E-7	2.13E-6	1.58E-6	1.46E-5	3.98E-4	9.54E-5	8.42E-5	1.34E-3	9.81E-7	2.34E-6	6 00E-5	2.79E-5	1.98E-4	1.43E-7
33	PRA ANALOG MUX DATA	7.09E-5	5.27E-2	2.96E-5	1.91E-5	1.45E-2	4.71E-2	1.32E-2	3.62E-4	2.32E-3	9.93E-3	4.75E-5	1.52E-5	1.58E-4	3.72E-4	2.36E-2	1.43E-3	1.74E-3	9.94E-3	6.32E-5	1.58E-5	7.20E-5	1.45E-4	9.86E-3	2.38E-6
34	PRA ELECTRONICS TEMP	7.25E-5	8.35E-2	3.31E-5	2.01E-5	1.46E-2	4.98E-2	1.34E-2	3.70E-4	2.69E-3	1.38E-2	4.78E-5	1.63E-5	1.60E-4	3.79E-4	2.47E-2	1.61E-3	1.90E-3	1.36E-2	6.48E-5	1.70E-5	8.14E-5	1.93E-4	1.05E-2	2.88E-6
35	PRA CMD WORD	1.00E-8	2.31E-3	2.35E-6	3.72E-6	1.84E-4	4.24E-3	1.79E-4	2.70E-5	2.39E-4	8.84E-4	6.02E-7	7.33E-6	2.24E-6	2.40E-5	5.23E-4	9.81E-5	6.95E-5	8.88E-4	1.14E-6	2.50E-6	6.24E-6	1 81E-5	2.78E-4	1.44E-7
36	LECP CMD WORD A	7.44E-9	1.06E-5	4.76E-8	1.91E-7	6.16E-6	2.89E-4	1.58E-6	3.71E-7	3.62E-6	1.34E-5	2.38E-8	3.18E-7	5.63E-5	1.06E-3	9.81E-6	4.72E-6	5.81E-6	1.04E-4	4.37E-10	2.01E-9	2.72E-7	1.67E-6	4.07E-2	2.76E-6
37	LECP ANALOG DATA	5.15E-6	3.93E-3	5.77E-6	1.19E-5	6.32E-3	4.46E-2	1.59E-3	5.84E-5	2.08E-4	1.67E-3	2.07E-6	2.80E-5	4.48E-2	1.25E-1	3.82E-3	9.19E-4	6.59E-4	1.33E-2	1.76E-7	1.72E-7	4.57E-5	1.26E-4	8.58E 0	8.10E-4
38	PPS COMMAND WORD	1.28E-8	1.95E-5	9.14E-8	3.73E-7	1.07E-5	5.47E-4	2.85E-6	7.08E-7	7.29E-6	2.62E-5	4.20E-8	6.24E-7	5.20E-4	1.17E-3	1.93E-5	8.79E-6	1.15E-5	2.03E-4	8.47E-10	3.94E-9	5.47E-7	3.35E-6	3.02E-0	4.88E-6
39	PPS SOLAR SENSOR	8.34E-6	6.16E-3	9.54E-6	1.96E-5	1.08E-2	6.90E-2	2.75E-3	9.25E-5	3.81E-4	2.59E-3	3.40E-5	4.56E-5	2.76E-1	1.66E-1	7.03E-3	1.42E-3	1.15E-3	2.07E-2	3.11E-7	2.80E-7	2.81E-5	2.07E-4	6.03E-2	1.20E-3

FOLDOUT FRAME 1

FOLDOUT FRAME 2

TABLE 2-9. TABLE OF INDUCED VOLTAGES. RUN 8, 6-17-78 (CONT'D)

RECEPTORS		GENERATOR PARAMETERS																							
		BREWSTER PLATE		MAG CABLE		SEP CONN		MAG TEFLON		HGA OB PAINT		PLUME SH SEP CONN		LECP TEFLON		FSS		HGA IB PAINT		PLUME SH RTG		RTG OXIDE		MIRIS KAPTON	
NO.	NAME	RECPL	LOOP	RECPL	LOOP	RECPL	LOOP	RECPL	LOOP	RECPL	LOOP	RECPL	LOOP	RECPL	LOOP	RECPL	LOOP	RECPL	LOOP	RECPL	LOOP	RECPL	LOOP	RECPL	LOOP
40	UVS MODE CONTROL	1.32E-8	2.03E-5	8.57E-8	3.91E-7	1.11E-5	5.72E-4	2.97E-6	7.40E-7	7.65E-8	2.74E-5	4.37E-8	6.54E-7	5.14E-4	1.23E-3	2.01E-5	9.17E-8	1.20E-5	2.12E-4	8.85E-10	4.12E-9	5.74E-7	3.51E-6	2.98E 0	5.07E-6
41	UVS HV MONITOR	8.81E-8	6.41E-3	9.93E-6	2.16E-5	1.09E-2	7.30E-2	2.85E-3	9.82E-5	3.98E-4	2.68E-3	3.52E-5	4.89E-5	2.51E-1	1.76E-1	7.30E-3	1.48E-3	1.19E-3	2.14E-2	3.22E-7	3.00E-7	2.82E-5	2.16E-4	5.41E-2	1.23E-3
42	UVS SCIENCE DATA I	1.32E-8	2.04E-5	9.61E-8	3.92E-7	1.11E-5	5.74E-4	2.97E-6	7.44E-7	7.65E-6	2.74E-5	4.37E-8	6.55E-7	5.30E-7	1.23E-3	2.02E-5	9.18E-8	4.98E-5	2.12E-4	8.86E-10	4.13E-9	5.75E-7	3.15E-6	3.06E 0	5.08E-6
43	MAG SAMPLE B	1.53E-7	2.15E-4	4.34E-7	1.63E-6	1.59E-5	7.33E-4	1.43E-5	3.35E-6	2.48E-4	9.21E-4	6.13E-8	8.02E-7	1.98E-7	2.86E-6	8.50E-5	3.34E-5	4.98E-5	8.95E-4	2.02E-7	9.11E-7	3.67E-6	2.27E-5	4.06E-5	4.97E-8
44	MAG IBHFM CLOCK 50.4 KHz	7.39E-7	7.57E-4	2.07E-6	6.88E-8	3.85E-5	3.16E-3	2.98E-5	1.22E-5	1.38E-3	5.32E-3	1.88E-7	3.69E-6	5.27E-7	9.88E-6	4.18E-4	1.95E-4	2.83E-4	5.23E-3	9.58E-7	4.56E-6	1.88E-5	1.21E-4	1.94E-4	3.13E-7
45	MAG OBLFM SENSOR TEMP	3.91E-10	1.12E-6	8.14E-3	6.36E-3	2.68E-5	1.04E-3	8.68E-2	2.56E-4	6.53E-7	1.07E-6	8.75E-8	4.51E-7	4.76E-8	6.71E-7	8.30E-3	1.97E-3	1.20E-5	6.88E-5	5.21E-9	9.24E-5	1.93E-4	1.35E-4	4.38E-4	7.71E-8
46	ISS-WA ADC START	8.34E-8	1.43E-4	4.90E-7	8.46E-7	1.24E-4	2.98E-3	3.57E-5	4.63E-6	7.38E-6	2.63E-5	3.93E-7	1.76E-6	6.45E-3	8.25E-3	1.24E-4	2.47E-5	1.63E-5	2.02E-4	4.78E-9	1.06E-8	9.46E-7	2.77E-6	3.55E 1	1.31E-5
47	ISS-WA ADC VIDEO DATA	4.18E-8	8.61E-5	2.61E-7	6.50E-7	6.18E-5	1.93E-3	1.76E-5	2.99E-6	3.97E-6	1.39E-5	1.97E-7	1.23E-6	3.24E-3	5.25E-3	6.27E-5	1.53E-5	8.57E-6	1.11E-4	2.42E-9	7.41E-9	5.08E-7	1.55E-6	1.81F 1	7.73E-6
48	ISS-NA ANALOG ENGR TLM	6.27E-6	5.42E-3	7.57E-6	5.48E-6	1.02E-2	3.88E-3	2.69E-3	7.76E-5	8.59E-5	3.68E-4	3.26E-6	1.41E-5	2.34E-1	1.54E-1	5.76E-3	4.17E-4	4.38E-4	2.88E-3	2.67E-7	8.24E-8	1.31E-5	2.82E-5	5.01E-2	2.77E-4
49	MAG OBLFM SENSOR TEMP	1.84E-8	6.10E-5	2.64E-3	1.84E-2	4.76E-5	2.65E-3	4.63E-2	1.74E-4	7.62E-7	2.79E-6	1.90E-7	1.77E-6	5.11E-7	1.01E-5	2.56E-3	1.86E-3	5.84E-6	7.64E-5	1.99E-5	1.09E-4	5.14E-5	1.34E-4	3.27E-5	2.27E-8
50	IRIS FRAME START	1.28E-8	1.94E-6	9.11E-8	3.64E-7	1.14E-5	5.34E-4	3.05E-6	6.97E-7	7.01E-6	2.51E-5	4.38E-8	6.00E-7	5.69E-4	1.16E-3	1.94E-5	8.47E-8	1.11E-5	1.94E-4	8.50E-10	3.78E-9	5.29E-7	3.21E-8	3.46E 0	4.89E-6
51	IRIS RAD-MTR H-G ANALOG	3.35E-6	1.61E-3	3.33E-6	1.60E-5	2.09E-3	3.83E-2	6.08E-4	2.58E-5	3.45E-4	2.68E-3	6.79E-6	3.64E-5	7.43E-2	3.25E-2	2.44E-3	1.18E-3	3.72E-4	2.06E-2	9.44E-8	2.31E-7	1.88E-5	2.06E-4	1.47E 2	1.08E-3
52	IRIS PLL CARRIER	1.81E-6	1.08E-3	1.85E-6	6.05E-7	2.72E-3	7.05E-3	7.33E-4	1.42E-5	1.60E-5	3.23E-5	8.66E-6	1.89E-6	4.21E-2	3.11E-2	1.56E-3	6.86E-5	1.00E-4	2.58E-4	7.22E-9	1.11E-8	3.00E-6	2.83E-6	2.60E 1	3.72E-5
53	PITCH CRUISE SS/1 POSN	1.80E-10	4.13E-7	1.43E-9	8.04E-9	2.07E-8	6.14E-7	7.10E-8	1.68E-8	4.05E-7	1.61E-6	9.01E-11	7.68E-10	1.54E-9	2.07E-8	1.82E-6	6.26E-7	5.16E-8	1.01E-6	4.26E-10	1.84E-9	1.72E-8	1.18E-7	3.41E-7	6.98E-10
54	CSTI CONE ANGLE CMD A	3.89E-9	2.72E-5	3.50E-9	1.89E-7	6.30E-7	6.30E-5	5.06E-7	3.77E-7	1.16E-6	7.80E-6	2.49E-9	5.51E-8	6.23E-9	3.18E-7	9.63E-7	1.30E-5	2.68E-7	7.72E-6	2.70E-9	6.14E-8	2.00E-8	1.83E-7	4.44E-7	1.47E-9
55	CSTI STAR INTENSITY	1.22E-9	5.53E-6	1.79E-9	4.01E-8	1.40E-7	1.34E-5	1.09E-7	7.60E-8	1.23E-6	5.83E-6	5.92E-10	1.27E-8	1.45E-9	6.32E-8	3.96E-7	3.73E-7	2.50E-7	5.67E-6	1.06E-9	1.42E-8	1.81E-8	1.37E-7	1.73E-7	5.38E-10
56	CSTI CONE ANGLE POSITION	3.70E-9	3.33E-5	3.81E-9	2.74E-7	6.30E-7	8.71E-5	5.06E-7	5.03E-7	1.19E-6	9.35E-5	2.49E-9	7.80E-8	6.24E-9	4.26E-7	9.70E-7	1.75E-6	2.73E-7	9.30E-6	2.72E-9	8.72E-8	2.07E-8	2.20E-7	4.48E-7	1.89E-9
57	OBLFM X OUT % COAX <	3.70E-8	3.47E-5	4.19E-2	2.00E-2	2.63E-3	1.24E-2	2.24E 0	3.78E-3	9.77E-6	5.67E-6	8.27E-6	2.50E-6	3.75E-6	1.12E-5	3.56E-1	2.70E-2	4.07E-4	3.67E-4	2.85E-3	4.76E-4	3.04E-3	4.50E-4	1.33E-2	1.20E-6
58	IBHFM X OUT % COAX <	9.64E-7	8.03E-4	3.86E-3	3.39E-2	2.73E-3	6.78E-3	9.86E-1	6.73E-4	2.94E-6	1.48E-5	8.80E-6	1.79E-6	2.29E-6	4.56E-5	6.06E-2	7.88E-3	8.36E-5	4.00E-4	6.62E-4	1.03E-4	2.11E-4	3.88E-4	5.99E-4	1.38E-7
59	CRS ANALOG DATA	5.15E-6	3.72E-3	4.79E-6	1.03E-5	6.32E-3	3.88E-2	1.58E-3	4.92E-5	2.07E-4	1.67E-3	2.06E-5	2.50E-5	4.35E-2	8.62E-2	3.77E-3	8.88E-4	8.57E-4	1.34E-2	1.74E-7	1.54E-7	1.45E-5	1.26E-4	6.84E 0	7.93E-4
60	HGA S-BAND FEED TEMP	8.75E-9	9.09E-6	2.83E-8	1.19E-8	1.21E-7	3.85E-6	9.98E-8	1.31E-8	7.11E-6	2.45E-4	4.70E-10	6.33E-9	7.66E-8	5.97E-7	2.23E-1	8.30E-3	5.01E-7	8.71E-5	1.71E-10	7.61E-10	4.03E-9	2.63E-8	1.07E-5	1.05E-8
61	X-BAND FEED TEMP	7.79E-9	8.42E-6	2.36E-8	1.06E-7	8.46E-7	2.95E-5	8.60E-7	1.26E-7	1.94E-5	6.79E-5	3.27E-9	4.44E-8	1.20E-8	1.06E-7	5.07E-6	1.70E-6	3.68E-5	6.47E-5	1.27E-8	5.15E-8	2.89E-7	1.82E-6	2.17E-6	2.52E-9
62	IRIS SEC MIRROR TEMP	8.05E-6	5.74E-3	7.27E-6	1.34E-5	1.07E-2	5.23E-2	2.80E-3	7.37E-5	3.08E-4	2.10E-3	3.44E-5	3.31E-5	1.14E-1	1.36E-1	6.73E-3	1.15E-3	9.86E-4	1.67E-2	3.04E-7	2.04E-7	2.20E-5	1.66E-4	1.30E-2	9.79E-4
63	IRIS SEC MIRROR HTR ANLG	8.53E-6	5.87E-3	7.63E-6	1.71E-5	1.08E-2	5.36E-2	2.81E-3	7.58E-5	3.89E-4	2.65E-3	3.47E-5	4.08E-5	1.13E-1	1.37E-1	7.02E-3	1.39E-3	1.17E-3	2.12E-4	3.14E-7	2.52E-7	2.61E-5	2.13E-4	1.18E 2	1.19E-3
64	SS 1 SYNC	2.41E-8	8.27E-5	4.05E-7	4.45E-6	1.45E-6	3.76E-4	5.11E-6	8.13E-6	8.74E-5	3.39E-4	7.44E-9	3.93E-7	1.42E-7	1.08E-5	3.88E-4	2.07E-4	1.12E-5	2.14E-4	8.27E-8	9.31E-7	3.71E-6	2.48E-5	7.72E-5	1.72E-7
65	PITCH SS BIAS	1.33E-11	3.42E-8	3.58E-11	2.73E-10	1.79E-9	3.57E-8	6.29E-9	1.20E-9	9.25E-9	6.47E-8	7.00E-12	2.71E-11	1.29E-10	1.48E-9	8.45E-8	3.04E-8	1.43E-9	3.47E-8	2.00E-11	6.41E-11	3.81E-10	3.16E-9	1.47E-8	4.26E-11
66	RTG CASE TEMP	7.35E-8	4.72E-5	1.63E-6	5.15E-6	1.82E-4	3.75E-3	8.75E-5	5.99E-6	9.80E-5	3.66E-4	7.11E-7	6.18E-6	1.13E-5	4.51E-5	1.19E-5	3.71E-3	2.03E-5	3.60E-4	1.73E-6	5.08E-6	4.43E-2	2.92E-1	3.86E-5	4.32E-8
67	RTG POWER	2.89E-6	1.13E-3	1.76E-5	2.58E-6	1.61E-2	2.64E-2	7.93E-3	8.84E-5	8.30E-5	6.34E-5	4.55E-5	5.21E-6	8.87E-4	1.03E-3	4.00E-4	6.94E-3	7.73E-5	6.26E-5	6.14E-5	3.67E-6	8.43E-3	1.04E-1	1.19E-3	6.26E-8
68	X-BAND FEED TEMP	3.72E-9	1.98E-5	1.72E-8	1.17E-7	7.67E-7	6.77E-5	8.65E-7	3.70E-7	5.42E-7	2.38E-6	2.34E-9	4.82E-8	1.11E-8	3.27E-7	2.95E-6	1.19E-6	2.03E-7	2.53E-6	5.75E-9	5.26E-8	3.39E-8	5.44E-8	1.58E-6	1.79E-9
69	X-BAND FEED TEMP	3.72E-9	1.98E-5	1.72E-8	1.17E-7	7.67E-7	6.77E-5	8.65E-7	3.70E-7	5.42E-7	2.38E-6	2.34E-9	4.82E-8	1.11E-8	3.27E-7	2.95E-6	1.19E-6	2.03E-7	2.53E-6	5.75E-9	5.26E-8	3.39E-8	5.44E-8	1.58E-6	1.79E-9
70	X-BAND FEED TEMP	3.72E-9	1.98E-5	1.72E-8	1.17E-7	7.67E-7	6.77E-5	8.65E-7	3.70E-7	5.42E-7	2.38E-6	2.34E-9	4.82E-8	1.11E-8	3.27E-7	2.95E-6	1.19E-6	2.03E-7	2.53E-6	5.76E-9	5.26E-8	3.39E-8	5.44E-8	1.58E-6	1.79E-9
71	X-BAND FEED TEMP	7.82E-9	8.15E-6	2.39E-8	1.04E-7	8.46E-7	2.85E-5	8.60E-7	1.20E-7	1.99E-5	6.92E-5	3.28E-9	4.39E-8	1.20E-8	1.01E-7	5.09E-6	1.69E-6	3.75E-6	6.60E-5	1.28E-8	5.09E-8	2.96E-7	1.86E-6	2.17E-6	2.50E-9
72	X-BAND FEED TEMP	3.61E-9	1.00E-5	1.12E-8	4.63E-8	7.57E-7	3.04E-5	8.54E-7	1.71E-7	3.08E-7	8.08E-7	2.27E-9	1.99E-8	1.10E-8	1.54E-7	2.70E-6	5.20E-7	1.56E-7	8.73E-7	5.29E-9	2.19E-8	2.20E-8	1.83E-8	1.37E-6	7.89E-10
73	HGA DISH TEMP	1.23E-8	6.71E-5	2.67E-8	1.76E-7	1.07E-6	9.65E-5	1.25E-6	5.63E-7	6.91E-8	3.05E-7	3.32E-9	6.83E-8	6.12E-8	1.91E-6	9.22E-6	4.92E-6	1.95E-7	2.56E-6	2.08E-9	2.02E-8	1.30E-8	2.12E-8	3.64E-5	3.00E-8
74	HGA DISH TEMP	1.23E-8	6.71E-5	2.67E-8	1.76E-7	1.07E-6	9.65E-5	1.25E-6	5.63E-7	6.91E-8	3.05E-7	3.32E-9	6.83E-8	6.12E-8	1.91E-6	9.22E-6	4.92E-6	1.95E-7	2.56E-6	2.08E-9	2.02E-8	1.30E-8	2.12E-8	3.64E-5	3.00E-8
75	HGA DISH TEMP	1.23E-8	6.71E-5	2.67E-8	1.76E-7	1.07E-6	9.65E-5	1.25E-6	5.63E-7	6.91E	3.05E-7	3.32E-9	6.83E-8	6.12E-8	1.91E-6	9.22E-6	4.92E-6	1.95E-7	2.56E-6	2.08E-9	2.02E-8	1.30E-8	2.12E-8	3.64E-5	3.00E-8
76	HGA DISH TEMP	2.64E-8	2.71E-5	3.40E-8	1.53E-7	1.18E-6	3.99E-5	1.24E-6	1.78E-7	2.33E-6	8.39E-6	4.60E-9	8.10E-8	6.59E-8	5.74E-7	1.63E-5	6.95E-6	3.58E-6	6.33E-5	4.63E-9	1.90E-8	1.06E-7	6.71E-7	4.88E-5	5.72E-8
77	HGA DISH TEMP	1.19E-8	3.36E-5	1.68E-8	6.92E-8	1.06E-6	4.29E-5	1.24E-6	2.56E-7	3.77E-8	1.03E-7	3.21E-9	2.80E-8	6.00E-8	8.92E-7	8.30E-6	2.14E-8	1.45E-7	8.75E-7	1.89E-9	8.22E-9	8.14E-9	7.07E-9	3.08E-5	1.34E-8

FOLDOUT FRAME 2

FOLDOUT FRAME 1

Table 2-10. Voltage Thresholds and Negative dB Margins of Immunity

Run 8 6/17/77

RECEPTORS			GENERATOR PARAMETERS																					
NO.	NAME	VOLTAGE THRESHOLD	BREWSTER PLATE		MAG CABLE		SEP CONN		MAG TEFLON		HGA OB PAINT		PLUME SH SEP CONN		LECP TEFLON		FSS		HGA/B PAINT		PLUME SH RTG		RTG OXIDE		MIRIS KAPTON	
			RECPL	LOOP	RECPL	LOOP	RECPL	LOOP	RECPL	LOOP	RECPL	LOOP	RECPL	LOOP	RECPL	LOOP	RECPL	LOOP	RECPL	LOOP	RECPL	LOOP	RECPL	LOOP	RECPL	LOOP
1	TLM BAY 6 TEMP	0.01		-20			-8	-18	-7			-6					-13			-6					-6	
2	S-TWTA HI/LO STAT	2.00																								
3	S-TWTAI ON STAT<	10.00																								
4	50.4 KHz % 02-05	2.00																								
5	TLM S-BAND TWT REG V	0.01		-14			-2	-9									-4									
6	S-TWTA RF DR MONITOR	0.01		-6				-13				-18								-18						
7	CMPST CMD, RCVR 1 TO CDU-A	0.01		-6				-9																		
8	TLM S-BAND EX CURR	0.01		-18			-5	-19	-4		-4	-22					-10			-22					-2	
9	TLM RCVR VCO TEMP	0.01		-16			-4	-12	-3								-8									
10	TLM RCVR LO DR	0.01		-17			-4	-17	-4			-4					-9			-4					-2	
11	TLM S-BAND TWT DR	0.01		-17			-4	-17	-4			-4					-9			-4					-2	
12	CDU-A COMMAND DATA, XR	2.00																								
13	TMU A SYMBOL SYNC	2.00																								
14	HGH RATE CHAN DATA TMU-A	1.50																								
15	CC STROBE XR	4.50																								
16	CCS BIT SYNC 1	4.50																								
17	CCS DATA TO AACS XR	4.00																								
18	POWER CODE B XR	1.20																								
19	BOT/EOT XR	1.20																								
20	POWER CODE	1.00																								
21	POWER CODE	1.00																								
22	TLM SUN SENSOR TEMP	0.01															-21								-6	
23	AACS DATA	4.00																								
24	AACS ADDRESS DATA	2.00																								
25	TLM PYRO AMP IND A	4.00																								
26	TLM TCAPU TANK TEMP 1	0.01		-8				-10			-2	-21					-2			-21						
27	CC DATA 2	4.00																								
28	PLAYBACK DATA	4.00																								
29	TLM DSS MOTOR V	0.01		-14				-16				-18					-5			-18						
30	CRS CMD WORD	4.00																								
31	CRS TELESCOPE TEMP	0.01						-6							-12	-19									-54	
32	PWS ADC BIT SYNC	2.00																								
33	PRA ANALOG MUX DATA	0.01		-16			-3	-13	-2								-7									
34	PRA ELECTRONICS TEMP	0.01		-16			-3	-14	-3			-3					-8			-3						
35	PRA CMD WORD	2.00																								
36	LECP CMD WORD A	4.00																								
37	LECP ANALOG DATA	0.01						-13							-13	-22				-2					-59	
38	PPS COMMAND WORD	4.00																								
39	PPS SOLAR SENSOR	0.01						-17							-29	-24				-6					-96	

Table 2-10. Voltage Thresholds and Negative dB Margins of Immunity (Cont)

Run B 6/17/77

RECEPTORS			GENERATOR PARAMETERS																					
			BREWSTER PLATE		MAG CABLE		SEP CONN		MAG TEFLON		HGA OB PAINT		PLUME SH SEP CONN		LECP TEFLON		FSS		HGA IB PAINT		PLUME SH RTG		RTG OXIDE		MIRIS KAPTON	
NO.	NAME	VOLTAGE THRESHOLD	RECPL	LOOP	RECPL	LOOP	RECPL	LOOP	RECPL	LOOP	RECPL	LOOP	RECPL	LOOP	RECPL	LOOP	RECPL	LOOP	RECPL	LOOP	RECPL	LOOP	RECPL	LOOP	RECPL	LOOP
40	UVS MODE CONTROL	4.00																								
41	UVS HV MONITOR	0.01					-1	-17							-28	-25				-7						-95
42	UVS SCIENCE DATA I	2.00																								-5
43	MAG SAMPLE B	4.00																								
44	MAG IBHFM CLOCK 50.4 KHz	4.00																								
45	MAG OBLFM SENSOR TEMP	0.01				-4			-19																	
46	ISS-WA ADC START	2.00																								-25
47	ISS-WA ADC VIDEO DATA	4.00																								-13
48	ISS-NA ANALOG ENGR TLM	0.01						-12							-27	-24										-94
49	MAG OBLFM SENSOR TEMP	0.01				-5			-13											-6						
50	IRIS FRAME START	4.00																								
51	IRIS RAD-MTR H-G ANALOG	0.01						-12							-17	-10				-6						-83
52	IRIS PLL CARRIER	0.20																								-42
53	PITCH CRUISE SS/I POSN	0.01																								
54	CSTI CONE ANGLE CMD A	3.50																								
55	CSTI STAR INTENSITY	0.01																								
56	CSTI CONE ANGLE POSITION	0.60																								
57	OBLFM X OUT % COAX	1.00E-7		-51	-112	-108	-88	-102	-147	-92	-40	-35	-38	-28	-31	-41	-131	-109	-72	-71	-89	-74	-90	-73	-102	-22
58	IBHFM X OUT % COAX	9.99E-7		-58	-72	-91	-69	-77	-120	-57	-9	-23	-19	-5	-27	-33	-96	-78	-38	-62	-56	-40	-46	-52	-56	
59	CRS ANALOG DATA	0.01						-12							-13	-19									-57	
60	HGA S-BAND FEED TEMP	1.00																								
61	X-BAND FEED TEMP	1.00																								
62	IRIS SEC MIRROR TEMP	1.00																							-42	
63	IRIS SEC MIRROR HTR ANLG	1.00																							-41	
64	SS 1 SYNC	1.00																								
65	PITCH SS BIAS	1.00																								
66	RTG CASE TEMP	1.00																								
67	RTG POWER	1.99																								
68	X-BAND FEED TEMP	1.00																								
69	X-BAND FEED TEMP	1.00																								
70	X-BAND FEED TEMP	1.00																								
71	X-BAND FEED TEMP	1.00																								
72	X-BAND FEED TEMP	1.00																								
73	HGA DISH TEMP	1.00																								
74	HGA DISH TEMP	1.00																								
75	HGA DISH TEMP	1.00																								
76	HGA DISH TEMP	1.00																								
77	HGA DISH TEMP	1.00																								

high-field magnetometers. These cables carry narrow-band (∿20 Hz) signals and thus the threshold levels have been set to 0.1 μv and 1.0 μv, respectively. A 1 volt signal level in these cases would therefore correspond to -140 db and -120 db margins. Digital or bilevel signal lines have much higher thresholds. Receptor No. 38 (LECP CMD WORD A) a command line for the Low Energy Charged Particle Experiment has a threshold of 4.0 volts. Whether a bilevel threshold is crucial or not depends on its particular function and whether or not further protection against anomalous operation, e.g., coincidence gating or sequential signal recognition, has been implemented. The more crucial the function, the greater the protection should be.

2.3 STUDY OF COUPLING EFFECTS OF ARCS TO SPACE

The modeling of the replacement current generators as shown in Figure 2-1 involved coupling only via the stray capacitance to space. The boom replacement current was calculated by

$$I_{boom} = I_{arc} \cdot P_1(f),$$

$$P_1(f) = I_{boom}/I_{arc} = [G'] \, (4\pi^2 f^2 C_{eq} L_{boom} + 1)^{-1},$$

$$G' = C_F/(C_F + C_x) \text{ (in-band gain)}.$$

Thus, $P_1(f)$, the ratio of boom replacement current or its frequency-independent component, G', is essentially the ratio of the capacitance to space, C_F, to the capacitance of the arcing item, C_x. G' is therefore, usually, a very small ratio, in the order of 10^{-4}. What is being assumed, then, is that the arc discharges are of the "flashover" type in which all of the stored charge is released in the front-to-back mode, and the replacement currents arise only as a result of displacement currents. Runs 9 and 10 were performed to study the effects of increasing G' over the pure displacement current value. Since Runs 11 and 12 were made to investigate the simulated kapton thermal blanket, optical solar reflector, and solar array, the remaining nine sources were included in this study with other intermediate and larger values of G'.

In Run 9, an increase of the currents-to-space was incorporated by increasing the value of G´. If the arcs were to be completely of the arcs-to-space variety, then G´ would be unity. Instead of unity, the value of G´ for Run 9 was computed on the basis that the boom voltage, V_{boom}, due to the boom replacement current, I_{boom}, was 10% of the breakdown voltage, V. The boom impedance, Z_{boom}, was evaluated at a frequency, f_x, defined by

$$f_x = (3\ t_p)^{-1}.$$

Table 2-11 compares the parameters, including G´, between Runs 8 and 9, and also shows the parameters which were unchanged. Also shown in Table 2-11 are the areas, A, and thickness, d, of dielectric surfaces associated with each generator. The area, A, satisfies the equation

$$C_x = \varepsilon_r\ \varepsilon_o\ A/d \text{ (MKS units), or } A(cm^2) = C_x(pf) \cdot d(mils)/70$$

$$\text{for } \varepsilon_r = 2, \text{ and } \varepsilon_o = 8.85 \cdot 10^{-12}.$$

It may be noted in Table 2-11 that the G´ values are appreciably ($\sim$ 100 times) larger for Run 9 than for Run 8. In only two cases, the LECP teflon and the FSS, are G´ values equal to unity.

Table 2-12 lists the parameters of the twelve generators for four cases in addition to Run 8. Runs 9, 10, 11, and 12 are various representations of arc parameters which were derived from the literature survey, Task 1.1 of the present study. In Table 2-12, the lower eight generator parameters in Table 2-1, having to do with their physical position and geometrical configuration on the spacecraft, are not repeated. These parameters were retained unchanged for all of the cases. The receptor parameters, which include the harnessing layout, were also unchanged throughout. In all of the four runs in which variable G´ effects were studied, the breakdown voltages of Run 8 were retained. The discharge waveform was, however, taken to be as per one of the area dependent expressions from the literature survey:

$$t_p = 54.9\ A^{.28};\quad t_r = 0.10\ t_p,$$

and the peak arc current was then computed from

$$I_{arc} = .774\ C_x\ V/t_p.$$

Table 2-11. Voyager Arc Characterization Comparison Between Runs 8 and 9

	COMMON PARAMETERS				OLD PARAMETERS (RUN 8)				NEW PARAMETERS (RUN 9)			
GENERATOR	V (kV)	C_x (pf)	f_c (MHz)	G''(Ω)	G'	t_r (ns)	t_p (ns)	I (A)	†G'	A (cm^2) /d (mils)	*t_p (ns)	I_A (A)**
BREWSTER PLATE	1	2E4	104	1250	6E-4	3	10	2	.08	571/2	325	98
MAGNETIC CABLE	5	5E4	8	82E3	5E-4	10	1700	20	.002	7143/10	659	607
SEP. CONN.	5	150	159	9500	6.6E-3	10	15	36	.161	12.9/6	112	11
MAG. TEFLON	1	38	81	3.8E4	4E-2	5	13	3	.10	5.43/10	88	.69
HGA PAINT (OB)	1	4E5	15.9	1250	1.25E-3	5	3000	150	.031	22,857/4	912	702
PLUME SHIELD (SEP. CONN.)	1	4500	290	9400	4E-5	20	8	.26	1.0	42.9	157	.12
LECP TEFLON	1	12	-9	1.6E4	0.25	3	8	.26	1.0	42.9/250	157	.12
FSS	7	14	34	12E3	1.0	8	80	80	1.0	4750/--	588	.27
HGA PAINT (IB)	1	3E5	42	1250	2.3E-4	5	2400	150	.035	17,143/4	842	570
PLUME SHIELD (RTG)	1	5200	83	9500	2.5E-4	20	330	16	.046	743/10	349	24
RTG OXIDE	3.5	3.4E5	12	1.1E4	2.5E-4	20	3700	925	.0026	9,714/2	718	2652
MIRIS KAPTON	1	40 (5400)	12	2.5E4	1.0	5	26	150	.086	103/2	786	11

†G' FOR NEW VALUE IS ADJUSTED TO MAKE V_{BOOM} 1% OF V AT $f_x = 1/(3t_p)$.

*RISETIME, t_r, FOR NEW VALUE IS 10% OF PULSE WIDTH, t_p.

**Currents should be divided by 2.

Table 2-12. Generator Parameters for Voyager SEMCAP Runs

RUN		1 BREWSTER PLATE	2 MAG CABLE	3 SEP CONN	4 MAG TEFLON	5 HGA OB PAINT	6 PLUME SH SEP CONN	7 LECP TEFLON	8 FSS	9 HGA IB PAINT	10 PLUME SH RTG	11 RTG OXIDE	12 MIRIS KAPTON
8	$V_{BREAKDOWN}$ (kV)	1	5	5	1	1	1	1	7	1	1	3.5	1
	I_{ARC} (amps)	2	20	36	3	150	16	.26	80	150	16	925	160
	G' (ratio)	6E-4	5E-4	6.6E-3	4E-2	1.25E-3	4E-5	.25	1.0	2.3E-4	2.5E-4	2.5E-4	1.0
	t_r (ns)	3	10	10	5	5	20	3	8	5	20	20	5
	t_p (ns)	10	1700	15	13	3000	285	8	80	2400	330	3700	26
9	$V_{BREAKDOWN}$ (kV)	1	5	5	1	1	1	1	7	1	1	3.5	1
	I_{ARC} (amps) *	98	607	11	.69	702	18	.12	.27	570	24	2652	11
	G' (ratio)	.08	.002	.161	.10	.031	.06	1.0	1.0	.035	.046	.0026	.086
	t_r (ns)	32.5	65.9	11.2	8.8	91.2	33.6	15.7	58.8	84.2	34.9	71.8	78.6
	t_p (ns)	325	659	112	88	912	336	157	588	842	349	718	786
10	$V_{BREAKDOWN}$ (kV)	1	5	5	1	1	1	1	7	1	1	3.5	1
	I_{ARC} (amps) *	98	607	11	.69	702	18	.12	.27	570	24	2652	11
	G' (ratio)	6E-4	5E-4	6.6E-3	4E-2	1.25E-3	4E-5	.25	1.0	2.3E-4	2.5E-4	2.5E-4	1.0
	t_r (ns)	32.5	65.9	11.2	8.8	91.2	33.6	15.7	58.8	84.2	34.9	71.8	78.6
	t_p (ns)	325	659	112	88	912	336	157	588	842	349	718	786
11	$V_{BREAKDOWN}$ (kV)	7	5	5	1	12	1	1	7	1	1	9	1
	I_{ARC} (amps) *	249	607	11	.69	2018	18	.12	.27	570	24	3254	11
	G' (ratio)	18E-4	1E-3	2E-2	7E-2	1.25E-3	2E-3	.50	1.0	5E-4	1E-3	7.5E-4	1.0
	t_r (ns)	30	65.9	11.2	8.8	380.5	33.6	15.7	58.8	84.2	34.9	50	78.6
	t_p (ns)	300	659	112	88	3805	336	157	588	842	349	500	786
12	$V_{BREAKDOWN}$ (kV)	2	5	5	1	8	1	1	7	1	1	1	1
	I_{ARC} (amps) *	71.1	607	11	.69	741	18	.12	.27	570	24	90.4	11
	G' (ratio)	18E-4	4E-3	5E-2	.2	1.25E-3	1E-2	.75	1.0	5E-3	1E-2	7.5E-4	1.0
	t_r (ns)	30	65.9	11.2	8.8	690	33.6	15.7	58.8	84.2	34.9	200	78.6
	t_p (ns)	300	659	112	88	6900	336	157	588	842	349	2000	786

*Currents should be divided by 2.

In Run 10, the G´ values were returned to those for Run 8, displacement currents only, but with t_p, t_r and I_{arc} values the same as for Run 9. In Runs 11 and 12 intermediate values were assumed as shown in Table 2-12 except for the Brewster Plate, high gain antenna outboard paint (HGA OB Paint), and RTG Oxide. Table 2-13 summarizes the G´ values for all of the runs for the 12 sources. It should be noted that the G´ values do not increase or decrease with run number in any systematic manner.

The results of Runs 9, 10, 11, and 12 are shown in Tables 2-14, 2-15, 2-16 and 2-17, respectively. Each table lists the threshold voltage at each receptor and the db margin over the threshold if negative.

Runs 8 and 10 had the same G´ value and breakdown voltage, but different peak arc currents and waveforms. Comparing Table 2-15 (Run 10) with Table 2-10 (Run 8), the comparable negative db margin tables, it may be noted that the frequency of negative db entries is not significantly increased. Even though the Run 10 currents are larger, the pulse widths are also larger, tending to equalize the induced voltages.

Comparing the results of these runs for the effect of increasing G´ shows, as may have been expected, that the induced voltage varies directly as G´. For example, the replacement current induced voltage margin in Receptor No. 1 is tabulated below in the order of increasing G´:

RUN	G´	RECEPTOR NO. 1 db MARGIN
10	.0005	0-8
11	.001	4-14
9	.002	8-20
12	.004	-26

Each succeeding value of G´ doubles the previous value and the -db margin increases by 6 db; i.e., the induced voltage also doubles. At the bottom of Table 2-13 are listed the db's required to increase the G´ values from those in Run 9 to a value of unity; i.e., all of the stored charge goes off to space. Thus, adding these db's to those for Run 9 will give the db margins for a completely-to-space discharge model. Table 2-18 lists the negative db margins that would be obtained for this model. It is emphasized that such a

Table 2-13. G´ Values for the Various Runs

RUN	BREWSTER PLATE	MAG CABLE	SEP CONN	MAG TEFLON	HGA OB PAINT	PLUME SH SEP CONN	LECP TEFLON	FSS	HGA IB PAINT	PLUME SH RTG	RTG OXIDE	MIRIS KAPTON
8	.0006	.0005	.0066	.04	.00125	.00004	.25	1.0	.00023	.00025	.00025	1.0
9	.08	.002	.161	.10	.031	.06	1.0	1.0	.035	.046	.0026	.086
10	.0006	.0005	.0066	.04	.00125	.00004	.25	1.0	.00023	.00025	.00025	1.0
11	.0018	.001	.02	.07	.00125	.002	.5	1.0	.0005	.001	.00075	1.0
12	.0018	.004	.05	.2	.00125	.01	.75	1.0	.005	.01	.00075	1.0
db's to 1 from Run 9	-22 db	-54 db	-16 db	-20 db	-30 db	-24 db	0 db	0 db	-29 db	-27 db	-52 db	0 db

FOLDOUT FRAME 1

FOLDOUT FRAME 2

Table 2-14. Voltage Thresholds and Negative dB Margins of Immunity *

Run 9 - 9/14/78

RECEPTORS			GENERATOR PARAMETERS																							
NO.	NAME	VOLTAGE THRESHOLD	BREWSTER PLATE		MAG CABLE		SEP CONN		MAG TEFLON		HGA OB PAINT		PLUME SH SEP CONN		LECP TEFLON		FSS		HGA IB PAINT		PLUME SH RTG		RTG OXIDE		MIRIS KAPTON	
			RECPL	LOOP	RECPL	LOOP	RECPL	LOOP	RECPL	LOOP	RECPL	LOOP	RECPL	LOOP	RECPL	LOOP	RECPL	LOOP	RECPL	LOOP	RECPL	LOOP	RECPL	LOOP	RECPL	LOOP
1	TLM BAY 6 TEMP	0.01	-24	-14	-20		-20	-9	-3		-36	-5	-7						-36	-4	-8		-10			
2	S-TWTA HI/LO STAT	2.00																								
3	S-TWTA I ON STAT<	10.00																								
4	50.4 KHz % 02-06	2.00																								
5	TLM S-BAND TWT REG V	0.01	-15		-12		-13				-27								-27		-1		-2			
6	S-TWTA RF DR MONITOR	0.01	-20	-24			-3	-5			-34	-16							-34	-15						
7	CMPST CMD, RCVR 1 TO CDU-A	0.01	-5		-2		-2	-5			-18								-18							
8	TLM S-BAND EX CURR	0.01	-27	-28	-16		-17	-11			-41	-21	-4						-40	-19	-5		-7			
9	TLM RCVR VCO TEMP	0.01	-18		-16		-16	-1			-30		-3						-30		-4		-6			
10	TLM RCVR LO DR	0.01	-20	-12	-16		-16	-10			-33	-3	-4						-33	-2	-4		-6			
11	TLM S-BAND TWT DR	0.01	-20	-12	-16		-16	-10			-33	-3	-4						-33	-2	-4		-6			
12	CDU-A COMMAND DATA, XR	2.00																								
13	TMU A SYMBOL SYNC	2.00																								
14	HGH RATE CHAN DATA TMU-A	1.60																								
15	CC STROBE XR	4.50																								
16	CCS BIT SYNC 1	4.50																								
17	CCS DATA TO AACS XR	4.00																								
18	POWER CODE B XR	1.20																								
19	BOT/EOT XR	1.20																								
20	POWER CODE	1.00																								
21	POWER CODE	1.00																								
22	TLM SUN SENSOR TEMP	0.01	-3		-13						-19								-15				-2			
23	AACS DATA	4.00																								
24	AACS ADDRESS DATA	2.00																								
25	TLM PYRO AMP IND A	4.00																								
26	TLM TCAPU TANK TEMP 1	0.01	-24	-28	-3		-6	-9			-38	-20							-37	-18						
27	CC DATA 2	4.00																								
28	PLAYBACK DATA	4.00																								
29	TLM DSS MOTOR V	0.01	-22	-24	-11		-12	-7			-36	-16							-36	-15			-2			
30	CRS CMD WORD	4.00																								
31	CRS TELESCOPE TEMP	0.01					-7								-19	-1			-13						-15	
32	PWS ADC BIT SYNC	2.00																								
33	PRA ANALOG MUX DATA	0.01	-18	-8	-15		-15	-5																		
34	PRA ELECTRONICS TEMP	0.01	-19	-10	-15		-15	-5			-31		-2						-31		-3		-5			
35	PRA CMD WORD	2.00									-31		-2						-31		-3		-5			
36	LECP CMD WORD A	4.00																								
37	LECP ANALOG DATA	0.01	-1	-2			-8	-6			-4				-20	-10			-21						-19	
38	PPS COMMAND WORD	4.00																								
39	PPS SOLAR SENSOR	0.01	-5	-6	-1		-13	-10			-9		-1		-37	-10			-26	-5					-55	

*NEGATIVE MARGINS SHOULD BE REDUCED BY 6 dB.

FOLDOUT FRAME 1

FOLDOUT FRAME 2

Table 2-14. Voltage Thresholds and Negative dB Margins of Immunity (Cont)*

Run 9 9/14/78

RECEPTORS			GENERATOR PARAMETERS																							
NO.	NAME	VOLTAGE THRESHOLD	BREWSTER PLATE		MAG CABLE		SEP CONN		MAG TEFLON		HGA OB PAINT		PLUME SH SEP CONN		LECP TEFLON		FSS		HGA IB PAINT		PLUME SH RTG		RTG OXIDE		MIRIS KAPTON	
			RECPL	LOOP	RECPL	LOOP	RECPL	LOOP	RECPL	LOOP	RECPL	LOOP	RECPL	LOOP	RECPL	LOOP	RECPL	LOOP	RECPL	LOOP	RECPL	LOOP	RECPL	LOOP	RECPL	LOOP
40	UVS MODE CONTROL	4.00																								
41	UVS HV MONITOR	0.01	-6	-7	-2		-13	-11			-9		-1		-36	-12			-27	-6					-55	
42	UVS SCIENCE DATA I	2.00																								
43	MAG SAMPLE B	4.00																								
44	MAG IBHFM CLOCK 50.4 KHz	4.00																								
45	MAG OBLFM SENSOR TEMP	0.01			-38	-12			-20												-1					
46	ISS-WA ADC START	2.00																								
47	ISS-WA ADC VIDEO DATA	4.00																								
48	ISS-NA ANALOG ENGR TLM	0.01			-1		-12	-4							-35	-8			-18						-54	
49	MAG OBLFM SENSOR TEMP	0.01			-33	-20			-11																	
50	IRIS FRAME START	4.00																								
51	IRIS RAD-MTR H-G ANALOG	0.01	-2	-6			-1	-5			-6				-26				-24	-6					-43	
52	IRIS PLL CARRIER	0.20																							-5	
53	PITCH CRUISE SS/I POSN	0.01																								
54	CSTI CONE ANGLE CMD A	3.50																								
55	CSTI STAR INTENSITY	0.01																								
56	CSTI CONE ANGLE POSITION	0.60																								
57	OBLFM X OUT % COAX <	1.00E-7	-54	-33	-159	-123	-101	-93	-145	-81	-81	-35	-89	-26	-39	-24	-80	-92	-117	-70	-136	-73	-130	-76	-67	
58	IBHFM X OUT % COAX <	9.99E-7	-60	-46	-133	-107	-80	-66	-116	-44	-56	-18	-68	-3	-34	-12	-47	-58	-84	-46	-103	-39	-98	-52	-25	
59	CRS ANALOG DATA	0.01	-1	-2			-6	-4			-4				-20	-1			-21						-18	
60	HGA S-BAND FEED TEMP	1.00																								
61	X-BAND FEED TEMP	1.00																								
62	IRIS SEC MIRROR TEMP	1.00																							-2	
63	IRIS SEC MIRROR RTR ANLG	1.00																							-1	
64	SS 1 SYNC	1.00																								
65	PITCH SS BIAS	1.00																								
66	RTG CASE TEMP	1.00																								
67	RTG POWER	1.00																								
68	X-BAND FEED TEMP	1.00																								
69	X-BAND FEED TEMP	1.00																								
70	X-BAND FEED TEMP	1.00																								
71	X-BAND FEED TEMP	1.00																								
72	X-BAND FEED TEMP	1.00																								
73	HGA DISH TEMP	1.00																								
74	HGA DISH TEMP	1.00																								
75	HGA DISH TEMP	1.00																								
76	HGA DISH TEMP	1.00																								
77	HGA DISH TEMP	1.00																								

*NEGATIVE MARGINS SHOULD BE REDUCED BY 6 dB.

Table 2-15. Voltage Thresholds and Negative dB Margins of Immunity *

Run 10 9/15/78

RECEPTORS			GENERATOR PARAMETERS																					
			BREWSTER PLATE		MAG CABLE		SEP CONN		MAG TEFLON		HGA OB PAINT		PLUME SH SEP CONN		LECP TEFLON		FSS		HGA IB PAINT		PLUME SH RTG		RTG OXIDE		MIRIS KAPTON	
NO.	NAME	VOLTAGE THRESHOLD	RECPL	LOOP	RECPL	LOOP	RECPL	LOOP	RECPL	LOOP	RECPL	LOOP	RECPL	LOOP	RECPL	LOOP	RECPL	LOOP	RECPL	LOOP	RECPL	LOOP	RECPL	LOOP	RECPL	LOOP
1	TLM BAY 6 TEMP	0.01		-14	-8			-9			-8	-5								-4						
2	S-TWTA HI/LO STAT	2.00																								
3	S-TWTA I ON STAT<	10.00																								
4	50.4 KHz % 02-06	2.00																								
5	TLM S-BAND TWT REG V	0.01																								
6	S-TWTA RF DR MONITOR	0.01		-24				-5			-4	-16								-15						
7	CMPST CMD, RCVR 1 TO CDU-A	0.01						-6																		
8	TLM S-BAND EX CURR	0.01		-28	-4			-11			-11	-21								-19						
9	TLM RCVR VCO TEMP	0.01			-4			-1			-2															
10	TLM RCVR LO DR	0.01		-12	-4			-10			-4	-3								-2						
11	TLM S-BAND TWT DR	0.01		-12	-4			-10			-4	-3								-2						
12	CDU-A COMMAND DATA, XR	2.00																								
13	TMU A SYMBOL SYNC	2.00																								
14	HGH RATE CHAN DATA TMU-A	1.50																								
15	CC STROBE XR	4.50																								
16	CCS BIT SYNC 1	4.50																								
17	CCS DATA TO AACS XR	4.00																								
18	POWER CODE B XR	1.20																								
19	BOT/EOT XR	1.20																								
20	POWER CODE	1.00																								
21	POWER CODE	1.00																								
22	TLM SUN SENSOR TEMP	0.01			-1																					
23	AACS DATA	4.00																								
24	AACS ADDRESS DATA	2.00																								
25	TLM PYRO AMP IND A	4.00																								
26	TLM TCAPU TANK TEMP 1	0.01		-28				-9			-8	-20								-18						
27	CC DATA 2	4.00																								
28	PLAYBACK DATA	4.00																								
29	TLM DSS MOTOR V	0.01		-24				-7			-7	-16								-16						
30	CRS CMD WORD	4.00																								
31	CRS TELESCOPE TEMP	0.01													-7	-1									-37	
32	PWS ADC BIT SYNC	2.00																								
33	PRA ANALOG MUX DATA	0.01		-8	-3			-5			-2															
34	PRA ELECTRONICS TEMP	0.01		-10	-3			-5			-3															
35	PRA CMD WORD	2.00																								
36	LECP CMD WORD A	4.00																								
37	LECP ANALOG DATA	0.01		-2				-6							-8	-10									-41	
38	PPS COMMAND WORD	4.00																								
39	PPS SOLAR SENSOR	0.01		-6				-10							-25	-10				-5					-77	

*NEGATIVE MARGINS SHOULD BE REDUCED BY 6 dB.

FOLDOUT FRAME 1

FOLDOUT FRAME 2

C-2

FOLDOUT FRAME 1

FOLDOUT FRAME 2

Table 2-15. Voltage Thresholds and Negative dB Margins of Immunity (Cont)*

Run 10 9/15/78

RECEPTORS			GENERATOR PARAMETERS																							
		VOLTAGE	BREWSTER PLATE		MAG CABLE		SEP CONN		MAG TEFLON		HGA OB PAINT		PLUME SH SEP CONN		LEOP TEFLON		FSS		HGA IB PAINT		PLUME SH RTG		RTG OXIDE		MIRIS KAPTON	
NO.	NAME	THRESHOLD	RECPL	LOOP	RECPL	LOOP	RECPL	LOOP	RECPL	LOOP	RECPL	LOOP	RECPL	LOOP	RECPL	LOOP	RECPL	LOOP	RECPL	LOOP	RECPL	LOOP	RECPL	LOOP	RECPL	LOOP
40	UVS MODE CONTROL	4.00																								
41	UVS HV MONITOR	0.01		-7				-11							-24	-12				-5					-76	
42	UVS SCIENCE DATA 1	2.00																								
43	MAG SAMPLE B	4.00																								
44	MAG IBHFM CLOCK 50.4 KHz	4.00																								
45	MAG OBLFM SENSOR TEMP	0.01			-28	-12			-12																	
46	ISS-WA ADC START	2.00																							-6	
47	ISS-WA ADC VIDEO DATA	4.00																								
48	ISS-NA ANALOG ENGR TLM	0.01						-4							-23	-8									-75	
49	MAG OBLFM SENSOR TEMP	0.01			-21	-20			-3																	
50	IRIS FRAME START	4.00																								
51	IRIS RAD-MTR H-G ANALOG	0.01		-6				-5							-14					-5					-64	
52	IRIS PLL CARRIER	0.20																							-26	
53	PITCH CRUISE 55/1 POSN	0.01																								
54	CSTI CONE ANGLE CMD A	3.50																								
55	CSTI STAR INTENSITY	0.01																								
56	CSTI CONE ANGLE POSITION	0.60																								
57	OBLFM X OUT % COAX <	1.00E-7	-12	-33	-147	-123	-74	-93	-137	-81	-53	-35	-26	-26	-26	-24	-80	-92	-73	-70	-90	-73	-110	-76	-88	
58	IBHFM X OUT % COAX <	9.99E-7	-18	-46	-121	-107	-53	-66	-108	-44	-28	-18	-4	-3	-22	-12	-47	-58	-41	-46	-58	-39	-77	-52	-46	
59	CRS ANALOG DATA	0.01		-2				-4							-8	-1									-39	
60	HGA S-BAND FEED TEMP	1.00																								
61	X-BAND FEED TEMP	1.00																								
62	IRIS SEC MIRROR TEMP	1.00																							-23	
63	IRIS SEC MIRROR HTR ANLG	1.00																							-22	
64	SS 1 SYNC	1.00																								
65	PITCH SS BIAS	1.00																								
66	RTG CASE TEMP	1.00																								
67	RTG POWER	1.00																								
68	X-BAND FEED TEMP	1.00																								
69	X-BAND FEED TEMP	1.00																								
70	X-BAND FEED TEMP	1.00																								
71	X-BAND FEED TEMP	1.00																								
72	X-BAND FEED TEMP	1.00																								
73	HGA DISH TEMP	1.00																								
74	HGA DISH TEMP	1.00																								
75	HGA DISH TEMP	1.00																								
76	HGA DISH TEMP	1.00																								
77	HGA DISH TEMP	1.00																								

*NEGATIVE MARGINS SHOULD BE REDUCED BY 6 dB.

FOLDOUT FRAME 1

FOLDOUT FRAME 2

Table 2-16. Voltage Thresholds and Negative dB Margins of Immunity*

Run 11 10/19/78

NO.	RECEPTORS NAME	VOLTAGE THRESHOLD	GENERATOR PARAMETERS: BREWSTER PLATE RECPL	BREWSTER PLATE LOOP	MAG CABLE RECPL	MAG CABLE LOOP	SEP CONN RECPL	SEP CONN LOOP	MAG TEFLON RECPL	MAG TEFLON LOOP	HGA OB PAINT RECPL	HGA OB PAINT LOOP	PLUME SH SEP CONN RECPL	PLUME SH SEP CONN LOOP	LECP TEFLON RECPL	LECP TEFLON LOOP	FSS RECPL	FSS LOOP	HGA IB PAINT RECPL	HGA IB PAINT LOOP	PLUME SH RTG RECPL	PLUME SH RTG LOOP	RTG OXIDE RECPL	RTG OXIDE LOOP	MIRIS KAPTON RECPL	MIRIS KAPTON LOOP
1	TLM BAY 6 TEMP	0.01		-24	-14		-2	-9			-6	-5								-4			-4			
2	S-TWTA HI/LO STAT	2.00																								
3	S-TWTA I ON STAT<	10.00																								
4	50.4 KHz % 02-08	2.00																								
5	TLM S-BAND TWT REG V	0.01		-4	-6																					
6	S-TWTA RF DR MONITOR	0.01		-33				-5			-6	-16								-15						
7	CMPST CMD, RCVR 1 TO CDU-A	0.01		-9				-5																		
8	TLM S-BAND EX CURR	0.01		-37	-10			-11			-13	-21							-4	-19			-1			
9	TLM RCVR VCO TEMP	0.01		-11	-10			-1																		
10	TLM RCVR LO DR	0.01		-22	-10			-10			-3	-4								-2						
11	TLM S-BAND TWT DR	0.01		-23	-10			-10			-3	-4								-2						
12	CDU-A COMMAND DATA, XR	2.00																								
13	TMU A SYMBOL SYNC	2.00																								
14	HGH RATE CHAN DATA TMU-A	1.50																								
15	CC STROBE XR	4.50																								
16	CCS BIT SYNC 1	4.50																								
17	CCS DATA TO AACS XR	4.00																								
18	POWER CODE B XR	1.20																								
19	BOT/EOT XR	1.20																								
20	POWER CODE	1.00																								
21	POWER CODE	1.00																								
22	TLM SUN SENSOR TEMP	0.01		-5	-7																					
23	AACS DATA	4.00																								
24	AACS ADDRESS DATA	2.00																								
25	TLM PYRO AMP IND A	4.00																								
26	TLM TCAPU TANK TEMP 1	0.01		-36				-9			-10	-20								-18						
27	CC DATA 2	4.00																								
28	PLAYBACK DATA	4.00																								
29	TLM DSS MOTOR V	0.01		-33	-6			-7			-7	-16								-15						
30	CRS CMD WORD	4.00																								
31	CRS TELESCOPE TEMP	0.01													-13	-1									-15	
32	PWS ADC BIT SYNC	2.00																								
33	PRA ANALOG MUX DATA	0.01		-18	-9			-5																		
34	PRA ELECTRONICS TEMP	0.01		-20	-9			-5			-1															
35	PRA CMD WORD	2.00																								
36	LECP CMD WORD A	4.00																								
37	LECP ANALOG DATA	0.01		-11				-6							-14	-10									-19	
38	PPS COMMAND WORD	4.00																								
39	PPS SOLAR SENSOR	0.01		-15				-10							-31	-10				-5					-55	

*NEGATIVE MARGINS SHOULD BE REDUCED BY 6 DB.

FOLDOUT FRAME 1

FOLDOUT FRAME 2

Table 2-16. Voltage Thresholds and Negative dB Margins of Immunity (Cont) *

Run 11 10/19/78

RECEPTORS			GENERATOR PARAMETERS																					
			BREWSTER PLATE		MAG CABLE		SEP CONN		MAG TEFLON		HGA OB PAINT		PLUME SH SEP CONN		LECP TEFLON		FSS		HGA IB PAINT		PLUME SH RTG		RTG OXIDE		MIRIS KAPTON	
NO.	NAME	VOLTAGE THRESHOLD	RECPL	LOOP	RECPL	LOOP	RECPL	LOOP	RECPL	LOOP	RECPL	LOOP	RECPL	LOOP	RECPL	LOOP	RECPL	LOOP	RECPL	LOOP	RECPL	LOOP	RECPL	LOOP	RECPL	LOOP
40	UVS MODE CONTROL	4.00																								
41	UVS HV MONITOR	0.01		-15				-11							-30	-12				-5					-55	
42	UVS SCIENCE DATA I	2.00																								
43	MAG SAMPLE B	4.00																								
44	MAG IBHFM CLOCK 50.4 KHz	4.00																								
45	MAG OBLFM SENSOR TEMP	0.01			-32	-12			-17																	
46	ISS-WA ADC START	2.00																								
47	ISS-WA ADC VIDEO DATA	4.00																								
48	ISS-NA ANALOG ENGR TLM	0.01						-4							-29	-8									-54	
49	MAG OBLFM SENSOR TEMP	0.01			-27	-20			-8																	
50	IRIS FRAME START	4.00																								
51	IRIS RAD-MTR H-G ANALOG	0.01		-15				-6							-20					-5					-43	
52	IRIS PLL CARRIER	0.20																							-6	
53	PITCH CRUISE SS/1 POSN	0.01																								
54	CSTI CONE ANGLE CMD A	3.50																								
55	CSTI STAR INTENSITY	0.01																								
56	CSTI CONE ANGLE POSITION	0.60																								
57	OBLFM X OUT % COAX <	1.00E-7		-46	-153	-123	-83	-93	-142	-81	-50	-36	-60	-26	-32	-24	-80	-92	-80	-70	-102	-73	-124	-82	-67	
58	IBHFM X OUT % COAX <	9.99E-7	-14	-57	-127	-107	-62	-66	-113	-44	-25	-17	-38	-3	-28	-12	-47	-68	-47	-46	-70	-39	-92	-57	-25	
59	CRS ANALOG DATA	0.01		-11				-4							-14	-1									-18	
60	HGA S-BAND FEED TEMP	1.00																								
61	X-BAND FEED TEMP	1.00																								
62	IRIS SEC MIRROR TEMP	1.00																							-2	
63	IRIS SEC MIRROR HTR ANLG	1.00																							-1	
64	SS 1 SYNC	1.00																								
65	PITCH SS BIAS	1.00																								
66	RTG CASE TEMP	1.00																								
67	RTG POWER	1.00																								
68	X-BAND FEED TEMP	1.00																								
69	X-BAND FEED TEMP	1.00																								
70	X-BAND FEED TEMP	1.00																								
71	X-BAND FEED TEMP	1.00																								
72	X-BAND FEED TEMP	1.00																								
73	HGA DISH TEMP	1.00																								
74	HGA DISH TEMP	1.00																								
75	HGA DISH TEMP	1.00																								
76	HGA DISH TEMP	1.00																								
77	HGA DISH TEMP	1.00																								

*NEGATIVE MARGINS SHOULD BE REDUCED BY 6 dB.

FOLDOUT FRAME 1

FOLDOUT FRAME 2

Table 2-17. Voltage Thresholds and Negative dB Margins of Immunity *

Run 12 10/20/78

RECEPTORS			GENERATOR PARAMETERS																							
NO.	NAME	VOLTAGE THRESHOLD	BREWSTER PLATE		MAG CABLE		SEP CONN		MAG TEFLON		HGA OB PAINT		PLUME SH SEP CONN		LECP TEFLON		FSS		HGA IB PAINT		PLUME SH RTG		RTG OXIDE		MIRIS KAPTON	
			RECPL	LOOP	RECPL	LOOP	RECPL	LOOP	RECPL	LOOP	RECPL	LOOP	RECPL	LOOP	RECPL	LOOP	RECPL	LOOP	RECPL	LOOP	RECPL	LOOP	RECPL	LOOP	RECPL	LOOP
1	TLM BAY 6 TEMP	0.01		-13	-26		-10	-9	-9			-35							-19	-4						
2	S-TWTA HI/LO STAT	2.00										-3														
3	S-TWTA I ON STAT<	10.00																								
4	50.4 KHz % 02-08	2.00																								
5	TLM S-BAND TWT REG V	0.01			-18		-3		-2			-23							-10							
6	S-TWTA RF DR MONITOR	0.01		-22	-6			-5				-24							-17	-15						
7	CMPST CMD, RCVR 1 TO CDU-A	0.01			-8			-5				-40							-1							
8	TLM S-BAND EX CURR	0.01		-26	-22		-7	-11	-5			-28							-24	-19						
9	TLM RCVR VCO TEMP	0.01			-22		-6	-1	-5			-30							-13							
10	TLM RCVR LO DR	0.01		-12	-22		-6	-10	-5			-43							-16	-2						
11	TLM S-BAND TWT DR	0.01		-12	-22		-6	-10	-5			-42							-16	-2						
12	CDU-A COMMAND DATA, XR	2.00										-8														
13	TMU A SYMBOL SYNC	2.00																								
14	HGH RATE CHAN DATA TMU-A	1.50																								
15	CC STROBE XR	4.50																								
16	CCS BIT SYNC 1	4.50																								
17	CCS DATA TO AACS XR	4.00																								
18	POWER CODE B XR	1.20																								
19	BOT/EOT XR	1.20										-8														
20	POWER CODE	1.00										-3														
21	POWER CODE	1.00																								
22	TLM SUN SENSOR TEMP	0.01			-19				-2			-19														
23	AACS DATA	4.00																								
24	AACS ADDRESS DATA	2.00																								
25	TLM PYRO AMP IND A	4.00																								
26	TLM TCAPU TANK TEMP 1	0.01		-25	-9			-9				-27							-20	-18						
27	CC DATA 2	4.00																								
28	PLAYBACK DATA	4.00																								
29	TLM DSS MOTOR V	0.01		-22	-17		-2	-7				-23							-19	-15						
30	CRS CMD WORD	4.00																								
31	CRS TELESCOPE TEMP	0.01			-2										-16	-1									-15	
32	PWS ADC BIT SYNC	2.00																								
33	PRA ANALOG MUX DATA	0.01		-7	-21		-5	-5	-4			-33							-14							
34	PRA ELECTRONICS TEMP	0.01		-9	-21		-5	-5	-4			-31							-14							
35	PRA CMD WORD	2.00																								
36	LECP CMD WORD A	4.00																								
37	LECP ANALOG DATA	0.01			-3			-6				-4			-19	-10			-4						-19	
38	PPS COMMAND WORD	4.00																								
39	PPS SOLAR SENSOR	0.01		-4	-7		-3	-10				-10			-35	-10			-9	-5					-55	

*NEGATIVE MARGINS SHOULD BE REDUCED BY 6 dB.

FOLDOUT FRAME 2

FOLDOUT FRAME 1

Table 2-17. Voltage Thresholds and Negative dB Margins of Immunity (Cont)*

Run 12 10/20/78

RECEPTORS			GENERATOR PARAMETERS																							
		VOLTAGE	BREWSTER PLATE		MAG CABLE		SEP CONN		MAG TEFLON		HGA OB PAINT		PLUME SH SEP CONN		LECP TEFLON		FSS		HGA B PAINT		PLUME SH RTG		RTG OXIDE		MIRIS KAPTON	
NO.	NAME	THRESHOLD	RECPL	LOOP	RECPL	LOOP	RECPL	LOOP	RECPL	LOOP	RECPL	LOOP	RECPL	LOOP	RECPL	LOOP	RECPL	LOOP	RECPL	LOOP	RECPL	LOOP	RECPL	LOOP	RECPL	LOOP
40	UVS MODE CONTROL	4.00																								
41	UVS HV MONITOR	0.01		-5	-8		-3	-11		-14					-34	-12			-10	-6					-55	
42	UVS SCIENCE DATA I	2.00																								
43	MAG SAMPLE B	4.00																								
44	MAG IBHFM CLOCK 50.4 KHz	4.00																								
45	MAG OBLFM SENSOR TEMP	0.01			-44	-12			-26																	
46	ISS-WA ADC START	2.00																								
47	ISS-WA ADC VIDEO DATA	4.00																								
48	ISS-NA ANALOG ENGR TLM	0.01			-7		-2	-4		-6					-33	-8			-1						-54	
49	MAG OBLFM SENSOR TEMP	0.01			-39	-20			-17																	
50	IRIS FRAME START	4.00																								
51	IRIS RAD-MTR H-G ANALOG	0.01		-4				-5		-3															-43	
52	IRIS PLL CARRIER	0.20													-23				-7	-5					-5	
53	PITCH CRUISE SS/I POSN	0.01																								
54	CSTI CONE ANGLE CMD A	3.50																								
55	CSTI STAR INTENSITY	0.01																								
56	CSTI CONE ANGLE POSITION	0.60																								
57	OBLFM X OUT % COAX <	1.00E-7	-19	-36	-165	-123	-91	-93	-151	-81	-37	-79	-74	-26	-36	-24	-80	-92	-100	-70	-122	-73	-82	-104	-67	
58	IBHFM X OUT % COAX <	9.99E-7	-25	-46	-139	-107	-70	-66	-122	-44	-11	-50	-52	-3	-31	-12	-47	-58	-67	-46	-90	-39	-49	-68	-25	
59	CRS ANALOG DATA	0.01			-2			-4							-17	-1			-4						-18	
60	HGA S-BAND FEED TEMP	1.00																								
61	X-BAND FEED TEMP	1.00																								
62	IRIS SEC MIRROR TEMP	1.00																							-2	
63	IRIS SEC MIRROR HTR ANLG	1.00																							-1	
64	SS 1 SYNC	1.00																								
65	PITCH SS BIAS	1.00																								
66	RTG CASE TEMP	1.00																								
67	RTG POWER	1.00																								
68	X-BAND FEED TEMP	1.00																								
69	X-BAND FEED TEMP	1.00																								
70	X-BAND FEED TEMP	1.00																								
71	X-BAND FEED TEMP	1.00																								
72	X-BAND FEED TEMP	1.00																								
73	HGA DISH TEMP	1.00																								
74	HGA DISH TEMP	1.00																								
75	HGA DISH TEMP	1.00																								
76	HGA DISH TEMP	1.00																								
77	HGA DISH TEMP	1.00																								

*NEGATIVE MARGINS SHOULD BE REDUCED BY 6 DB.

FOLDOUT FRAME 1

FOLDOUT FRAME 2

Table 2-18. Voltage Thresholds and Negative DB Margins of Immunity for COMPLETE-ARCS-TO-SPACE Model (G=1) *

RECEPTORS			GENERATOR PARAMETERS																					
			BREWSTER PLATE		MAG CABLE		SEP CONN		MAG TEFLON		HGA OB PAINT		PLUME SH SEP CONN		LECP TEFLON		FSS		HGA IB PAINT		PLUME SH RTG		RTG OXIDE		MIRIS KAPTON	
NO.	NAME		RECPL	LOOP	RECPL	LOOP	RECPL	LOOP	RECPL	LOOP	RECPL	LOOP	RECPL	LOOP	RECPL	LOOP	RECPL	LOOP	RECPL	LOOP	RECPL	LOOP	RECPL	LOOP	RECPL	LOOP
1	TLM BAY 5 TEMP	0.01	-46	-36	-74	-19	-38	-25	-23		-66	-35	-31						-65	-33	-35		-62	-24		
2	S-TWTA HI/LO STAT	2.00			-19						-9								-8				-7			
3	S-TWTAI ON STAT<	10.00			-5																					
4	50.4 KHz % 02-06	2.00		-4	-14						-22	-4							-21	-1			-5			
5	TLM S-BAND TWT REG V	0.01	-37	-9	-66		-29	-13	-16		-57		-24						-56		-28		-54			
6	S-TWTA RF DR MONITOR	0.01	-42	-46	-54	-28	-19	-21	-3		-64	-46	-15						-63	-44	-19		-46	-34		
7	CMPST CMD, RCVR 1 TO CDU-A	0.01	-27	-17	-56	-6	-18	-21	-6		-48	-12	-14						-47	-11	-17		-44	-2		
8	TLM S-BAND EX CURR	0.01	-49	-50	-70	-33	-33	-27	-19		-71	-51	-26						-69	-48	-32		-59	-39		
9	TLM RCVR VCO TEMP	0.01	-40	-19	-70	-4	-32	-17	-19		-60	-15	-27						-59	-13	-31		-58	-4		
10	TLM RCVR LO DR	0.01	-42	-34	-70	-18	-32	-26	-19		-63	-33	-28						-62	-31	-31		-58	-22		
11	TLM S-BAND TWT DR	0.01	-42	-34	-70	-18	-32	-26	-19		-63	-33	-28						-62	-31	-31		-58	-22		
12	CDU-A COMMAND DATA, XR	2.00			-21						-18								-17				-11			
13	TMU A SYMBOL SYNC	2.00			-13						-12								-10				-2			
14	HGH RATE CHAN DATA TMU-A	1.50			-25						-16								-15				-13			
15	CC STROBE XR	4.50			-9																					
16	CCS BIT SYNC 1	4.50			-8						-6								-5							
17	CCS DATA TO AACS XR	4.00			-13						-5								-4				-1			
18	POWER CODE B XR	1.20			-28						-17								-16				-11			
19	BOT/EOT XR	1.20			-19						-17								-19				-8			
20	POWER CODE	1.00			-24						-18								-17				-12			
21	POWER CODE	1.00	-4	-6	-24						-26	-6							-24	-3			-13			
22	TLM SUN SENSOR TEMP	0.01	-25	-17	-67	-14	-16	-6	-16		-49	-19	-11						-44	-13	-21		-54	-17		
23	AACS DATA	4.00																								
24	AACS ADDRESS DATA	2.00			-15						-17								-15				-5			
25	TLM PYRO AMP IND A	4.00																								
26	TLM TCAPU TANK TEMP 1	0.01	-46	-50	-57	-32	-22	-25	-6		-68	-50	-19						-66	-47	-22		-49	-38		
27	CC DATA 2	4.00			-2						-2								-1							
28	PLAYBACK DATA	4.00																								
29	TLM DSS MOTOR V	0.01	-44	-46	-65	-29	-28	-23	-13		-66	-46	-23						-65	-44	-27		-54	-34		
30	CRS CMD WORD	4.00																								
31	CRS TELESCOPE TEMP	0.01	-15	-6	-50		-23	-13			-25		-19		-19	-1			-42	-10			-35		-15	
32	PWS ADC BIT SYNC	2.00																								
33	PRA ANALOG MUX DATA	0.01	-40	-30	-69	-13	-31	-21	-18		-61	-28	-26						-60	-26	-30		-57	-17		
34	PRA ELECTRONICS TEMP	0.01	-41	-32	-69	-15	-31	-21	-18		-61	-30	-26						-60	-28	-30		-57	-19		
35	PRA CMD WORD	2.00																								
36	LECP CMD WORD A	4.00																								
37	LECP ANALOG DATA	0.01	-23	-24	-51	-14	-24	-22			-34	-13	-20		-20	-10			-50	-29			-36	-16	-19	
38	PPS COMMAND WORD	4.00																								
39	PPS SOLAR SENSOR	0.01	-27	-28	-55	-19	-29	-26	-4		-39	-18	-25		-27	-10			-55	-34			-41	-20	-55	

*NEGATIVE MARGINS SHOULD BE REDUCED BY 6 DB.

FOLDOUT FRAME /

FOLDOUT FRAME 2

Table 2-18. Voltage Thresholds and Negative DB Margins of Immunity for COMPLETE-ARCS-TO-SPACE Model (G=1) (Cont) *

RECEPTORS			GENERATOR PARAMETERS																					
			BREWSTER PLATE		MAG CABLE		SEP CONN		MAG TEFLON		HGA OB PAINT		PLUME SH SEP CONN		LECP TEFLON		FSS		HGA IB PAINT		PLUME SH RTG		RTG OXIDE		MIRIS KAPTON	
NO.	NAME		RECPL	LOOP	RECPL	LOOP	RECPL	LOOP	RECPL	LOOP	RECPL	LOOP	RECPL	LOOP	RECPL	LOOP	RECPL	LOOP	RECPL	LOOP	RECPL	LOOP	RECPL	LOOP	RECPL	LOOP
40	UVS MODE CONTROL	4.00																								
41	UVS HV MONITOR	0.01	-28	-29	-56	-19	-28	-27	-5		-39	-18	-25		-36	-12			-56	-34			-41	-21	-55	
42	UVS SCIENCE DATA I	2.00																								
43	MAG SAMPLE B	4.00																								
44	MAG IBHFM CLOCK 50.4 KHz	4.00																								
45	MAG OBLFM SENSOR TEMP	0.01			-92	-66			-40										-17		-28		-49	-19		
46	ISS-WA ADC START	2.00																								
47	ISS-WA ADC VIDEO DATA	4.00																								
48	ISS-NA ANALOG ENGR TLM	0.01	-20	-12	-66	-3	-28	-20	-4		-30	-1	-24		-35	-8			-47	-16			-40	-3	-54	
49	MAG OBLFM SENSOR TEMP	0.01			-87	-74		-3	-31										-11		-20		-40	-19		
50	IRIS FRAME START	4.00																								
51	IRIS RAD-MTR H-G ANALOG	0.01	-24	-28	-41	-18	-17	-21			-36	-18	-14		-26				-53	-34			-31	-20	-43	
52	IRIS PLL CARRIER	0.20			-18														-9				-2		-5	
53	PITCH CRUISE SS/I POSN	0.01																								
54	CSTI CONE ANGLE CMD A	3.50																								
55	CSTI STAR INTENSITY	0.01																								
56	CSTI CONE ANGLE POSITION	0.60																								
57	OBLFM X OUT % COAX <	1.00 E-7	-76	-55	-213	-177	-117	-109	-165	-101	-111	-65	-113	-50	-39	-24	-80	-62	-148	-99	-163	-100	-182	-128	-67	
58	IBHFM X OUT % COAX <	9.99 E-7	-82	-68	-187	-161	-96	-82	-136	-64	-86	-48	-92	-27	-34	-12	-47	-58	-113	-75	-130	-66	-150	-104	-25	
59	CRS ANALOG DATA	0.01	-23	-24	-50	-14	-24	-20			-34	-13	-20		-20	-1			-50	-28			-36	-15	-18	
60	HGA S-BAND FEED TEMP	1.00																								
61	X-BAND FEED TEMP	1.00																								
62	IRIS SEC MIRROR TEMP	1.00			-15														-14				-1		-2	
63	IRIS SEC MIRROR HTR ANLG	1.00			-15														-15				-1		-1	
64	SS I SYNC	1.00																								
65	PITCH SS BIAS	1.00																								
66	RTG CASE TEMP	1.00																					-50	-42		
67	RTG POWER	1.00			-25																		-49	-31		
68	X-BAND FEED TEMP	1.00																								
69	X-BAND FEED TEMP	1.00																								
70	X-BAND FEED TEMP	1.00																								
71	X-BAND FEED TEMP	1.00																								
72	X-BAND FEED TEMP	1.00																								
73	HGA DISH TEMP	1.00																								
74	HGA DISH TEMP	1.00																								
75	HGA DISH TEMP	1.00																								
76	HGA DISH TEMP	1.00																								
77	HGA DISH TEMP	1.00																								
		1.00																								

*NEGATIVE MARGINS SHOULD BE REDUCED BY 6 DB.

model represents a completely worst case situation which most likely does not exist. It does, however, correspond to the configuration in which nearly all laboratory measurements of arc characteristics are made, i.e., arc currents measured with a small (∿10 ohm) resistance to the vacuum tank walls and the return (replacement) currents from the walls to the sample reported. In space, the spacecraft (wall) potential is not fixed, but rather, rises to a value consistent with the ability of the entire spacecraft to collect the return current. As indicated in Section 1.2, a serious deficiency in the laboratory definition of arc characteristics lies in the test-setup differences from in-flight conditions. Although the proper values of G' that should be used in the SEMCAP analysis are undefined at the present time, we feel that the smaller displacement current values used in Run 9 are more nearly appropriate than the unity G' values.

REFERENCES

1. Inouye. G. T., A. C. Whittlesey, S. R. Ponamgi, B. D. Cooperstein, and A. K. Thomas, "Voyager Spacecraft Electrostatic Discharge Immunity Verification Tests," presented at 2nd Symposium on the Effect of the Ionosphere on Space and Terrestrial Systems, IES '78, Arlington, VA., Jan 24-26, 1978.

2. Boeing Aerospace Company, "Electrostatic Charging and Discharging of Mariner-Jupiter/Saturn Spacecraft Parts" dated April 1977.

3. THREAT DETERMINATION

The susceptibility of typical spacecraft components to disruption by arc discharges is discussed in this section. The SEMCAP analyses performed under Task 2 on the Voyager spacecraft model provided the estimates of induced voltages on each receptor or victim wire from each of the sources modelled, and since the anomalous operation thresholds for each receptor are included in the SEMCAP model, db margins of immunity are also provided. The determination of the threat to typical spacecraft components, as indicated in the previous section, is not directly indicated by the fact that a negative db margin exists. Further insight into this question and the susceptibility of typical components in two other spacecraft, the DSCS II and HEAO, are presented in this section.

The information presented in this section can be used to develop rough assessments of the threat of circuit upset due to arc discharges or other transient voltages coupled into a circuit. In addition to upset levels for bistable circuits, thresholds for certain types of analog circuits are also presented here. Although analog circuits will not be upset by transients, bit errors can be introduced in the digitizing process. The degree of error is a function of the amplitude, duration, and moment of occurrence of the transient event.

Tables 3-1 and 3-2 are lists of the noise threshold characteristics of circuits likely to be found on a communications satellite and a scientific satellite, respectively. The range of parameters will, of course, vary from satellite to satellite and from contractor to contractor, so generalizing these parameters to include other satellites is not recommended, as serious errors could result. The three parameters shown are DC Noise Margin (DCNM), cutoff frequency (F_c), and the frequency response roll-off rate (slope). These parameters are shown graphically in Figure 3-1. It is obvious that these three parameters define the frequency response of circuits having low-pass filter characteristics. Such circuits account for almost all of the circuits on a satellite likely to respond to transients. In special circumstances, circuits having band-pass characteristics may be encountered in the

Table 3-1. Typical DSCS II Noise Threshold Characteristics

Subsystem	Circuit Type	DCNM (Volts)	F_c (Hertz)	Slope
Communications	TWTA ON CMD	7	1.28×10^6	2
	TDAL CH 1	.45	1×10^6	2
	EC BEACON	15	1×10^6	2
	RF ASSY A GEN	.45	1×10^6	2
	EC BEACON (MAX)	2.5	3400	1
	EC BEACON (-10 DB)	.1	16000	1
Elec. Integ.	BATTERY DISC	12	1×10^6	2
	500 HZ CLOCK	2.5	1×10^6	2
	EIA/DEA CMD EX	.5	100	1
	EIA/CTA CMD EX	.5	100	1
ACS	PLAT REF PLS 25	.083	1×10^6	1
	PLAT REF PLS 0	.5	1×10^6	1
	EARTH SENS SIG	.7	2×10^6	1
	DEA RESET	1.5	18×10^6	1
	GIM MOT ADV	.5	18×10^6	1
TT&C	TLM CLOCK A	2.5	40×10^6	2
	TANK PRESS	.013	125	1
	TLM SYNC	2.5	20×10^6	2
	SLA CONV OV-A	1	40×10^6	1
	SIGNAL PRESENT	1.2	14×10^6	1
	TWTA TEMP	.02	12000	1
	TWTA HELIX I	.02	12000	1
	TWTA CATHODE V	.02	12000	1
HTR Control	DESPUN TEMP SENS	.03	3000	1
	BUS V LIMITER	.6	1000	1
PWR DIST	PRESS XDUCER PWR	4.5	340	1
	CTA 5V SEL CMD	5	1000	2
	DEA 5V SEL CMD	5	3000	2
	GEA SEC PWR	5	700	2

Table 3-2. Samples of HEAO-A Noise Threshold Characteristics

Subsystem	Circuit Type	DCNM (Volts)	F_c (Hertz)	Slope
Command	DHA/CIA PRI DIFF CMD	3.9	$15x10^6$	1
	DHA/CIA SEC PAR CMD	1	$10x10^6$	2
	SIA/DHA CONV OFF	2	16000	1
	SIA/XPNDR XMTR OFF	.6	$35x10^6$	2
	SIA/XPNDR XMTR ON	7.5	$35x10^6$	2
	SIA/XPNDR XMTR OVERRIDE	8.5	$1x10^6$	2
	SIA/XPNDR XMTR ENABLE	.47	$1x10^6$	2
	SIA/XPNDR RANGING OFF	1.5	$7.8x10^6$	2
	SIA/XPNDR AUX OSC	4.2	30000	1
	SIA/CIA FAILURE MODE	4	$14x10^6$	1
	DHA/TR ALL TAPE REC CMD	3.8	$11x10^6$	1
	CIA/DPA INT REQ LEV	1	$7.5x10^5$	1
Control Data	ZERO ENT/SIA SEP SIG 1	1	10000	1
	ZERO ENT/SIA SEP SIG 2	.7	24000	2
	PCU/SM SHNT VOLT SEQ	2	$1.4x10^5$	1
Telemetry	PCU/DHA MAIN BUS CURR	.1	88000	1
	DCA/CIA CPU CLOCK	3.9	$15x10^6$	1
	CIA/DHA CLOCK	.9	$19x10^6$	1
	EAA/DHA CLOCK	.9	$30x10^6$	1
	PCU/DHA BUS VOLTAGE	1.5	$1.8x10^6$	1
	PCU/DHA BATT DISCH	3.5	88000	1
Analog Control	ZSSA/CIA NA INPUT S	.01	16000	1
	ZSSA/CIA SUN SENS PRES	.001	3200	1
	YSSA/CIA YSSA OUTPUTS	.005	5000	1
	ADM/PCU BUS SENSE	.004	$1.5x10^5$	1

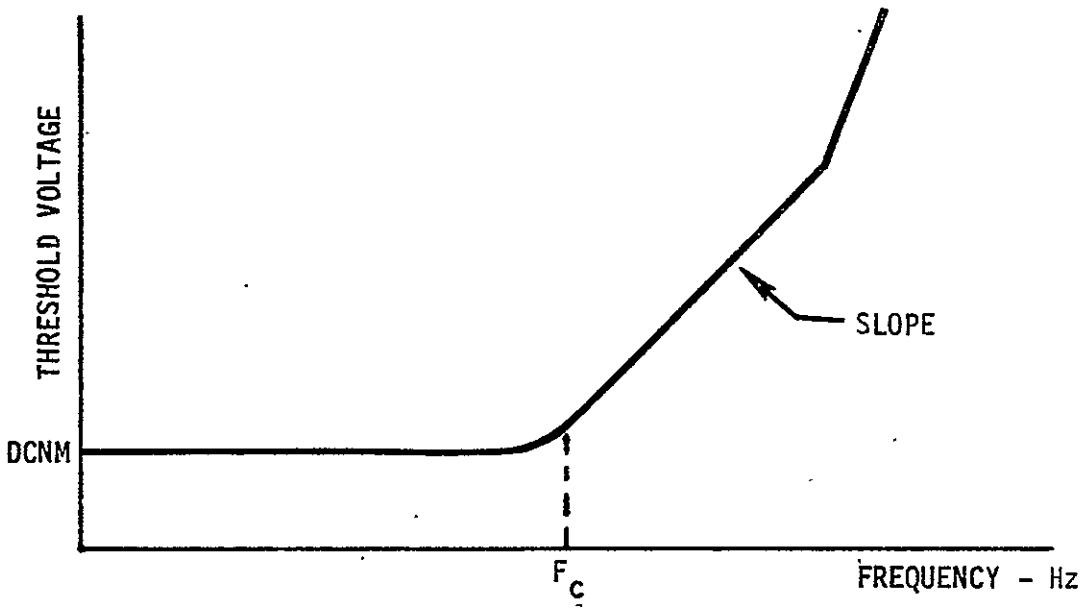

Figure 3-1A. Frequency Response Curve

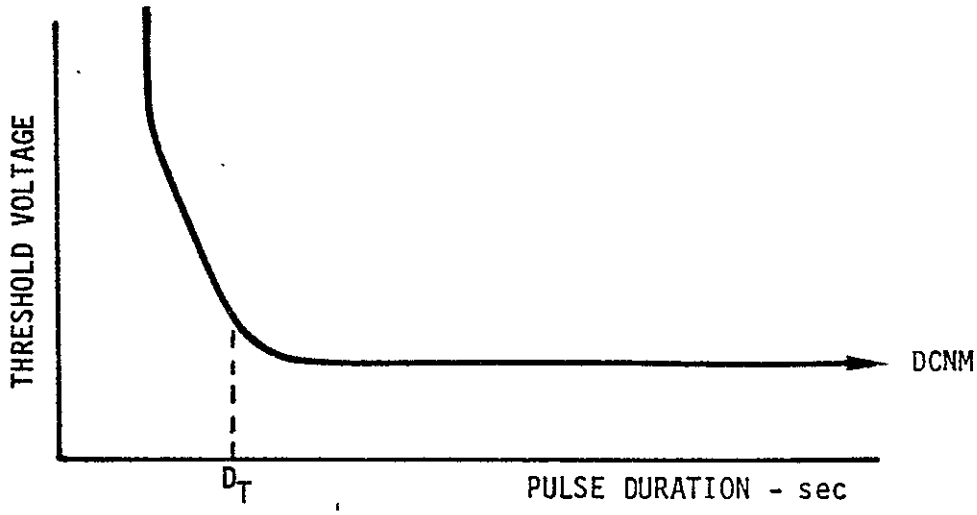

Figure 3-1B. Pulse Response Curve

frequency spectrum of interest, but these are likely to be RF analog circuits which tend to be more tolerant of non-destructive transient interference.

In Figure 3-1A, the DCNM is that value of constant voltage which, when added to the existing signal-plus-noise on a circuit, will result in an undesired output (e.g., upset of a bi-stable circuit). The curve shown in Figure 3-1A is developed analytically according to the component values found on a schematic diagram, or by test. Testing involves the injection of a sine-wave signal into the circuit at that level which results in the undesired response. As the frequency of the sine-wave is increased, a point will eventually be reached where the original signal level is insufficient to cause the undesired response. The level is then increased until the response is obtained. This process is continued until sufficient data is taken to plot the frequency response curve. F_c is the frequency at which the signal level is 3 db higher than the DCNM. The slope is typically 6 db per frequency octave (slope = 1) or 12 db per frequency octave (slope =2) for these kinds of circuits, although steeper slopes are occasionally encountered. The slope is normally a function of the number of reactive elements in the front end of the circuit.

Figure 3-1B is the time-domain response of a similar circuit and is usually developed by testing, although it can be developed analytically. The DCNM is the same as was described above, and D_T is that pulse duration for which the pulse amplitude is 3 db higher than the DCNM to obtain the undesired response. F_c and D_T are related by the following equation:

$$F_c \approx \frac{0.35}{D_T} .$$

As the pulse response of a circuit can be very accurately determined by testing, it is usually considered to be the best way of determining the threshold characteristic of a circuit, although it is a more expensive method than by analytically determining its frequency response.

Given this basic understanding of the parameters shown in Tables 3-1 and 3-2, it is obvious that the most sensitive circuit, in terms of threshold characteristics, is that having a low DCNM and a high F_c. However, it is unusual for the circuit with the lowest DCNM to have the highest F_c. For this reason, the real sensitivity is also a function of the imposed electromagnetic spectrum. A spectral density function with most of its energy above F_c of a circuit with a low DCNM, may not result in an upset of that circuit, but might result in the upset of another circuit having a higher DCNM, but also a much higher F_c. Because the conditions are not always simple, it is necessary to exercise caution in drawing any generalizations from partial information about a situation, as represented by threshold characteristics alone. Other complicating factors are those which influence the coupling of energy into a circuit (e.g., circuit impedance, shielding, proximity to ground, etc.).

The following example will illustrate the use of the noise threshold characteristics of a hypothetical circuit. The given information is the noise threshold characteristic of the circuit and the transient waveform postulated to exist across the input of the circuit. This waveform, therefore, is that which has been coupled to the wire, and is a function of the impinging electromagnetic field and the field-to-wire transfer function. The following parameters will be used for the example:

THRESHOLD CHARACTERISTICS

DCNM = 1 volt

F_c = 100 kHz

Slope = 2

TRANSIENT CHARACTERISTICS

Amplitude (A) = 2 volts

Pulse Duration (d) = 1 μsec

Rise Time (t) = 100 nsec

The induced transient amplitude of 2 volts, in terms of some of the SEMCAP run results is somewhat large. A few cases of negative margins greater than -46 dB for a .01 volt threshold (2 volts) may be seen in the tabulated results for Runs 9-12. A greater number of negative margins larger than -46 dB are seen in Table 2-18 for the complete-arcs-to-space source model in which G´ = 1. The largest, -86 dB for Receptor 45 (Magnetometer Temperature Sensor Line) corresponds to 200 volts. The 100 ns/

1 μs waveform parameters of pulse width are typical as may be seen from Table 2-12.

At first glance, it may appear that the 2 volt transient will upset a circuit having a 1 volt DCNM. A more careful examination of the data shows that an F_c of 100 kHz corresponds to a D_T of 3.5 μsec. As the pulse duration is only 1 μsec, it becomes evident that the DCNM alone can not be used as the determining parameter (see Figure 3-1B). On the other hand, if F_c > 500 kHz, it would be an obvious upset situation, because D_T would be 0.7 μsec. In order to determine whether there would be an upset for the data given in the example, the approach taken will be to convert the transient data into the frequency domain, normalize it by the frequency response curve, integrate the result over a wide frequency range, and compare the integrated value with the DCNM. This is normally done by a computer, but a reasonable approximation can be obtained by manual calculations, and graphical analysis.

Using the equation $E = 2Ad \cdot \frac{\sin\pi fd}{fd} \cdot \frac{\sin\pi ft}{ft}$ the envelope of the spectral density function can be obtained. The real frequency representation of this envelope is shown in Figure 3-2A. For the example, the frequencies corresponding to $1/\pi d$, $1/d$, and $1/\pi t$ are 318 kHz, 1 MHz, and 3.18 MHz, respectively.

Disregarding phase reversals, the envelope can be represented as in Figure 3-2B. The envelope of that envelope, shown on a log-log scale, is shown on Figure 3-2C. This common representation is sometimes erroneously accepted as the actual spectral density of a pulse. However, it can be used for simple graphical analysis, so long as the user is fully aware of its derivation, and is careful to avoid using it incorrectly. At frequencies below $1/\pi d$, its inaccuracies are insignificant; at frequencies above $1/\pi d$, large errors can result from its use, especially when segments of the area under the curve are used.

Figure 3-3 shows how a graphical analysis of our example can be done. The envelope of the spectral density function is plotted as shown. Note that between 318 kHz and 3.18 MHz, the function declines at a rate of 6 db/octave. The normalized frequency response curve is plotted against the numerical scale at the right of the graph. Note that above F_c, the response curves falls at 12 db/octave. The resulting composite spectral density envelope has been modified by the frequency response of the circuit, and can

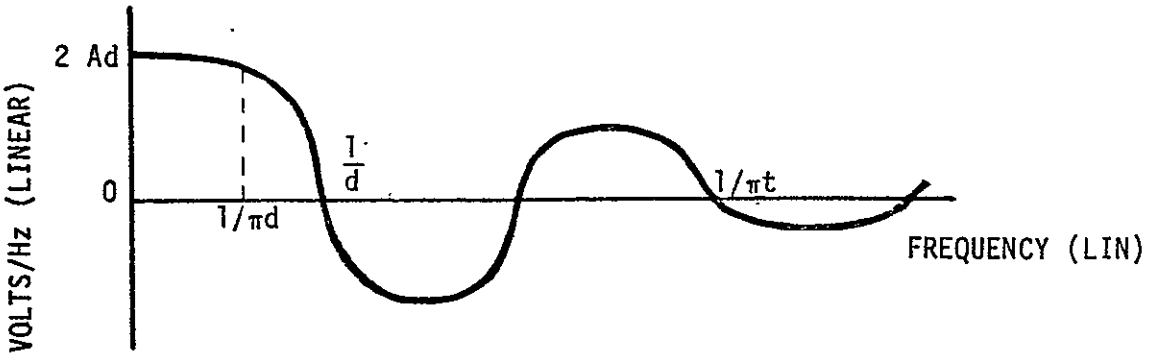

Figure 3-2A

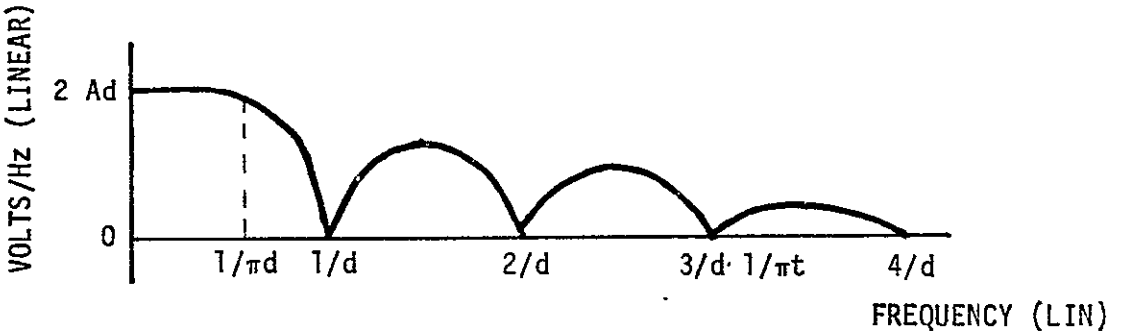

Figure 3-2B

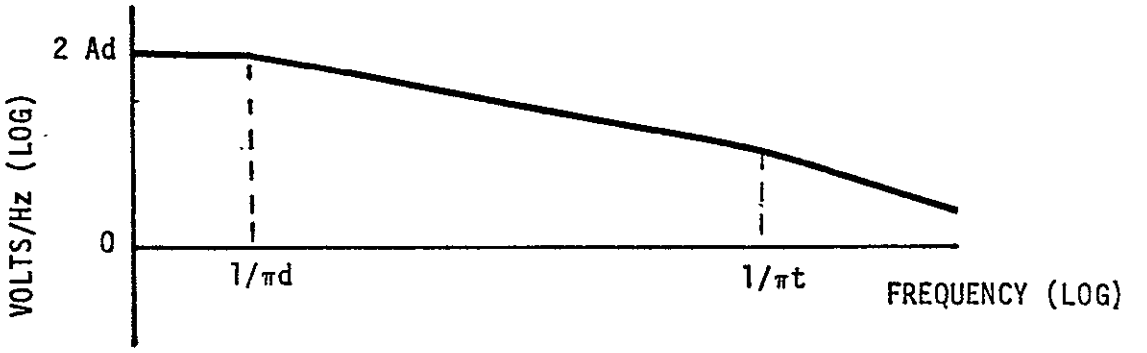

Figure 3-2C

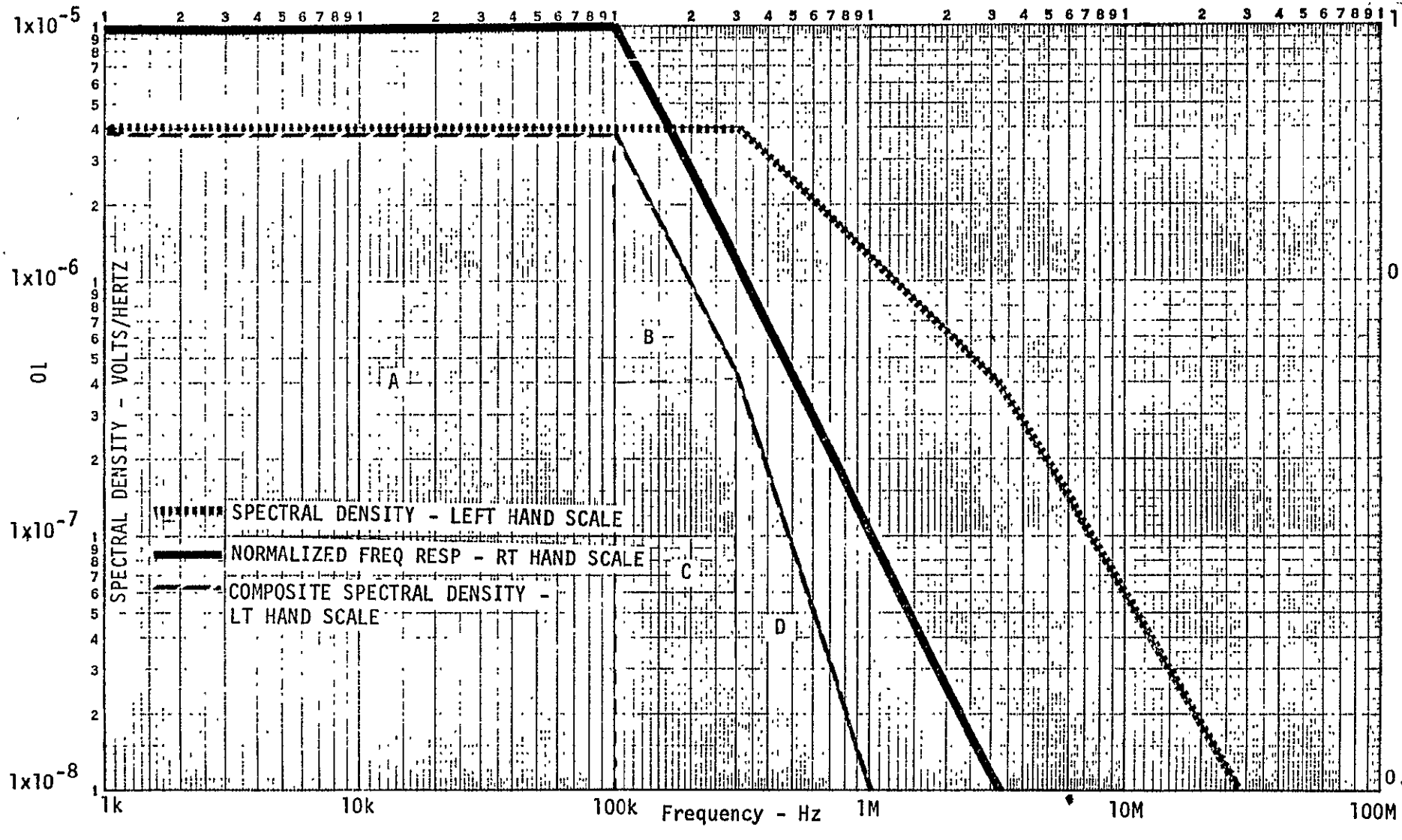

Figure 3-3. Graphic Analysis of Threat Determination

now be related to the DCNM, after integration over its frequency spectrum. Note that the composite envelope falls at 12 db/octave between F_c and $1/\pi d$, and at 18 db/octave above $1/\pi d$. At a still higher frequency ($1/\pi t$) the slope will increase to 24 db/octave.

The area under the composite curve can be calculated by simple geometry as follows:

$$\text{Area A} = 4 \times 10^{-6}\ (\text{V/Hz}) \times 10^{5}(\text{Hz})$$

$$= .4\ \text{V}$$

$$\text{Area B} = [(4 \times 10^{-6}) - (4 \times 10^{-7})]\ (2 \times 10^{5})/2$$

$$= .36\ \text{V}$$

$$\text{Area C} = 4 \times 10^{-7} \times 2 \times 10^{5}$$

$$= .36\ \text{V}$$

$$\text{Area D} = (4\text{=x}\ 10^{-7} \times 7 \times 10^{5})/2$$

$$= .14\ \text{V}$$

$$\text{A+B+C+D} = .98\ \text{volts.}$$

A note of caution is now in order. It is obvious that Area D is much larger than .14 V if its base is taken at 0 V/Hz, as this would result in a base abscissa of infinite frequency. However, it is observed on Figure 3-2A, that the spectrum goes through zero at 1 MHz (1/d) and then becomes negative. For this reason, Area D is calculated as shown, with the result that the total calculated area is 0.98 volts. The integrated value of the remainder of the spectrum will be slightly negative, assuming no phase reversals in the frequency response of the circuit.

The conclusion to be reached from this simplified analysis is that the circuit is marginally secure relative to the injected pulse. A more accurate computer aided analysis is likely to result in the same conclusion. The margin, expressed in decibels is:

$$\text{Margin} = 20 \log \frac{1}{.98}$$

$$= .18\ \text{db}$$

This represents a high risk situation requiring additional protection of a critical circuit.

The above discussion is intended to demonstrate a technique for determining the threat margin to a circuit when the characteristics of the circuit and the waveform of the applied pulse (or transient) are known. More complex circuit and transient characteristics can be more accurately evaluated using computer aided techniques such as those presently in use by TRW (EMCD).

4. TASK 4 - SPACECRAFT DESIGN PRACTICES REVIEW

4.1 INTRODUCTION

In this task the spacecraft design guidelines and recommended practices available at TRW have been reviewed. This information is summarized and discussed in this report. We have further reviewed countermeasures which can be used to control and reduce the hazard due to spacecraft charging and examined the resulting tradeoffs. Recommendations for changes in recommended practices and guidelines are made.

4.2 DESIGN GUIDELINES

In September, 1974, TRW's Space Systems Division issued an electrical design standard on the subject of spacecraft charging. These standards defined the procedures and guidelines to be used at TRW for design of spacecraft to be resistant to the effects of geomagnetic substorms. The standard applied to mechanical design, electrical grounding and interface circuit design procedures. A summary of those design procedures is given below:

The following design procedures shall be applied to all spacecraft which are exposed to the geomagnetic substorm environment.

1. Ground all metallic surfaces of area greater than approximately (25 cm^2) exposed to the space plasma in order to prevent significant metal to metal arcs. Grounding of smaller metallic surfaces is required only if the energy stored by the differential voltage can be shown to be sufficiently large to cause circuit upset.

2. Provide shields grounded to structure for spacecraft cables exposed to the plasma or to sunlight in order to attenuate EMI and to avoid direct arcing to a cable which can conduct the arc energy to an electronic component.

3. Investigate the effects of apertures and spacecraft surface materials on differential voltage buildup to determine necessity for charge balancing and closure of apertures.

4. Institute handling and assembly procedures which maintain the electrical continuity of grounded metallic surfaces.

5. Design electronic circuits for the minimum bandwidth required to perform their function or provide sufficient filtering in order to minimize their susceptibility to EMI.

6. Perform physical and electrical inspections and additional tests to insure that all design criteria are implemented.

These procedures recognized the need to prevent the exposure to the environment of isolated metallic surfaces. It concerned itself not only with the hazard due to the EMI produced by a discharge but also with the possibility of direct conduction of the arc energy to electronic components. Although the procedures were not very specific, they identified the requirement for an analysis of each spacecraft to determine the necessity for specific countermeasures.

Table 4-1 gives a more recent set of design guidelines and recommended practices generated by TRW which cover some of the concerns addressed in the earlier design standard but recognizes the hazard of dielectric-to-metal arcs.

Table 4-1. Design Guidelines and Recommended Practices

GROUNDING

GROUND ALL BOXES TO PLATFORM.

GROUND CABLE SHIELDING AS FREQUENTLY AS POSSIBLE.

PROVIDE GOOD GROUNDS TO STRUCTURE FOR ALL METALLIZED LAYERS IN THERMAL BLANKETS.

GROUND ALL ISOLATED OR INSULATED METAL STRUCTURES, E.G., THE ALUMINUM HONEYCOMB IN THE SOLAR CELL PANELS.

SHIELDING

PROVIDE ADEQUATE SHIELDING FOR EXPECTED ELECTRIC FIELD LEVELS AND SPECTRA.

PROVIDE ADEQUATE SHIELDING OF CABLING AND CONNECTORS.

USE TWISTED PAIR WIRING AND COMMON-MODE REJECTION TECHNIQUES WHERE NECESSARY.

CIRCUIT DESIGN

EACH INTERBOX WIRE SHOULD BE GROUNDED AT EACH BOX FOR FREQUENCIES HIGHER THAN THE INTENDED PURPOSE FOR THAT WIRE.

FILTERING: CIRCUITS SHOULD BE DESIGNED TO MINIMIZE REQUIRED BANDWIDTHS OR MAXIMIZE REQUIRED RISE-TIMES ON INTERBOX WIRING.

CHARGE BALANCE

REDUCE VOLTAGE STRESS LEVELS AT SPECIFIC LOCATIONS AS DETERMINED BY CIRCUIT SUSCEPTIBILITY BY SELECTING THE PROPER SURFACE MATERIAL AND RATIO OF CONDUCTOR TO INSULATOR.

APERTURES AND SLITS

CLOSE OFF ALL APERTURES AND SLITS TO REDUCE VOLTAGE STRESS LEVELS AT SPECIFIC LOCATIONS.

GENERAL

PERFORM VERIFICATION TESTING TO ASSURE THE INTEGRITY OF GROUNDS, SHIELDS, CIRCUIT DESIGN, AND CHARGE BALANCE

INCLUDE HIGH-INTENSITY, HIGH-FREQUENCY (ARC DISCHARGE) SOURCES IN SPACECRAFT EMI ANALYSES. ONCE THIS IS DONE PROPERLY, STANDARD EMI PROBLEM-SOLVING TECHNIQUES MAY BE BROUGHT TO BEAR ON EACH PROBLEM AREA.

MINIMIZE EXPOSED INSULATED SURFACE AREAS TO REDUCE THE OCCURRENCE OF DIELECTRIC-TO-METAL ARCS, E.G., USE GROUNDED CONDUCTIVE COATING ON SOLAR CELLS AND EXPOSED MYLAR THERMAL BLANKET SURFACES.

In these guidelines some of the countermeasures that can be taken are more explicitly stated. These guidelines identify the need for including the arc discharge characteristics in the spacecraft EMI analyses (SEMCAP)[1] thus bringing to bear on each problem area the standard EMI problem solving techniques.

4.2.1 Solar Array Guidelines

The set of guidelines listed in Table 4-2 for solar array design resulted from tests performed at TRW. The data from these tests were included in the literature survey results of Task 1.1.[1,2] The most interesting results of those tests were obtained when the solar array samples were irradiated with electrons on the backside and with ultraviolet on the solar cell side.

Table 4-2. Design Guidelines and Recommended Practices for Solar Arrays

1. THE BACK SURFACES OF THE SOLAR ARRAY PANELS MUST BE CONDUCTIVE
2. THE CONDUCTIVE BACK SURFACE MUST BE CONNECTED TO STRUCTURE
3. THE ALUMINUM HONEYCOMB CORE MUST BE GROUNDED TO STRUCTURE
4. THE SOLAR PANEL EDGES MUST BE COVERED WITH CONDUCTIVE TAPE AND GROUNDED
5. THE SOLAR CELL COVERGLASS MAY BE FUSED SILICA OR CERIA GLASS
6. THE SOLAR ARRAY WIRING MAY BE ON THE FRONT SIDE OR THE BACKSIDE - THE BACKSIDE IS PREFERRED
7. THE BLOCKING AND SHUNT DIODES MAY BE LOCATED ON THE FRONTSIDE OR THE BACKSIDE - THE BACKSIDE IS PREFERRED.
8. THE BLOCKING AND SHUNT DIODES SHOULD HAVE THE LARGEST POSSIBLE FORWARD CURRENT RATINGS
9. DESIGN VERIFICATION TESTS MUST BE PERFORMED

The test sample was isolated from ground (tank walls) so that the sample potentials were determined predominantly by the "environmental" fluxes of electrons and UV. An enhanced photo-induced emission of electrons was observed only when the backside was coated with conducting paint. This effect leads to the elimination of a major part of the charge buildup and energy storage which is the source of potentially hazardous arc discharges.

The first two items of the design guidelines in Table 4-2 result directly from the test observations. The requirement for electrically connecting all metallic parts, Items 2, 3 and 4, is always a recommended practice for electromagnetic compatibility reasons. For substorm immunity, this requirement is even more essential because of the very large discharge currents that could flow in metal-to-metal arcs. Item 4, regarding the tape around the edges of the solar panel, was included because the prior practice was to use kapton tape. Wiring crossing panel edges would be subject to arcing if the tape was not made conductive and grounded. Item 5 was included because both fused silica and ceria glass were tested and found to behave similarly. Items 6 through 8, having to do with component and wiring locations, frontside and backside, are based on the test results, and minimize the probability of arcing to components or to wiring. With the dark side made conductive and connected to spacecraft ground, all wiring and diode potentials are low with respect to the backside.

The final recommendation, that a design verification test be performed, is included since the tests were performed on an incomplete sample. Diodes and wiring and panel edges were not in the in-flight configuration.

4.3 COUNTERMEASURE REVIEW

In this section of the report, we review the countermeasures available to reduce the hazard due to spacecraft charging. Recommendations made for changes or additions to the guidelines and the recommended practices are summarized.

Countermeasures to reduce the hazard due to spacecraft charging fall into two broad categories, spacecraft charge control and post-discharge hazard reduction. In the first category the amount of charge on the spacecraft surface is controlled so that discharges do not occur or are sig-

nificantly weakened in energy, thus eliminating the hazard to the spacecraft. In the second category, the discharge is permitted to take place but the spacecraft equipment (components, circuits, etc.) are immunized to the effects of the discharge. A successful spacecraft charge hazard countermeasure program should utilize both of these methods. This is reflected in the guidelines summarized in Section 4.2.

A summary of spacecraft charging countermeasures is shown in Figure 4-1. In this section we will discuss each of the elements in that figure and point out the advantages and/or disadvantages of each measure.

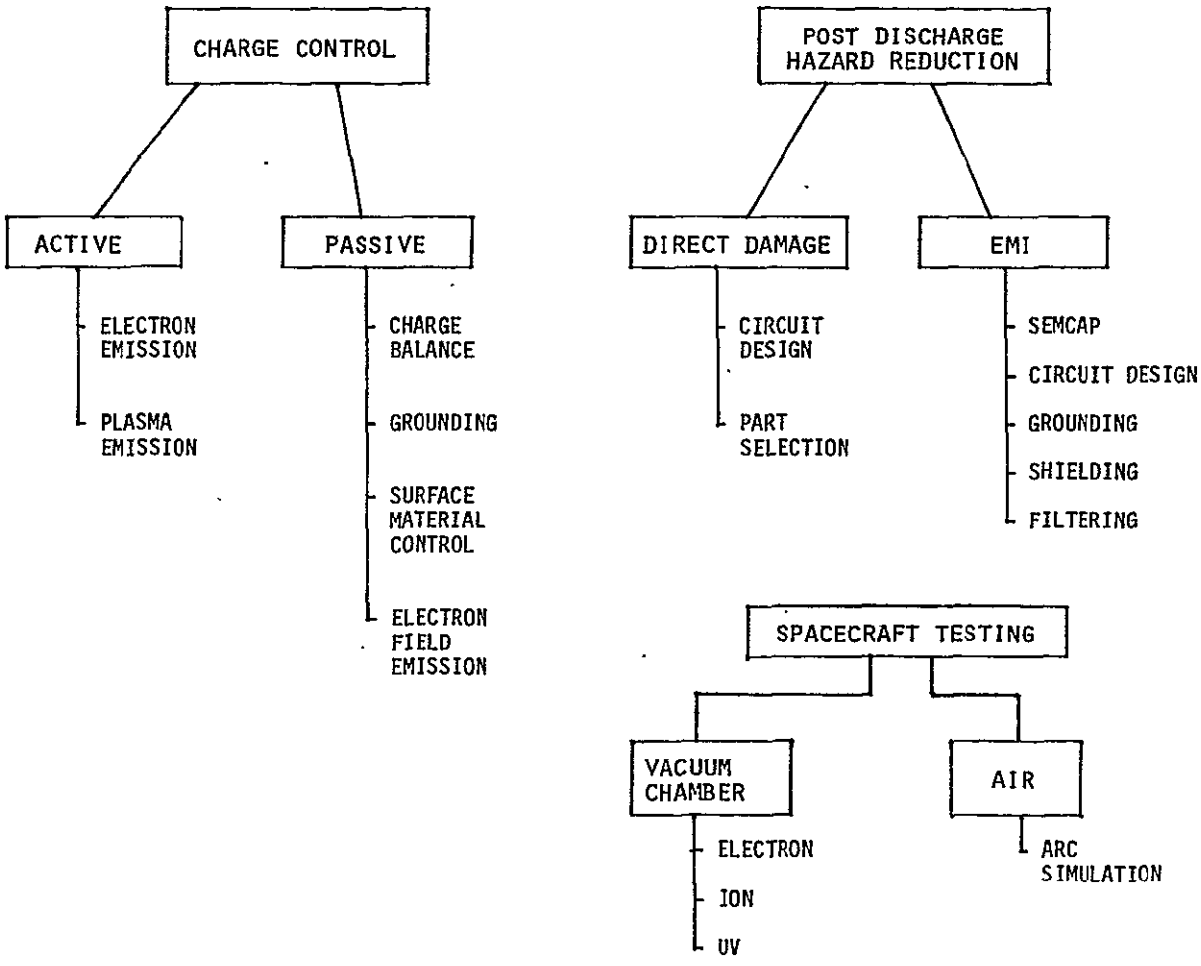

Figure 4-1. Spacecraft Charging Countermeasures

4.3.1 Active Charge Control

Control of the spacecraft charge can be performed by active or passive means. To control actively the charge on the spacecraft, electrons and/or ions are emitted from the spacecraft by means of a powered device.

General demonstrations of the effectiveness of active control methods to bring the spacecraft potential near to the ambient plasma potential has been demonstrated by experiments on ATS-5 and ATS-6.(3) Both spacecraft carry cesium ion thrusters. The thrusters produce a beam of singly charged cesium ions. This beam is neutralized by electrons extracted from a second plasma source. The neutralizers as well as the thrusters themselves can be used to control the spacecraft potential. The ATS-5 neutralizer consists of a hot wire filament operating at less than 10 volts, whereas the ATS-6 neutralizer is a small plasma bridge which emits a cesium plasma of less than 10 volt energy. Tests were performed to investigate the effectiveness of thrusters and neutralizers to control the spacecraft potential. The results are discussed below:

a) The ATS-6 ion thruster was operated for over 90 hours in daylight. During this period of time it clamped the ATS-6 spacecraft potential of several hundred volts negative to within a few volts of ground.(3) In this case, the engine is probably compensating for charge influx during charged particle events.

b) The ATS-6 neutralizer is mounted about 17cm. outboard of the vehicle. The neutralizer was operated both in eclipse and in daylight. In daylight, it apparently reduced the spacecraft potential from -100 volts to within 10 volts of ground and also reduced the differential charge on the spacecraft. This results from the fact that the ions from the ATS-6 plasma bridge can be attracted to nearby negative surface thus providing a mechanism for discharging insulator surfaces as well as the spacecraft frame.(4)

Laboratory experiments at TRW(5) have shown that ion currents at levels from tens to hundreds of microamperes can be easily drawn from a thruster neutralizer plasma plume to relatively remote surface locations, thus supporting the conjecture of a reduction in ATS-6 differential charge during neutralizer operation.

During eclipse operation the ATS-6 neutralizer was able to reduce the charge on the spacecraft from -3000 volts to "within 40 volts(3) of ground".

c) Operation of the ATS-5 thermal electron emission neutralizer was less successful in reducing the spacecraft potential. This instrument was recessed about 2.5 cm. into the spacecraft and no electron acceleration bias was employed. Therefore the electron energy was about 2 volts. The test results showed that the hot-wire electron emitter lowered the spacecraft potential in eclipse but does not always bring that potential near the ambient plasma ground. In the ATS-5 case, the emitter was less effective in lowering large magnitude potentials than small. These results would probably be improved by accelerating the electrons to higher energies to insure that they had sufficient energy to penetrate any emission suppression barriers.

These tests clearly demonstrate that active control methods decrease spacecraft surface potentials below the breakdown levels.

4.3.2 Passive Charge Control

The state of art of passive charge control to minimize the charge-up of a spacecraft surface consists of a large number of techniques, many of which are used to solve special spacecraft surface charging problems. Many of these techniques such as grounding, charge balancing, material selection have been used in flight spacecraft programs whereas others such as the passive field emitter have been reported in the literature but not yet demonstrated.

In this section we will review the various techniques for passive charge control.

4.3.2.1 Grounding as a Charge Control Measure

Grounding is required for spacecraft charge control and prevention of metal-to-metal arcs. The avoidance of large isolated conductors exposed to the environment is imperative to prevent high energy metal-to-metal arcs. This includes conductors inside of spacecraft but exposed through spacecraft apertures. Thus a primary countermeasure is to electrically connect to structure all large (>25 cm^2) isolated conductors.

To prevent arcing between the metallic layers of thermal blankets, the various layers are frequently tied to structure. However, grounding of the metallic layers of thermal blanket cannot prevent arcing of the outer (usually kapton) dielectric surface. The grounding of the metallic film

on thermal blankets, usually VDA, has been a recommended practice in spacecraft design for EMC for a long time. However, the need for ground straps from the metallic film to carry the many amperes associated with the outerlayer arc discharges increases the requirements on the durability of these straps many fold. Various techniques have been used to connect ground straps to the metallic films. Figure 4-2 shows four different techniques used at TRW. Tests performed at TRW[6] showed that the relative durability of the different groundstrap configurations to standardized pulses of 100 amperes peak and 1 microsecond decay time-constant shows a wide variation, from less than 50 to greater than 10,000 pulses, before burnout. The standardized pulse used is typical of the pulse obtained in the discharge of 100 cm^2 of kapton (See Task 1.1 - Figures 1-3 and 1-6).

The test results are shown in Figure 4-3a, b, c, and d as curves of groundstrap resistance vs the number of current bursts. The results are also summarized in Table 4-3. The wide variation in the number of pulses required to cause the groundstrap to open-circuit seemed to depend on the peripheral length of the contact between the metallizing VDA film and the aluminum foil of the groundstrap itself. An estimate made in the same study showed that from 500 - 2000 discharges in the blanket could be expected in a year. Therefore, the test results indicate that only the modified strap would survive one year in geosynchronous orbit. These results point out the futility of using the standard EMI grounding techniques for arc discharge prevention without careful consideration of the unique requirements imposed by the spacecraft charging phenomena.

Table 4-3. Number of Pulses to Burn Out Various Groundstrap Configurations

DSP	20 to 60 pulses
FSC	40 to 200 pulses
DSCS II	600 to 1200 pulses
Modified	Greater than 10,000 pulses

A. DSP GROUNDSTRAP/ALUMINUM TAPE WITH CONDUCTIVE ADHESIVE

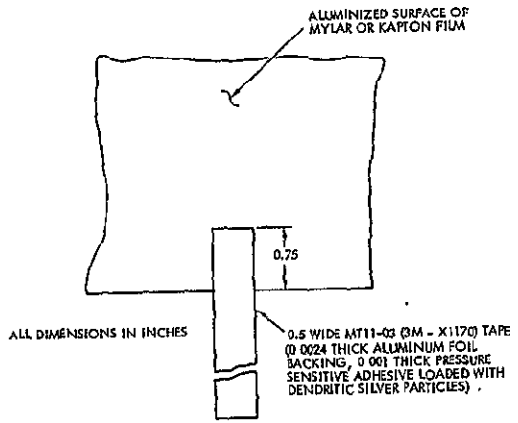

B. FSC GROUNDSTRAP/GROUND LEAD WITH MECHANICAL FASTENER

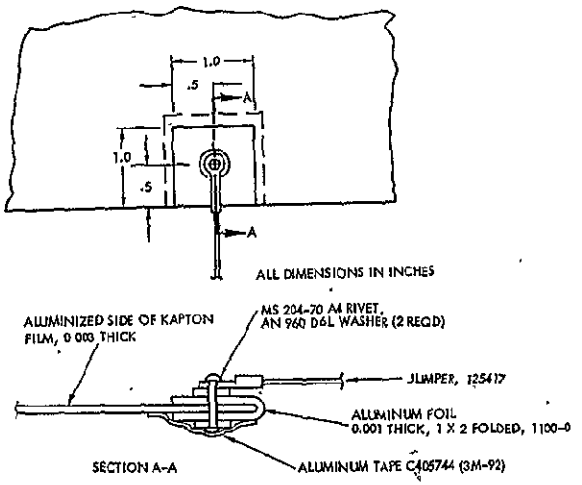

C. DSCS II GROUNDSTRAP/GROUND LEAD WITH MECHANICAL FASTENER

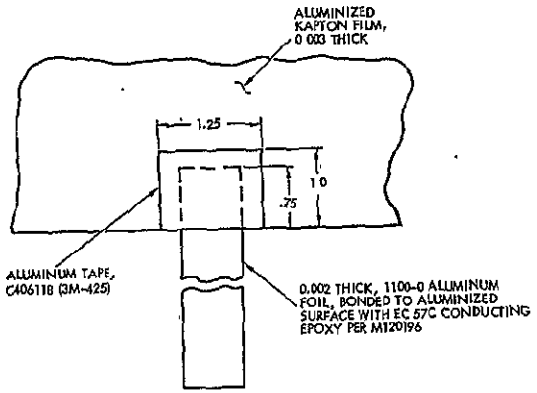

D. MODIFIED FILM AND GROUNDSTRAP

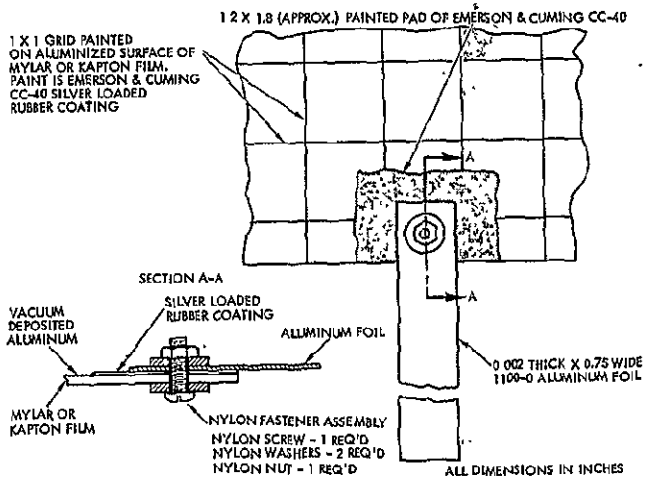

Figure 4-2. Four Thermal Blanket Groundstrap Configurations

a. Mod. 35 Type Groundstrap (0.75 inches Wide Strap)

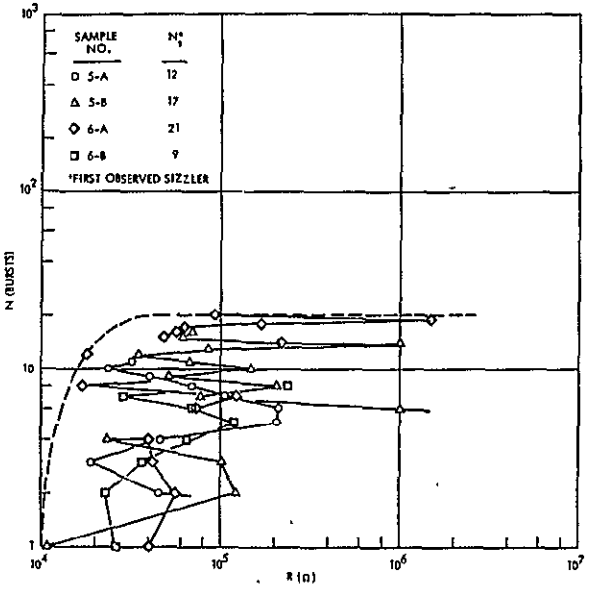

b. FSC Groundstrap

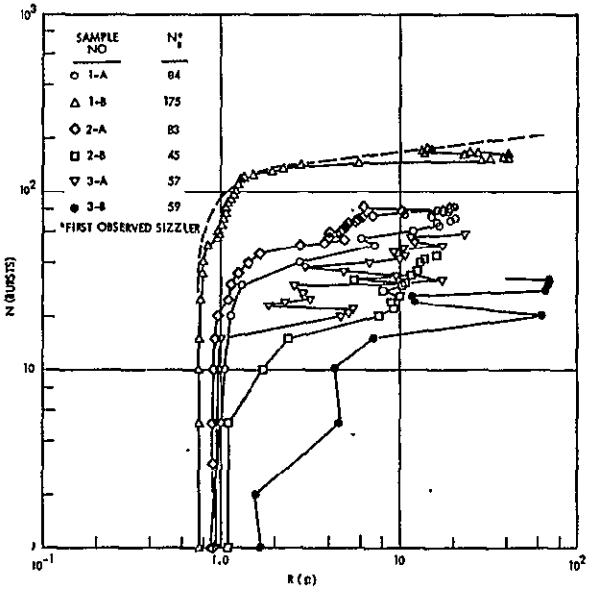

c. DSCS Groundstrap

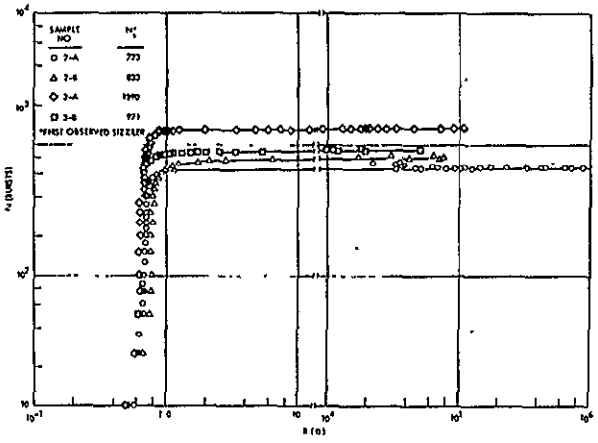

d. Modified Film/Groundstrap (Sample I-A)

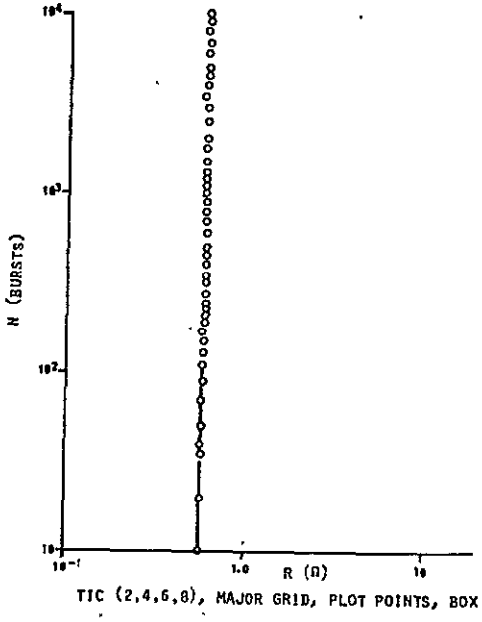

Figure 4-3. Groundstrap Test Results

It is clearly not as easy to remove the charge from isolated dielectrics as from isolated conductors. In some cases, "grounding" of isolated dielectrics can be performed by bonding the dielectric to the spacecraft structure with a sufficiently conductive adhesive. In this manner the capacitor formed across the adhesive is sufficiently "leaky" to prevent chargeup to breakdown electric fields. The conductivity of the adhesive required and whether this technique will work depends on the resistivity, thickness and configuration of the dielectric. Therefore, an analysis should be performed to determine whether conductive adhesives are necessary or will be effective in bleeding off the charge from dielectrics. For example, OSR's are usually bonded to the spacecraft with approximately three mils of silicone adhesive having a bulk resistivity of about 7×10^{13} Ω-cm. If the cover glass is made of fused silica, as is often the case, the leakage current through the approximately 6-8 mil thick coverglass will be so small that the use of conductive adhesive to bond the OSR to the structure will be of no help. On the other hand, work at TRW (See Section 4.3.2.3) has shown that if the coverglass is made of borosilicate glass, the leakage is sufficiently great to prevent chargeup to breakdown fields. Even in this case, however, a highly conductive epoxy is not needed. The same TRW study has shown that some adhesives used to bond the mirrors have sufficiently low resistivity to prevent the chargeup to break down fields of the capacitor formed by the mirrored surface, the adhesive and structure. Care should be taken in selection of adhesives to assure that the charge can leak through.

In some cases, highly conductive adhesives may be necessary, but quite frequently the properties of conductive adhesives are incompatible with other spacecraft requirements. For example, conductive adhesives having the flexibility required by OSR's to accommodate thermal stresses are not easily found. Another case in point is the bonding of solar cells. In this case, conducting adhesive serves no purpose since the capacitor formed by the solar cell, adhesive and ground has an adequate parallel leakage path through the spacecraft loads. In any case, this path will not help in removing the charge from the coverglass unless a transparent conductive coating connected to the adhesive is used (see Section 4.3.2.3).

4.3.2.2 Charge Balance

Charge balancing consists of modifying the configuration, properties and location of surfaces of a spacecraft exposed to the environment in such a manner as to reduce the high voltage stresses resulting from spacecraft charging. To employ the technique, stresses in different parts of the spacecraft are computed by modeling the entire spacecraft. Changes are then made to the spacecraft properties (such as judiciously insulating or removing the insulation from exposed metal surfaces or closing apertures in the spacecraft) to minimize the potential difference below the hazard level. This method is very useful for reducing the hazard of a previously designed spacecraft. Charge balancing was used on the DSCS II Spacecraft. In that spacecraft the results of the analysis showed the minor modifications of the spacecraft that could be made to reduce or eliminate the stress at several critical locations. These modifications were incorporated into the following spacecraft of the same generic configuration. A description of the application of charge balance to DSCS II follows:

Figures 4-4 and 4-5 are photographs of the DSCS II spacecraft which depict their general configuration. A notable and important feature is that less than 2% of the total external surface area is metallic and tied to the common spacecraft ground. Structural pipes, which constituted the major portion of this metallic area, are shown in the underside view of Figure 4-5. The solar array panels are removed in this photograph. Nearly all exterior surfaces are covered or wrapped with thermal blankets, second surface mirrors, solar cell coverglasses, paint, etc. Subsequent examination of a number of other spacecraft configurations has shown that the small proportion of exposed metallic surfaces relative to surface areas is a common feature that has been dictated primarily by thermal control considerations.

Figure 4-6 shows the seasonal and diurnal variation of the (projected) metallic area exposed to sunlight. The seasonal variation mainly is caused by the structural pipes, seen in Figure 4-5, which are sunlit only during the winter months. The diurnal variation mainly is due to the daily rotation of the antennas resulting in the exposure of the waveguides in front

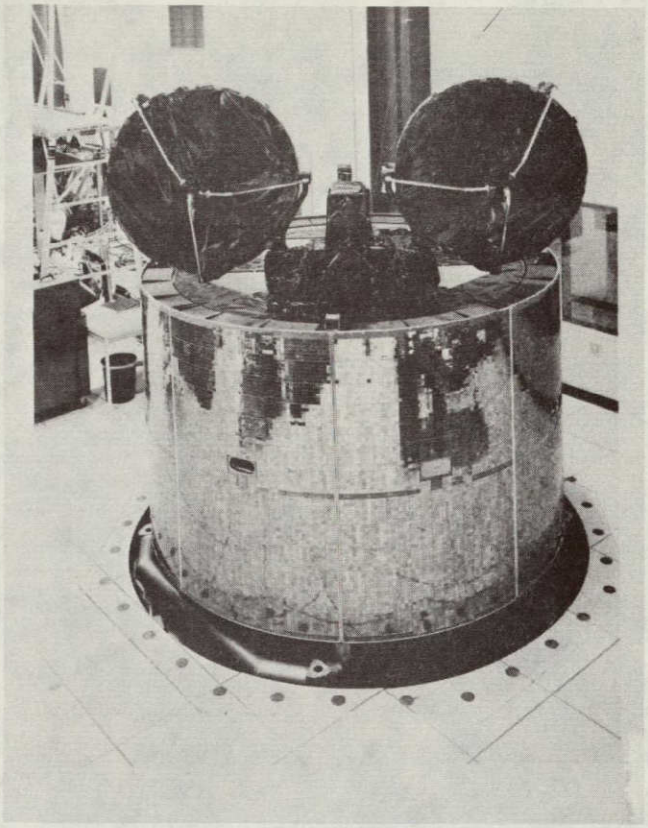

Figure 4-4. DSCS II Spacecraft

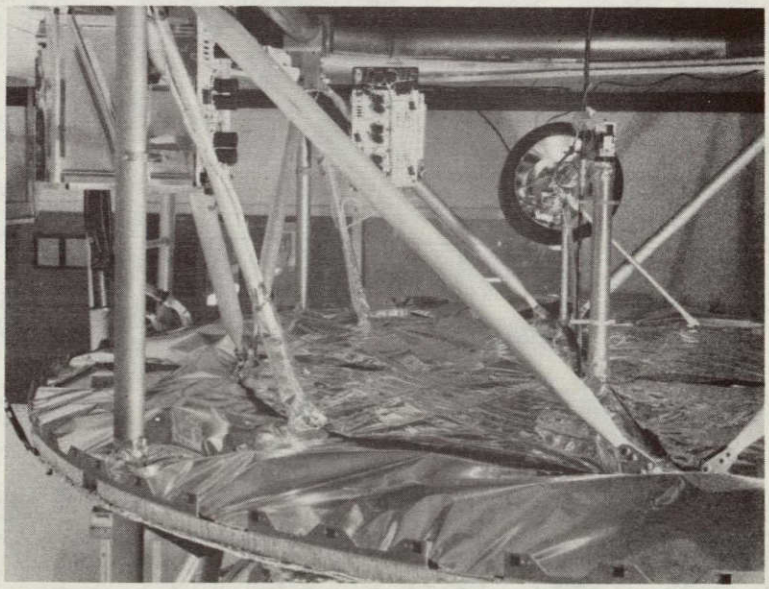

Figure 4-5. Underside View of the DSCS II Spacecraft

Figure 4-7 is a schematic representation of the spacecraft for purposes of showing charging potentials at various locations as a function of the seasonal changes of the sun aspect angle. Figure 4-7a applies to the original configuration (Mod 0) and Figure 4-7b to the modified configuration (Mod 2) in which the metallic pipes of Figure 4-5 have been covered with thermal blankets and all apertures to the interior volume, in which most of the electronic hardware are located, have been baffled. The steady-state potential differences (V_n-V_0) are compared in Table 4-4 for the two configurations. The main features to be noted in Table 4-4 are that the (V_1-V_0) stress, which has been identified as being critical, has been reduced greatly at all seasons, as have all of the aperture related stresses.

4.3.2.2.1 Stress Analyses

The determination of the potentials on the spacecraft and the stresses resulting from those potentials is an important part of the charge balance technique and a stress analysis should be performed for each synchronous orbit spacecraft.

Two approaches have been predominantly used to determine the spacecraft potential. The first of these consists of an electrical circuit representation of the satellite. This method uses Langmuir probe approximations to the various portions of the satellite surface. This method was used to compute the potentials in the example discussed in the previous section and also in estimating the charging of Voyager at Jupiter. A detailed description of the method is given in Reference 16.

The second approach used to evaluate the stresses on the spacecraft involves the use of large machine computer programs. One program specifically designed for this purpose is NASCAP (NASA Charging Analyzer Program) which was developed by Science, Systems and Software Corporation under contract to NASA Lewis. The program performs a 3-dimensional time dependent simulation of the chargeup of a spacecraft. The spacecraft can be modeled by up to 1200 surface cells. The cells can be made up of different surface materials described by up to 20 different material properties. NASCAP computes the potential on each of the cells as well as the potential of the underlying conducting substrate. NASCAP also computes the potentials

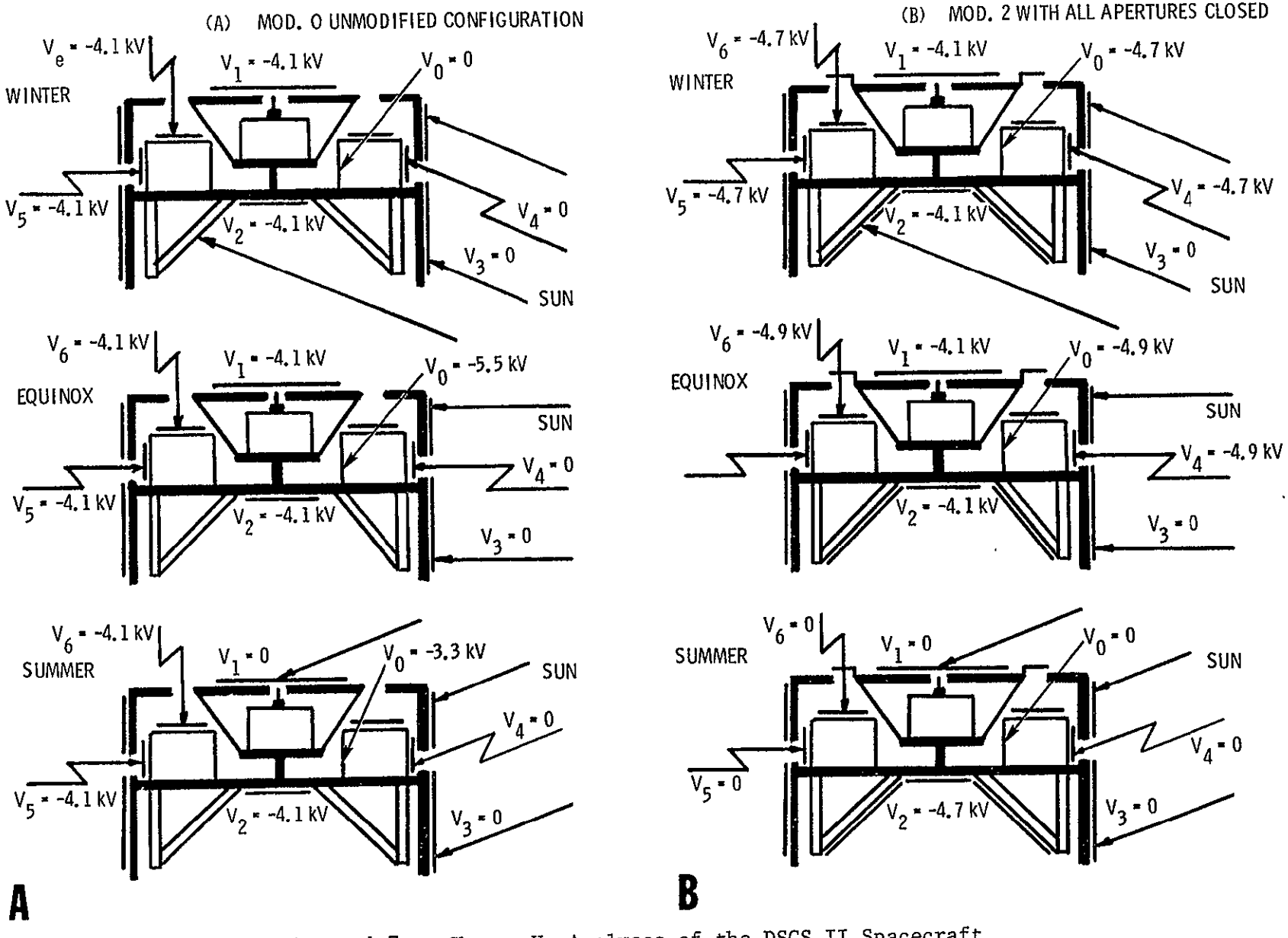

Figure 4-7. Charge-Up Analyses of the DSCS II Spacecraft

Table 4-4. Potential Differences, kv, at a) External Surfaces and b) Apertures

a

MOD	WINTER			EQUINOX			SUMMER		
	V_1-V_0	V_2-V_0	V_3-V_0	V_1-V_0	V_2-V_0	V_3-V_0	V_1-V_0	V_2-V_0	V_3-V_0
0	-4.1	-4.1	0	1.4	1.4	-5.5	3.3	-0.8	3.3
1	-2.4	-2.4	1.7	-1.4	-1.4	2.7	0	-4.1	0
2	0.6	0.6	4.7	0.8	0.8	4.9	0	-4.1	0

b

POTENTIAL DIFFERENCES (KV) AT APERTURES

MOD.	APERTURES CLOSED	WINTER			EQUINOX			SUMMER		
		V_4-V_0	V_5-V_0	V_6-V_0	V_4-V_0	V_5-V_0	V_6-V_0	V_4-V_0	V_5-V_0	V_6-V_0
0	NONE	0	-4.1	-4.1	5.5	1.4	1.4	3.3	-0.8	-0.8
M2	6	4.7	0.6	0	4.9	0.8	0	0	-4.1	0
	4,6	0	0.6	0	0	0.8	0	0	-4.1	0
	4,5,6	0	0	0	0	0	0	0	0	0

MOD. 0 = ORIGINAL CONFIGURATION
MOD. 1 = PIPES WRAPPED ONLY (5462 CM^2)
MOD. 2 = PIPES WRAPPED (5462 CM^2), METAL EXPOSED (3406 CM^2)
SURFACE 0 = METALIC STRUCTURE (SPACECRAFT GROUND)
SURFACE 1 = FORWARD CLOSURE
SURFACE 2 = BOTTOM OF SPINNING PLATFORM
SURFACE 3 = SOLAR CELL COVER GLASS
APERTURE 4 = PORTHOLES AND SLIT ON SOLAR PANELS FOR SUNLIGHT
APERTURE 5 = PORTHOLES AND SLIT ON SOLAR PANELS FOR PLASMA
APERTURE 6 = ANNULAR GAP ON FORWARD CLOSURE FOR PLASMA
V_n = POTENTIAL OF SURFACE n WHERE n = 0, 1, 2, 3, 4, 5, 6

around the spacecraft and plots the equipotential contours around the spacecraft. A detailed description of NASCAP is given in Reference 17. The program has been used by AFGL to analyze the charging of the SCATHA spacecraft and more recently by TRW where it was used in a stress analysis of the DSP satellite.

4.3.2.3 Material Selection

The properties of the surface materials of the spacecraft play a major role in the determination of the floating as well as the differential potential of the spacecraft in the charging environment. The resulting potentials will depend upon the conductivity and the dielectric properties of the surface as well as its secondary emission, photoemission and backscattering properties. Therefore surface material selection is to some extent part of every charge control technique. The principal problem common to all these techniques is to select materials that have the desirable properties from the point of view of spacecraft charging which at the same time have satisfactory thermal properties and can withstand the space environment. In this section, we discuss some of the specific methods that have been considered for charge control directly based on the selection of surface materials.

4.3.2.3.1 Conducting Coatings

A much-discussed method of controlling the charge on the spacecraft surface is to cover the entire surface with conducting material. In principle, this would eliminate differential charging. In practice, however, it is usually not possible to eliminate all exposed insulators or close all spacecraft apertures. This method was used on the Voyager spacecraft. In that case, most of the spacecraft surface was coated with a black Sheldahl conducting paint which had a resistance of about 10^6 ohms per square corresponding to a resistivity of 10^3 ohm-cm for a coating thickness of 0.4 mil. For Voyager, with the elimination of solar cells by the use of a RTG power source, only a small portion of the external surface was dielectric. Out of a total Voyager surface area of 351,700 cm^2, only 6800 cm^2 were dielectrics. Even in this case, however, the possibility of dielectric to metal arcs at Jupiter was not completely eliminated.(7) Several materials have been developed which can be used for electrically conducting paints for spacecraft which do not seriously compromise the thermal radiative properties of the surface and are spaceworthy. Greater conductivity is required of paints which will be used over insulators than those over conductors. A review of these materials is given in Reference 8.

A related but more serious problem with conductive coatings arises if the coating must also be transparent for use on solar cell coverglasses or second surface mirrors. The European Space Agency satellites GEOS and HELIOS

used a conductive solar array coating of antimony doped tin oxide. Other materials[9] and techniques such as the use of conducting grids have been considered for the same purpose.

4.3.2.3.2 Emissive Surfaces

A different approach to reducing the spacecraft charge by controlling the spacecraft surface materials employs highly emissive surface materials. The use of spacecraft surface materials having secondary emission coefficients greater than unity to reduce the maximum negative potential to which a spacecraft can charge has been suggested[10,11]. The secondary emission coefficient $\delta(E)$ is defined as the number of secondary electrons emitted per incident electron of energy, E. If $\delta(E)$ is greater than unity at high incident energies, the current due to secondaries can dominate the incident electron current and force the spacecraft surface potential positive. Kapton has a relatively low secondary yield at high energies whereas the teflon coefficient remains greater than unity for incident electrons as high as 1500 eV. This approach has not been used to date to control spacecraft surface charge. One of the problems associated with the approach is the lack of data available on the secondary emission properties of surfaces used for spacecraft materials. The problem is that the available secondary emission data is typically for clean surfaces at zero potential. On the other hand, the effect of secondary emission on the floating potential must be considered in the spacecraft design for minimum potential difference between spacecraft elements.

Solar reflecting coatings have been produced from high purity silica and are available from J. P. Stevens Company, under the trade name of Astroquartz. These fabrics are apparently space worthy and can be used as thermal control surfaces. Tests performed on Astroquartz fabrics[12] have shown that this material will not sustain a differential charge greater than 100 V when exposed to a mono-energetic electron beam simulating the geosynchronous orbit environment. The resistivity of the material is found to decrease suddenly as the potential across the material increases to about 50 volts, the actual point of decrease depending on the beam current and voltage. This effect is explained in the referenced study as being due to secondary emission conductivity (i.e., free charge carriers are provided by the relatively large number of secondary emission electrons produced in the material). The conductivity of the material becomes sufficiently high to

prevent charge buildup to breakdown potentials and sufficiently low so as not to interfere with the propagation of electromagnetic radiation. Although not yet tried in space, the materials apparently will make good arc-proof solar reflectors for thermal control.

Another technique that can be used for spacecraft charge control is the selection of surface materials for their photoemissive properties. In this case, the decision to use a highly photoemissive surface or a poor emitter will depend on the configuration and orientation of the spacecraft. In some situations, it may be desirable to have a highly photoemissive surface so that the photoelectron current will reduce the surface negative charge. In other cases, it may be better if the surface exposed to the sun was a poor photoemitter so that the potential difference between the solar exposed side of the spacecraft and the eclipsed side of the spacecraft be minimized. The utility of this method may be reduced because of the "barrier" effect; a barrier to the emission of the photoelectrons from the sunlit side of the spacecraft by the large electric field produced by a highly charged portion of the spacecraft in the dark. In any case, the use of photoemitting surfaces to control spacecraft charge must be employed judiciously along with a spacecraft charge analysis. Furthermore, as in the case of secondary emission surface selection, this technique also suffers from the lack of appropriate photoemission property data for spacecraft materials in the synchronous orbit environment.

4.3.2.3.3 "Leaky" Materials

Selection of dielectric materials which have high surface and bulk leakage can be an effective countermeasure for arc prevention. Frequently, however, this requirement cannot be satisfied at the same time as the thermal requirements on the surface materials. For example, tests performed at TRW[6] showed that quartz window OSR's charge up to breakdown voltages when exposed to an electron beam of 1 na/cm^2 whereas OSR's with borosilicate glass windows because of its poorer insulating properties do not. At higher incident electron currents, 10 na/cm^2, the quartz window OSR's arced at all temperaturesfrom 20°C to 100°C, but the glass window devices did not arc for temperatures above 50°C. Since OSR's are usually used on hot surfaces, even at the higher current glass OSR's would be practically "arc-proof". The use of glass OSR's is there-

fore recommended over quartz OSR's to control arcing due to spacecraft charging. Unfortunately, spacecraft requiring long lifetimes use quartz OSR's because of their superior retention of their thermal control properties in the geosynchronous enivornment.

4.3.2.4 Field Emission Electron Emitter

Calculations have shown that the use of a probe consisting of a hundred tungsten needles (with 0.1 μm radius tips) connected to a spacecraft by a long conducting boom can limit the negative potential of a spacecraft to about -300 V by field emission.[13] In the absence of the probe, the potential of the vehicle was estimated to be -3800 V. The principle employed here is that electrons will be emitted from a cold metal when the electric field on its surface is of the order of 10^9 Vm^{-1}. Fields of this size are generated at the tips of the tungsten needles. The separation from the spacecraft is required so that the field, at the needle tips, is not reduced by charge induced on the main body.

This device has not yet been tried on a spacecraft or for that matter tested under space flight conditions.

4.4 HAZARD REDUCTION

Countermeasures to reduce the threat of an environmentally induced arc discharge by controlling the chargeup of the spacecraft were discussed in the previous section. In this section we will examine the countermeasures that can be taken to prevent an arc discharge that does occur from interfering with the spacecraft operation.

The hazards of the arc discharge are twofold, i.e., direct damage to components and material by the arc, and electrically induced degradation or interference. In the category of direct damage we have included contamination by the arc byproducts, e.g., contamination of optical surfaces by materials expelled in an arc discharge.

4.4.1 Direct Damage

Very little can be done to reduce the threat of direct damage to components once the arc has occurred apart from removing the sensitive component from the region where arcs might occur. The probability that an arc to a cable would damage an electronic component can be reduced by shielding the cable and tying the shields to ground at both ends. Another precaution that should be taken is to design circuits for maximum threshold for burnout or provide circuit protection. This is usually not practical therefore it is often easier to remove sensitive components from regions where high stress might occur. This was actually done on the Voyager spacecraft where thermistor wires near the dielectric low gain antenna support cone were removed to prevent arcing to the cables. Similarly, in the case of surface contamination due to arc products, the recommended practice is to prevent the arc intensity using the methods of the previous sections.

4.4.2 EMI Hazard

The hazard due to the arc electromagnetic radiation can frequently be reduced and eliminated using standard EMI techniques. This can be most successfully performed if the arc discharge electromagnetic signal can be characterized and if the susceptibility of the various elements (receptors) in the system can be identified.

4.4.2.1 SEMCAP

The SEMCAP electromagnetic compatibility analysis program, developed and maintained by TRW, is a powerful tool for determining whether circuits will be upset by the arc discharge interference. SEMCAP can identify incompatibilities in the sensitivities of circuits to electromagnetic energy and the onboard source of that energy. Although SEMCAP was originally designed to identify incompatibilities between various onboard circuit recptors

and circuit EMI generators, it has been modified so that it can accept coupled electromagnetic pulses from arc discharges as a generator. The modified program was used on the Voyager spacecraft program. A detailed example of SEMCAP application to the spacecraft charging problem has been performed in Task 2 and is described in Section 2. In that example the arc discharge pulse characteristics used were obtained through the literature survey of Task 1.1.

4.4.2.2 Precautions

Once the SEMCAP program has identified circuits which will be disrupted by the electromagnetic radiation associated with the arc discharge, a variety of fixes can be applied to the susceptible circuits. We assume that the normal EMI/RFI precautions such as the following have been taken:

a. The circuit is in an RF-tight assembly
b. The assembly is electrically bonded to the spacecraft structure
c. The cables to and from the assemblies are shielded and grounded as frequently as possible
d. The acceptance bandwidths of the circuits are made only as wide as necessary.

If these precautions have been taken then special precautions could be applied such as

a. Design circuits with maximum possible trigger threshold. Consider the use of relays rather than solid state switches.
b. Use command and data line interface circuits that provide protection against short high-level transients.
c. Design circuitry for minimum sensitivity in the frequency range up to 400 MHz.
d. Consider the use of differential circuits for common mode rejection.

4.4.3 Testing

An important part of any arc discharge hazard reduction program is the verification testing to determine the efficacy of the countermeasures taken. Two types of verification tests have been considered. In the first type of test, arcs are induced by exposing the spacecraft to an electron beam in a vacuum chamber. In this type of test consideration has also been given to irradiating the spacecraft with ions and ultraviolet light. This type of

vacuum chamber test has never been performed on a flight spacecraft although the Air Force Weapons Laboratory has plans to test FLTSATCOM or DSCS in this manner.

The problems associated with the vacuum chamber test are numerous. The impracticality of putting an all-up spacecraft in a vacuum chamber can often result in a non-realistic test configuration, e.g., without deployed solar arrays. The problems associated with generating large area electron, ion and/or ultraviolet light beams are usually so great that compromises resulting in exposures not typical of the space environment are required. Furthermore, the presence of factors in the test configuration not typical of the space environment such as the chamber walls can lead to effects which do not occur in space, e.g., chamber resonances or arcing to walls.

The second method of testing consists of examining the response of the spacecraft and its subsystems using arc simulation sources. These tests are performed in air. This approach has been employed on Voyager[7], the Communications Technology Satellite[14], and the Viking Lander.[15] The problems associated with this approach are

a. The design of an arc simulation source that realistically simulates the arc and coupling occurring in the geosynchronous orbit environment.

b. The isolation of the spacecraft arc sources and diagnostics from ground to prevent unrealistic current paths for the discharge currents.

Since the simulated arc tests are performed in air an "all-up" flight configuration can be more readily assumed than in the chamber tests. Furthermore, these tests are relatively inexpensive to perform. A brief description of the arc simulation tests performed on Voyager follows:

4.4.3.1 Voyager Arc Simulation Tests

The basic test philosophy adopted for the Voyager I flight spacecraft tests was that all of the tests would be performed in a manner such that none of the onboard equipment would be exposed to test stimulus levels which could be considered hazardous to its in-flight performance, while the maximum immunity verification information was obtained. Many other facets of the real-life situation had to be considered such as the unavailability of developed test

equipment, the realities of possible spacecraft test configurations in view of schedule and manpower limitations, and the paucity of applicable information and prior experience within the scientific and engineering community in testing for the phenomena at hand. The schedule restrictions, in general, were the most limiting as may be deduced from the fact that the immunization effort was begun at the first of the year and the successful launch of both Voyager spacecrafts occurred near the end of August, 1977.

The SEMCAP computer program (Section 4.4.2.1) played an important part in the Voyager spacecraft testing. A SEMCAP model which had been generated for EMC purposes for Voyager earlier in the program was modified to include arc discharge sources. The modifications included modeling of the arcs and the coupling. A description of these modifications are given in Task 2 (Section 2). Among the functions provided by the modified SEMCAP for the Voyager tests were

- Selection of diagnostic points and stimulus location
- Prediction of spacecraft responses to test stimuli
- Limitation of stimuli to benign levels
- Extrapolation of responses to those expected at other locations
- Prediction of spacecraft responses to in-flight arcs.

The two types of arc discharge simulation sources used in the Voyager tests are shown in Figure 4-8. The radiated field arc source shown at the top of the figure was conceptually derived from Section 6.5.2.4.1, Electrostatic Discharge of MIL-STD-1541 (USAF). The coil used was a Transpack 400:1 automotive ignition coil. It was operated in parallel with a 2 μf capacitor which was discharged by a relay about once per second. Although radiated fields are not expected to occur in flight, this type of test stimulus was carried over from preceeding Proof Test Model (PTM) spacecraft tests to the flight spacecraft test to provide comparative data on the immunity improvements implemented. Tests with this type of stimulus also provided some of the data essential to establishing a measure of the accuracy of the SEMCAP model. The surface arc simulation source is shown in the lower part of Fig. 4-8. The aluminum foil is insulated from the surface to be tested with a 3 mil sheet of mylar. Its capacitance, determined by the test area, is charged by the high voltage power supply through 500 megohm isolation resistors. The maximum arcing potential is adjusted by means of pre-adjusted arc gaps. It

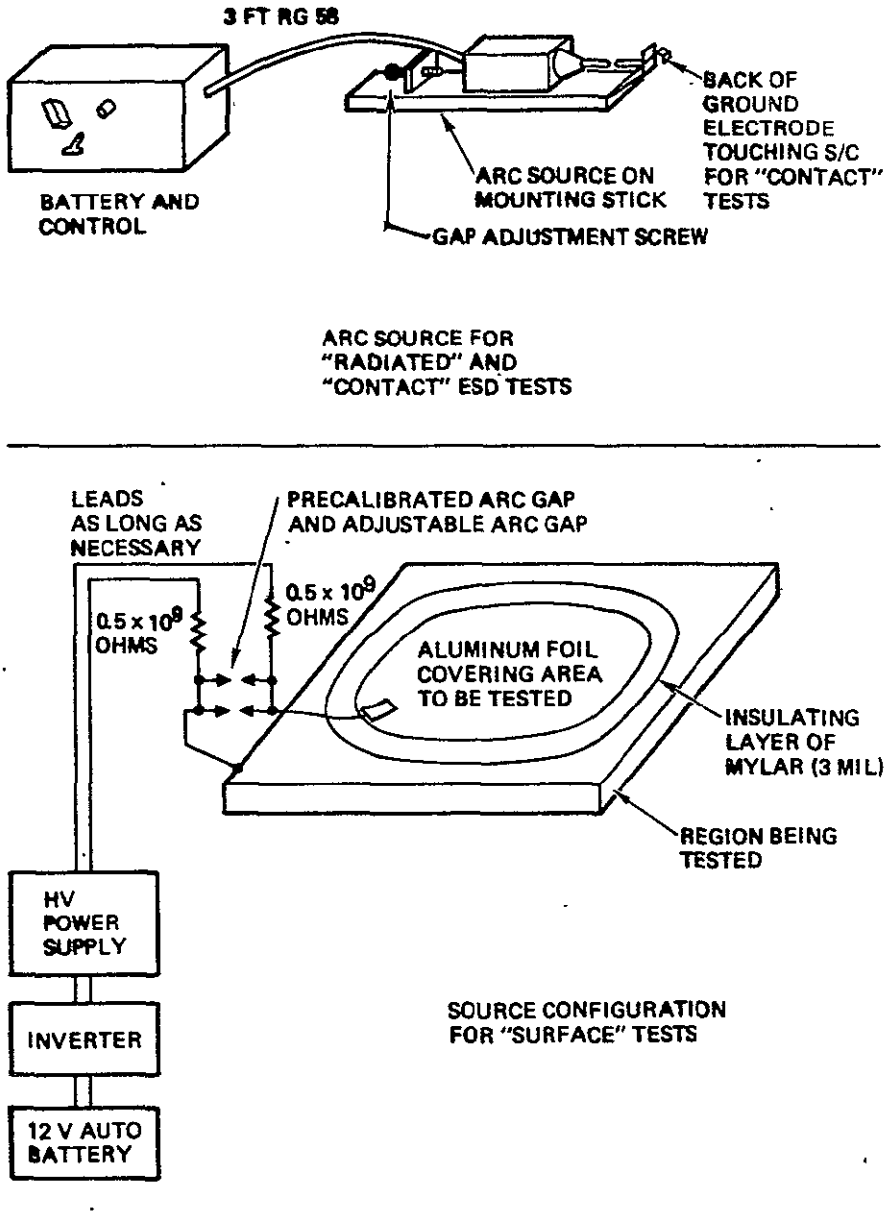

Figure 4-8. Test Sources for Voyager

was recognized that unintentional coupling from the source to "target" circuits, including diagnostic equipment, could generate false data. For this reason the sources were battery operated in order to eliminate coupling into power lines. In addition, the radiation and coupling from the supporting equipment, batteries and power supplies were minimized as best as permitted by available time constraints.

Figure 4-9 shows the calibration data for the sources. The spark coil arcing voltage is adjusted by means of the gap adjusting screw shown in Figure 4-8. The relation between gap width and arcing voltage turned out to be nearly linear at about 1 kV/mm (actually 18 kV for 16mm). The spark coil pulse shape as shown in Figure 4-9 was approximately 20 ns in duration irrespective of arc breakdown voltage. The gap width to peak current relation, a function of the coil self-capacitance (35 pf) and the external circuit inductance, was in the order of 50 amperes peak at 14 mm or 15 kV. The surface arc source was triggered at 5 kV for the test data shown in Figure 4-9. The approximately 35 ns risetime observed was determined by the associated circuit inductance, and the 100-200 ns fall time increased as the area of aluminum foil.

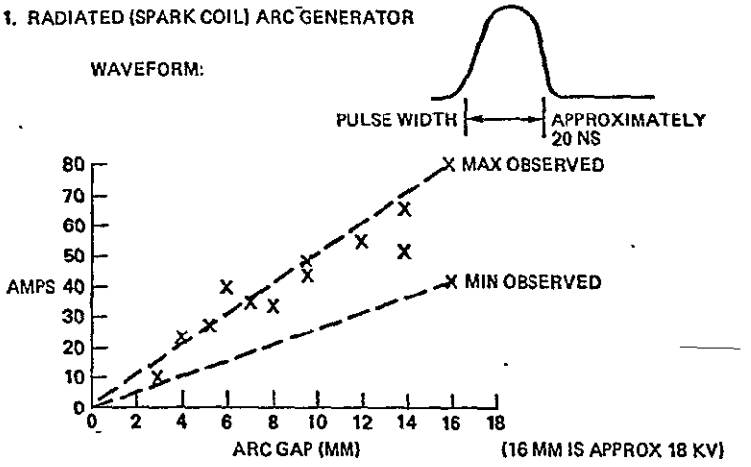

2. SURFACE ARC SOURCE WITH ALUMINUM FOIL (5 KV ARC)

	OBSERVED PEAK CURRENT	
CAPACITANCE	WITH 11 OHMS	WITHOUT 11 OHMS
2600 PF	70A	80A
1300 PF	62A	70A

	OBSERVED 50% AMPLITUDE TIME DURATION	
CAPACITANCE	WITH 11 OHMS	WITHOUT 11 OHMS
2600 PF	250 NS	200 NS
1300 PF	125 NS	100 NS

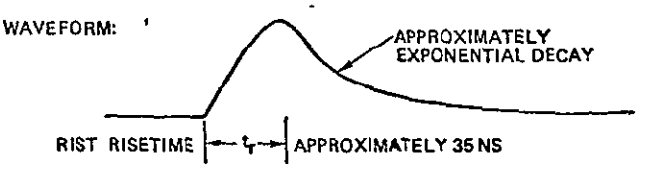

Figure 4-9. Source Characteristics for the Voyager Program

The possible test configurations were limited by schedule considerations such as the unavailability of the RTG power source for this test. Furthermore, an objective of the test plan was to obtain the most crucial data in the most "efficient" manner. That is, to minimize the number of test locations and diagnostic points and to depend to a major extent on the analytical capabilities inherent in the use of the SEMCAP model.

Figure 4-10 shows the diagnostic setup used for the flight spacecraft tests as well as for the initial tests performed on the PTM spacecraft. As indicated in Figure 4-10, four diagnostic test points were selected. These test points, made accessible with breakout connectors, were monitored differentially with high impedance probes on two oscilloscopes. The full-up spacecraft with the science boom deployed, as shown in the photograph of Figure 4-11 was insulated from the floor to minimize unreal coupling effects. Power was brought in on cables from an external power supply, but the spacecraft was otherwise completely isolated electrically. The spacecraft systems were monitored via "air" using its telemetry system.

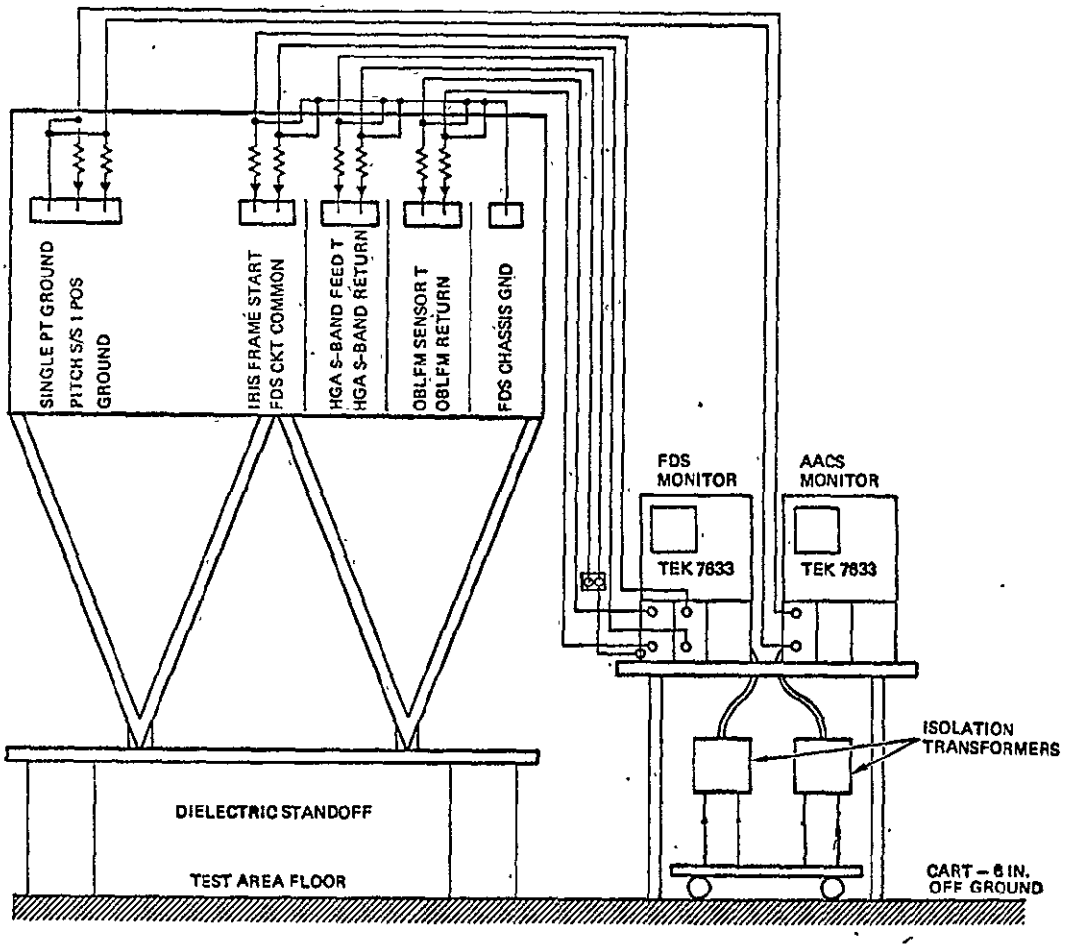

Figure 4-10. Voyager Test Setup

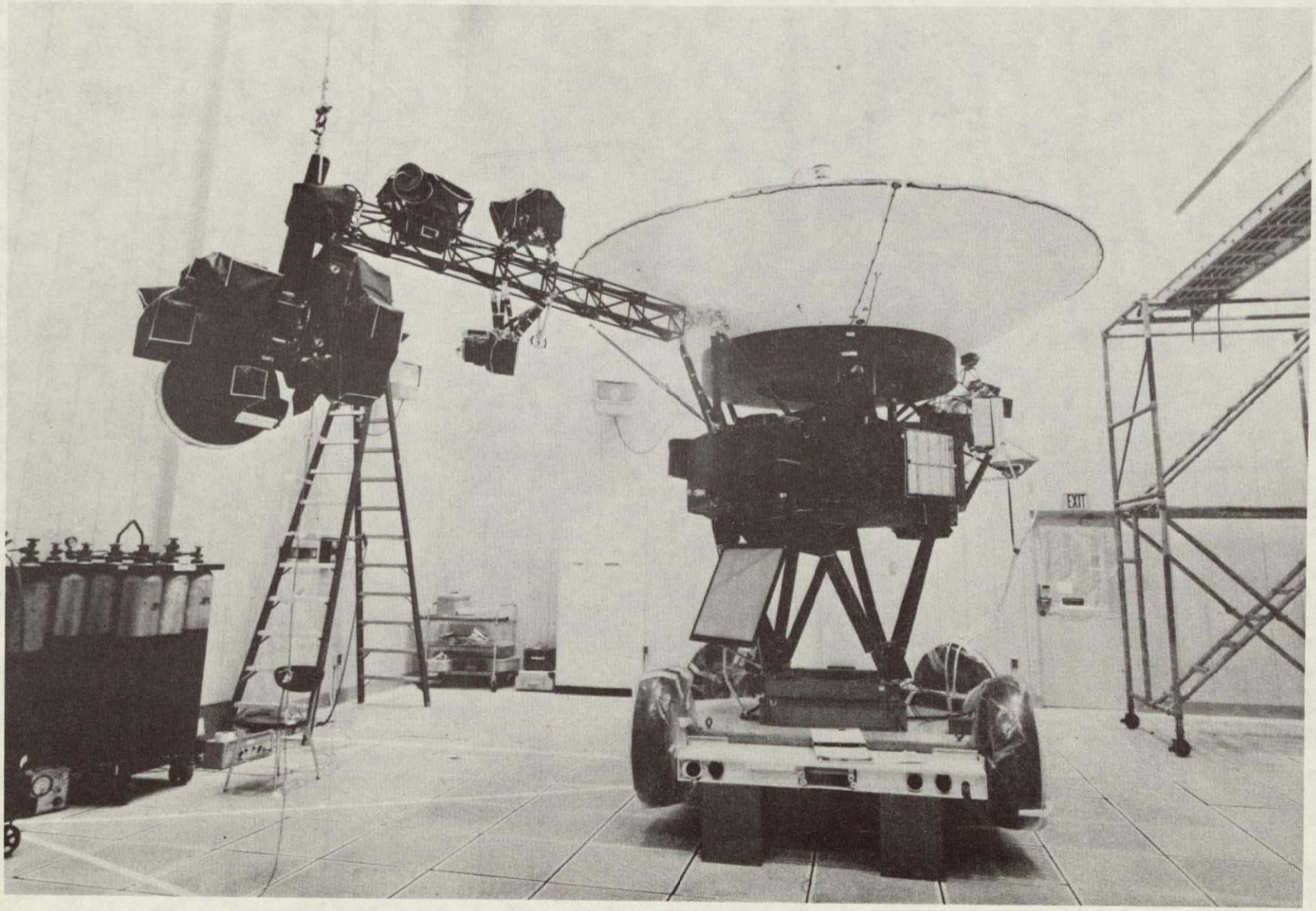

VOYAGER—SPACECRAFT CHARGE VERIFICATION TEST SETUP

Figure 4-11.

Table 4-5. SEMCAP Predictions vs ESD Test Results (Flight Spacecraft)

LOCATION OF ARC	HGA		IRIS		OBLFM		SUN SENSOR	
	PRED(V)	MEAS(V)	PRED(V)	MEAS(V)	PRED(V)	MEAS(V)	PRED(V)	MEAS(V)
RADIATED TESTS								
IRIS/ISS	0.9	1.2	2.0	0.8	0.09	1.0	0.08	2.5
LECP	1.5	0.8	6.0	0.45*	0.4	0.7	0.1	1.6
SUN/SENS	0.84	1.0	0.48	0.3*	0.9	0.4*	4.0	1.6
MAG	0.4	0.4*	0.8	0.5*	3.6	1.2	0.4	0.5
FSS	4.9	4.0	0.96	1.5	2.1	1.4	0.002	2.0
BREWSTER PLATE(1)	2.2	4.0	1.5	4.0	0.9	3.3	0.54	17.7
SURFACE TESTS								
LECP	0.27	0.6	15.0	0.6*	0.04	0.6	0.017	0.8
BREWSTER PLATE	6.8	1.0	0.37	0.6	0.6	0.7	0.4	0.9
FSS	57.0	10.0+	0.09	4.2+	0.2	1.7+	0.001	4.0+

*BACKGROUND NOISE; NOISE DUE TO ARC UNNOTICEABLE

+EXTRAPOLATED

MEAN ERROR = -12 dB (UNDERPREDICTING) } NOT INCLUDING *(STARRED) ENTRIES

STANDARD DEVIATION = 20 dB }

(1) PREDICT WAS "CONTACT" TEST. MEASURED WAS "RADIATED" TEST.

Table 4-6. Parameters of Test Arc Discharge Source Models

Arc Source	Type of Arc	Breakdown voltage V	Discharge current $I_{(A)}$	Risetime of discharge current t_r	Discharge current pulse width t_p	Replacement current path inductance $L_{(\mu h)}$	Main discharge capacitor C_x	Equiv stray capacitance C_f	I_{repl} / I_{arc} G'_I	$V_{repl\ volt} / I_{arc}$ G''_I	Corner frequency f_c	Looplength ℓ(m)	Loopheight $h_{(m)}$	Wire radius $r_{(m)}$
IRIS/ISS	Radiated	12 kV	60	2 ns	20 ns	N/A	N/A	N/A	N/A	N/A	N/A	N/A	N/A	N/A
Sun Sensor	Radiated	12 kV	60	2 ns	20 ns	N/A	N/A	N/A	N/A	N/A	N/A	N/A	N/A	N/A
MAG Canister	Radiated	12 kV	60	2 ns	20 ns	N/A	N/A	N/A	N/A	N/A	N/A	N/A	N/A	N/A
FSS	Radiated	12 kV	60	2 ns	20 ns	N/A	N/A	N/A	N/A	N/A	N/A	N/A	N/A	N/A
Brewster Plate	Contact	12 kV	60	2 ns	20 ns	N/A	N/A	N/A	N/A	N/A	N/A	N/A	N/A	N/A
LECP	Surface	5 kV	25	10 ns	10 ns	1.8	56 pf	7 pf	0.12	1.9E4	35 MHz	0.3	0.15	0.07
Brewster Plate	Surface	5 kV	37.5	10 ns	20 ns	0.25	150 pf	12 pf	74E-3	1.5E3	95 MHz	0.25	0.15	0.07
FSS	Surface	5 kV	12	10 ns	10 ns	2.0	12 pf	13 pf	0.5	1.25E4	45 MHz	0.3	0.15	0.07

Table 4-7. Parameters of In-Flight Surface Arc Models

Assumes Arc Discharge Current Greater Than Measured "Replacement" Current by Factor $\frac{C_x + C_f}{C_f}$ (of test setup)

Arc Source	Breakdown Voltage V	Discharge or Arc Current I	Discharge Current Rise Time t_r	Discharge Current Pulse Width t_p	Replacement Current Path Inductance $L_{B(\mu h)}$	Main Discharge Capacitance C_x	Equivalent Stray Capacitance C_f	G'_I I_{repl}/I_{arc}	G''_I $\frac{V_{repl\ volt}}{I_{arc}}$	Corner Frequency f_c	Looplength ℓ	Loopheight $h_{(m)}$	Wire Radius $r_{(m)}$
MAG Cable	5 kV	20 A	10 ns	1.7 μs	2.3	0.05 μf	30 pf	5.0 E-4	82 E3	8 MHz	0.6 m	6 E-5	2.5 E-4
HGA Paint (OB)	1 kV	150 A	5 ns	3 μs	0.4	0.4 μf	500 pf	1.25 E-3	1.25 E3	15.9 MHz	1.8 m	2 E-4	5 E-5
Plume Shield (Sep Conn)	1 kV	16 A	20 ns	285 ns	1.5	4500 pf	0.2 pf	4 E-5	9.4 E3	290 MHz	0.2 m	5 E-5	2.5 E-5
FSS	7 kV	80 A	8 ns	80 ns	1.9	14 pf	53 pf	1.0	12 E3	34 MHz	0.35 m	0.025	5 E-5
HGA Paint (IB)	1 kV	150 A	5 ns	2.4 μs	0.4	0.3 μf	70 pf	2.3 E-4	1.25 E3	42 MHz	1.0 m	2 E-4	5 E-5
Plume Shield (RTG)	1 kV	16 A	20 ns	330 ns	0.8	5200 pf	2.5 pf	2.5 E-4	9.5 E3	83 MHz	0.17 m	5 E-5	2.5 E-5
RTG Oxide	3.5kV	925 A	20 ns	3.7 μs	2.8	0.34 μf	90 pf	2.5 E-4	1.1 E4	12 MHz	0.85 m	7.6 E-5	3.8 E-5
MIRIS KAPTON	1 kV	150 A	5 ns	26 ns	4	40 pf	0.032 pf	1.0	2.5 E4	12 MHz	0.24 m	5 E-5	2.5 E-5

G'_I = Replacement Curr/Arc Curr

G''_{II} = Repl Line Voltage/Arc Curr

Table 4-8. Revised SEMCAP Predictions of Interference (Volts) on Interface with RC Filters Due to In-Flight Arcs

RECEPTOR NAME	ARC SOURCE						
	MAG CABLE	HGA OUTBOARD FACE	FSS	HGA INBOARD FACE	PLUME SHIELD ON RTG STRUT	RTG OXIDE	KAPTON ON MIRIS
PLAYBACK DATA		---	---	---			---
CRS CMD WORD		---	---	---			0.044
PWS ADC BIT SYNC		0.001	---	0.001			---
PRA COMD WORD		---	---	---			---
LECP COMD WORD A		---	---	---			0.04
PPS COMD WORD		---	---	---			3.0
UVS MODE CONTROL		---	---	---			3.0
UVS SCIENCE DATA 1		---	---	---			3.0
MAG SAMPLE B		---	---	---		---	---
MAG OBLFM SENSOR TEMP		0.014	0.01	---	---	---	---
ISS-WA ADC START			---	---			35
ISS-WA ADC VID DATA							18
MAG IBHFM SENSOR TEMP	0.02		0.004	---	---	---	---
IRIS FRAME START		---	---	---			3.46
PITCH CRUISE S/S1 POSN		---	---	---		---	---
HGA S-BAND FEED TEMP		---	0.23			---	---
RTG CASE TEMP		---	0.004			0.3	---

---DENOTES LESS THAN A MILLIVOLT, PREDICITONS FROM RUN OF 06/17/77
ARC SOURCE PARAMETERS PER TABLE 4-7

4.5 MODIFIED GUIDELINES AND RECOMMENDED PRACTICES

Additional guidelines have been generated as a result of this study. These guidelines are essentially a summary of the countermeasures discussed in the previous sections. Added guidelines using arc control techniques such as electron or plasma guns or electron emitters are not recommended. These devices can be useful in special cases but in general more passive techniques should be adequate and with less disruption to the spacecraft program. Furthermore, techniques and materials that have not been previously qualified for flight spacecraft application have also been avoided. The added guidelines follow.

4.5.1 Analysis

- Analysis should be performed on each synchronous orbit spacecraft to determine the locations of voltage stresses. This analysis should consider apertures and seasonal effects.
- Charge balance techniques based on analysis should be employed to reduce hazardous stresses.
- SEMCAP-type analyses should be performed to determine susceptibility and margin of spacecraft components to interference from arc discharges. Arc characteristics based on laboratory tests (such as those given in Table 1-10, Task 1.1) should be used as an input.

4.5.2 Grounding Guidelines

- Ground straps should be sufficiently heavy to carry currents associated with pulses described in Task 1.1.
- Grounding of thermal blanket VDA should be able to tolerate at least 2000 discharges a year having the pulse characteristics described in Table1-10, Task 1.1.

4.5.3 Materials Guidelines

- Use low resistivity surface materials wherever possible. Borosilicate OSR's are preferred over fused silica.
- Use conductive adhesives to bond exposed dielectric components such as OSR's to structure if analysis and tests show need.
- Use conductive coating only if analysis or tests show need. Ground coating to structure.

4.5.4 Guidelines Related to Direct Arc Damage

- Do not run cabling or mount components near dielectrics predicted to be at high voltages.
- Design circuits with maximum threshold for burnout and provide protection circuitry.
- Locate contamination-sensitive components to avoid regions of high voltage stress.

4.5.5 EMI Guidelines

- Mount susceptible circuits in RF-tight enclosures.
- Bond enclosures to spacecraft structure.
- Ground cables to and from assemblies as often as practical.
- Minimize circuit acceptance bandwidth.
- Design circuits with maximum possible trigger threshold. Consider use of relays rather than solid state switches.
- Use command-and data-line interface circuits that provide protection against short high level transients.
- Design circuitry for minimum sensitivity in the frequency range up to 400 MHz.
- Consider the use of differential circuits for common mode rejection.

4.5.6 Testing Guidelines

- Testing to verify efficacy of countermeasure program should be performed. Testing in air with simulated arc discharges sources can be useful.
- If air tests are performed
  - Design arc simulator sources to realistically simulate arcs and coupling to spacecraft
  - Isolate spacecraft, sources, and diagnostics from ground to prevent unrealistic current paths for the discharge currents
  - Use SEMCAP-type program to
    - Select diagnostic points and stimulus location
    - Predict spacecraft response to test stimuli
    - Limit stimuli to benign levels
    - Extrapolate responses to those expected at other locations
    - Predict spacecraft response to in-flight arcs.

REFERENCES

1. Inouye, G. T. and J. M. Sellen, Jr., "TDRSS Solar Array Design Guidelines for Immunity to Geomagnetic Substorm Charging Effects," Proc. of Thirteenth IEEE Photovoltaic Specialists Conference - 1978, June 5-8, 1978, Washington D.C., pp. 309-312.

2. Inouye, G. T., and J. M. Sellen, Jr., "TDRSS Solar Array Arc Discharge Tests," presented at the Spacecraft Technology Conference, U. S. Air Force Academy, Colorado Springs, CO, Oct. 31-Nov. 2, 1978 and to be published in the Proceedings.

3. Olsen, R. C., E. C. Whipple and C. K. Purvis, "Active Modification of ATS-5 and ATS-6 Spacecraft Potentials," presented at 1978 Symposium on the Effect of the Ionosphere on Space and Terrestrial Systems, Arlington, VA, January 1978.

4. Purvis, C. K., R. O. Bartlett and S. E. DeForest, "Active Control of Spacecraft Charging on ATS-5 and ATS-6," presented at Spacecraft Charging Technology Conference, U. S. Air Force Academy, Colorado Springs, CO., Oct. 27-29, 1976. Published in the Proceedings, AFGL-TR-77-0051 and NAS TMX-73537, Ed. C. P. Pike and R. R. Lovell, 24 February 1977.

5. Komatsu, G. K., and J. M. Sellen, Jr., "A Plasma Bridge Neutralizer for the Neutralization of Differentially Charged Spacecraft Surfaces," Proc. of Thirteenth IEEE Photovoltaic Specialist Conference - 1978, June 5-8, 1978, Washington D.C.

6. Inouye, G. T., N. L. Sanders, G. K. Komatsu, J. R. Valles, and J. M. Sellen, Jr., "Thermal Blanket Metallic Film Groundstrap and Second Surface Mirror Vulnerability to Arc Discharges," presented at the Spacecraft Technology Conference, U. S. Air Force Academy, Colorado Springs, CO, Oct. 31-Nov. 2, 1978 and to be published in the Proceedings.

7. Sanders, N. L. and G. T. Inouye, "Voyager Spacecraft Charging Model," presented at 1978 Symposium on the Effect of the Ionosphere on Space and Terrestrial Systems, Arlington, VA, January 1978.

8. "Electrically Conductive Paints for Satellites," IIT Research Institute, Dec. 1976, AFML-TR-76-252.

9. "Transparent Antistatic Satellite Materials," General Electric Space Division, Oct. 1977, AFML-TR-77-74, Part 1.

10. Knott, K., "The Equilibrium Potential of a Magnetospheric Satellite in an Eclipse Situation, Planet. Space Sci., 20:1137-1146.

11. Ruben, A. G., P. L. Rothwell and G. K. Yates, "Reduction of Spacecraft Charging using Highly Emissive Surface Materials," presented at 1978 Symposium on the Effect of the Ionosphere on Space and Terrestrial Systems, Arlington, VA, January 1978.

12. Belanger, V. J. and A. E. Eagles, "Secondary Emission Conductivity of High Purity Silica Fabric," presented at Spacecraft Charging Technology Conference, U. S. Air Force Academy, Colorado Springs, CO, Oct. 27-29, 1976. Pub. in the Proceedings, AFGL-TR-77-0051 and NASA TMX-73537, Ed. C. P. Pike and R. R. Lovell, 24 February 1977.

13. Grard, R., "Spacecraft Potential Control and Plasma Diagnostic Using Electron Field Emission Probes," Space Science Instrumentation, Vol. 1, Aug. 1975, pp. 363-376.

14. Gore, J. Victor, "Design, Construction and Testing of the Communications Technology Satellite Protection Against Spacecraft Charging," presented at the Spacecraft Charging Technology Conference, U. S. Air Force Academy, Colorado Springs, CO, Oct. 27-29, 1976. Pub. in the Proceedings, AFGL-TR-77-0051 and NASA TMX-73537, Ed. C. P. Pike and R. R. Lovell, 24 February 1977.

15. Lewis, R. O., Jr., "Viking and STP P78-2 Electrostatic Charging Designs and Testing," presented at the Spacecraft Charging Technology Conference, U. S. Air Force Academy, Colorado Springs, CO, Oct. 27-29, 1976. Pub. in the Proceedings, AFGL-TR-77-0051 and NASA TMX-73537, Ed.. C. P. Pike and R. R. Lovell, 24 February 1977.

16. Inouye, G. T., "Spacecraft Potentials in A Substorm Environment", Progress in Astronautics and Aeronautice, Vol. 47, Series edited by Martin Summerfield.

17. Katz, I, et al., "A Three Dimensional Dynamic Study of Electrostatic Charging in Materials", Report No. NAS-CR-135256 and SSS-R-77-3367 (Systems, Science and Software Corp.).

APPENDIX A

(TO TASK 1.1)

Modification of Task 1.1 to incorporate results of Aron-Staskus experiments.

The Experiment

A series of experiments were recently performed at NASA Lewis on the area scaling of teflon samples (P. R. Aron and J. V. Staskus, "Area Scaling Investigations of Charging Phenomena," to be published). The data taken is the most comprehensive study of charging and discharging of teflon samples, particularly those of large (>300 cm^2) area. We received a preliminary copy of that study too late to include the data in the main body of this report. However, the data are sufficiently unique as to warrant inclusion in this report as an appendix. In this appendix we will summarize those aspects of that study that relate to the characterization of the arcs of teflon. Furthermore, we will identify those changes in the pulse-characteristic estimates made in Task 1.1 which result from this new data. The only changes that will be necessary will be to the discharge parameters for teflon.

The teflon charging and discharging experiments were performed in the vacuum facility at LeRC. The samples were exposed to a 1-2 nanoamp/cm^2 electron beam at energies of 10 kV, 15 kV and 20 kV. Although breakdown occasionally occurred at 10 kV most of the discharge experiments were performed at beam voltages of 15 kV and 20 kV, and discharge data were given only at those energies.

Area effects were studied by irradiating teflon samples of 232 cm^2, 1265 cm^2 and 5058 cm^2. Each sample consisted of strips of silvered FEP type A teflon tape, .011 cm thick and 5.08 cm wide. Each tape is backed with a layer of vacuum-deposited silver covered with vacuum deposited Inconel and a 0.03 mm thick layer of adhesive. The three different sample areas are made up of several of these strips applied to a 0.318 cm square aluminum plate. Two different runs were takne with each sample. In the first run a 50Ω coax ($\sim$ 10 m long) brought out the current from the aluminum backplate. The current was grounded through 50Ω and measured by a current probe. In the second series of runs (labelled LI, low impedance), the sample backplate

current was brought out on a low impedance (5 cm diameter) aluminum cylinder through the core of the current transformer. The sample backing in this case was within a few milliohms of tank ground.

Discharge Parameters

Three parameters were used to characterize the discharge current pulses: the peak current (I), the total charge (Q) and the pulse duration (τ). Several discharges were examined for each sample. From these a maximum value and a most probable value of each parameter was deduced. Using this data the authors computed the area effect for both the peak current and the pulse duration for the maximum current and pulse duration measured. The equations deduced are given in Table A-1 along with all the other teflon discharge parameters determined. Table A-1 should be used as an extension of Table 1-6 of Task 1.1.

Comparison with Results of Task 1.1

Comparison of the Aron and Staskus (A-S) data with the area effect for teflon deduced under Task 1.1 and summarized in Figures 1-5A and 1-7 is given in Figure A-1 and A-2. In determining the area effect we have only used the 20 kV data since most of the data used in determining the original results were taken with a 20 kV electron beam. In Figure A-1 and A-2 we have plotted the A-S, 50Ω and low impedance (LI) data on the curves for the area effect for teflon obtained under Task 1.1. Both the worst case (maximum) and most probable data is shown. Power curves of the form $I = aA^b$ and $\tau = aA^b$ were determined for the data. For this purpose the LI and 50Ω data were combined.

From Figure A-1 we notice that the worst case A-S current is about an order of magnitude less than our worst case teflon estimate. Furthermore, the most probable A-S current actually decreases for increasing area for areas greater than 232 cm^2. From Figure A-2 we notice that the A-S pulse durations increase more steeply at higher areas than our estimates. Both the maximum and most probable values reach values about three times higher than our estimates for these values at 5000 cm^2.

Conclusions and Update for Teflon Discharge Parameters

The Aron and Staskus data are the only arc discharge data available for teflon samples having areas greater than 300 cm^2. The estimates we made for teflon for large area samples were extrapolations from the Balmain ('78)

Table A-1. Teflon (VDA or Silvered)

	Aron ('78)	Aron ('78)	Aron ('78)
1. Sample Size	232 cm^2	1265 cm^2	5058 cm^2
2. Thickness	.011 cm	.011 cm	.011 cm
3. Configuration	Teflon strips on 1/8" thick Al substrate	SAME	SAME
4. Technique	Electron Swarm Tunnel (EST)	EST	EST
5. Beam Voltage at Breakdown	15 kV/20 kV*	15 kV/20 kV	15 kV/20 kV
6. Beam Current	1-2 na/cm^2	1-2 na/cm^2	1-2 na/cm^2
7. Load to Ground from Metallic Backing	50Ω/LI**	50Ω/LI	50Ω/LI
8. Breakdown Voltage	∿ 7.5 kV	∿ 7.5 kV	∿ 7.5 kV
9. Peak Pulse Current(amps)			
Most Probable:***			
15 kV/20 kV, 50Ω	58/55	60/63	108/52
15 kV/20 kV, LI	22/135	20/50	20/63
Maximum:***			
15 kV/20 kV, 50Ω	60/62	73/110	128/240
15 kV/20 V, LI	23/140	45/138	32/330
10. Pulse Duration (μS)			
Most Probable:			
15 kV/20 kV, 50Ω	.2/.22 μs	.5/.6	1.4/1
15 kV/20 kV, LI	.85/.28 μs	.7/.6	1.4/1
Maximum:			
15 kV/20 kV, 50Ω	.2/.25 μs	1/1.1	3.5/3.6
15 kV/20 kV, LI	.95/.2 μs	2.1/1.3	4/2.7
11. Charge in Pulse (μC)			
Most Probable:			
15 kV/20 kV, 50Ω	25/13	38/50	155/30
15 kV/20 kV, LI	5/30	20/50	25/135
Maximum:			
15 kV/20 kV, 50Ω	32/23	50/68	223/260
15 kV/20 kV, LI	7/30	65/80	75/340
12. Area Effect	$I = 5.49A^{.44}$ (20 kV, 50Ω max)	$I = 14.3A^{.25}$ (15 kV, 50Ω max)	

*2 different beam voltages used.
**2 different loads used 50Ω and a low impedance (LI) connection.
***Several runs taken. Most probable and maximum values given.

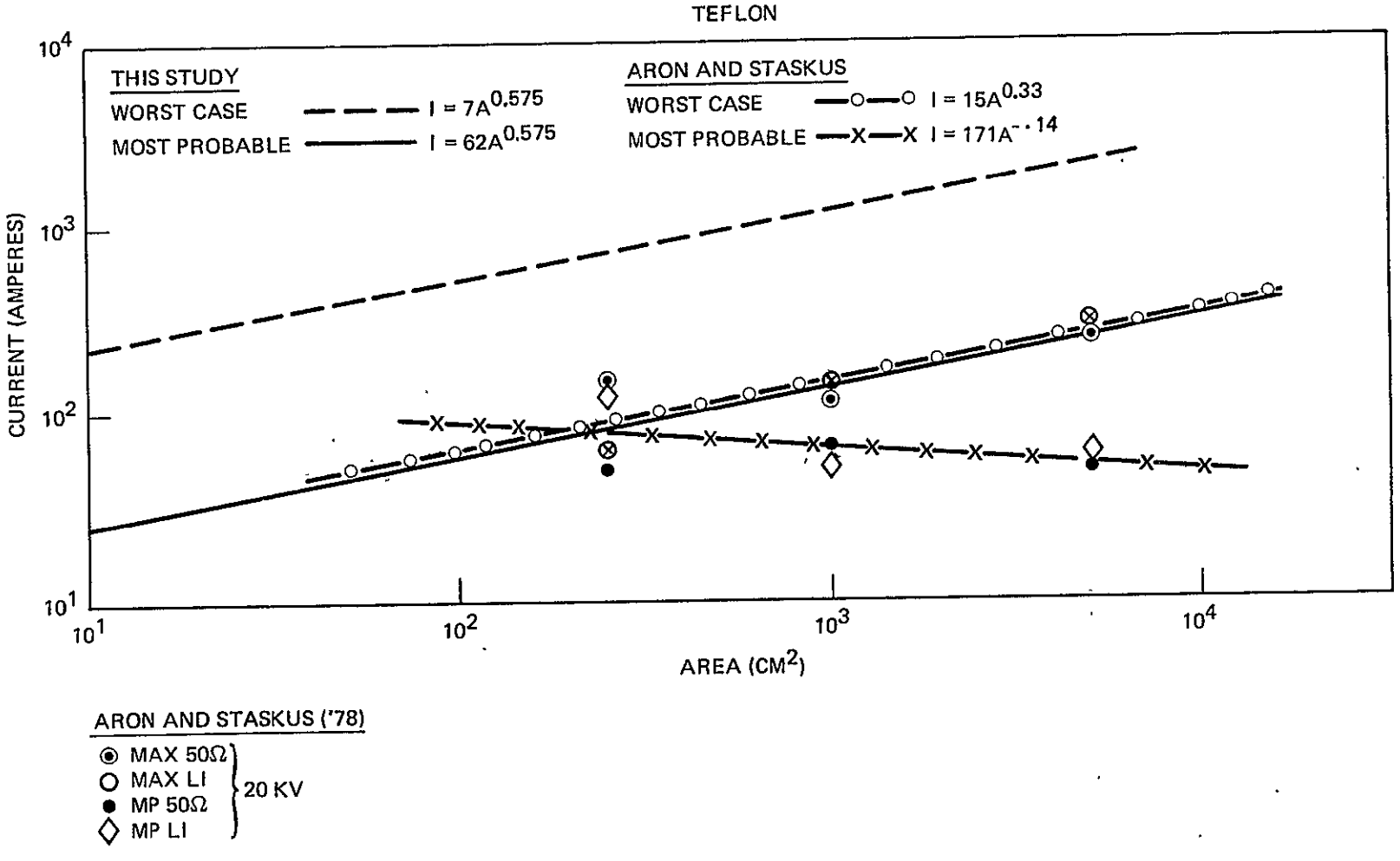

Figure A-1. Comparison of Peak Discharges Currents Obtained in This Study to Those of Aron and Staskus

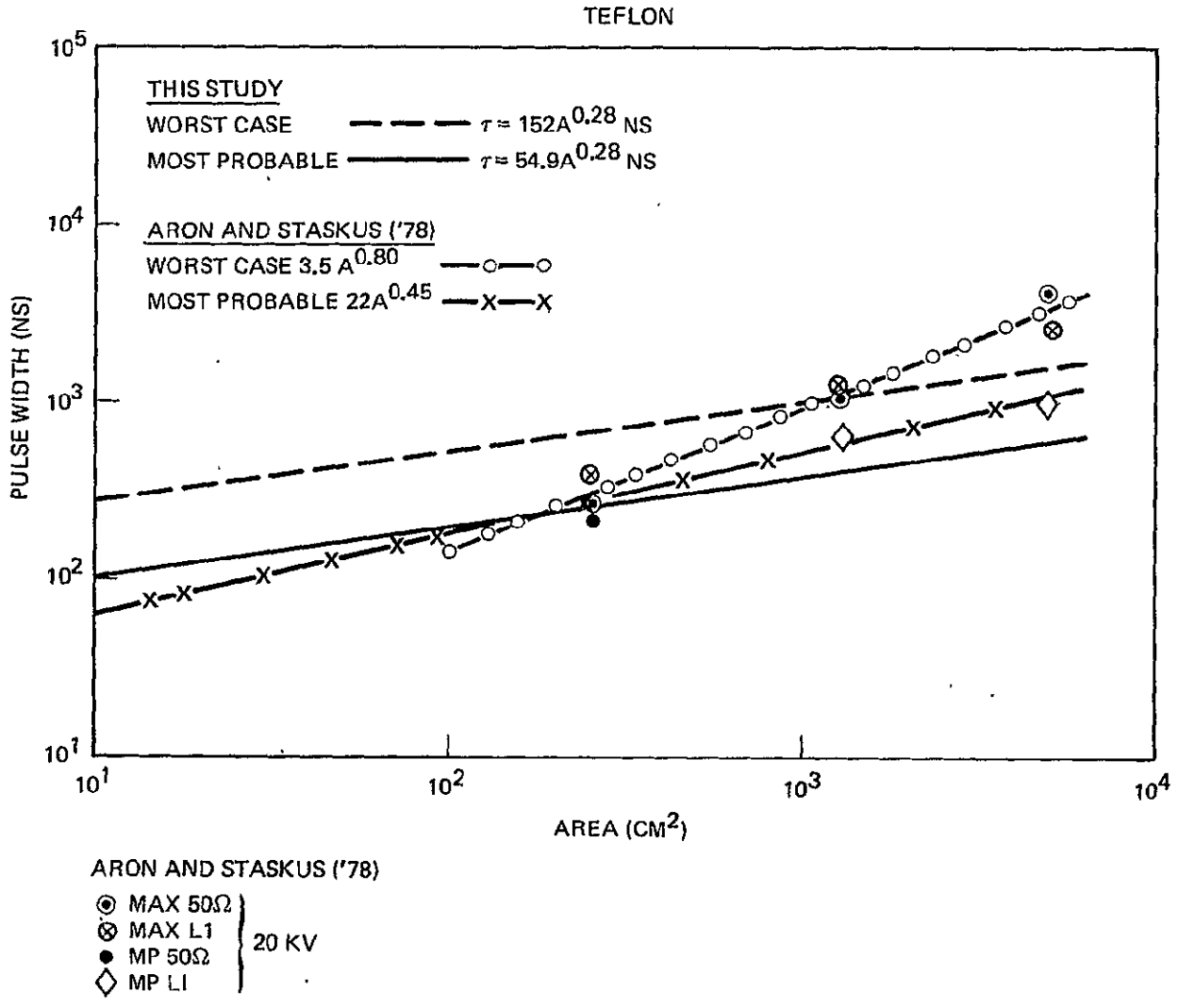

Figure A-2. Comparison of Discharge Pulse Width Obtained in This Study with Results of Aron and Staskus

experiment using small areas (less than .10 cm^2). Furthermore very little data was available to permit a good worst-case estimate. The A-S experiment gives excellent results in this case also. We therefore have updated the arc discharge summary given in Table 1-10 under Task 1.1 to reflect the A-S experiment as follows:

- The peak-current and pulse-duration area effects for teflon use the most probable values obtained from the A-S experiment for teflon samples with areas greater than 200 cm^2. Most-probable values estimated under Task 1.1 are kept for areas less than 200 cm^2.
- The worst-case (maximum) values for the peak current and pulse duration deduced from A-S are used for teflon in place of those deduced under Task 1.1.
- The breakdown voltage determined by A-S for teflon is used.

In Table A-2, we show the changes made to the arc-discharge characterization parameters resulting from the A-S experiments.

Table A-2. Arc Discharge Characterization Summary*

MATERIAL		BREAKDOWN VOLTAGE		PEAK PULSE CURRENT (AMPS)		PULSE WIDTH (ns)	
		ESTIMATE	WORST CASE	ESTIMATE	WORST CASE(1)	ESTIMATE	WORST CASE (1)
TEFLON		~~1.2 kV (2)~~ 9.5 kV	4 kV (3)	**$I=7A^{.575}$, $A<200\ cm^2$. (4) $I=171A^{-.14}$, $A>200\ cm^2$	**~~$I=62A^{.575}$ (5)~~ $I = 15A^{.33}$	**$\tau=54.9A^{.28}$, $A<200\ cm^2$. (4) $\tau=22A^{.45}$, $A>200\ cm^2$.	**$\tau=152A^{.28}$, $A<200\ cm^2$. $\tau=3.5A^{.8}$, $A>200\ cm^2$.
KAPTON		12 kV (6)	8 kV (6)	$I=9.9A^{.43}$ (7)	$I=.002A^{2.1}$ (8)	$\tau=203A^{.292}$ (7)	$\tau=44A^{.6}$ (8)
MYLAR		<20 kV (9)	<20 kV (9)	$I=17.2A^{.764}$ (4)	$I=12.5A^{1.33}$ (10)	$\tau=24.9A^{.39}$ (4)	$\tau=56A^{.39}$ (5)
SOLAR CELLS COVERGLASS NEGATIVE		9 kV (11)	9.4 kV (11)	20 (12)	20 (12)	500 (12)	500 ns (12)
SOLAR CELLS COVERGLASS POSITIVE		1 kV (13)	1 kV (13)	0.5 (13)	0.6 (13)	2000 (13)	2000 (13)
SECOND SURFACE MIRRORS(QUARTZ WINDOW)		7 kV	2 kV	40 (14)	40 (14)	300 (14)	300 (14)
THERMAL BLANKETS	SEWN EDGE	10.4 kV (15)	10.4 kV (15)	(17)	(17)	(17)	(17)
	OPEN EDGE	16.5 kV (15)	5 kV (16)	(17)	(17)	(17)	(17)

* LOAD FOR DIAGNOSTICS FOR ALL EXPERIMENTS USED IN SUMMARY IS R < 2000 Ω. INSUFFICIENT DATA TO DETERMINE THICKNESS DEPENDENCE.

**UPDATE OF TEFLON DATA FOR AREAS GREATER THAN 200 cm^2 BASED ON ARON AND STASKUS ('78) 20 kV DATA.

APPENDIX B

FUTURE PROGRAMS: THE SPACE TEST PROGRAM; P78-2 SPACECRAFT

As part of the cooperative NASA/AF Spacecraft Charging Program, initiated in 1975, a satellite devoted to spacecraft charging investigations, the P78-2 spacecraft was launched on January 30, 1979. The spacecraft was spin stabilized at one revolution per minute and placed in a near synchronous, near equatorial earth orbit. In its final orbit, achieved 2 February 1979, the satellite was at an apogee of 43,200 km ($L \sim 7.8\ R_e$); perigee of 27,500 km ($L \sim 5.3\ R_e$); an inclination of $\sim 7.8°$, with apogee and perigee points near the geographic equator. On 5 February apogee was at 190° east longitude and drifting eastward at $\sim 5.4°$ per day. The spin axis of the satellite was located in the orbit plane and maintained approximately perpendicular to the satellite-sun line.

Table A, identifying the experiments and principal investigators, was taken from SAMSO publication TR-78-24 "Description of the Space Test Program P78-2 Spacecraft and Payloads". This publication also presents a detailed description of the experiments and spacecraft.

The objective of the P78-2 mission is to obtain information for a military standard concerning spacecraft charging and EMI/RFI encountered at synchronous orbit. In addition, it is hoped that data from the P78-2 spacecraft will be applicable to the validation of the NASCAP charging model and EMI coupling models.

It is too early to evaluate the effects on spacecraft survival of the data already obtained and that which will be obtained from P78-2. However, there are two important tasks that should be undertaken, in light of the information generated in the present study; the effects of arcing due to spacecraft charging on spacecraft survival. These are (a) an analytical and experimental determination of G´ and (b) a direct correlation and comparison of the engineering data ordinarly obtained during spacecraft assembly and test, with the "in-orbit" data obtained by the P78-2 payload instrumentation. These two tasks should be aimed at a quantitative determination of hazard posed to spacecraft by the environment and the extent to which present day "ground"

test programs simulate that hazard. With the launch of P78-2, there is a promise of a data return that is directly applicable to the definition of standards and procedures that will be effective in eliminating the deleterious effects associated with spacecraft charging/arcing.

Table A. Principal Investigators/Sponsors

Experiment Number	Title	Principal Investigator/ Sponsor	Address
SC1	Engineering Experiments	Dr. H. C. Koons/ USAF/AFSC/SAMSO	The Aerospace Corporation P.O. Box 92957 Los Angeles, CA 90009
SC2	Spacecraft Sheath Electric Fields	Dr. J. F. Fennell/ USAF/AFSC/SAMSO	The Aerospace Corporation P.O. Box 92957 Los Angeles, CA 90009
SC3	High Energy Particle Spectrometer	Dr. J. B. Reagan Office of Naval Research	Lockheed Palo Alto Research Lab, 3251 Hanover Street Palo Alto, CA 94304
SC4	Satellite Electron and Positive Ion Beam System	Dr. H. A. Cohen/ USAF/AFSC	Hanscom AFB/LKB Bedford, MA 01731
SC5	Rapid Scan Particle Detector	Lt. D. Hardy/ USAF/AFSC	Hanscom AFB/PHE Bedford, MA 01731
SC6	Thermal Plasma Analyzer	Dr. R. C. Sagalyn/ USAF/AFSC	Hanscom AFB/PHR Bedford, MA 01731
SC7	Light Ion Mass Spectrometer	Dr. D. L. Reasoner/ Office of Naval Research	NASA Marshall Space Flight Center, Code BS-23 Huntsville, AL 35815
SC8	Energetic Ion Composition Experiment	Dr. R. G. Johnson/ Office of Naval Research	Lockheed Palo Alto Research Lab, 3251 Hanover Street Palo Alto, CA 94304
SC9	UCSD Charged Particle Experiment	Dr. S. E. Deforest/ Office of Naval Research/USAF/AFSC/ SAMSO	University of California B019 Dept. of Physics La Jolla, CA 92093
SC10	Electric Field Detector	Dr. T. L. Aggson/ Office of Naval Research	NASA Goddard Space Flight Center, Code 625 Greenbelt, MD 20771
SC11	Magnetic Field Monitor	Dr. B. G. Ledley/ Office of Naval Research	NASA Goddard Space Flight Center, Code 625 Greenbelt, MD 20771
ML12	Spacecraft Contamination	Dr. D. F. Hall/ USAF/AFSC/AFML	The Aerospace Corporation P.O. Box 92957 Los Angeles, CA 90009